Characterisation of PRT1, an E3 Ligase of the N-end Rule Pathway in *Arabidopsis thaliana*

Christopher John Till (4235052)

Supervisors: Professor Michael Holdsworth &
Professor Frederica Theodoulou

Thesis Submitted to the University Of Nottingham for the Degree of Doctor of Philosophy

September 2018

Abstract

The N-end rule pathway of targeted protein degradation links the half-life of a protein to the identity of its amino (N-) terminal residue. Proteins become substrates for the pathway following proteolytic cleavage which may be followed by enzymatic modification to produce novel N-termini. In *Arabidopsis thaliana*, proteins with aromatic N-termini are targeted for degradation by the PROTEOLYSIS1 (PRT1) E3 ligase (Potuschak *et al.,* 1998). This component of the plant N-end rule pathway has received little attention by the scientific community with no definitive physiological role or substrate profile established to date.

Several approaches were taken to address unanswered questions regarding this enigmatic ligase. Promoter-reporter, activity reporter and tagged lines were used to identify tissues and cell types in which *PRT1* is expressed and active. Loss of function mutants and complementing lines were screened to identify processes which require PRT1-mediated protein degradation.

Although the *prt1-1* loss of function mutant did not exhibit robust phenotypes in response to a range of abiotic stresses, a role for PRT1-mediated degradation as a regulator of plant responses to biotic stresses was established. A consistent and reproducible phenotype of increased resistance of *prt1-1* to *Pseudomonas syringe* pv *tomato* DC3000 inoculation was demonstrated. Transcript analysis and proteomic data revealed increased expression and abundance of key components of the plant immune response in the *prt1-1* background which prime it for defence against infection by bacteria. Interestingly, the other plant E3 ligase PRT6, which targets substrates with basic N-termini, exhibits a similar phenotype in response to *Pseudomonas* challenge. Taken together, the data support a role for the N-end rule in suppressing the immune response in uninfected plants.

Acknowledgements

I would like express particular appreciation and thanks to my supervisors Professor Freddie Theodoulou and Professor Michael Holdsworth for their advice, flexibility, patience and drive which, through great collaborative efforts, have enabled me to produce a thesis I can say I am personally extremely proud of.

“If I have seen further than others, it is by standing upon the shoulders of giants” Isaac Newton

I would like to thank all members of the Theodoulou and Holdsworth groups, past and present: Dr Maria Oszvald, Dr Hongtao Zhang, Dr Theresia Schaedler, Lucy Gannon, Dr Kirsty Hasall, Charlene Dambire, Julietta Marquez, Dr Jorge Vicente Conde, Natasha Gladstone, Dr Mohammed Abbas, Dr Guillermina Mendiondo, Dr Gunjan Sharma, Dr Kamal Swarup, Dr Sophie Berckhan, Dr Tinne Boeckx, Dr Cristina Mariana Sousa Correia, Agata Zubrycka and Ken Davies. I would like to extend especial gratitude to Dr Jorge Vicente Conde who has not only invested a lot of time teaching me but is a supportive and really inspiring colleague. A great deal of appreciation is owed also to Dr Hongtao Zhang whose scientific rigour, unrivalled work ethic and patience enabled me particularly to get through very long days of proteomic experimentation in the lab.

Additional thanks are extended to Professor Julie Gray and Joanne Landymore at the University of Sheffield, Katherine Lilley and Mike Deery at the University of Cambridge and Professor Andreas Bachmair (University of Vienna) for their collaborations.

I would like to thank my friends and family, in particular my father John Till and partner Jasmine Burr-Hersey. They have been unwavering bastions during turbulent periods of my life and helped push me over the finish line.

Contents

List of figures

4. Screening abiotic factors for a physiological function requiring PRT1-mediated protein degradation

Appendix

List of tables:

1. Introduction

2. Materials and Methods

5. The role of PRT1 in plant immunity

1 Introduction

1.1 Arabidopsis thaliana as a model organism

Arabidopsis thaliana has remained a 'work horse' for genetic and molecular biology research since it was originally adopted as a model organism approximately 30 years ago (Woodward and Bartel, 2018). The plant has a plethora of desirable characteristics making it well suited to this task despite it being an agriculturally insignificant plant. Arabidopsis has a small diploid genome consisting of approximately 27,000 genes over 5 chromosomes and was the first plant to have its genome mapped and sequenced. It has a short generation time of between 6-7 weeks and produces a prolific seed set following self-pollination. The plant is small in size and has very basic growth requirements meaning no specialist lab setup is required. Rapid and efficient means of genetic transformation are possible such as *Agrobacterium tumerfaciens* methods.

1.2 Regulated Proteolysis

The central dogma in molecular biology, first published in 1958 by Francis Crick traditionally describes flow of information from DNA which is transcribed into RNA and translated into protein. Upon transfer of this information into the protein, it cannot alter the DNA sequence. (Crick, 1958). The conversion of proteins into constituent amino acids, and subsequent recycling of these back into proteins was only proposed in 1942. Prior to this, proteins were viewed as stable components that only deteriorated due to the inevitable rigours of the cell environment (Ciechanover, 2005), thus this central dogma was viewed as a one-way process. The regulated degradation of proteins is an essential process for eukaryotes (Choi *et al.,* 2010; Gibbs *et al.,* 2014). Proteolysis involves the targeted breakdown of proteins into their constituent peptides and amino acids which not only plays an essential role in signalling and fundamental development processes but can also prevent accumulation of misfolded/irregular proteins and those which may be deleterious to cellular viability.

1.3 The ubiquitin proteasome system (UPS)

In eukaryotes, protein turnover is primarily mediated by the ubiquitin proteasome system and the covalent attachment of the abundant regulatory protein called ubiquitin (Ub) is essential for protein turnover. Ub is a 76-amino acid protein highly conserved between yeasts, mammals and plants, with only three of these residues differing between them (Sadanandom *et al*., 2012). In a process called ubiquitylation, it is covalently attached lysine (Lys) or amine terminals (Nt) of target proteins (Komander and Rape, 2012). Plant genome-wide studies have revealed that approximately 6% of the *Arabidopsis* genome is implicated in the ubiquitin proteasome system (Vierstra, 2009).

1.3.1 The E1-E2-E3 cascade

The ubiquitin-activating enzyme (E1) activates free ubiquitin molecules at their carboxyl–terminal (C-terminal) glycine residue through a thioester bond (Figure 1.1). This high energy thiol ester intermediate is transferred to a ubiquitin conjugating enzyme (E2) which interacts with ubiquitin ligases (E3) (Chen and Hellman, 2013). E3 ligases largely determine substrate specificity in the E1-E2-E3 cascade, although the importance of E2s in substrate specificity has recently been demonstrated (Turek *et al.,* 2018). The E1-E2-E3 cascade results in the formation of an isopeptide bond between the C-terminal glycine residues of activated ubiquitin and internal lysine *ε*-NH_2 groups of the target substrate (Matta-Camacho *et al.,* 2010; Tasaki *et al.,* 2005; de Bie & Ciechanover, 2011). After attachment of the first ubiquitin moiety to the target protein substrate, further Ub moieties are ligated specifically to one of seven available lysine residues (K6, K11, K27, K29, K31, K48, and K63) on the initial Ub residue (Kim *et al.,* 2007). Linear peptide bonds can also be generated with α-NH_2 groups, ester bonds with threonine or serine as well as thiol ester bonds with internal cysteine, although these are less frequent (de Bie & Ciechanover, 2011).

It not clear whether poly-ubiquitin chains are generated by linkage of pre-formed Ub moieties or through successive rounds of E3-mediated ligations. Proteins are earmarked for degradation by the presence of a multi-ubiquitin Gly-76-Lys-48 chain (Sadanandom *et al.,* 2012; Hanna and Finley, 2007) (Figure 1.2 & 1.3). This protein conformation is recognised by the 26S proteasome, whose ATP-dependent protease activity breaks the substrate protein down into small peptides and recycles ubiquitin moieties for further use (Stary *et al.,* 2003; Tasaki *et al.,* 2012; Zhou, 2005). Poly-ubiquitin chains in which the ubiquitin moieties are sequentially attached to available Lys residues other than 48 may fulfil roles other than proteolytic ones (de Bie & Ciechanover, 2011). Polyubiquitin chains stemming from Lys63 regulate activation of kinases as well as DNA repair mechanisms (Jacobson *et al.*, 2009; Walsh and Sadanandom, 2014). Furthermore, monoubiquitylation has been demonstrated to cause protein translocation, degradation via the lysosome as well as degradation of small, loosely folded proteins (Tanaka *et al.,* 2008; Cai *et al.,* 2012; Nordgren *et al.,* 2015; Kwon and Ciechanover, 2017). Polyubiquitin chains which are linear, branched as well as heterogenous can be attached to a substrate, although the specific function of these is currently unknown (Park and Ryu, 2014).

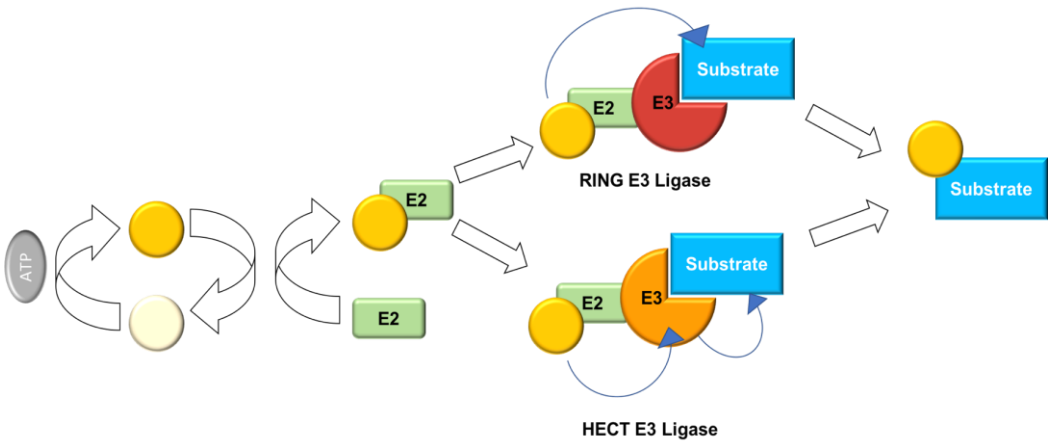

Figure 1.1: The E1-E2-E3 cascade for ubiquitin attachment to the target substrate (grey oval indicates ATP; circles indicate ubiquitin moieties; blue indicates protein substrate; yellow indicates ATP-activated; beige indicates inactivated ubiquitin).

In plants, only one or two E1 enzymes are present, but they are expressed and active in most tissues (Callis *et al.,* 1995). By contrast, there are 37 isoforms of E2 enzymes grouped into 12 classes in Arabidopsis, indicating there is a greater specificity in terms of tissue and developmental expression of these E2 enzymes and interactions with E3 ligases. It has recently been shown that a given E3 may pair with more than one E2, potentially resulting in different types of Ub linkage and different subcellular localisation (Turek *et al*., 2018). The E3 ligases, being specific for particular substrates, are highly diverse and numerate in plants, with thousands of distinct enzymes predicted in plants alone (Hotton and Callis, 2008; Hua and Vierstra, 2011). Such diversity enables plants to respond to environmental changes and facilitate developmental processes in a highly precise, co-ordinated and rapid fashion (Chen and Hellmann, 2013).

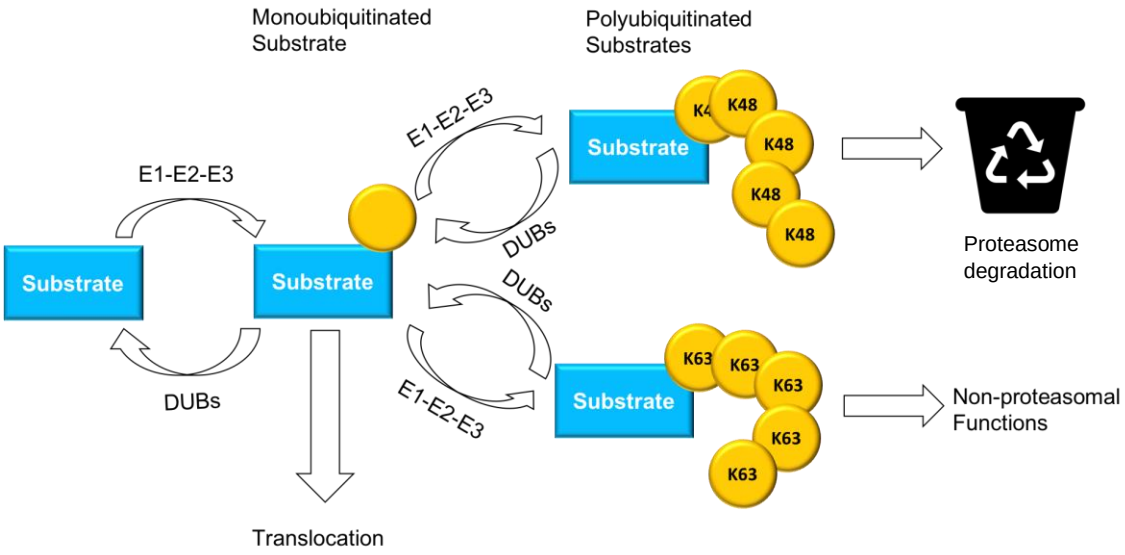

Figure 1.2: Formation of ubiquitin chains and substrate fates. Successive E1-E2-E3 cascades form polyubiquitin chains whereas DUB enzymes remove Ub moieties (yellow circles). Lys48 and Lys63 polyubiquitin chains result in different fates for the tagged protein.

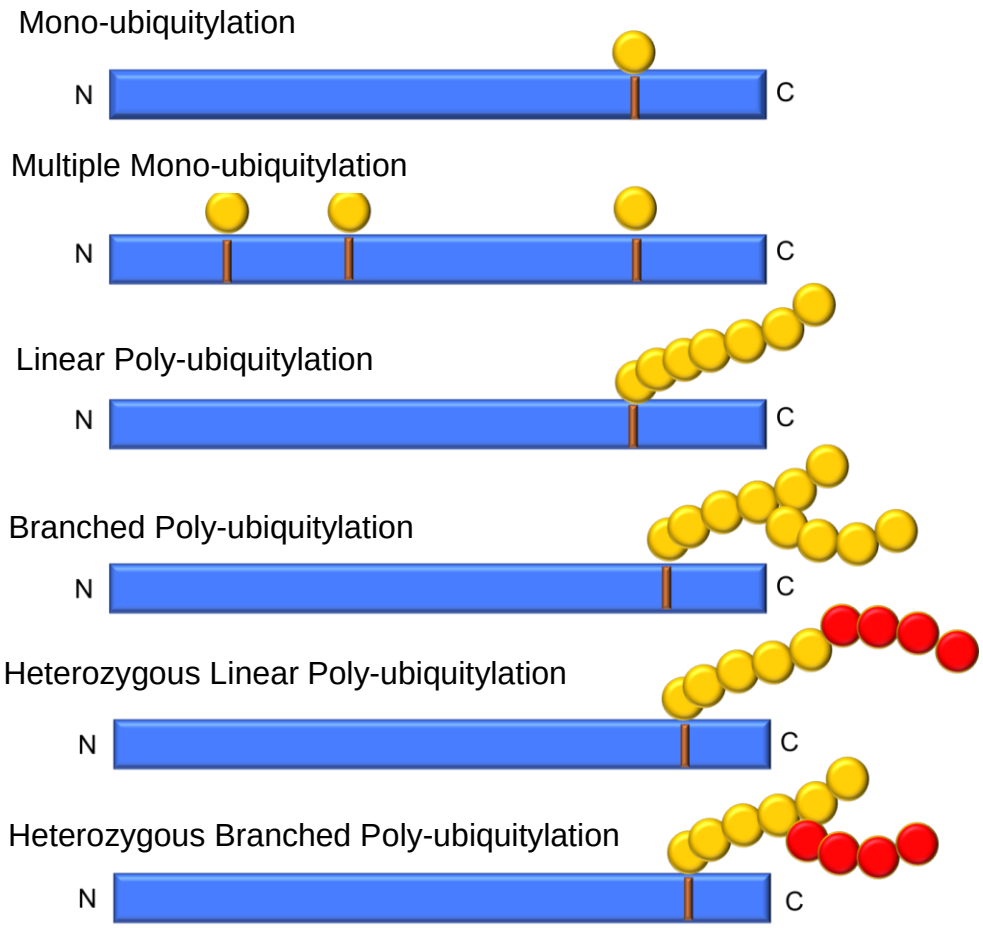

Figure 1.3: Variation of protein target ubiquitylation. (N= amine terminal; C=carboxyl terminus; circles indicate ubiquitin moieties; blue indicates protein substrate; orange indicates internal lysine residues).

1.3.2 Types of E3 ligases

There are three major groups of E3 ligases in plants called Really Interesting New Gene (RING), Homologous to the E6-AP Carboxyl Terminus (HECT) and U-box.

1.3.2.1 HECT domain E3 ligases

HECT domain containing E3 ligases are generally large proteins, with ~350 amino acids and molecular weights in excess of 100 kDa. The HECT domain is relatively conserved but other regions of the structure

can vary considerably. They contain an active Cys residue within the C-terminal HECT domain which co-ordinates a thiol-ester intermediary with the ubiquitin moiety before it is transferred to the substrate (Schneffner *et al.,* 1995). In Arabidopsis, HECT E3 ligases are referred to as UBIQUITIN–PROTEIN LIGASE (UPL) and 7 members have been identified which are further divided into four subfamilies based on domain sequence similarity and structure (UPL1/2, UPL3/4, UPL5, and UPL6/7) (Downes *et al.,* 2003; Huibregtse *et al.* 1995; Marin*,* 2013).

1.3.2.2 RING domain E3 ligases

RING-domain E3 ligases can simultaneously bind with ubiquitin conjugating E2 enzymes and their substrate without requirement for an adaptor protein. (Chen & Hellmann, 2013). RING-finger containing E3 ligases are similar to zinc-finger proteins in that they contain 8 conserved cysteine and histidine residues which co-ordinate the binding of two ions in a cross-braced manner (Fang & Weissman, 2004). However, RING-fingers only modulate protein-protein interactions for E3-E2 proteins (Chen & Hellmann, 2013). Conservative estimates put the number of different plant RING proteins in excess of 450, although not all these proteins function as E3 ligases. RING proteins are classified according to the metal residue ligand present (Stone *et al.,* 2005). The abundance of RING E3 ligases reflects the diversity of the roles they take place in plant response to stresses and involvement in plant development (Cho *et al.,* 2017).

Monomeric RING-type E3s can exist in single-chain enzymes, homodimers and heterodimer forms. In single protein RING E3 ligases, as the name implies, the substrate binding domains and E2-binding domain are fulfilled by a single protein. Both RING E3 ligases RING-domains are capable of interacting with E2 enzymes in homodimeric RING E3s, whereas in heterodimeric RINGs E3s, one RING-domain may interact with the E2 and the other serving to enhance the stability or

activity (Chen & Hellmann, 2013). The E2 binding surfaces in homo- and hetero-dimer tend to face away from one another (Metzger *et al.,* 2014). In complex, multimeric RING-finger E3 ligases, a central cullin protein acts as a scaffold for C-terminal RING-finger recruitment and binding substrate adaptor proteins at the N-terminus. In plants, there are four major groups of cullin-containing E3 ligases including CUL1, CUL3, CUL4 or the cullin-like protein APC (Chen and Hellmann, 2013).

1.3.2.3 U-box E3 ligases

U-box E3 ligases are a class of E3 ligases containing a conserved ~70 amino acids U-box motif which are a modified form of the RING-domain E3 ligases which lacks the ability to co-ordinate zinc ions (Morreale & Walden, 2016). In *Arabidopsis*, there are at least 64 PLANT U-box (PUB) which fulfil a diverse range of roles in plant development and responses to stress (Mudgil *et al.,* 2004).

1.3.2.4 RING between RING fingers (RBR)

RING between RING finger E3 ligases comprise a group of eukaryotic complex multimeric enzymes involving concerted RING/HECT action. Ubiquitin conjugation is catalysed through a mechanism in which a RING1 domain interacts with E2-ubiquitin complexes and a thioester intermediate forms with the cysteine residue of the RING2. The HECT domain of this E3 then modifies the target protein (Smit & Sixma, 2014; Dove & Klevit, 2017).

1.3.3 Degradation of Target Proteins

Irrespective of the way in which substrates were generated, they are ultimately delivered to and consequently degraded by the organism's proteolytic machinery. This takes the form of ClpAP, 26S proteasome and ClpCP in bacteria, eukaryotes and mitochondria respectively. These mechanisms are distantly related yet similar in terms of their structure. The following section focuses primarily on the degradation of proteins in

eukaryotic systems, and prokaryotic substrate degradation will be addressed later.

The eukaryotic 26s proteasome consists of a 20S protein subunit (CP) and a 19S regulatory particle (RP) (Dougan *et al.,* 2012). The RP (19S in eukaryotes) in the 26S proteasome degradation machinery may be located at either one or both ends of the peptidase and acts as a gatekeeper. Consisting of approximately 19 subunits, the RP excludes native proteins from entering the peptidase core by creating a compartment. This facilitates the ATP-dependent unfolding of the target proteins and entry into the proteolytic core (Dougan *et al.,* 2012; Wickner *et al.,* 1999). Peptide movement through the core component is controlled by narrow openings at either end of the proteolytic chamber. If no such gatekeepers exist, the N-terminal ends of the α-subunits obstruct the passage of the protein (Groll *et al.,* 1997). These regulators also make proteins ready for degradation before entry into the proteasome. The removal of ubiquitin is performed by the lid of the RP whilst the base is responsible for unfolding of peptides, activation of the core particle and translocation of the target protein. Unfoldase components which facilitate this protein unfolding events belong to the AAA+ superfamily of proteins, which form ring-like hexameric structures when ATP is present. These AAA+ proteins interact in a few ways with the peptidase and are responsible for its activation although the true nature of eukaryotic AAA+ machinery is limited mainly only to the type II bacterial ClpAP (Dougan, Truscott & Zeth, 2010).

The ClpP or 20S core particles form the peptidase machinery in prokaryotes and eukaryotes, respectively. In eukaryotes, the 20S core particle consists of 28 subunits forming four-heptameric rings. Two of these rings are catalytically inactive α-subunits (α1 to α7) which make up the outer rings. Catalytically active β-subunit sites lie within the central aspects of the machinery (2 rings of 7 different subunits β1- β7) (Groll *et al.,* 1997). The activation of the core particle entry portal, known as ‘gate opening’, is achieved by the docking of a tri-peptide motif, HbYX where

the ‘Hb’ signifies a hydrophobic residue and ‘X’ can take the form of any amino acid. These are located in the C-terminal side of Rpt2 and Rpt5 of the core particle within an inter-subunit pocket (Dougan, Truscott & Zeth, 2010). As stated previously, this highly targeted ubiquitin proteasome system (UPS) is ATP-dependent process and following translocation of the substrate to the CP, it is broken down into constituent amino acids which are recycled by the cell similarly to ubiquitin molecules (Zhou *et al.,* 2005; Dougan *et al.,* 2012).

1.3.4 Regulation of the ubiquitin system

Substrate modification and degradation through the UPS is reasonably well understood. However, information regarding regulation of the ubiquitin system (the E3 ligase aspect in particular) is only recently emerging. For instance, phosphorylation plays a crucial role in the regulation of E3 ligases (Broad, Ling & Jarvis, 2016). Additional mechanisms of UPS regulation are discussed in the following section.

1.3.4.1 Self-ubiquitylation

Modulation of E3 activity can be achieved through ubiquitylation, either self-catalysed or through exogenous ligase activity. Self-regulatory function of E3 ligase have been observed through self-ubiquitylation proposed to target the enzyme to the 26S proteasome for degradation. Self-ubiquitylation can be substrate-dependent, substrate-independent or prevented during the substrate-E3 ligase interaction (Ryan *et al.,* 2006; Petroski & Deshaies, 2005; Okamoto, Taya & Nakagama, 2009). Furthermore, exogenous ligases target E3 ligases for degradation, even those that are capable of self-ubiquitylating. Physiological adaptation may abolish the ability of a ligase to self-ubiquitinate or the E3 ligase may be incapable of self-destruction which could be mitigated by the presence of exogenous ligases. Specific stimuli may also result in external ligase-mediated ubiquitylation. An E3 ligase may be degraded exclusively by the external E3 ligase(s), such as *Drosophila melanogaster* inhibitor of apoptosis1 (DIAP1) degradation by DIAP2 (Hermann-Bachinsky *et al.,* 2007). Alternatively, a combination of self- and external-ubiquitylation

may be required, such as GP79 targeting by HRD1 as well as itself (Fang *et al.,* 2001; Ballar *et al.,* 2010; Shmueli *et al.,* 2009). These mechanisms of E3 ligase degradation may be arranged into a hierarchy for protein and E3 regulation through multiple proteolytic pathways. This can occur in a linear or closed circular fashion (de Bie & Ciechanover, 2011).

Self-ubiquitylation of E3 ligases have also been reported to demonstrate a non-proteolytic function of this process. Self-ubiquitylation can regulate the ubiquitylation state of the E3 ligase to alter the potential for ubiquitylation of the substrate either positively or negatively. For example, the ubiquitylation of histone H2A by RING1B requires self-ubiquitinated RING1B (Ben-Saadon *et al.,* 2006). Whereas DIAP1 self-ubiquitylation through poly-ubiquitin chain formation at Lys63 diminishes preference for the substrate Dronc, potentially through altered binding capacity (Herman-Bachnisky *et al.,* 2007).

1.3.4.2 Deubiquitylation

Additionally, E3 ligases can be regulated by the isopeptidase action of deubiquitinating enzymes (DUBs). These cleave Ub moieties, processing poly-ubiquitin chains into mono-ubiquitin units, completely removing ubiquitin from the substrate (Isono and Nagel, 2014) or reversing the process of self- or exogenous-ubiquitylation (de Bie & Ciechanover, 2011). This process allows the pool of free ubiquitin moieties to be replenished and also a final proof-reading opportunity before the fate of a protein is ultimately decided (Kelderon, 1996; Lilienbaum, 2013). Furthermore, ubiquitin can be modified post-translationally by phosphorylation, acetylation and ribosylation, which may result in structural changes and influence ubiquitylation/deubiquitylation cascades (Kwon & Ciechanover, 2017).

1.3.4.3 SUMOylation

The action of the small ubiquitin-like modifier (SUMO) family of proteins is another way in which ubiquitylation can be regulated and responses to

stress and plant development post-translationally adjusted. SUMOylation consists of the covalent attachment of a 100-115 amino acid SUMO protein, through a cascade of enzymatic reactions reminiscent of ubiquitin conjugation (Verma, Croley and Sadanandom, 2018). These proteins can compete for ubiquitylation sites or alter the stability and/or localisation of modified proteins, or differentially modulate partner protein interactions or with DNA (Wilkinson and Henley, 2010). Arabidopsis encodes eight genes encoding for SUMO proteins which differ in terms of expression patterning and functionality (van den Burg *et al*., 2010). The process of SUMOylations has been implicated in a diverse range of plant processes including thermotolerance (Kurepa *et al.,* 2003), plant growth (Conti *et al.,* 2014), timing of flowering (Murtas *et al.,* 2003), salt stress (Conti *et al.,* 2008) and plant responses pathogens (Lee *et al.,* 2007; Bailey *et al.,* 2016).

The SUMO peptidase activity of ubiquitin-like proteases (ULPs) which begin SUMO precursor maturation by removing 10 amino acids preceding a carboxyl- terminal diglycine which exposes a motif for SUMO conjugation to target proteins (Johnson, 2004). SUMO-activating E1 enzyme generates a high-energy thioester bond between the Cys sulfhydryl group of the large subunit in the E1 enzyme and a glycine carboxyl group in the SUMO protein via ATP hydrolysis (Johnson, 2004; Lucyshyn & Wigge, 2009; Park *et al.,* 2011). This activated SUMO is then transferred to the Cys residue present in a SCE1 SUMO conjugating enzyme and finally, SUMO is transferred from SCE1 to the ε-amino group of Lys in the target protein. This reaction is catalysed by SUMO E3 ligases, although some reports suggest that E3 ligase activity may not be required and conjugation of SUMO to the target is done by directly by E2s (Wilkinson and Henley, 2010). The equilibrium of SUMO signalling is maintained by deSUMOylation of SUMOylated proteins (Saracco *et al.,* 2007). This is fulfilled by the same set of ULPs that were used during SUMO maturation, although some ULPS may play a distinct role in deSUMOylation only (Castro *et al.,* 2016). To date, only HIGHPLOIDY2

(HPY2) and SAP & MIZ1 (SIZ1) SUMO E3 ligases have been identified in *Arabidopsis* (Ishida *et al.,* 2012) in contrast to the huge diversity of UPS E3 ligases. This suggests that rather than SUMO E3 ligases, SUMO deconjugation enzymes are the source for the diversification of SUMO role in plants (Verma *et al.,* 2017).

Furthermore, SUMO proteins fulfil non-covalent interactions with target proteins. SUMO interaction motif (SIM)-SUMO interaction plays a key role in SUMO-mediated processes. The SUMO–SIM interaction offers a vital point of control in regulating SUMO-mediated cellular processes, and SIMs can be integral for SUMOylation of groups of target proteins. SIMs therefore physically interacts with groups of proteins via E3 ligases, which recruits them on to pre-formed protein complexes for protein group SUMOylation (Merrill *et al*., 2010; Jentsch & Psakhye, 2013; Conti *et al*., 2014).

1.4 The autophagy-lysosome pathway (ALP)

Independent studies concurrently discovered a membrane-closed organelle containing digestive enzymes with protease activity against a broad range of targets with the potential to mediate cellular proteolysis, called the lysosome (Ciechanover, 2005). The lysosome fulfils extracellular protein digestion through endocytosis and degradation of organelles and proteins. Compartmentalisation prevents uninhibited degradation of the cellular components, meaning degradation requires uptake of the cellular proteins by the lysosome. This is facilitated by double-membrane autophagosomes, in which endoplasmic reticulum-derived vesicles enclose the organelle/small areas of cytoplasm and fuse with lysosomes whereby proteolysis occurs. Vesicles appear randomly distributed throughout the cytoplasm which move along microtubules toward a microtubule-organising centre, where lysosomes are concentrated (Kwon & Ciechanover, 2017). Ubiquitin is used as a signal for internalisation by vesicles and mono-ubiquitylation, via interaction with endosomal sorting complexes required for transport (ESCRTs) and is sufficient for internalised proteins to be directed to the lysosome for

degradation (Clague & Urbé, 2010). The ALP is divided into micro-autophagy, chaperone-mediated autophagy, and macro-autophagy depending on means of cargo delivery to the lysosome/vacuole.

10-20% of cellular proteolysis is facilitated by the ALP whilst the remaining 80-90% of degradation occurs via the UPS, although this is subject to the physiological state (Kwon & Ciechanover, 2017). Protein uptake by autophagosomes can be a basal, non-selective process responsible for degradation of long-lived or defective proteins (Nedelsky, Todd & Taylor, 2008; Weidberg, Shvets & Elazar, 2011). Starvation and cellular stress induce autophagy in which non-essential cellular components are recycled into amino acids and for cellular energy so essential cellular processes can continue (Tasaki *et al.,* 2013).

Autophagy is regulated by upstream signalling pathways, formation of autophagosomes and their maturation and fusion with lysosomes. B-oxidation of fatty acids is done through single-membrane enclosed organelles called peroxisomes. Mono-ubiquitylation of surplus or damaged peroxisomes have recently demonstrated a role for selective degradation through autophagy (Zhang *et al.,* 2015a). Despite previous categorisation of the autophagy and the ubiquitin proteasome system as distinct catabolic pathways, recent research has revealed they are related processes, with careful orchestration required to maintain cellular homeostasis (Lilienbaum, 2013; Cohen-Kaplan *et al.,* 2016; Kwon and Ciechanover; 2017; Grumati & Dikic, 2018). Autophagy can therefore be a tightly regulated aspect of the lysosomal degradation pathway, which may act as a backup mechanism where the UPS dominates proteolysis (Lilienbaum, 2013).

1.5 The N-end Rule Pathway:

1.5.1 Discovery

The N-end rule pathway is a conserved mechanism of ubiquitin-dependent proteolysis found in mammals, yeasts, plants and bacteria which was first discovered by Bachmair, Finley and Varshavsky (1986) in *Saccharomyces cerevisiae.* The group used artificial reporter fusion proteins consisting of N-terminal ubiquitin molecules attached to a range of different amino acid residues ('X') and a β-galactosidase reporter gene at the C-terminus. Cleavage of the N-terminal ubiquitin molecule by deubiquitinating enzymes produces a β-galactosidase reporter protein with the 'X' amino acid at the N-terminus. Whilst some of the X-residues brought about a stabilisation of β-galactosidase, other residues resulted in a reduction in reporter protein accumulation thus were termed 'destabilising residues'. The different half-lives of the reporter- 'X'-residue proteins were correlated with variation in accumulation of β-galactosidase. Therefore, the group concluded that the *in vivo* stability of a protein is governed by the identity its amino-terminal (N-terminal) amino acid residue, hence the term N-end rule pathway (Bachmair *et al.,* 1986). Further investigation revealed that, as well as a destabilising N-terminal residue, proteins targeted for degradation in this pathway also require an internal lysine residue to which ubiquitin is conjugated and a flexible region of amino acids which lies between the two (Bachmair *et al.,* 1989). The N-end rule pathway will be discussed in this review with the focus being chiefly on the plant N-end rule pathway and more specifically, within the model organism *Arabidopsis thaliana.*

1.5.2 The Arginine/N-end rule pathway

1.5.2.1 Introduction

The eukaryotic N-end rule pathway consists of two distinct branches: one which involves substrate N-terminal arginylation called the Arginine branch (Arg/N-end rule), although not all proteins are arginylated in this branch. The other branch involves the co-translational N^{α}-terminal acetylation of nascent proteins (Ac/N-end rule). The N-end rule pathway

follows a hierarchical structure shared in bacteria, fungi, yeast, mammals and plants; although the details differ slightly between organisms. Generally speaking, this hierarchy is based on the modifications required for E3 Ub ligases to bind to the target substrate and undergo subsequent degradation by the 26S proteasome (Figure 1.4).

1.5.2.2 Structure

In ascending order, primary destabilising residues do not require additional modification and are further sub-divided into type I & II. Type I primary destabilising residues are basic (arginine, lysine and histidine). Type II residues include bulky, hydrophobic and/or aromatic residues, such as phenylalanine, tryptophan and tyrosine. These features of proteins, known as N-degrons, are directly recognised by corresponding E3 ligase N-terminal recognition domains called N-recognins and subsequently degraded by the proteasome (Tasaki *et al.,* 2012; Graciet & Wellmer, 2010).

Other amino acids can be considered to be secondary and in the case of eukaryotes, tertiary destabilising residues. These pre-N-degrons need to be modified enzymatically in order to become functional N-degrons recognised by the N-recognins. In the eukaryotic N-end rule pathway, the secondary destabilising residues, aspartic acid, glutamic acid or oxidised cysteine must undergo post-translational arginylation to become substrates for the N-end rule. In *Arabidopsis*, this reaction is catalysed by two distinct yet closely related arginine-tRNA protein transferases (R-transferases) called *ATE1* and *ATE2*. Mammalian and yeast systems have a single *ATE1* gene, although this undergoes alternate splicing in mammals (Gonda *et al.,* 1989; Graciet & Wellmer, 2010; Yoshidam *et al.* 2002). These enzymes conjugate an arginine residue to the N-terminus of the protein chain, thus producing primary destabilising residues which can be recognised by N-recognins as ready for degradation (Balzi *et al.,* 1990).

Tertiary destabilising residues must be altered to generate secondary destabilising residues. Glutamine and asparagine are eukaryotic tertiary destabilising residues which require deamination. Glutamine (Q) is deamidated into glutamic acid by Nt^{Q}-amidases called NTAQ1 and AtNTAQ1 in mammals and plants respectively (Wang *et al.,* 2009). The conversion of asparagine into the secondary destabilising residue aspartic acid uses the independent Nt^{Asn}-amidase called NtTAN1 in mammals or AtTAN1 in plants (Grigoryev *et al.,* 1996; Graciet & Wellmer, 2010). In contrast, a single N-terminal amidohydrolyase called NTA1 facilitates this deamination in yeast. Furthermore, in plants and mammals, cysteine is also a tertiary destabilising residue (Hu *et al.,* 2005). Modification of this residue through oxidation involves nitric oxide or oxygen. This generates N-terminally oxidized Cys residues (Cys-sulfinic acid in plants or Cys-sulfonic acid) which bear structural resemblance to aspartic acid, a secondary destabilising residue (White *et al.,* 2017*;* Hu *et al.,* 2005; Dougan *et al.,* 2012). A conversion of the new secondary destabilising residue to a primary one by R-transferases earmarks the protein for degradation and thus, protein turnover can take place. In yeast, Nt cysteine is stabilising, perhaps because yeast does not synthesise nitric oxide (Gibbs *et al*., 2015). N-degrons, created through the above cascade, are first created by protein cleavage. Methionine amino-peptidases remove methionine from newly formed proteins to reveal the Nt-residues but only Cys can be made N-terminal by MetAPs (Graciet *et al.,* 2010). Internal cleavage by endopeptidases such as separases, caspases and calpains however can make any destabilising residue N-terminal (Varshavsky *et al.,* 1996; Ditzel *et al.,* 2003).

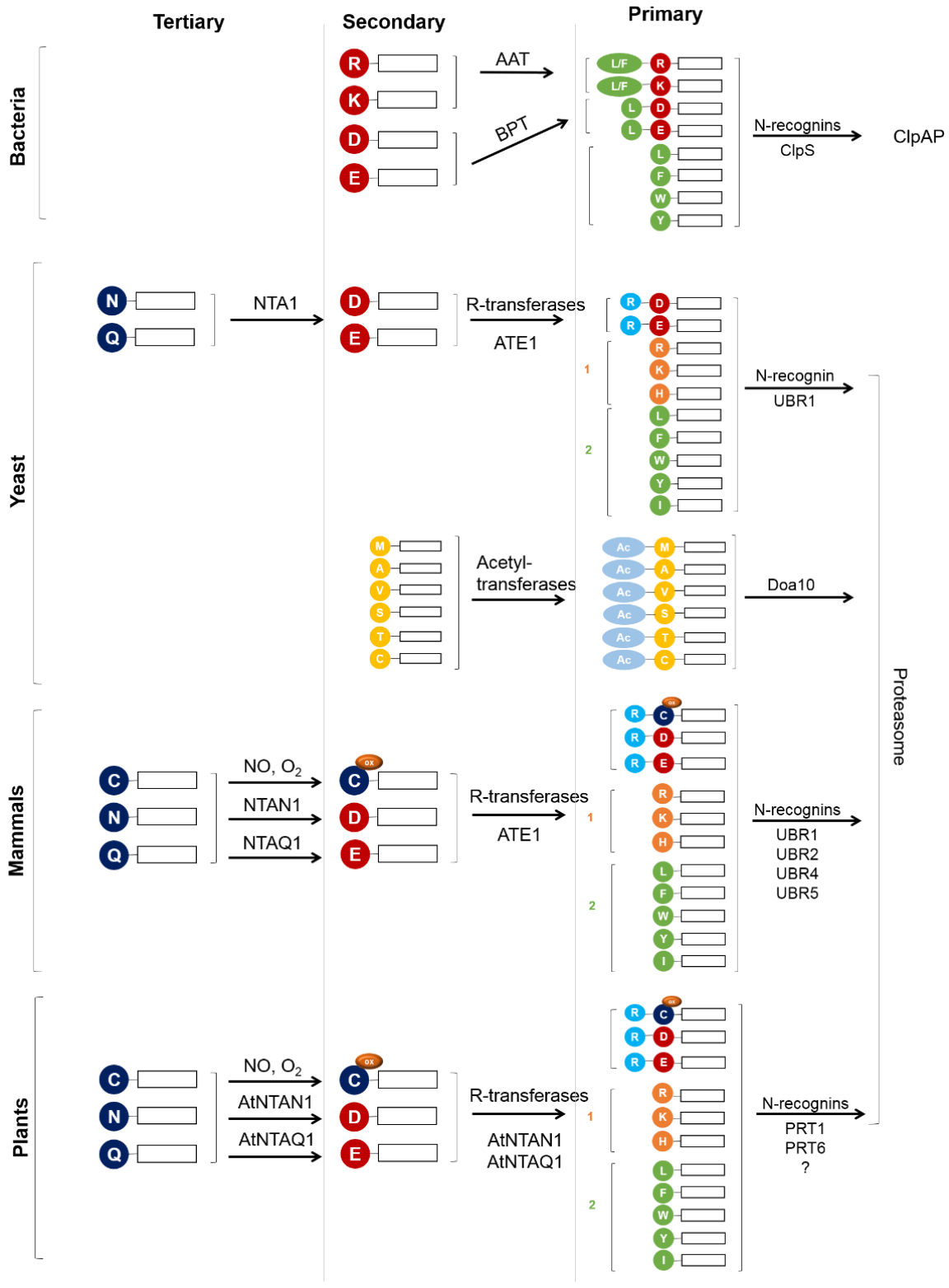

Figure 1.4: The hierarchical structure of the N-end Rule pathway in bacteria, yeast, mammals and plants. Protein substrates undergo sequential modification beginning at tertiary/secondary destabilising to primary destabilising residues. These primary residues are divided into type 1 and 2, which are recognised by N-recognins which leads to their degradation either through the ClpAP for bacterial or the proteasome in yeast, mammals and plants. The circles indicate the amino acid at the N-terminus of the protein and oval indicates oxidation modification. (Based on Graciet & Wellmer, 2010).

1.5.3 The Acetylation/N-end Rule Pathway

1.5.3.1 Introduction:

Another branch of the N-end rule pathway known as the acetylation/N-end rule or Ac/N-end rule exists. In contrast to the “Classic” or Arg/N-end rule pathway in which Nt-residues are unmodified and substrates for degradation by the 26S proteasome (Bachmair *et al.,* 1986), the Ac/N-end branch involves the co-translational or post-translational N-terminal acetylation of proteins (Lee *et al.,* 2016). Since no Nt-deacetylase enzymes have been identified to date, it is assumed that Nt-acetylation of substrates is irreversible (Starheim *et al.,* 2012). The role of N-terminal acetylation has remained enigmatic since its discovery (Narita, 1958), however a diverse set of novel roles have begun to emerge to the Ac/N-end rule including; plant-pathogen defence (Xu *et al.,* 2015), protein folding and quality (Kim & Hwang, 2014), and cell function, proliferation and apoptosis (Lee *et al.,* 2016).

1.5.3.2 Structure:

As with the Arg/N-end rule pathway, N-terminal residues can be described as stabilising or destabilising. This branch of the pathway is also arranged hierarchically into tertiary, secondary and primary destabilising residues. An evolutionarily conserved mechanism of removal of N-terminal methionine (Nt-Met) from nascent cellular proteins is completed by ribosome methionine-aminopeptidases (MetAPs). These MetAPs make tertiary destabilising residues secondary and target small residues in the penultimate amino acid site of the protein. Such small residues include; alanine, valine, serine, threonine, proline, glycine or cysteine (Lee *et al.,* 2016).

These are in turn acetylated by ribosome-associated N-terminal acetylases NatA-NatF to produce primary destabilising residues. These enzymes that facilitate Nt-acetylation are highly conserved within eukaryotes (Polevoda & Sherman, 2000; Gibbs *et al.,* 2014). Nat A contains the catalytic subunit Naa10 (Ard1) and the ancillary Naa15

subunit which acetylate N-termini with serine, alanine, glycine, cysteine, threonine and valine residues (Polevoda *et al*., 2003). Loss-of-function mutants demonstrate the importance of NatA in a diverse range of organisms including stress resistance and response, ribosome biogenesis, cell apoptosis, correct protein folding and photosynthesis (Lee *et al.,* 2016). Dorfel and Lyon (2015) demonstrate that a loss-of-function for the NatA subunit Naa10 may be lethal to *Drosophila* since it critically perturbs cell proliferation and survival. Additionally, roles for NatA in humans have been in observed cancers, neuronal diseases, X-linked human genetic disorders (Kalvik & Arnesen, 2013; Rope *et al.,* 2011).

Naa20 and Naa25 are the catalytic and accessory subunits respectively of NatB which have specificity for Nt-Met with asparagine, aspartate, glycine and glutamic acid (Lee *et al.,* 2016). NatB has pleotrophic effects including the regulation of development, including flowering in plants (Ferrandez-Ayela *et al.,* 2013), as well as maintenance of cell wall structure and formation of actin cables, and mitochondrial inheritance (Lee *et al.,* 2016). NatC principally acts on Nt-Met where bulky hydrophobic residues are present in the penultimate position, acetylating these through the action of the Naa30 catalytic, and Naa35 and Naa38 auxiliary subunits. Studies have demonstrated that NatC is implicated in stress responses, chloroplast organogenesis (Pesarsei *et al.,* 2003) and protein directing, growth and maintenance of cells (Aksnes *et al.,* 2015).

The catalytic subunits Naa40, Naa50, and Naa60 are present in NatD, NatE, and NatF respectively. Histone H2A or H4 Nts are acetylated by NatD for partial histone modification and rDNA silencing (Polevoda *et al*., 2009). NatE is implicated with microtubule development and segregation of chromosomes whereas NatF acetylates the Nt of Golgi transmembrane proteins in multicellular organisms to regulate their structural integrity. NatE and NatF share partially overlapping substrate profiles with NatC (Aksnes *et al.,* 2015).

These Nt-acetylated residues are known as ^{Ac}N-Degrons which are recognised by a distinct group of E3 ligases known as Ac/N-recognins. In yeast, Ac/N-end rule pathway E3 ligases are usually tethered to the endoplasmic reticulum membrane and nuclear membrane, where they serve to degrade nuclear and cytosolic proteins (Swanson *et al.,* 2005). Hwang *et al* (2010) suggested that, although acetylation plays an essential role in the recognition of protein targets, this alone is not sufficient for degradation to proceed. Instead the pathway may be a conditional one which oversees the formation and folding of proteins; a point which is backed up by the observation that between 50% and up to 80% of major yeast proteins remain stable despite being N-terminally acetylated (Dougan *et al.,* 2012).

Shemorry *et al* (2013) propose that Ac/N-end rule also regulates input stoichiometries in hetero-oligomeric protein complexes. COG1 and HIGH COPY SUPPRESSOR for CUT NINE1 (HCN1) are a conversed oligomeric Golgi complex and a subunit of anaphase promoting complex ubiquitin ligase. A technique known as 'subunit decoy' demonstrated that both aforementioned proteins are provisional substrates of the Nt-acetylation pathway. Association of the protein with its multi-subunit protein complex shields their N-terminal residue which protects them from degradation by the proteasome. Conversely, dissociation of the protein leaves the N-terminus vulnerable to recognition by N-recognins and can be degraded as described above. In this way proteins are only degraded at specific developmental stages (reviewed in Gibbs *et al.,* 2014b).

1.5.4 The Pro/N-end rule pathway

Aside from the Arg- and Ac/N-end rule pathway branches, the Pro/N-end rule pathway has recently been discovered which has specificity for Nt-proline residues. Gid4 is a recognition component of the Pro/N-end rule pathway, which is a subunit of the oligomeric GID ubiquitin ligase (Chen *et al.,* 2017). In *Saccharomyces cerevisiae,* the Pro/N-end rule pathway

functions to degrade gluconeogenic (involved in *de novo* glucose synthesis) enzymes, involved in glucose synthesis in deficient conditions. In *S. cerevisiae,* fructose-1,6-bisphosphatase (Fbp1), isocitrate lyase (Icl1), malate dehydrogenase (Mdh2), and phosphoenolpyruvate carboxykinase (Pck1) are gluconeogenic enzymes (Giardina & Chiang, 2013). Following return to glucose-replete conditions, gluconeogenic enzymes are degraded. Gid4 recognises Nt-proline residues, polyubiquitylates proteins and earmarks them for degradation by the proteasome (Chen *et al.,* 2017). The Pro/N-end rule pathway has not been demonstrated in the plants.

1.5.5 The N-end Rule Pathway in prokaryotes

Prokaryotic organisms lack ubiquitin. A mechanism of protein degradation independent of Ub evolved in these organisms for substrate recognition and degradation (Mogk, Schmidt & Bukau, 2007). In spite of these major differences, the prokaryotic branch mirrors the eukaryotic N-end rule pathway in many respects (Dougan, Truscott & Zeth, 2010).

In bacteria, protein synthesis initiates with formyl-Met (f-Met), which is not a destabilising Nt residue of the N-end rule pathway. Consequently, post-translational modification is required to form an N-degron. (Dougan, Truscott & Zeth, 2010). Nt f-Met is first removed by peptide deformylase (PDF) allowing Nt Met removal by methionine aminopeptidase (MetAP). This however only happens if the amino acid residue at position 2, which will become the new Nt, has a small side chain representing a stabilising residue (such as Gly, Cys, Ala and Ser) (Giglione *et al.,* 2003). Following this modification, proteins with secondary destabilising residues (Arg, Lys, Met, Asp, Glu) are processed by either aminoacyl-tRNA-protein transferase: aminoacyl transferase (AAT) or bacterial protein transferase (BPT) (Graciet *et al.,* 2006). These conjugate Leu or Phe to the secondary destabilising residues. N-terminal Leu, Trp, Tyr and Phe are primary destabilising residues in *E. coli* (Mogk, Schmidt & Bukau, 2007).

Recognition of substrates in the prokaryotic N-end rule pathway is facilitated by Hsp100 proteins such as ClpS that resemble the eukaryotic E3 ligases in their mode of action (Mogk, Schmidt & Bukau, 2007). Recognition domains of these proteins interact either directly or via adaptor proteins pre-bound to the substrate (Erbse *et al.,* 2006). Following recognition events, the ClpS-substrate complex is directly delivered to the AAA+ ClpA chaperone of ClpAP via specific interactions between the Nt-extra domain of ClpA and ClpS. Efficient transfer of the substrate from the ClpS to the ClpA requires an unstructured linker between the Nt-destabilising residue and substrate moiety. This permits efficient unfolding and translocation of N-end rule substrates into the chamber of ClpP in a ClpA-mediated ATP dependent fashion. Similar to eukaryotes, prokaryotes are reliant on a central proteasomal component to facilitate protein degradation. In *E coli* this is done by the ClpP peptidase and forms a narrow passage that physically prevents folded proteins from entering (Mogk, Schmidt & Bukau, 2007).

1.5.6 Plastid and mitochondrial N-end rule pathway

Mitochondria are gram-negative derived organelles in eukaryotic cells (Smith, 1975). These organelles contain the Leu/N-end rule pathway thought to be “inherited” during symbiosis. The mitochondrial matrix may contain the N-end rule pathway (Varshavsky, 2011). Nuclear-encoded mitochondrial matrix proteins are cleaved by mitochondrial processing proteases (MPP) upon import from the cytosol into the matrix, revealing Nt-destabilising residues of the bacterial Leu/N-end rule pathway and the eukaryotic Arg/N-end rule pathway, such as bulky hydrophobic N-degrons. Chloroplasts, being cyanobacteria derived organelles, may also contain the N-end pathway. A strong sequelog of the bacterial ClpS N-recognin has been identified indicating it may be a component of the Leu/N-end rule pathway (Varshavsky, 2011).

1.6 N-degron Recognition Domains (N-recognins)

1.6.1 Introduction

N-degron recognition domains or N-recognins are E3 ligases which bind proteins bearing primary destabilising residues (Graciet & Wellmer, 2010). *Saccharomyces cerevisiae* Ubr1p is the prototypical N-recognin. Analysis of Ubr1p has revealed at least three substrate binding sites: a UBR box which recognises N-degrons with basic residues, a ClpS-like domain which recognises hydrophobic N-termini, and a third domain which recognises an internal degron in CUP9 (Varshavsky, 2011).

1.6.2 The UBR box

The UBR box is a 70-residue domain which binds Type 1 degrons (i.e. basic N-termini). Biochemical and crystallographic studies have demonstrated that the UBR boxes of ScUBR1 and mammalian homologues, UBR1 and UBR2 interact with the target protein's N-terminal amino acid side chain and the peptide backbone of the first two amino acids in a similar fashion to bacterial ClpS-domain (Dougan *et al.,* 2012). The N-terminal side chain locates within a negatively-charged shallow groove on the UBR box interface, with an H-bond network serving essential functionality in modulating type 1 N-degron α-amino groups for binding in recognition events. The acidic residues in the Ubr1 side chain binding groove serve to modulate substrate specificity (Dougan *et al.,* 2012; Choi *et al.,* 2010; Tasaki *et al.,* 2009; Matta-Camacho *et al.,* 2010). Two conserved cysteine and histidine residues in this zinc-finger domain are likely to provide structural integrity to the UBR box (Matta-Camacho *et al.,* 2010). Tasaki *et al* (2009) speculate that these important structural features within the structure of the N-recognin perhaps house the active site residues and facilitate substrate binding. These Cys/Hys rich motifs co-ordinate three zinc ions with one motif being responsible for a single zinc ion and the other motif co-ordinating two zinc ions. For the most part, these zinc ions are highly conserved amongst the vast majority of UBR box proteins. However, one residue is poorly conserved, and its more unrestrained activity may be important for

the co-ordination of the final zinc ion. In yeast Ubr1 His118 fulfils this role and may be provided by two residues found at opposite ends of the UBR box (Choi *et al.,* 2010; Dougan *et al.,* 2012).

1.6.3 Beyond the UBR box

Despite the UBR box seemingly being an essential component for N-degron recognition, the capacity to recognise N-degrons does not extend to all UBR box proteins and not all UBR boxes bind N-degrons. Bartel *et al* (1990) demonstrated that although yeast contains Ubr1p and Ubr2p, only the former N-recognin fulfils its purpose. Furthermore, the mammalian N-end rule pathway features at least seven UBR box proteins (UBR1-7) although only UBR1, UBR2, UBR4 and UBR5 function as N-recognins (Graciet & Wellmer, 2010). The ability to bind both basic type 1 and hydrophobic type 2 destabilising residues is a feature common to yeast Ubr1 and mammalian UBR1 and UBR2. Mammalian UBR4 and UBR5 which both lack ClpS-like domain can still bind type 1 and type 2 N-degrons, and type 2 destabilising residues respectively (Tasaki *et al.,* 2009). Additionally, PRT1 in the plant N-end rule pathway lacks the conical UBR box but is able to target Nt-aromatic amino acids for degradation (Stary *et al.,* 2003).

1.6.4 Plant N-end Rule Pathway N-recognins

The Arabidopsis genome encodes three UBR box-containing proteins: PROTEOLYSIS6 (PRT6; At5g02310), BIG (At3g02260) and PRT7 (At4g23860). As stated previously, PROTEOLYSIS 1 is a component of the plant N-end Rule pathway lacking the UBR box.

1.6.4.1 PRT6

PRT6, the second identified N-recognin in plants, was identified based on its sequence homology to UBR1 of yeast and presence of the characteristic UBR domain common to N-recognins in mammalian and yeast systems (Garzón *et al*., 2007). However, unlike yeast Ubr1, studies exploiting X-GUS reporters in the *prt6* and wild type backgrounds

demonstrated that PRT6 is specific for basic N-termini and does not degrade proteins with N-terminal leucine or phenylalanine (Garzón *et al*., 2007). The inability of PRT6 to degrade proteins with hydrophobic N-termini corresponds with the lack of a ClpS homology region present in ScUbr1p.

1.6.4.2 BIG and PRT7

Queries based on the mouse UBR4 to the BLASTP database retrieve the plant protein *BIG*, aptly named due to its large size. Independent mutant screens have identified several *big* mutant alleles that indicate that *BIG* may be involved in cross-talk and regulation of hormone (auxin), light and other signalling pathways (Li *et al.,* 1994; Ruegger *et al.,* 1997; Sponsel *et al.,* 1997; Gil *et al.,* 2001; Kanyuka *et al.,* 2003; Graciet & Wellmer, 2010). The role of PRT7, which is a putative UBR7 homolog, is yet to be determined although it is speculated that it is not involved in the N-end rule pathway as it does not appear to be an E3 ligase, based on sequence comparisons (Andreas Bachmair, personal communication). Although BIG and PRT7 are UBR box proteins, they lack key amino acid residues required for recognition of N-degrons including the promiscuous residue involved in the co-ordination of the final zinc ion and so may not bind peptides (Dougan *et al.,* 2012). More research must be conducted to establish their involvement, if any, in the N-end rule pathway.

1.6.4.3 PRT1

Plants contain an N-recognin which lacks the UBR box as well as a ClpAP-like domain (Stary *et al.,* 2003). Bachmair and colleagues (1993) were the first to identify the plant N-recognin which they named PROTEOLYSIS1 or PRT1. To date, PRT1 has received little attention from the N-end rule community with only a handful of reports referring to work completed on PRT1 (Potuschak *et al.*,1998; Stary *et al.*, 2003; de Marchi *et al.*, 2016; Mot *et al.,* 2018; Dong *et al.,* 2017).

PRT1 of *Arabidopsis thaliana* was identified through a genetic screen and interestingly fulfils the biochemical functions of Ubr1 of yeast despite

not sharing homology (Stary *et al.,* 2003). Mutant *Arabidopsis thaliana* plants were generated through ethyl methanesulfonate treatment (EMS) and were screened for impaired protein degradation. Isolation of the mutants involved a transgenic reporter gene consisting of the model substrate Phe-dihydrofolate reductase (F-DHFR) fused to an N-degron recognised specifically by the ubiquitin dependent proteolysis pathway. This is known as the ubiquitin-fusion technique (UFT). In this way, a short half-life is conferred on the DHFR protein. The transgene-encoded DHFR is mutant mouse form, which has a significantly reduced affinity for the drug methotrexate (MTX). The endogenous Arabidopsis DHFR is inhibited by MTX, but the mouse-derived DHFR compensates, meaning F-DHFR is stabilised. The *prt1-1* mutation is manifested as an inability of Arabidopsis seedlings to degrade DHFR. At MTX concentrations which result in a sensitive phenotype in wild type plants, those mutated in the *PRT1* locus are able to accumulate the DHFR protein and are therefore resistant to MTX (Bachmair *et al.,* 1993; Potuschak *et al.,* 1998). Inactivation of the 26-proteomsome by MG132 also stabilises the F-DHFR construct in the wild type. This is the case for all model substrates tested bearing aromatic, hydrophobic residues such as Phe, Trp and Tyr (Potuschak *et al.,* 1998; Stary *et al.,* 2003).

PRT1 consists of a 410-residue unique protein with a predicted molecular weight of 46-kDa, a relatively small protein. PRT1 contains two RING-HCa finger domains (Figure 1.5). These are protein-protein interaction domains that may facilitate the substrate binding interactions of the E3 ligases (Stone *et al.,* 2005). Furthermore, a ZNF_ZZ domain is present in PRT1. The ZZ domain is suggested to weakly resemble part of the UBR box hinting that perhaps it is a UBR box variant and recognises structurally related molecules or N-degron subsets (Tasaki *et al.,* 2005; Kaur and Subramanian, 2015). PRT1 has the ability to bind two Zn^{2+} ions through histidine and cysteine residues (Potuschak *et al.,* 1998). Although PRT1 does demonstrate some similarity to the RAD18 DNA repair protein present in *Saccharomyces cerevisiae,* complementation

tests demonstrated that PRT1 was unable to complement the radiation sensitivity phenotype associated with *rad18* mutants (Stary *et al.,* 2003).

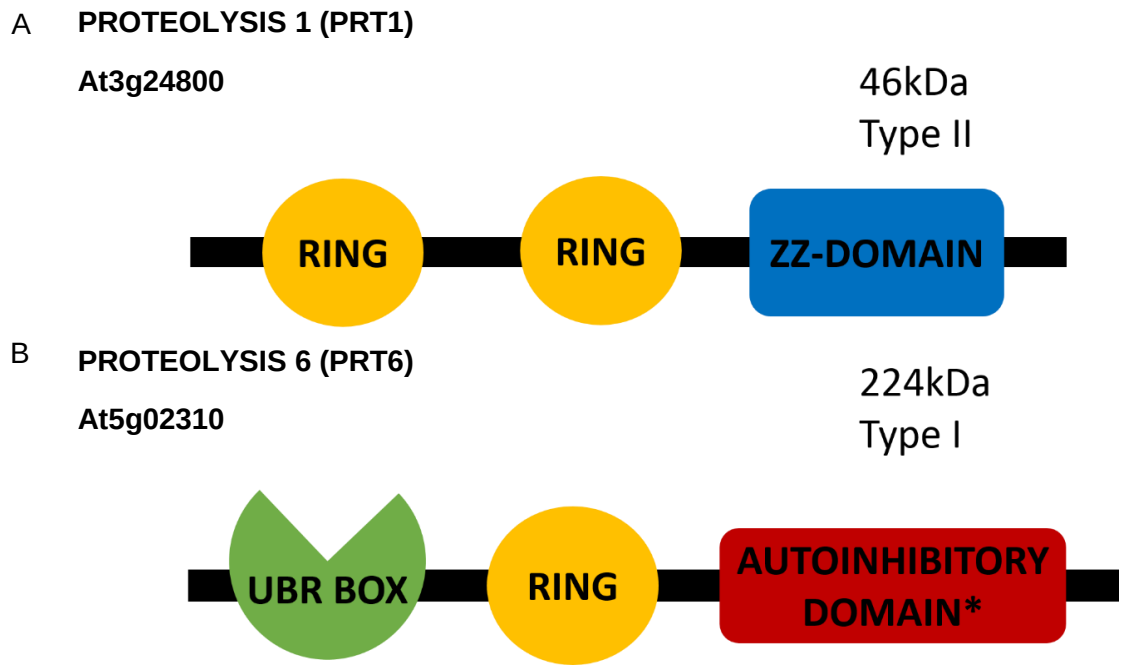

Figure 1.5: The structural features of *bona fide* plant N-end rule recognition domains: (A) PRT1, containing two RING-HCa domains for protein-protein interactions and a ZZ-domain, and (B) PRT6 containing the UBR box, RING domain. (*- predicted autoinhibitory domain) (Diagram based on Mott *et al.,* 2018).

PRT1 is suggested to function as a ubiquitin E3 ligase in the pathway and has been shown to successfully complement a non-functional *ubr1* mutant in yeast (despite its comparatively smaller size). Mot *et al* (2018) developed a protocol for the measurement and tracking of polyubiquitylation in real-time to understand the enzymological and mechanistic characteristics of the PRT1 E3 ligase. Their strategy allows the ubiquitylation to be monitored live via fluorescently labelled substrate proteins and fluorescence-based detection assays called fluorescence polarisation (FP) coupled to high-throughput scanning fluorescence in SDS-PAGE gel detection. Recombinant PRT1 was used with artificial protein substrates in an *in vitro* fluorescence based real time

ubiquitylation assay. The work confirmed that PRT1 is indeed an E3 ligase which can function with the promiscuous UBC8 E2-conjugating enzyme, which mono- and poly-ubiquitinate target substrates without a co-factor requirement.

In general, however, PRT1 bears no sequence resemblance to the E3 ligases present in yeast and mammal apart from targeting aromatic, bulky destabilising residues (Stary *et al.,* 2003). It is often referred to as a "plant pioneer" E3 ligase. Graciet & Wellmer (2010) speculate that some N-recognins may have evolved following the divergence of animal and plant lineages. PANTHER plant classification (http://www.pantherdb.org/; accessed September 2018) shows homologues for PRT1 in a range of different taxa including *Physcomitrella patens* (Moss), *Brachypodium distachyon* (Purple false brome) and *Chlamydomonas reinhardtii* (*Chlamydomonas*) indicating that PRT1 may be an evolutionary conserved component of the N-end rule pathway.

1.6.4.4 Other N-recognins in Plants:

The characterisation of other elusive plant N-recognins remains a challenge to those working on the N-end rule pathway. In addition to identifying PRT1 and PRT6, Bachmair and colleagues provided genetic evidence for the existence of an N-recognin for leucine and isoleucine (Garzon *et al.,* 2007), a finding which was confirmed by Graciet and colleagues (2010) using N-end rule reporter proteins in tobacco. Consequently, additional recognins must be at play in the pathway and more research is required to reveal their molecular identity.

1.7 Pathway Regulation:

Regulation of the N-end Rule Pathway can occur transcriptionally, post-transcriptionally by modification such as ubiquitylation and phosphorylation, and through interaction with Ub ligases (Tasaki *et al.,* 2012). The N-end pathway has been shown to be regulated by the

presence of small molecules, for example, in yeast, peptides regulate the activity of the Ubr1 N-recognin (Byrd *et al.,* 1998; Turner *et al.,* 2000). Additionally, Hu *et al* (2008) discovered that hemin (Fe^{3+} protoporphyrin IX) inhibits the action of R-transferases in yeast and mouse systems through redox mechanisms. Hemin also induces proteasomal degradation of R-transferases and thus acts as both a stoichiometric and catalytic regulator of the N-end rule pathway. Additionally, hemin interacts with the E3 ubiquitin ligases not by directly obstructing the binding site itself, but due to associated dipeptides. The pathway may be a means of controlling and responding to the redox reactions of aforementioned factors through degradation conditionally of transcription factors and G-protein regulators (Hu *et al.,* 2008).

1.8 Substrates of the N-end Rule Pathway

While the structure of the N-end rule pathway has been identified using artificial substrates, information regarding substrates of the Arg/N-end rule pathway has proven more elusive. The components of the N-end rule pathway and hierarchical structure are generally conserved between kingdoms. However, substrates, being functionally and structurally diverse, are not conserved. Consequently, very few substrates of the Arg/N-end rule pathway have been identified to date and are reviewed in this section.

1.8.1 *Saccharromyces cerevisiae* – Scc1 cohesin subunit

SCC1 was the first *in vivo* substrate of the N-end rule pathway discovered by Rao *et al* (2001). Sister chromatids of a replicated chromosomes are separated physically by microtubules which attach at their centromeres. Cohesion forces exist between these chromatids during anaphase that prevent their separation due to the action of the 4-subunit cohesin complex (formed of SMC1, SMC3, SCC1 & SCC3 in yeast). During the metaphase-anaphase transition, an ESP1-encoded separin, through its protease activity cleaves SCC1. This generates a C-terminal SCC1 fragment which bears Nt-Arg: a destabilising N-end rule substrate which

is quickly degraded in an Ubr1 dependent manner through the N-end rule pathway with a half-life of approximately 2 mins (Rao *et al.,* 2001; Sriram *et al.,* 2011).

1.8.2 *Drosophila melagaster* - DIAP1

Ditzel *et al* (2003) demonstrated that Drosophila inhibitor of apoptosis 1 (DIAP1) is the first metazoan substrate of the N-end rule pathway. Inhibitors of apoptosis are a family of proteins which supress cellular death by physical association and neutralisation of caspases. Furthermore, IAP-mediated ubiquitylation of caspases and the interacting DIAP is observed (Wilson *et al*., 2002). DIAP1 degradation lowers the cellular apoptotic threshold and is essential for regulation of cell death. The cleavage of DIAP1 at position 20 via caspases reveals Asn at the N-terminus of DIAP1, a destabilising residue which is a substrate of the N-end rule pathway. Mutants that inhibit the N-end rule pathway mediated degradation of DIAP1 prevent DIAP1 from suppressing apoptosis, possibly due to the inability of DIAP1 to regulate caspases. Cells with mutations that increase the stability of DIAP1 are more sensitised to cell apoptosis because they have increased caspase deregulation. DIAP1 may function as a sink that ensures basal caspase activity is quashed through co-ordinated self-destruction and destruction of the associated caspases, to ensure cellular viability (Ditzel *et al.,* 2003).

1.8.3 *Mus musculus*- Calpain generated peptides

Calpains are ubiquitous, non-lysosomal cysteine proteases which function in a calcium-dependent manner. C-terminal protein fragments generated through the action of calpains in mammals were demonstrated by Piatkov *et al* (2014) to be capable of bearing destabilising Nt-residue recognised by and undergo processive proteolysis through the Arg/N-end rule way. The Ubiquitin-reference technique used identified many mammalian peptides (see Table 1.1) which bear Nt-degrons recognised by the Arg/N-end rule pathway.

Table 1.1: The number and diversity of Calpain generated peptides in *Mus muculus* that are substrates for the N-end rule pathway (Piatkov *et al.,* 2014).

Nt-residue	Peptide	Identity	Role
Arg	Ankrd2	Member of Muscle Ankyrin Repeat Protein family	Negative regulator of muscle differentiation in muscle
	Atp2b2	Plasma membrane Ca^{2+} ATPase	Transmembrane pump that ejects Ca2+ from the cytosol to extracellular space
	Igfbp2	Insulin-like growth factor-binding proteins	Regulate insulin-like growth factors
	C-FOS	Leucine Zipper Transcription Factor	Implicated in cell proliferation, differentiation and transformation regulation.
	Bid	Member of the 'BH3 domain only' subgroup of BCL-2 family	Apoptotic regulatory protein promoting cellular death
Asp	Bclxl	Member of Bcl-2 family	Anti-apoptotic protein in mitochondria
	Capns1	Non-catalytic subunit of calpain-1 and calpain-2	Regulation of Calpain activity
Glu	Bak	Member of the Bcl-2 superfamily of apoptosis regulators	Contributes to the mitochondrial outer membrane permeabilisation, resulting in apoptosis
	Ikbα	Nuclear factor of kappa light polypeptide gene enhancer in B-cells inhibitor, alpha	Binds to the multifunctional transcriptional regulator nfκb and retains it in the cytosol
Leu	Capn1	Catalytic subunit of calpain-1.	Catalytic component of Calpain
Lys	Ica512	Member of the receptor protein phosphatase	Integral membrane proteins
Phe	Glun2a	Subunit of the NMDA receptor	Function as a ligand-gated Ca2+ channel
Tyr	Grm1	Isoform of a member of the group I subfamily of metabotropic glutamate receptors	Mediates a variety of functions, including (indirectly) Ca2+ transients

1.8.4 *Arabidopsis thaliana* – Group VII Ethylene Response Factors

Being sessile organisms, plants are subject to a huge range of abiotic and biotic stresses without the ability to move to mitigate or avoid these. Consequently, plants have evolved mechanisms to overcome and adapt to environment stresses; the N-end rule pathway plays a pivotal role in the perception of many of these pressures. Although *prt6* mutant phenotypes pointed to important roles for the N-end rule pathway, physiological substrates remained elusive until the demonstration that the stability of Group VII Ethylene Response Factor (ERF) transcription factors is controlled by PRT6. These were the first *bona fide* plant substrates of the Arg N-end rule pathway (Gibbs *et al.,* 2011; Licausi *et al.*, 2011).

A transcriptome analysis of PRT6 E3 ligase (*prt6-1)* and arginyl-tRNA:protein arginyltransferase (*ate1ate2*) mutants demonstrated that hypoxia response genes are constitutively expressed in these mutant backgrounds indicating that stabilised substrates of the Arg/N-end Rule pathway promote increased resistance to hypoxic stress in *prt6-1* and *ate1ate2* plants (Gibbs *et al.,* 2011). Licausi *et al.* (2010) demonstrated that overexpression of Ethylene Response Factor (ERF) transcription factors, *RELATED TO AP2 12* (*RAP 2.12*), *HYPOXIA RESPONSIVE ERF1* (*HRE1*) and *HRE2* leads to an increase in the expression of hypoxia response genes. RAP 2.12 and HRE1 are members of the Group VII Ethylene Response Factor (ERFVII) superfamily of transcription factors (Nakano *et al.,* 2006).

ERFVIIs contain a highly conserved N-terminal methionine-cysteine (MC) sequence and become N-end rule substrates following post-translational N-terminal methionine excision, catalysed by methionine aminopeptidases. Amino-terminal cysteine is oxidised when O_2 and NO is present, triggering arginylation of Nt-Cys bearing proteins through the action of arginyl transferases 1 and 2 (ATE 1/2). This makes them substrates for the PRT6 E3 ligase N-recognin which results in their

degradation through the action of the 26S-proteosome, hence the assumption of the term Cys-Arg/N-end rule pathway. When NO and O_2 are absent, cysteine oxidation is prevented, and the stabilised ERF transcription factors initiate the hypoxia response (Gibbs *et a*l., 2014; Weits *et al*., 2014). In this way, the pathway acts as a sensor of both oxygen and nitric oxide (Gibbs *et al*., 2011, 2014; Licausi *et al*., 2011). In Arabidopsis, there are ~250 MC proteins, although not all of these are substrates (Gibbs *et al.,* 2011).

1.9 Physiological Roles of the N-end Rule Pathway in Plants

1.9.1 Introduction

The N-end rule pathway is implicated in a wide array of various cellular processes in a diverse range of organisms, making it an attractive target for research and also for drug discovery (Sriram *et al*., 2013). The Arg/N-end pathway has been implicated in fundamental cellular processes such as DNA repair (Hwang *et al.,* 2009), NO and oxygen sensing (Gibbs *et al.,* 2014) as well as signalling of phytohormones like auxin and ABA (Graciet *et al.,* 2010), germination (Holman *et al.,* 2009) and senescence (Yoshida *et al.,* 2002) in plants. This makes the plant N-end rule pathway a potential target for breeders or biotechnologists to exploit to address the major shortfall between the global population and food stocks.

1.9.2 The Ac/N-end Rule pathway:

The Ac/N-end rule pathway was discovered in yeast and its existence has recently been confirmed in mammals (Park *et al*., 2015) but this branch of the N-end rule has received little attention in plants to date (Gibbs et al., *2014;* Graciet & Wellmer, 2010). Arabidopsis has a homologue of the yeast Ac/N-recognin, DOA10, identified independently by Lue *et al* (2012) as *CER9*, a gene involved in cuticle biosynthesis. This may fulfil a role as an Ac/N-end recognin in plants but a lot more research must be conducted to determine this (Licausi *et al.,* 2013; Graciet & Wellmer, 2010). A review by Gibbs (2015) does however highlight the recent developments in knowledge regarding the

acetylation-branch of the N-end rule pathway may play in plants. The studies presented in the review substantiate claims by Silva & Martinho (2015) that the Ac/N-end pathway is more dynamic than previously reported and plays an important role in plant growth and development. Nt-acetylation has been shown, subject to the sequence context of the modification, to have antagonistic effects on single protein half-life which paints a more complex view of acetylation with regard to proteolysis in plants (Xu *et al.,* 2015). Further studies are necessary to determine what functional significance as well as the complexity and prevalence the acetylation pathway plays in plants (Gibbs, 2015).

1.9.3 Arg-N-end Rule Pathway

1.9.3.1 PRT6 and the Cys-Arg/N-end Rule Pathway

The physiological importance of PRT6 has emerged in recent years as a result of comprehensive mutant analysis. Russell *et al.* (2000) conducted a forward genetic screen for mutants with perturbed germination potential and identified a mutant which was later shown to have a lesion in *PRT6* (Holman *et al.,* 2009). Decreased germination potential of *prt6* seeds was associated with a hypersensitive response to ABA. Since the *ate1 ate2* double mutant exhibited a similar phenotype to *prt6,* it was deduced that the N-end rule substrates accountable for defects in germination may first be arginylated by R-transferases before interaction with PRT6 (Holman et al., 2009). PRT6 also plays several roles in the seed to seedling transition, specifically regulation of seed storage reserves and photomorphogenesis (Holman *et al*., 2009; Abbas *et al.,* 2015; Zhang *et al*., 2018). Graciet *et al.* (2009) subsequently demonstrated the involvement of this “arginine branch” of the N-end rule (sequential action of ATE1/2 and PRT6) in the control of leaf morphology, stem elongation and apical dominance. In *ate1 ate2* and *prt6* mutant plants, *BREVIPEDICELLUS* (*BP)* is not expressed properly. Normally *BP* is not expressed in the leaves of Arabidopsis due to an ASYMMETRIC LEAVES1 (AS1) transcription factor and auxin. Genetic studies hint that AS1 acts redundantly with the N-end rule pathway to regulate leaf

morphology, and thus may be a potential physiological role for PRT6 (Graciet & Wellmer, 2010; Graciet *et al.,* 2009). Despite the plethora of physiological roles in which PRT6 has recently been implicated, a proteomic study by Zhang *et al* (2015) suggested that mutating or deleting this E3 ligase did not have a marked impact upon the Arabidopsis global proteome and consequently it is likely to be involved predominantly in the degradation of a few key regulatory proteins.

As mentioned previously, the Cys-Arg/N-end rule pathway is implicated in regulation of plant homeostasis during low NO and oxygen following degradation of ERFVIIs by the 26S proteasome via the PRT6 E3 ligase. Beyond this role in responses to hypoxia, the ERFVIIs have been associated with plant responses to other abiotic stresses (Qiao & Fan. 2008; Simontacchi *et al.,* 2015; Gibbs *et al.,* 2015), but no molecular mechanism has been validated to explain the role of the ERFVIIs and/or the Cys-Arg/N-end rule pathway in these stresses. The responses of *Arabidopsis thaliana* and *Hordeum vulgare* plants deficient in *PRT6* function (*prt6-1* and *HvPRT6i* respectively), in which ERFVIIs are constitutively stable were screened to a range of abiotic stresses including salinity drought, oxidative stress and high temperature. Following salt stress, a significant decrease in nitrate reductase (NR) activity is seen; the reduction in the activity of NR is correlated with a reduction in NO levels (Vicente *et al.,* 2017).

Vicente *et al* (2017) hypothesised that the NO-sensing role of the plant N-end rule pathway enhances tolerance to salt stress through regulation of downstream responses. There are hints emerging of how stabilised ERFVIIs mediate these functions. Interaction between stabilised ERFVIIs transcription factors and BRAHMA (BRM): a chromatin remodelling ATPase which has been shown to integrate plant responses to abiotic stress though hormone interactions such as ABA. Shani *et al* (2017) also demonstrated that RAP2.3 (an ERFVII) interacts with Aux/IAA promoters and is required for plant stress tolerance. The metabolic slowdown induced by stress is perhaps sensed indirectly by

the stability of the ERFVIIs due to the reduction in NO level. This elucidates the molecular mechanism that links the stress signalling to the environmental stress (i.e. salt). The group conclude that the Cys-Arg/N-end rule pathway enhances plant survival by integrating environmental and metabolic responses (Vicente *et al.,* 2017).

Two recent publications by de Marchi *et al* (2016) and Vicente *et al* (2018) demonstrate a role for the Arg/N-end rule pathway in plant-pathogen interactions. These publications however report contradictory roles for N-end rule mutants in defence against *Pseudomonas syringae* pv tomato DC3000 (*Pst* DC3000). An increased susceptibility to *Pst* DC3000 is reported in de Marchi *et al* (2016) for N-end mutants implying that the pathway is a positive regulator of plant immunity. On the other hand, Vicente *et al* (2018) demonstrated that the distinct Glu-deamidation and Cys-oxidation branches of the Arg/N-end rule pathway regulate the response to the *Pst* DC3000 through increased resistance in *prt6* and *ntaq* mutants. A consensus must be reached as to the involvement of the N-end rule pathway and response to biotic stresses.

1.9.3.2 PRT1

The physiological role(s) of PRT1-mediated protein degradation in plants remain elusive to date although it is an area gathering more attention from the scientific community. During this PhD, a number of papers were published ascribing functions to PRT1-mediated degradation in plants:

Dong *et al* (2017) demonstrated a potential role for PRT1 in the control of cell proliferation regulation. Cell proliferation patterns and final cell sizes determine the unique shapes and sizes of plant organs and must be a strictly controlled process. The duration of cell proliferation in *Arabidopsis* organ growth is limited by DA1: peptidase activated in a ubiquitin-dependent manner through the action of two RING E3 ligases called BIG BROTHER (BB) and DA2. The activated DA1 cleaves the cell proliferation promoting UBP15 deubiquitylase enzyme, and also cleaves

TEOSINTE BRANCED 1/CYCLOIDEA/PCF 15 (TCP15) and TCP22 transcription factors that work to promote proliferation but also repress endoreduplication. DA1 peptidase activity also cleaves BB and DA2 E3 ligases leading to their destabilisation. The mechanism of degradation of DA2 is unknown, but BB is destabilised through the action of PRT1 and the N-end rule pathway. DA1 is hypothesised to facilitate the transition from cell proliferation to endoreduplication and differentiation by degraded regulatory proteins in *Arabidopsis* organ formation, and PRT1 plays a role in the destabilisation of these peptides.

In the aforementioned publication by de Marchi *et al* (2016), *prt1-1* was among the N-end rule mutants reported to be more susceptible to challenge by pathogen, indicating there is a role of PRT1 in the regulation of plant responses to pathogens.

1.10 Objectives of this thesis:

As previously stated, PRT1 has been well characterised from a biochemical point of view. However, there are major gaps in knowledge regarding PRT1 and this thesis aims to elucidate more about the E3 ligase using *Arabidopsis thaliana* as a reference organism. Three major questions regarding the biology of PRT1 are the primary focus of this thesis.

1. In which tissues, cell types and subcellular components is *PRT1* expressed and where is it active?

2. What are the physiological functions of PRT1?

3. What are the substrates of PRT1 and with which other proteins does it interact?

In order to fulfil the first objective, a promoter-reporter construct was used to establish in which tissues and cell types the *PRT1* promoter is active, and how environmental cues influence the activity of the promoter. The ubiquitin-fusion technique was then employed to determine in which tissues and organs PRT1-dependent protein degradation occurs. Together, these approaches may give clues as to the physiological function of PRT1.

The *PRT1* loss-of-function knockout mutant, *prt1-1,* and lines overexpressing *PRT1* do not have obvious gross morphological or developmental phenotypes. To identify processes which require PRT1-mediated protein degradation, a wide variety of abiotic and biotic factors have been screened to assign a physiological function for PRT1.

To answer the final objective of the thesis, transgenic lines for isolating PRT1-interacting proteins have been developed. A *CaMv35s:PRT1*-GStag-GFP line was developed to allow *in vivo* pull down assays to be

conducted to study the weak and strong interactors of PRT1. Additionally, gene expression and proteomic approaches were trialled, with parameters influenced by localisation and physiological function experiments.

Chapter 2 Materials and Methods

2.1 Materials

2.1.1 Seed Material

All seeds were obtained from members of the Theodoulou (Rothamsted Research, Harpenden, UK) and Holdsworth groups (University of Nottingham, Sutton Bonington, UK) unless stated otherwise.

Dr Maria Oszvald generated several transgenic lines used in this study, under the supervision of Dr Hongtao Zhang. The 1.1kb promoter and full-length genomic sequence of *PRT1* without stop codon, was cloned into pDONR P4-P1R and pDONR221 vector (Invitrogen) to generate pEN-L4-promPRT1-R1 and pEN-L1-gPRT1-L2, respectively. Both of the entry vectors were sequenced, and recombination reactions were carried out with pEN-R2-GStag-L3 and pKCTAP (van Leene *et al.*, 2008) to generate MO14 construct following the instruction of Multisite Gateway® LR Recombination Reaction (Invitrogen). Transformation into *Agrobacterium tumefaciens* (strain AGL-1) and *Arabidopsis thaliana prt1-1* were performed according to established protocols (Clough and Bent, 1998) and transgenic plants were selected using kanamycin and subsequently methotrexate. Reporter line MO15 was generated using pEN-L4-promPRT1-R1 and pMK7S*NFm14GW (Karimi *et al.,* 2007), transformed into Col-0 and selected using kanamycin. MO16 was generated using pEN-L4-promPRT1-R1, pEN-L1-gPRT1-L2, pEN-R2-Y-L3 and pB7m34GW,0 and transformed to *prt1-1* and selected using DL-Phosphinothricin.

2.1.2 Selection Markers

Antibiotics and chemicals used to select for desired constructs in *Arabidopsis E. coli* and *Pseudomonas syringae* are listed in Table 2.1.

Table 2.1: List of antibiotics and chemicals for construct selection

Selection Marker	Abbreviation	Concentration (mg/ml)	Supplier
Ampicillin	Amp	100	Melford
Hygromycin	Hyg	50	Melford
Kanamycin	Kan	50	Sigma-Aldrich
Methotrexate hydrate	Mtx	100	Sigma-Aldrich
Rifampicin	Rif	50	Melford
Tetracyclin	Tet	10	Melford

2.1.3 Murashige & Skoog (MS) Media for *Arabidopsis* Growth

2.1.3.1 Basic MS Agar Media

Plants were routinely grown using agar plates Murashige and Skoog basal salt mixture at half strength referred to as 0.5 x MS (Murashige & Skoog, 1962) (See Table 2.2 for composition). For 500 ml of basic media: 1.25 g of MS basal salt mixture without vitamins (Sigma-Aldrich, Gillingham, UK was dissolved in 450 ml of deionised water to achieve half strength MS. The pH was adjusted to 6.2 using 1 M potassium hydroxide, 5 g of agar-agar granular powder (Fisher Scientific, Loughborough, UK) was added and the volume was brought to 500ml before autoclaving. Filter-sterilised plant hormones, antibiotics and other media components were added at desired concentrations to hand-warm media and mixed well. While still molten, 50 ml was poured into a sterile falcon tube (50 ml) (Sarstedt, Leicester, UK) a 100 x 100 x 20 mm, square petri dish (Sarstedt) inside a laminar flow cabinet. Half strength Murashige and Skoog plates (0.5 x MS) were stored at 4 ^{o}C up to 2 weeks prior to use.

Table 2.2: The composition of basic and modified Murashige & Skoog (MS) Media used for general growth or screening for physiological functions of *Arabidopsis* accessions.

Component	Sigma-Aldrich MS basal salt M0654 (mg/l)	Caisson labs MS without phosphate MSP11 (mg/l)	Caisson labs MS without nitrogen MSP21 (mg/l)
Ammonium Nitrate	1650.0	1650.0	0
Boric Acid	6.2	6.2	6.2
Calcium Chloride Anhydrous	332.2	332.2	332.2
Cobalt Chloride • $6H_2O$	0.025	0.025	0.025
Cupric Sulphate • $5H_2O$	0.025	0.025	0.025
Na_2-EDTA	37.26	37.26	37.26
Ferrous Sulphate • $7H_2O$	27.8	27.8	27.8
Magnesium Sulphate	180.7	180.7	180.7
Manganese Sulphate • H_2O	16.9	16.9	16.9
Molybdic Acid (Sodium Salt) • $2H_2O$	0.25	0.25	0.25
Potassium Iodide	0.83	0.83	0.83
Potassium Nitrate	1900.0	1900.0	0
Potassium Phosphate Monobasic	170.0	0	170.0
Zinc Sulphate • $7H_2O$	8.6	8.6	8.6

2.1.3.2 Modified Salt Concentration

Modifications were made to basic MS media (2.1.4.1) by adding sodium chloride (Fisher Scientific) to 0.5 x MS media at 4.38 g/L (75mM), 5.88 g/L (100 mM) and 7.32 g/L (125mM) prior to autoclaving. Plates were then poured as 2.1.4.1.

2.1.3.2 Modified Osmotic Stress

25ml polyethylene glycol (PEG) MW 8000 (Sigma-Aldrich) overlay solutions were prepared to -0.5 MPa (19 g/L), -0.75 MPa (250 g/L), -1.2 MPa (297 g/L) and -1.5 MPa (376 g/L). The overlay solution was passed through a 0.22 µm filter (Satorius, Epsom, UK) and poured directly on top of 0.5 x MS plates prepared as 2.1.3.1. Plates were left to infuse overnight with the overlay solution in a sterile laminar flow cabinet.

2.1.3.4 Altered Phosphate Content

Modified Murashige & Skoog agar medium without phosphate (composition in Table 2.2) (Caisson Labs, Smithfield, USA) was prepared as standard MS agar (section 2.1.3). MS with full phosphate content was prepared by adding 170mg/L potassium phosphate monobasic (Sigma-Aldrich) to MS without phosphate powder prior to autoclaving. Standard MS as prepared in 2.1.4.1 was used as a control.

2.1.3.5 Altered Nitrate Content

Stocks were prepared as in Table 2.3, and filter sterilised using 0.2µm Minisart filters (Satorius, Epsom, UK), with the exception of 10X Murashige and Skoog Basal Salt Micronutrient Solution (Sigma-Aldrich) which was purchased in a ready-prepared formulation.

Table 2.3: Components of nitrogen-free MS media

Component	Stock	Amount (g/50ml)
(1) Calcium Chloride, Anhydrous	X100	2..2
(2) Magnesium Sulphate, Anhydrous	X100	0.9035
(3) Potassium Phosphate, Monobasic, Anhydrous	X100	0.85
(4) MES	X100	2.5
(5) Potassium Sulphate	X50	4.0925
(6) Potassium Chloride	X50	1.775
(7) Ammonium Nitrate	X50	4.125
(8) Potassium Nitrate	X50	4.75
(9) MS Basal Salt Micronutrient Solution (MO529)	X10	N/A

Half strength MS medium without nitrogen was prepared by dissolving 2.5ml of stocks (1), (2), (3) and (4) in 400 ml of diH_20, 5ml of stocks (5) and (6), and 25ml of stock (9). The pH was adjusted to 6.2 using 1M KOH (pH 5.7 after autoclaving), water adjusted to 500 ml and 4 g of P1001 plant agar (0.8% final, Duchefa Biochemie, Haarlem, The Netherlands). The media was autoclaved at 121^{O}C for 15 min prior to pouring as 2.1.3.1. For 0.5 x MS with full nitrogen, stocks 5-6 were replaced with stocks 7-8 with the above media. For different ratios of nitrogen content in the 0.5 x MS media, the ratios of stocks 5-6 and 7-8 were adjusted accordingly (i.e. for 20% nitrogen 0.5 x MS, 1ml of stocks 5-6 and 4ml of stocks 7-8 were used). 0.5 x MS prepared as in 2.1.3.1 was used as a control.

2.1.4 King's B Media

King's B Media was prepared as fresh as possible prior to plating out bacteria. King's B media was prepared by dissolving 2% (w/v) Bacto Proteose Peptone No 3 (BD Biosciences) and 1.5% (v/v) glycerol (Fischer Scientific) in 800 ml sterile distilled water, then topped up to 1L before autoclaving. For King's B agar plates 1.5% (w/v) agar-agar

(Fischer Scientific) was added prior to autoclaving. To hand cool bottles, 6.5 mM K_2HPO_4 and 6 mM $SO_4Mg \bullet 7H_20$ were added and mixed by inverting the bottle. If antibiotics were required (Table 2.1) for appropriate selection, these were added to hand-warm media and mixed gently to avoid introducing air bubbles into the media. 20 ml of King's B media with appropriate selection marker was poured under sterile conditions to petri dishes and allowed to solidify. King's B media plates were stored at 4 ^oC up to 2 weeks prior to use, although fresh media is preferable for bacterial growth.

2.1.5 Hoagland's Media

2.1.5.1 Standard Hoagland's

Standard Hoagland's Media (HM) was prepared as in Table 2.4. All stocks were sterilised by autoclaving prior to storage. Components were combined, 1 % (w/v) agar-agar (Thermo Fisher Scientific) added and then autoclaved. For a standard agar plate, 50 ml of Hoagland's agar was poured per plate under sterile conditions and allowed to solidify for a minimum of 20 min.

Table 2.4: Components of standard Hoagland's media

Component	Final Concentration
$MgSO_4$	0.75 mM
KH_2PO_4	0.5 mM
KNO_3	1.25 mM
$Ca\ (NO_3)_2$	1.5 mM
KCl	50 µM
H_3BO_3	50 µM
$MnSO_4$	10 µM
$ZnSO_4$	2 µM
$CuSO_4$	1.5 µM
$(NH_4)_6Mo_7O_{24}$	0.075 µM
Fe EDTA	50 µM
Sucrose	1 % (w/v)

2.1.5.2 Iron Deficiency

For iron deficiency HM, standard media was prepared as described in 2.1.5.1 excluding Fe EDTA. Media with full iron content was used as a control.

2.1.5.3 Zinc Deficiency

For zinc deficiency HM, standard media was prepared as described in 2.1.5.1 excluding zinc EDTA. Media with full zinc content was used as a control.

2.1.6 Oligonucleotides

Oligonucleotide primers for genotyping *Arabidopsis* wild type and mutant allele accessions are listed in Table 2.5. Table 2.6 lists oligonucleotides used for qRT-PCR of genes of interest in this study. All oligonucleotides were ordered from Sigma-Aldrich unless stated otherwise at 0.025µM scale, with desalt purification and in dry format.

Table 2.5: Oligonucleotide primers for genotyping N-end rule mutants

Accession	*Type*	*Name*	*Sequence*
prt1-1	CAPS	prt1-1_F	CAGAGGAAGAGCAAGAACGAGAAT
	CAPS	prt1-1_R	CCACCTTCTGTTTATCTACAC
SALK_086253	SALK	prt1_SALK53_F	AAGAAAAGAAGAAGGTACGGCG
	SALK	prt1_SALK53_R	CGAACACTCTTCCACCTTCTG
prt6-1	SAIL	PRT61_F	GGAGTTTTCTATGTCCAGTGAGAGTTT
	SAIL	PRT61_R	GTCTCCAATGACACGTTCACTTGTCT
SAIL	T-DNA Primer	SAIL	GCCTTTTCAGAAATGGATAAATAGCCTTGCTTC
SALK	T-DNA Primer	SALK LBb 1.3	TGGTTCACGTAGTGGGCCATCG

Table 2.6: Oligonucleotide primers for qRT-PCR

AGI code	Description	ID	Sequence
AT5G18800	Housekeeping Gene, Cox19-like CHCH family protein, mitochondrial respiratory chain complex I	qCTRL3_F	CCTTTTGGCACT TCTGGTG
		qCTRL3_R	GAAGTGTCTCGA CAAAGGT
AT2G14610	*PATHOGENESIS RELATED-1, PR-1*	PR1_F	AAGTCAGTGAGA CTCGCATGTGC
		PR1_R	GGCTTCTCGTTC ACATAATTCCC
AT1G75040	*PATHOGENESIS RELATED-5, PR*-5	PR5_F	TCACATTCTCTT CCCTCGTCGT
		PR5_R	GTAGGGCAATTG TTCCTTAG
AT3G12500	*PATHOGENESIS RELATED-3, PR*-3	PR3_F	AAGTCCTTCCCC GGTTTTG
		PR3_R	CCCATCCACCTG TAGTTTCA
AT3G04720	*PATHOGENESIS RELATED4, PR-4*	PR4_F	GCAAGTGTTTAA GGGTGAAGAA
		PR4_R	CTACATCCAAAT CCAAGCCT
AT3G57260	ATBG2, ATPR2, *PR-2*, BETA-1, 3-GLUCANSE 2, PATHOGENESIS RELATED PROTEIN 2	PR2_F	AAAGAGCCACAA CGTCCGAT
		PR2_R	TCAACCACACAG CTGGACAA
AT3G48090	Alpha/beta hydrolases superfamily protein, ENHANCED DISEASE SUSPECTIBILITY 1, EDS1	EDS1_F	TTGCACCTCCTG AGGAATGTC
		EDS1_R	GCTTCTGTGGAA ATGGCTGT
AT1G08450	CALRETICULIN 3, CRT3, PRIORITY IN SWEET LIFE1	CRT3_F	GTCCTCGGGCT CTTTAGCTT
		CRT3_R	CGATGACCCCAA CGATGTCA

AT2G43570	CHITINASE, PUTATIVE, CHI, AED15	AED15_F	CATGAACCCTGTTTCTTGGGC
		AED15_R	TCGGTGCTTCCATCTCCAAA
AT5G03350	Legume lectin family protein, LLP1, AED9	LLP1_F	CCATGGCACCAGAAAAACCG
		LLP1_R	GAAGCCTTTGATCGTTGCCC
AT2G42530	Cold regulated 15B, COR15B	COR15_F	TCTTTGTGGCTTCGTTGAGGT
		COR15_R	CAGCGCAAGAAGTCGTTGAT
AT4G02520	Glutathione S-transferase PHI 2, GSTF2	GSTF2_F	GAACCTGACCAAAAGGGTTGC
		GSTF2_R	ACCTCGACTTTGAGCTCGTT
AT3G49120	Peroxidase CB, PEROXIDASE 34, AtPERX34	PERX34_F	CAATCTGTCACTTTGGCAGGA
		PERX34_R	ATGCTTGTAAACTGTCTCTCCTT
AT1G02930	Glutathione S-transferase 6, GSTF6	GSTF6_F	TTTACCAAAGGGGTTGCGAA
		GSTF6_R	CTTCACGAGAAGAATGTCGACT
AT1G02920	Glutathione S-transferase 7, GSTF7	GSTF7_F	CAAGGGAGACAAGTTGGTT
		GSTF7_R	CAAGCTTTTCGAATCAAGAGCAA
AT5G16880	Target of Myb protein 1	MYB1_R	AGTGTCGTTGTTAAGTCATCCTGT
		MYB1_F	AGCATTGAACTTCTTTCCACGG
AT4G24190	HEAT SHOCK PROTEIN 90-7, HSP-90.7, SHD,	HSP90_F	ACACTCTCATCCTCTGGGTCA
		HS90_R	GTCCTCGAGATCAACCCACG
AT3G07390	AIR12, AUXIN-INDUCED IN ROOT CULTURES 12, auxin-response family protein	AIR12_F	TCACGACGGTTAAGGTTCCG
		AIR12_R	GGGACGACCGTTGGTAACAT
AT1G21750	PDI-like 1-1, PROTEIN DISULFIDE ISOMERASE5, PDI-5	PDI_F	TCGCTAAGCTAGATGCAACCG
		PDI_R	ATGGTCGGGAATCCCTTCAC

2.1.7 Western Blotting

2.1.7.1 Crude Protein Extraction Buffers Recipe:

50 mM Tris-HCl pH 7.8, 0.1% SDS, 1x Complete™ Protease Inhibitor Cocktail (PIC) (Roche, Burgess Hill, UK).

2.1.7.2 RIPA Protein Extraction Buffer:

50 mM HEPES-KOH pH 7.8, 100 mM KCl, 5 mM EDTA, 5 mM EGTA, 50 mM NaF,10% v/v glycerol, 1% v/v IGEPAL, 0.5% w/v deoxycholate, 0.1% w/v SDS, 1mM Na_4VO_3, 1 mM phenylmethylsulfonylfluoride, 1x proteinase inhibitor cocktail (Roche), 1x phosphostop (Roche) and 50 µM MG-132.

2.1.7.3 Western Blot Polyacrylamide Gels Preparation

12% polyacrylamide gels were made just prior to loading using the recipe in Table 2.7 and Mini-PROTEAN Tetra Cell Casting Module (Bio-Rad, Watford, UK). Alternately NU-PAGE® 4-12% Bis-Tris 10/12/24-well pre-cast protein gels were used (Thermo Fisher Scientific, Paisley, UK).

Table 2.7: Running and stacking gel recipe sufficient for preparation of two 12% gels.

Component	Running Gel 12% (10ml)	Stacking Gel (5ml)
Molecular Grade Water	3.3ml	3.4ml
Acrylamide/ Bis-acrylamide Solution (30%) 29:1 (Sigma Aldrich)	4.0 ml	0.83 ml
Tris (BioRad)	2.5 ml pH 8.8	0.63 ml pH 8.8
SDS (10%) (Sigma Aldrich)	100 µl	50 µl
APS (Thermo Fisher Scientific)	100 µl	50 µl
TEMED (BioRad)	4 µl	40 µl

2.1.7.6 Running Buffer

If using polyacrylamide gels prepared manually, gels were electrophoresed in fresh buffer. 1 X running buffer was prepared from Ultra-Pure 10X Tris/Glycine/SDS (TGS) stock (Geneflow, National Diagnostics, and Lichfield, UK). NuPAGE™ MOPS or MES SDS Running Buffer (20X) were used for pre-cast gels (Thermo Fisher Scientific).

2.1.7.5 Transfer Buffer

Molecular grade water 70%, 20% methanol and Tris-glycine (10X) 10 % (Geneflow, National Diagnostics, Lichfield, UK).

2.1.7.6 Western Blotting Buffers

2.1.7.6.1 Phosphate Buffered Saline (PBS)

1 PBS tablet (Thermo Fisher Scientific) per 100 ml molecular grade water stirred for 2 h at RT.

2.1.7.6.2 Tris buffered saline (TBS)

0.1576% (w/v) Tris-HCl (Fisher Scientific) and 1.461% NaCl (Fisher Scientific) in sterile distilled water and adjusting the pH to 7.6 using HCL.

2.1.7.6.3 PBS-tween (PBST) or TBS-Tween (TBST)

0.1% Tween-20 (w/v/) (Thermo Fisher Scientific).

2.1.7.6.4 PBST/TBST milk

For blocking and antibody preparation, 5% (w/v) Skim Milk (Tesco, Welwyn Garden City) was added to PBS-T/TBS-T and mixed for 5 min . Stock can be kept for 1 d at 4^{o}C.

2.1.7.7 Coomassie Brilliant Blue

2.1.7.7.1 Fixing solution

50% (v/v) methanol and 10% (v/v) glacial acetic acid and 40% (v/v) molecular grade water.

2.1.7.7.2 Staining solution

0.1 % (w/v) Coomassie Brilliant Blue R-250 (Sigma Aldrich), 50% (v/v) methanol, 10% (v/v) glacial acetic acid and 40% (v/v) molecular grade water.

2.1.7.7.3 De-staining solution

40% (v/v) methanol, 10% (v/v) glacial acetic acid and 50% (v/v) molecular grade water.

2.1.7.7.4 Storage solution

5% (v/v) glacial acetic acid and 95% molecular grade water.

2.1.7.8 Ponceau Stain

1% (v/v) glacial acetic acid, 0.11% (w/v) Ponceau S (Sigma Aldrich) and 98.89% molecular grade water. Ponceau stain was stored at room temperature in a 50 ml falcon tube wrapped in foil as the solution is light sensitive.

2.1.8 DNA Extraction

Crude DNA extracts for genotyping were carried out using a buffer containing 100 mM Tris-HCl, 250 mM KCl and 10 mM EDTA.

2.1.9 PCR Reaction Mixtures

2.1.9.1 cDNA Synthesis master mix A (X1)

On ice, master mix A was prepared just prior to use by mixing by pipetting 0.5 µl 50 µM Oligo $(dT)_{20}$ (Thermo Fisher Scientific) and 0.5 µl 10 mM dNTP (Thermo Fisher Scientific).

2.1.9.1.2 cDNA Synthesis master mix B (X1)

On ice, master mix A was prepared just prior to use by mixing by pipetting 2 µl Superscript VI buffer (x 5), 0.5 µl 0.1 mM dTT, 0.5 µl RNase OUT (40 U/µl), 0.5 µl Superscript III enzyme (200 U/µl).

2.1.9.3 qRT-PCR Standard master mix

SyBr Green Taq Polymerase (Qiagen) is light sensitive so prolonged exposure to light must be avoided and all components were prepared on ice. For each gene, qRT-PCR Master mixes were prepared just prior to use by mixing by pipetting 6 µl SensiFAST™ SYBR® Hi-ROX polymerase (BIO-92005, Bioline), 0.1 µl forward oligonucleotide primer, 0.1 µl reverse oligonucleotide primer and 0.8 µl molecular grade water.

2.1.9.4 PCR master mix components for *prt1-1* genotyping

On ice, (X1) PCR master mix was prepared by pipetting 10 µl high fidelity (HF) buffer (X5), 1 µl 10 mM dNTP, 28.5 µl molecular grade water, 2.5 µl prt1-1_F primer (section 2.1.7), 2.5 µl prt1-1_R primer and 0.5 µl Phusion Taq (2000 U/ml) (NEB).

2.1.9.5 PCR master mix components for *prt6-1* genotyping

On ice, (X1) PCR master mix was prepared by pipetting 0.5 µl 10mM dNTPS, 5 µl HF buffer (X5), 15 µl molecular grade water, 0.5 µl PRT61F primer (section 2.1.7), 0.5 µl PRT61R primer, 0.5 µl SAIL primer and 0.5 µl Phusion Taq (2000 U/ml).

2.1.10 Proteasome inhibitors

Proteasome inhibitor stock aliquots were prepared in by dissolving powder in dimethyl sulfoxide (DMSO) ≥99% (Sigma-Aldrich) and were stored in -20ºC. 30 µl aliquots of 100 mM (X2000) of Z-Leu-Leu-Leu-al/MG-132 (Sigma-Aldrich) and Bortezomib (Santa Cruz Biotechnologies, Texas, USA) were prepared and used at 50 µM working concentration. Freeze-thaw cycles were avoided to prevent inactivation.

2.1.11 Soil

2.1.11.1 Composition

For general growth of *Arabidopsis* plant material, crosses or seed collection, soil composition in Table 2.8 was used.

Table 2.8: standard soil composition

Component	Supplier	Grade	Amount (Parts)
Levington Pot & Bedding High Nutrient M3 compost	Scott's, Surrey, UK	N/A	4
Vermiculite	Sinclair, Lincoln, UK	Medium 2-5mm	2
Perlite	Sinclair, Lincoln, UK	Standard 2-5mm	1

2.1.11.2 Soil Mixtures

The standard soil mixture (section 2.1.11.1) was used in all experiment unless stated otherwise. For general plant growth, Levington Pot & Bedding High Nutrient M3 compost was used (Scott's, Surrey, UK). For low nitrate growth experiments, Levington's M3 soil was replaced with the lower nitrate containing Tray Substrat (Klassmann & Deilmann, Geeste, Germany). To further reduce the nitrate content of this mixture,

Tray Substrate was mixed 50% v/v with sharp sand (Tarmac, Wolverhampton, UK).

Table 2.9: pH and nutrient compositions of soil mixtures

Soil	pH	N (mg/L)	P (mg/L)	K (mg/L)
Levington Pot & Bedding High Nutrient M3	5.3-6.0	204	104	339
Levington Advance F2 Seed & Modular	5.3-6.0	144	73	239
Klasmann Deilmann Tray Substrate	6.0	180	130	240
Klasmann Deilmann Tray Substrate with Sharp Sand (50% V/V)	6.0	90	65	120

2.1.11.3 Growth Apparatus

For pathogenesis experiments, two 24-cell insert trays were placed in a 520 mm (W) 434 mm (D) gravel tray (Verve). These were filled with Levington Pot & Bedding High Nutrient M3 compost in the standard composition (section 2.1.11.1) excluding the perlite component. Trays were well watered before sowing seeds directly to the soil.

2.1.12 Preparation Hoyer's Solution

30g gum Arabic, 200g chloral hydrate and 20g glycerol were added to 50 ml sterile water and mixed well.

2.1.13 Reagent for histochemical assay of GUS reporter protein

For preparation of β-glucuronidase (GUS) reaction mix, 10% (v/v) 50 nM Potassium ferricyanide, 10% (v/v) 10 ml 50 nM Potassium ferrocyanide, 50% (v/v) sodium phosphate buffer, 0.2% (v/v) 0.5 M Sodium EDTA, 10%

(v/v) Triton X-100 and 17.8% (v/v) molecular grade water were mixed well in a foil wrapped falcon tube. X-Gluc (5-Bromo-4-Chloro-3-Indoyl-Beta-D-Glucuronide) was dissolved in N, N- Dimethylformamide at a concentration of 2.5% (w/v). The GUS reaction mix was combined with X-Gluc mix 352 μl: 48 μl. The solution can be stored at -20^{O}C.

2.1.14 Tandem Affinity Purification

2.1.14.1 TAP Extraction buffer (50-ml) 50-ml extraction buffer:

25 mM Tris-HCl pH 7.6, 15 mM $MgCl_2$, 5 mM EDTA, 150 mM NaCl, 15 mM p-nitrophenylphosphate, 60 mM β-glycerophosphate, 0.1% nondet P-40, 0.1 mM sodium vanadate, 1 mM sodium fluoride, 1mM DTT, 1mM PMSF, 10 μg/μl leupeptin, 10 μg/μl aprotinin, 1X PIC tablet and 1X PhosSTOP tablet. Mixed thoroughly by vortexing and kept at 4^{O}C.

2.1.14.2 IgG Sepharose Wash Buffer (50-ml, ice cold)

10mM Tris-HCl pH 8.0, 150 mM NaCl, 0.1% NP-40 and 5% ethylene glycol.

2.1.14.3 TEV Buffer (100-ml, ice cold)

10 mM Tris-HCl pH 8.0, 150 mM NaCl, 0.1% NP-40, 0.5 mM EDTA, 1 μM E64, 1 mM PMSF and 5% ethylene glycol.

2.1.14.4 Streptavidin Elution Buffer (5-ml, ice cold)

10mM Tris-HCl pH 8.0, 150 mM NaCl, 0.1% NP-40, 0.5 mM EDTA, 1 μM E64, 1 mM PMSF, 5% ethylene glycol and 20 mM DTT.

2.2 Methods

2.2.1 Growth conditions

Different experimental light conditions are described in Table 2.10. Growth cabinet refers to an enclosed room where plated plants were grown routinely, whereas growth room is a room in which plants on soil were grown routinely. Humidity readings and temperature readings were taken using a TinyTag Ultra 2 (Gemini Data Loggers UK LTD, Chichester, UK).

Table 2.10: Characteristics of growth cabinets and rooms.

Growth Condition	Day Length (hours)	Day Temp (^oC)	Night Temp (^oC)	Light Intensity ($\mu mol\ m^{-2}\ S^{-1}$)
Constant Light Growth Cabinet	24	22	N/A	60
Neutral Days Growth Room	12	23	18	120
Long Days Growth Room	15	21	15	100
Long Days Growth Cabinet	16	21	15	60
Short Days Growth Cabinet	9	20	15	60
Long Day Cabinet (Rothamsted Research)	16	23	18	
Heat Stress Cabinet (Rothamsted Research)	16	28	28	

2.2.2 Seed sterilisation

Seeds for surface sterilisation were aliquoted into a 1.5ml Eppendorf tube, prior to 1ml of 5% bleach (Parazone®, Jeyes, Cambridge, UK). Tubes were shaken for 5 min at a low speed (60 rpm) Seeds were then washed 4 times using sterile water with 5 min.

For larger batches of seed for sterilisation, the vapour-phase method was used. A desiccator jar was placed into a fume hood in which seeds to be sterilised in 2ml Eppendorf tubes was placed. The lids of the tubes were left open. A 250ml beaker containing 100ml of Parazone® bleach was placed in the desiccator jar and 3ml of concentrated HCl was added to this. The lid of the desiccator jar was immediately sealed. The chlorine gas produced in the reaction was used for seeds sterilisation between 4-16 hours, although 3-4 hours was usually sufficient for sterile seed while minimising the amount of seed killing. The desiccator lid was removed, and the chlorine gas left to dissipate for a period of at least 30 minutes.

2.2.3 Seed Plating

Seeds were plated directly onto the surface of agar media using Ultipipette tips (Barky instruments International, Folkestone, UK) mounted on a P20 Gilson pipette. Generally, seeds were sown individually on media 10mm from the outer plate edges with sufficient space left between seeds. Plates were sealed using 15mm wide microporous tape (3M, Neuss, Germany).

2.2.4 Cold pre-treatment of imbibed seeds

Plated seeds or 1.5ml Eppendorf tubes with seeds suspended in water were placed in a $4^{O}C$ refrigerator to break the dormancy on the seed. The period required to break this dormancy depends on the age of the seedling, however this was standardised as 3 days.

2.2.5 Grinding Plant Material

Tissue for DNA, RNA or protein extraction consisted of whole seedlings or leaf material ≤100 mg snap frozen in liquid nitrogen and ground into a fine powder using either a mortar and pestle, a tissue lyser or plastic mortars in a 1.5ml Eppendorf tube.

2.2.6 Crude DNA extraction for genotyping

Fresh plant leaf discs were collected in 1.5ml Eppendorf tubes containing 40µl of extraction buffer (100 mM Tris-HCl, 250 mM KCl and 10 mM EDTA). The plant material was disrupted using a pipette tip for 10 seconds and the tubes were heated for 10 minutes at 95^{o}C before placing directly on ice. 40µl of dilution buffer (250 mM KCl) was added, briefly vortexed and then the tubes were centrifuged for 30s at 13,000rpm. The supernatant was removed and stored at 4^{o}C. For high quality material, DNA was extracted from ground plant material (2.2.5) with a DNeasy® Plant Mini Kit from Qiagen®. DNA quality and yield were quantified with a NanoDrop 1000 spectrophotometer (Thermo Scientific).

2.2.7 RNA Extraction from Plant Material

RNA was extracted using a RNeasy Plant Kit (Qiagen) according to the manufacturer's protocol. RNA quality and yield were quantified with a NanoDrop 1000 spectrophotometer (Thermo Scientific).

2.2.8 Genotyping *Arabidopsis thaliana* lines

2.2.8.1 *prt1-1* genotyping using CAPS marker

The *prt1*-1 mutant was genotyped using Cleaved Amplification Polymorphism Sequence (CAPS) markers (Prof. Andreas Bachmair). Total DNA was extracted from leaf or seedlings material as described in 2.2.5. PCR master mix was made as described in section 2.1.9.4 and 45 µl of the master mix is mixed with 5 µl of the sample DNA. The PCR conditions are described in Table 2.11. The PCR products (1 µl) were restricted using a reaction containing 1µl CutSmart®, 5µl Mn1L (NEB)

and 18µl of molecular grade water. The reaction mixture was incubated for 1 hour at 37^{O}C, which restricts the wild type fragment to yield fragments of 141 and 39 bp. The *prt1-1* mutant remains undigested. This difference is visualised by electrophoresis in a 2% agarose gel.

Table 2.11: PCR conditions for *prt1-1* CAPS marker genotyping:

PCR Step	Temperature (^{o}C)	Time (s)	
Initial Denaturation	98	30	
Denaturation	98	10	30 Cycles
Annealing	58	30	
Extension	72	30	
Final Extension	72	600	
Hold	4	∞	

2.2.8.2 *prt6-1* genotyping using SAIL PCR primers

A crude extract was prepared from leaf or seedling material as described in 2.2.5. PCR master mix was made as described in section 2.1.9.5 and 22.5 µl of the master mix was combined with 2.5 µl of the sample DNA. For SALK or SAIL lines, wild type alleles are identified using the forward and reverse primers. Mutant alleles were identified using the SALK or SAIL T-DNA primers and the reverse primer. The PCR conditions are shown in Table 2.12. PCR products were separated by electrophoresis in a 2% agarose gel, with the band for Col-0 being ~600bp and *prt6-1* ~500bp. For genotyping the *prt1-1 prt6-1* double mutant, both the CAPS marker (2.2.8.1) and PRT6 SAIL primers were used to confirm the presence of both alleles in these plants.

Table 2.12: PCR conditions for *prt6-1* genotyping

PCR Step	Temperature (°C)	Time (s)	
Initial Denaturation	98	30	
Denaturation	98	20	25 Cycles
Annealing	56	30	
Extension	72	120	
Final Extension	72	600	
Hold	8	∞	

2.2.9 Histochemical assay of GUS reporter protein

Specimens to be stained were completely immersed in GUS working solution (2.1.13) for 12-16 hours at 37°C. Upon removal from the incubator, samples were de-stained using 70% EtOH at RT on an orbital shaker until the chlorophyll has been cleared (~4 h to overnight). Samples were then mounted on glass slides for imaging. For rapid permanent mounting of samples on microscope slides, specimens were mounted in Hoyer's solution (section 2.1.12) rather than water.

2.2.10 Quantification of germination and establishment

Half strength Murashige and Skoog agar plates were divided equally into four and 25 surface sterilised seeds per line sown into each quadrant for Col-0, *prt1-1* and the complementing line. This was repeated three times with the location of each quadrant changing per plate to avoid any potential media location bias. Plates were stratified at 4°C for 3 d and placed into constant light. Germination was quantified in two ways: as the rupturing of the testa and emergence of a radicle, as observed by close examination of the seed surface under a stereo microscope (Lecia MZ6) and scoring. Establishment was quantified as the appearance of two fully expanded cotyledons. These were scored at 24 h intervals at

the same time of day. Three separate biological replicates were conducted, and data pooled.

2.2.11 Fresh Weight Determination

Surface sterilised seeds were sown on 0.5 x MS media plates, stratified for 3 d before transferring to long days. After 5 days after germination, seedlings were transferred from plates to soil and placed in long day light condition for 7.5 weeks. Plants were harvested, the root and shoots separated, and excess soil and water removed from the plant before determining the fresh weight.

2.2.12 Soil Nitrate Experiments

Seeds were geminated on agar plates with MS salts at half strength for 7 Days in constant light (24 h 22^{O}C) before transferring to soil. A nutrient rich Levington's M3 compost was used as a control. Klasmann Deilmann Traysubstrat compost was chosen as it has a comparatively low nutrient and therefore nitrogen content compared to M3 soil (2.1.11). To further reduce the nitrogen content of the soil, a 50:50 by volume traysubstrat: sharp sand soil mixture was made.

For experiments investigating the impact of low nitrate soil content on seed set, the soil mixture consisted of 4 parts soil: 2 parts vermiculite: 1-part perlite, with the latter two components included for their water retentive properties. Four *prt1-1* and Col-0 plants were grown for 8 weeks on soil or just prior to silique dehiscence, whereby whole plants were harvested by inverting pots in glassine bags and cutting the stems at the base to ensure minimal seed loss. Harvested plant material was left for a week to allow seeds to dry and then seeds were harvested from the plants using a fine 335 μm mesh sieve.

The soil types used were the same as previous nitrate-soil experiments, but no vermiculite or perlite was included in the soil composition to enable easier removal of soil material. After 8 weeks, the pots were removed

from 4 of *prt1-1* and Col-0 plants, the excess soil removed and then the roots were carefully washed in warm water until the roots were free of soil. These were left for dry between paper towels for an hour or until excess water had been removed, imaged, the shoots and roots excised using a scalpel and then both aspects weighed individually.

2.2.13 *Pseudomonas syringae* DC3000 growth quantification.

2.2.13.1 Inoculation of *Arabidopsis* with *Pst* DC3000

Soil was prepared as 2.1.11 Plants to be inoculated with bacteria were sown directly to soil following cold pre-treatment (2.2.4) using Ultipipette tips (Barky instruments International, Folkestone, UK) mounted in a P20 pipette. Genotypes were sown in a random distribution to avoid treatment bias and plants were grown in neutral day growth conditions (2.2.1) until the 10-12 leaf stage (~3.5 weeks after sowing) (Figure 2.1). For systemic acquired resistance (SAR) assays ~32 DAG plants were used. During growth, a propagator lid with the vents fully closed was used to increase the humidity until germination. After the 4 Leaf stage the vents on the propagator lid were fully opened, and after 6 leaf stage the lid was slightly skewed to increase the air flow to the plants.

For bacterial inoculations, *Pseudomonas syringae* pv. *tomato* (*Pst*) DC3000 strains were grown overnight at 30^{O}C on King's B media (2.1.4) supplemented with appropriate selection (Table 2.13). Following overnight growth, bacteria was resuspended using autoclaved 10mM $MgCl_2$ and a sterile blue spreader. This bacterial resuspension was poured into a 50ml falcon tube, and the process repeated to resuspend more bacteria. The Falcon tube was topped up to 50ml using sterile $MgCl_2$ and the OD_{600nm} was determined using a spectrophotometer (usually ~1.5 to 2.0). The bacterial suspension was then diluted further with 10mM $MgCl_2$ to the appropriate bacterial inoculum concentration. Silwet (Round Ruck, Texas, USA) was added to the spray treatment bottles at 0.02% (v/v).

Figure 2.1: Showing the plant growth stage for plant treatments and the white arrows indicate the correct order leaves that should be injected and also taken for growth curved analysis in both the injection and spray treatment methodologies.

Table 2.13: showing the selection markers and inoculum concentrations for the different *Pst* DC3000 strains used.

***Pst* DC3000 Strain**	**Selection (mg/L)**	**Inoculum Concentration (OD_{600nm}/CFU ml^{-1})**	
		Direct Infiltration	**Spray**
Virulent	Rifampicin (50)	$0.001/10^6$	$0.1/10^8$
Avirulent *AvrRpm1*	Rifampicin (50), Tetracycline (10)	$0.1/10^8$	N/A
hrpA-	Rifampicin (50), Kanamycin (50)	$0.1/10^8$	N/A
SAR Avirulent	Rifampicin (50), Tetracycline (10)	$0.1/10^8$	N/A
SAR Virulent	Rifampicin (50)	$0.001/10^6$	N/A

Bacterial treatments were conducted ~4 hours post-light switch in neutral days light conditions. One-hour pre-infection, the plants were watered from the bottom and the propagator lid placed fully on the tray with all vents closed to increase the humidity and open stomata. Disposable 1-ml blunt syringes were used for direct infiltration of the plant leaves on their abaxial side. Injected leaves were selected as shown in Figure 2.1 and were marked with a dot for later identification. The abaxial side of the leaf was supported by the operator's thumb, the blunt syringe was pressed against the adaxial surface and the plunger was slowly pressed until the inoculant is observed in the apoplast either side of the central vein as shown in Figure 2.2. It is paramount that during injection plant leaves are not damaged, the plant rosette size is comparable between plants, leaves selected are in the same order and the amount of inoculant injected is similar between treatments. For spray treatment, the bacterial inoculum with Silwet was mixed in a spray bottle and sprayed directly on to the plant leaf surface ~1/2 m away from the tray. Forty minutes post direct injection, the propagator lids were replaced slightly skewed with the air vents fully open. This was done 1 day following infection by the spray treatment. For SAR assays, half the population of 32 DAG plants were pre-treated with avirulent *AvrRpm1* strain and 2 days post-infection (dpi) plants were re-infected with virulent *Pst* DC3000 (see Table 2.13).

2.2.13.2 Growth Curve Determination

4 dpi tissue was taken for bacterial growth determination analysis. King's B media plates with the appropriate selection markers were removed from the fridge to allow to reach room temperature before plating. One genotype at a time, the leaves injected or those marked pre-spray treatment were carefully removed from the plant and placed on blue towel briefly to reduce excess water and for imaging. The leaves were randomised according the severity of infection (i.e. a leaf displaying most severe symptoms was placed with a leaf with the least severe symptoms and another leaf with moderate symptoms) to reduce the noise in the data and give an accurate representation of the plant population. Leaf discs (⌀= 6mm) were taken using a single hole-punch (5 Star Easy Office Supplies, London, UK) from the infection site on the leaf and placed in a 2 ml safe-lock Eppendorf tube containing 500 µl 10 mM $MgCl_2$ and sterile 1mm glass beads (Assistent, Sondheim, Germany) on ice. Three discs from three leaves of the same line were placed in each tube and samples were homogenised for 15 seconds at 4.0 m/s using FastPrep-24™ 5G (MP Biomedicals, UK). These were placed back on ice.

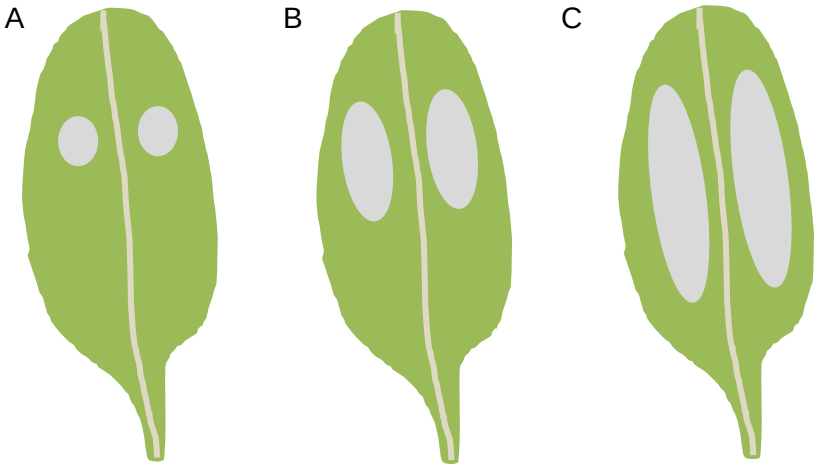

Figure 2.2: Showing the bacterial inoculant inside Arabidopsis leaf apoplast following direct infiltration with a blunt syringe: (A) too little inoculant injected, (B) ideal amount of inoculant injected and (C) too much inoculant

Under sterile conditions, six 3mm glass beads (Assistent) were placed onto each King's B media plate. 100 µl of the crude extract was serially diluted 1:10 in $MgCl_2$ according to the bacteria strain used (Table 2.14). 100 µl of these final dilutions was pipetted onto the surface of the corresponding plate and the plates agitated to spread the bacteria evenly across the plate. The lids were removed from plates to allow the surface to air dry (~5 minutes). Once dry, the glass beads were removed from the plate surface, plates were stacked with lids down and placed in a 28^{o}C incubator. This was repeated with the other lines as quickly as possible.

Table 2.14: The dilution factor used for plate-based quantification of different *Pseudomonas syringae* infection assays

***Pst* DC3000 Strain**	**Infection Mode**	**Quantification Dilution Factor**
Virulent	Direct Infiltration	-4 & - 5
	Spray	-5 & -6
Avirulent *AvrRpm1*	Direct Infiltration	-2 & -3
hrpA-	Direct Infiltration	-3 & -4
SAR Virulent Control	Direct Infiltration	-4 & -5
SAR Pre-treated	Direct Infiltration	-3 & -4

2.2.13.3 Quantification of Bacterial Growth

Bacterial counts were taken at 24 h, 48 h and 72 h time points after growth in the incubator and the bacterial load inside each sample (3 combined leaf discs) calculated according the equation below:

$$\text{Bacterial Load} = \log\left(\frac{\left(\frac{\left(5 \times \left(10^{-\text{Dilution Factor}}\right)\right)}{3}\right) \times \text{Bacterial Count}}{0.2827}\right)$$

The bacterial load per genotype was determined by taking the sum bacterial load and dividing by the sample number. The standard error of the mean was determined and used for graphical representation and statistics.

2.2.14 Western Blotting:

2.2.14.1 Gel Preparation:

All components listed in section 2.1.7.3 were combined in a 50 ml falcon tube without ammonium persulfate (APS) and tetramethylethylenediamine (TEMED). Mini-PROTEAN® Tetra Cell Casting Modules (BioRad) were set up according to the manufacturer's instructons. APS and TEMED were added to the running gel falcon, shaken to mix and quickly pipetted between the glass plates (~3.5ml). 1 ml of butanol was added on top of the running gel. Running gel was polymerised for 20 minutes. Butanol was removed, washed with molecular grade water and dried using filter paper. APS and TEMED were added to the stacking gel falcon tube and mixed before pipetting on top of the running gel. A comb (10-well/15-well, 1.0mm) was placed into the stacking and the stacking gel was polymerised for 20 minutes. Gels were washed briefly with molecular water and can be stored for up to one week at 4^{o}C.

2.2.14.2 Protein Extraction:

Plant material was snap frozen in liquid nitrogen and ground into a fine powder by disposable polypropylene pellet pestle (DWK Life Sciences) in a microcentrifuge tube, manually grinding with liquid nitrogen using a mortar and pestle or homogenising for 2X 30 seconds at 4.0m/s using FastPrep-24TM 5G (MP Biomedicals, UK). 120µl of appropriate extraction buffer was applied to homogenised tissues and incubated on ice for 30 minutes with occasional vortexing. Lysate was centrifuged for 15 min at 13,000rpm at 4^{O}C and the supernatant was placed in a new pre-chilled 1.5ml Eppendorf tube. This step was repeated to ensure minimal tissue debris is carried forward. Protein concentrations were

determined by Bradford assay according to the manufacturer's instructions (BioRad) reagent in triplicate. Proteins were diluted to appropriate concentrations using extraction buffer.

2.2.14.3 Running Gels

2.2.14.3.1 Pre-cast gels

Gels were placed into the gel tank with fresh running buffer and the wells washed carefully. Samples were loaded into the gel with an appropriate protein ladder used for reference. Gels were typically run for 1.5 hours at 120V or until the gel front had run off the gel. Upon completion, the casing of the gel was opened, the wells and bottom of the gel carefully removed before placing the gel in distilled water.

2.2.14.3.2 Manually Cast Gels

Running buffer (2.1.7.6) was prepared prior to use. Manually cast gels were then placed into the electrophoresis module and a Mini-PROTEAN Tetra cell tank (BioRad). Samples were loaded into the gel with an appropriate protein ladder used for reference. Gels were typically run for 10 min at 80V before 1.5 - 2 hours at 120V or until the gel front had run off the gel. Upon completion, the glass plates were separated, and the wells of the gel carefully removed before placing the gel in distilled water.

2.2.14.4 Coomassie Staining

2.2.14.4.1 Commercial Coomassie-based staining

Following electrophoresis, the gel was placed in a clean tray and washed three times (5 min) with ultrapure water. Imperial™ Protein Stain (Thermo Fisher Scientific), InstantBlue® (Expedeon) or SimplyBlue™ SafeStain (Invitrogen) was prepared immediately before use by inverting the bottle several times. The water was removed from the gel before pouring enough stain on so as to completely cover the gel and placing on a shaker for ~1 hour or until desired staining was achieved. The staining reagent was discarded and replaced with 200ml ultrapure water to reduce the background. This was repeated until the desired signal to

background ratio had been achieved, and then the gel was imaged using a Calibrated Imaging densiometer (BioRad, GS-800).

2.2.14.4.2 Coomassie Brilliant Blue

Following electrophoresis, the gel was placed in a clean tray and washed three times (5 min) with ultrapure water. The gel was then fixed in fixing solution (2.1.7.7.1) for 1 hr to overnight with gentle shaking. This solution was changed once at hour 1. The gel was stained for 20 min in staining solution (2.1.7.7.2) with gentle agitation at room temperature. The gel was then de-stained using de-staining solution (2.1.7.7.3) until the desired signal to background ratio had been achieved, and then the gel was imaged. The gel was then stored in storage solution (2.1.7.7.4) for future reference.

2.2.14.5 Blotting

2.2.14.5.1 Wet transfer

Transfer Buffer (2.1.7.5) was prepared just prior to use. Gels were equilibrated in transfer buffer and transferred to PVDF membrane (activated for 1 min in 100% methanol). The blot cassette was prepared according to manufacturer's instructions and placed in the Mini Trans-Blot® module (BioRad) with transfer buffer. Proteins were transferred for 2 hours at 80V minimum. When the run was completed, the sandwich was disassembled, and membrane is removed immediately then placed into deionised water/PBST/TBST.

2.2.14.5.2 iBlot® 7-Minute Blotting System

The iBlot system was set up according to manufacturer's instructions with protein gel and membrane. The setting P3 was typically used (7 min transfer). When the run was completed, the sandwich was disassembled, and membrane is removed immediately then placed into ultrapure water, PBST or TBST.

2.2.14.6 Ponceau staining

Following blotting but before blocking, the PVDF membrane was placed in a clean tray and washed three times (5 min) with ultrapure water before the membrane immerse the blotted membrane in a sufficient amount of Ponceau S staining solution (2.1.8.8) and incubated with shaking for 5 minutes. The membrane is then immersed in an aqueous solution containing 5% acetic acid (v/v) for 1 minute to remove the background. This step was repeated until the desired contrast between the bands and the background was achieved and imaged. The membrane was washed until the stain is removed completely, washed twice with ultrapure water and blocking of the membrane was completed.

2.2.15 Tandem Affinity Purification

2.2.15.1 Material preparation

Seeds (Col-0, *prt1-1* and MO14-7-1, the TAP tag line) were plated at high density on 0.5 x MS medium overlaid with sterile mesh. Seeds were stratified for 2 d at 4 °C for in the dark before being transferred to a constant light growth chamber at 21 °C for 8 d. A preliminary expression analysis of the TAP fusion protein was conducted prior to carrying out affinity purification. Bortezomib (50 µM) was spotted onto seedlings which were then incubated at room temperature for 8 h. Untreated plates were also harvested. Material was harvested from plates by dissecting the roots and shoots using a sharp razor blade, and snap freezing in liquid nitrogen. Snap-frozen root and shoot samples were ground into a fine powder using a SPEX SamplePrep 2010 Geno/Grinder® (Stanmore, UK).

2.2.15.2 Protein Extraction

TAP extraction buffer (2.1.14.1) was applied to homogenised tissues and incubated on ice for 30 min with occasional vortexing. All reagents in protein extraction and TAP were precooled and steps were performed at 4°C to minimise protein degradation, and to minimise protein interference, a clean and dust-free environment was maintained

throughout the procedure. Lysate was clarified twice by centrifugation for 15 min at 13,000 rpm. Samples were heated to 70ºC in 1 X LDS (NuPAGE, Invitrogen) with 100 mM DTT. 10 µl PageRuler Plus and 20 µl of sample were loaded on 5-12% Bis-tris gel (Invitrogen). The gel was run for 3 h at 80V in 1 X MES (NuPAGE, Invitrogen) buffer before transferring to membrane using iBlot system (Invitrogen) on programme 3.

Following transfer, the PVDF membrane was blocked in 5% TBST milk for at least 1 h and then incubated overnight at 4^{O}C with 1º antibody in 5% TBST milk with 1:300 mouse anti-SBP antibody (Santa Cruz Biotechnology). The membrane was washed 3 times in TBST and twice in molecular grade water. The membrane was incubated for 2 hours at room temperature with 1:10000 goat anti-mouse IgG 2º antibody in 5% TBST milk (Santa Cruz Biotechnology).

The membrane was washed as previous and bound antibody visualised using ECL WestFemto substrate (Thermofisher). Following confirmation of TAP tag presence in the MO14-7-1 seedlings, more material was prepared (15 plates) as previously described with bortezomib treatment and whole seedlings were harvested in liquid nitrogen. Total protein extract was prepared as described previously using 50 ml ice-cold TAP extraction buffer, 0.1% Benzonase® was added and incubated for 2 min on ice. The mixture was transferred to precooled Ultra High-Performance 50-ml centrifugation tubes (VWR), and incubated for 30 min at 4 °C on a tube rotator prior to centrifugation the tubes at 36,900 g for 20 min at 4 °C. The supernatants were carefully isolated, and centrifugation repeated. The supernatant was then filtered through a 0.45µm Minisart filters (Satorius, Epsom, UK). 100 µl of protein extract was set aside for western blot analysis, labelled as “input”, combined with 5X SDS buffer prior to heating to 95^{O}C and stored at -20 ^{O}C. The remaining protein extracts were pooled.

2.2.15.3 IgG- and streptavidin-based affinity purification

IgG Sepharose® (GE Healthcare) beads were prepared in Lo-bind 2-ml tubes by washing three times in buffer 2.1.14.2 whilst Ultra High-Performance 50 ml centrifugation tubes were pre-cooled. After the final wash, 125 μl of IgG-Sepharose beads was pipetted into each of the input samples, placed into a rotator at 4^{O}C for 1 hour. The base of Poly-Prep column was removed and attached to a peristatic pump. The sample was transferred to the column and drawn through the column at a rate of 1 ml/min. 100 μl of sample that passed through the column was taken, labelled as “flow through”, combined with 5X SDS buffer prior to heating to 95^{O}C and stored at -20 ^{O}C. The column was washed once with IgG Sepharose Wash Buffer and twice with Tobacco Etch Virus (TEV) Buffer (2.1.14.3). 100 μl of each of these washes was taken for later analysis to monitor the purification. With ~1ml of the final wash buffer remaining in the column, the column cap was replaced and using a cut 200 μl pipette tip, the beads were transferred to lo bind 2ml Eppendorf tubes. 1 ml of TEV buffer and 400 μl of TEV protease were added to the tube, which was incubated at room temperature on a tube rotator. After 30 min, a second aliquot (200 μl) of TEV protease was added and the reaction was incubated for a further 30 min. 500 μl of the sample was loaded step-wise into a spin column and centrifuged at 8,000 rpm until all the liquid as passed through. The column was transferred to a Lo Bind Eppendorf tube and washed twice with 250 μl TEV buffer (20 μl of each of these washes is taken for testing called “TEV flow through”) and the eluates were combined.

Streptavidin beads were prepared by washing three times with 1ml streptavidin wash buffer. 125 μl equilibrated streptavidin beads were incubated with the combined eluates for 1 hour at 4^{o}C on tube rotor. These samples were loaded onto a new spin column with Lo Bind tube and spun down in a pre-chilled centrifuge. All the sample was passed through the column, the flow-through fractions were combined and labelled as “TEV eluate” which contains the proteins that weakly interact

with the bait protein. A 20 µl sample was taken and combined with 5X SDS buffer then heated to 90^{O}C for 10 min prior to storage for later testing. The columns were washed three times with 500 µl TEV buffer and samples taken for later testing. Columns were eluted using wash buffer + DTT (5 x 200 µl), and eluates were combined to yield "streptavidin Elute" which contain the proteins that strongly interact with the bait protein (a 20 µl sample was taken for testing). The beads remaining the column were boiled with 5X SDS for 10 min and a 20µl sample was taken called "streptavidin beads".

TEV and Streptavidin eluted proteins were precipitated overnight on ice using 25% v/v trichloroacetic acid (TCA). Proteins were centrifuged at 20,800 g for 15 min at 4^{o}C and the supernatant carefully removed. The pellets were washed twice in ice cold HCl/acetone by centrifugation and the supernatant was carefully removed the supernatant. The pellet was allowed to air dry whilst on ice and stored in -80^{o}C.

2.2.15.4 Protein quality control checking

The protein samples taken throughout the TAP procedure were thawed and heated to 70^{O}C before separation on 4-12% gradient Bis-Tris Gel in MOPS buffer for 3.5 h at 80 V. An anti-SBP Western blot with Coomassie and Ponceau stained as described in section 2.2.14 was conducted to monitor the TAP tag throughout the experiment.

2.2.15.5 In-gel digestion

Protein pellets for "TEV eluate" and "streptavidin eluate" were dissolved with 5X LDS + DTT and heated to 70 °C for 10 min. Samples were loaded onto precast 4–12% Bis-Tris gel run in MOPS buffer at 40 V for 10 min and 120 V for 60 min. Proteins were visualised by Pierce® Silver staining (Thermo Scientific) and a gel image taken for documentation. Lines were superimposed for excising gel pieces, and the gel was transferred to a glass plate and a broad protein zone per lane were excised with a fresh scalpel and put into LoBind tubes 600 µl of HPLC-grade water. Gel plugs

were washed twice with 600 µl of HPLC-grade water, water removed, and gel plugs dehydrated the in 600 µl of 95% (v/v) acetonitrile for 10 min. Acetonitrile solution was removed and rehydrated in 600 µl of HPLC-grade water with shaking for 10 min. The dehydration step was repeated, and the acetonitrile solution was removed, and tube transferred to ice. 90 µl of trypsin digest buffer was added, ensuring full plug coverage and incubated for 30 min at 4 °C to allow the gel plugs to rehydrate. Then the mixture was incubated for 3.5 h at 37 °C to digest the proteins. Samples were sonicated for 5 min. The solution covering the gel plugs, which contains the peptides, was transferred to a LoBind tube. 300 µl of 95% (vol/vol) acetonitrile was added to the gel plugs, which were agitated for 10 min until the plugs were completely dehydrated and had a white appearance. This acetonitrile solution was combined with the solution containing the peptides. A needle was used to punch a hole in the cap containing the trypsin digest of the 1.5-ml tube and placed in a SpeedVac (Eppendorf) to completely dry the trypsin digest (~2–3 h).

2.2.16 Leaf Proteome Preparation and Tandem Mass Tag™ (TMT) Labelling

2.2.16.1 Protein extraction:

Proteins were extracted from the three leaves described in Figure 2.1 at 4 hours after lights on for Col-0 and *prt1-1* plants. The buffer containing 8M urea, pH 8.5 50mM triethylammonium bicarbonate (TEAB), 1X Complete Mini Protease Inhibitor Cocktail (Roche), 1X PhosSTOP Inhibitor Cocktail (Roche) and 100µM MG-132 (Sigma-Aldrich) on ice for 30 min. Lysate was centrifuged for 15 min at 13,000rpm at 4^{O}C and the supernatant was placed in a new pre-chilled 1.5ml Eppendorf tube. This step was repeated to ensure minimal tissue debris is carried forward.

2.2.16.2 Protein Preparation:

Protein concentrations were determined by Bradford's reagent in duplicate and input aliquots (250 µg in 100 µl) were reduced with 5 µL 200 mM Tris [2-carboxylethyl] phosphine (TCEP) in 50 mM TEAB to final

concentration 10 mM at 55^{O}C for 1 hour, alkylated with 5 µL 375 mM iodoacetamide (IAA) to final 17 mM for 30 minutes in the darkness at RT and then diluted to total volume 800 µl 50 mM TEAB to dilute the final urea concentration below 1 M.

Proteins were precipitated by methanol/chloroform method in a 15ml falcon tube. To the 800µl sample, 4 volumes of methanol were added (3.2ml) and vortexed for 10seconds, 2 volumes of chloroform were added (1.6 ml) and vortexed for 10seconds, 3 volumes of sterile molecular grade water were added (2.4ml) and vortexed for 10seconds. Tubes were centrifuged at 4,700 rpm for 10 min and the supernatant was removed using a vacuum pump ensuring the pellet remains undisturbed. The pellet was washed by adding 3 volumes of methanol (2.4ml), centrifuging at 4,700rpm and the supernatant removed. This was repeated, and the samples were transferred to Eppendorf tubes and washed again and centrifuged at 5000 g for 10 min at RT. Precipitated protein pellets were air dried at room temperature (ensuring over drying of the pellet did not occur).

Pellets were resuspended in 100µl 50mM TEAB and a 10µl aliquot was taken for analysis, with the 100µl total volume restored by addition of 10µl 50mM TEAB. Samples were digested with 2µg trypsin (T8658-1VL, from bovine pancreas, Sigma-Aldrich) at 37^{o}C for 700 rpm for 4 hours (Thermomixer Comfort, 5355 000.011, Eppendorf). An additional 2µg trypsin was added and reaction incubated overnight. After trypsin digestion, to the sample aliquots of pre- and post-trypsin digestion, 2.5µl 4 X LDS Sample Buffer (NP0008, NuPAGE^{TM}, ThermoFisher Scientific) and 100mM Dithiothreitol (DTT) was added. Samples were heated at 70^{o}C for 10 min. 10 µl was loaded on to NuPage 4-12% Bis-Tris Gel (WG1403BOX, ThermoFisher Scientific) with 5µl PageRuler™ Plus Prestained Protein Ladder for reference (26619, ThermoFisher Scientific). Gels were run in NuPAGE™ MOPS SDS Running Buffer (NP0001, ThermoFisher Scientific) at 80V for 10 min followed by 150V for 75 min. Gels were removed from casing, washed briefly in di-H20 and

stained for 30 min in InstantBlue™ Protein Gel Stain (ISB1L, Expedeon). Gels were destained using di-H20 for 1 hour and imaged.

2.2.16.3 Protein Labelling with TMT reagents

Following quality control protein gel analysis, peptide concentration was determined using a Pierce™ Quantitative Colorimetric Peptide Assay kit (23275, Thermo Scientific to ensure equal peptide labelling per sample. 75µl 100µg peptide aliquots were labelled using TMT10plex™ Isobaric Label Regent Set (90110, Thermo Scientific). 5 biological replicates were performed: Col-0 was labelled with TMT10 -126, -127N, -127C, -128N, -128C and *prt1-1* was labelled with -129 N, -129C, -130N, -130C, -131. The labelling reaction was incubated for 1 h at RT with 350 rpm shaking and quenched using 8 µl 5% hydroxylamine prior to storage in -80^{o}C. 100 µl of from each TMT^{10} vial was combined, vortexed thoroughly, aliquoted into 1 X 40 µl (~36µg) and 10µl (~9µg) labelling test samples and 2 X 450 µl experiment aliquots were taken. These were dried down (Concentrator plus, 5305000.304, Eppendorf) and stored -80^{o}C before sending for MS analysis at the Cambridge Centre for Proteomics.

2.2.17 Statistical Analysis

Statistical analysis completed in this thesis was done so using mainly mean, standard deviation (STD) and standard error of the mean (SEM) functions in Microsoft excel or Prism 7 with statistical tests such as T-tests, one-way and two-way ANOVA analyses with post-hoc Tukey's or Sidak's multiple comparison tests building on these basic calculations.

n = sample size
x = sample values

(1) Mean

$$\bar{x} = \frac{\sum x}{n}$$

(2) Standard Deviation

$$\sigma = \sqrt{\frac{\sum (x - \bar{x})^2}{n - 1}}$$

(3) Standard Error of the Mean

$$SE = \frac{\sigma}{\sqrt{n}}$$

Chapter 3: Localisation and activity of PRT1

3.1 Introduction

The objectives of this chapter were to identify in which organs and tissues *PRT1* is expressed and to identify where the PRT1 protein is expressed and active at tissue, cellular and subcellular levels. These are important first steps to understanding more about the role of PRT1 in the whole plant context. Knowledge of where the E3 ligase is located and active provides potentially useful clues to the physiological function(s) it fulfils and informs future approaches for the identification of substrates.

3.2 Publicly available expression data

The electronic Fluorescent Pictograph (eFP) browser allows interpretation and visualisation of gene expression from large-scale publicly available microarray datasets. It is an informative tool to begin investigating gene expression patterns and was used as a starting point in this study. As the Plant eFP viewer enables the gene expression levels from multiple experiments to be visualised, different scales are observed between experimental views due to the experimental parameters therefore each experiment should be viewed in isolation. Consequently, expression is interpreted according to local max linear expression colour scales for each experiment, with high expression being manifest as a red colour and yellow indicating low expression. The AtGenExpress eFP (Schmidt *et al*., 2005; Nayabayashi *et al.,* 2005) and Klepikova eFP (Klepikova *et al*., 2016) browsers indicate that *PRT1* expression is expressed ubiquitously, although the expression level varies between tissues and throughout development (Figure 3.1). *PRT1* is highly expressed in stage 8-10 seeds, dry seeds and mature pollen. Following the transition from vegetative rosettes to flowering, absolute expression of *PRT1* falls. Tissue-specific eFP browsers (Figure 3.2) indicate that the absolute expression of *PRT1* is high in trichomes, stomata, stems, stigma, ovaries, shoot apical meristems, as well as in developing embryos, gametogenesis and pollen tube growth (Marks *et al*., 2009;

Yang *et al*., 2008; Casson *et al*., 2005; Suh *et al*., 2005; Honys & Twell, 2004; Swanson *et al*., 2005; Tian *et al*., 2014; Qian *et al.*, 2009; Yadav *et al*., 2009). However, given these are based on global micro-array and RNAseq transcript profiling experiments not intended specifically to investigate the localisation of PRT1, the results should be used tentatively. Nonetheless, they provide interesting avenues for localisation studies.

A

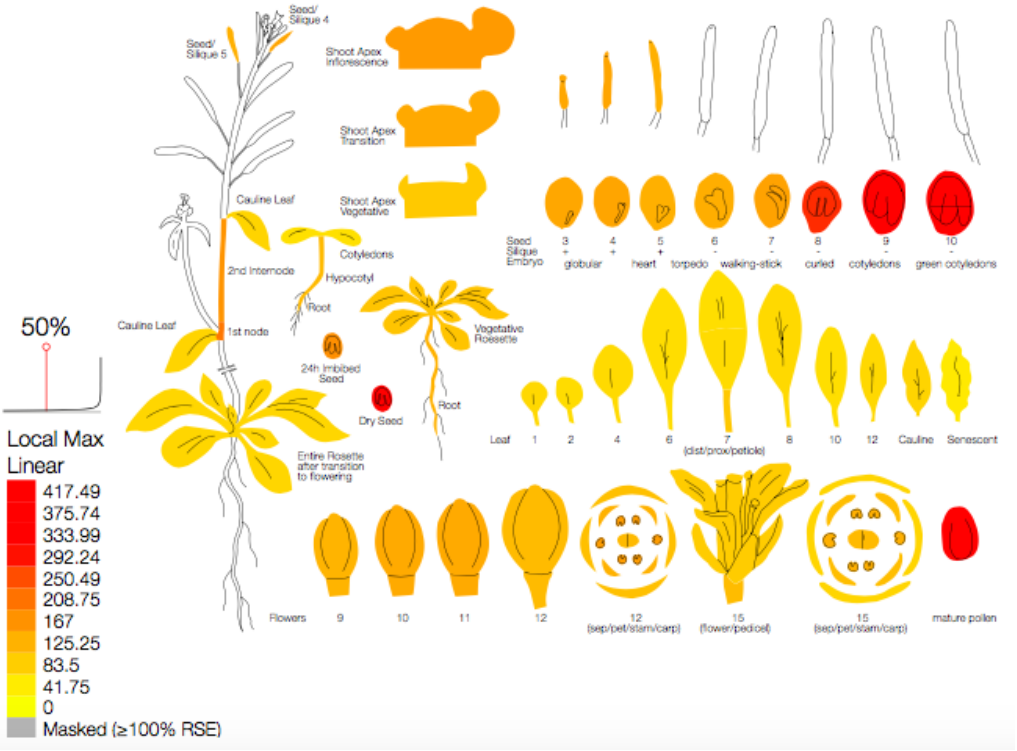

B

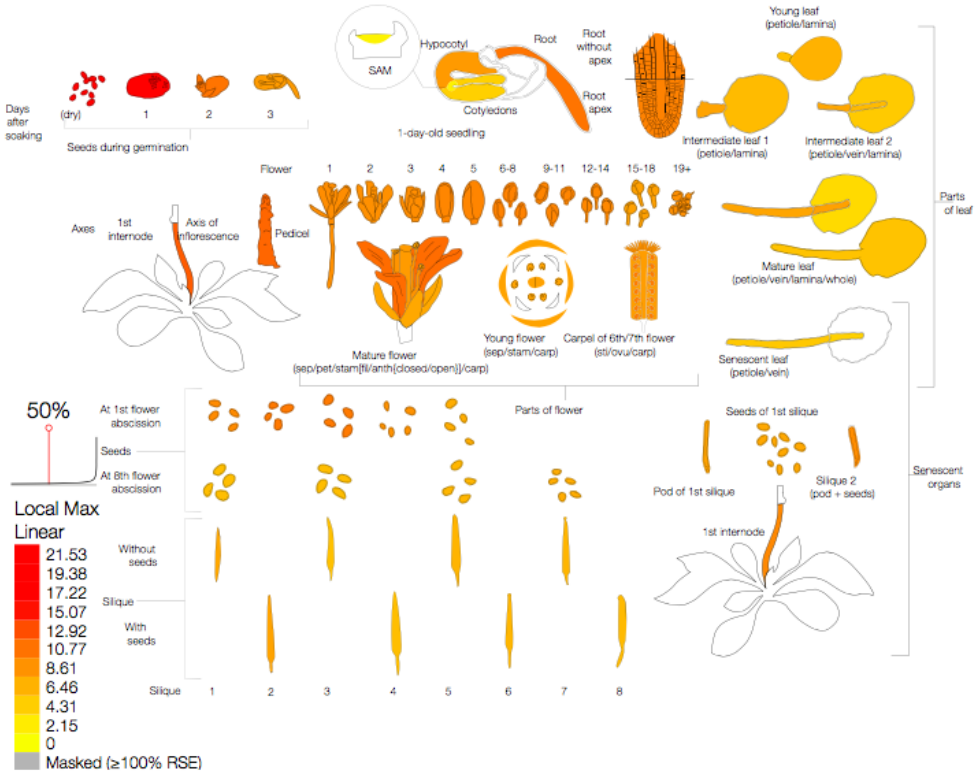

Figure 3.1: Expression of *PRT1* in public transcriptome datasets. Images adapted from the (A) AtGenExpress eFP (Schmidt *et al*., 2005; Nayabayashi *et al.,* 2005) and (B) Klepikova eFP (Klepikova *et al*. 2016), showing absolute Log2 quantification from gene expression of *PRT1* (At3g24800) (https://bar.toronto.ca/eplant/; accessed August 2018).

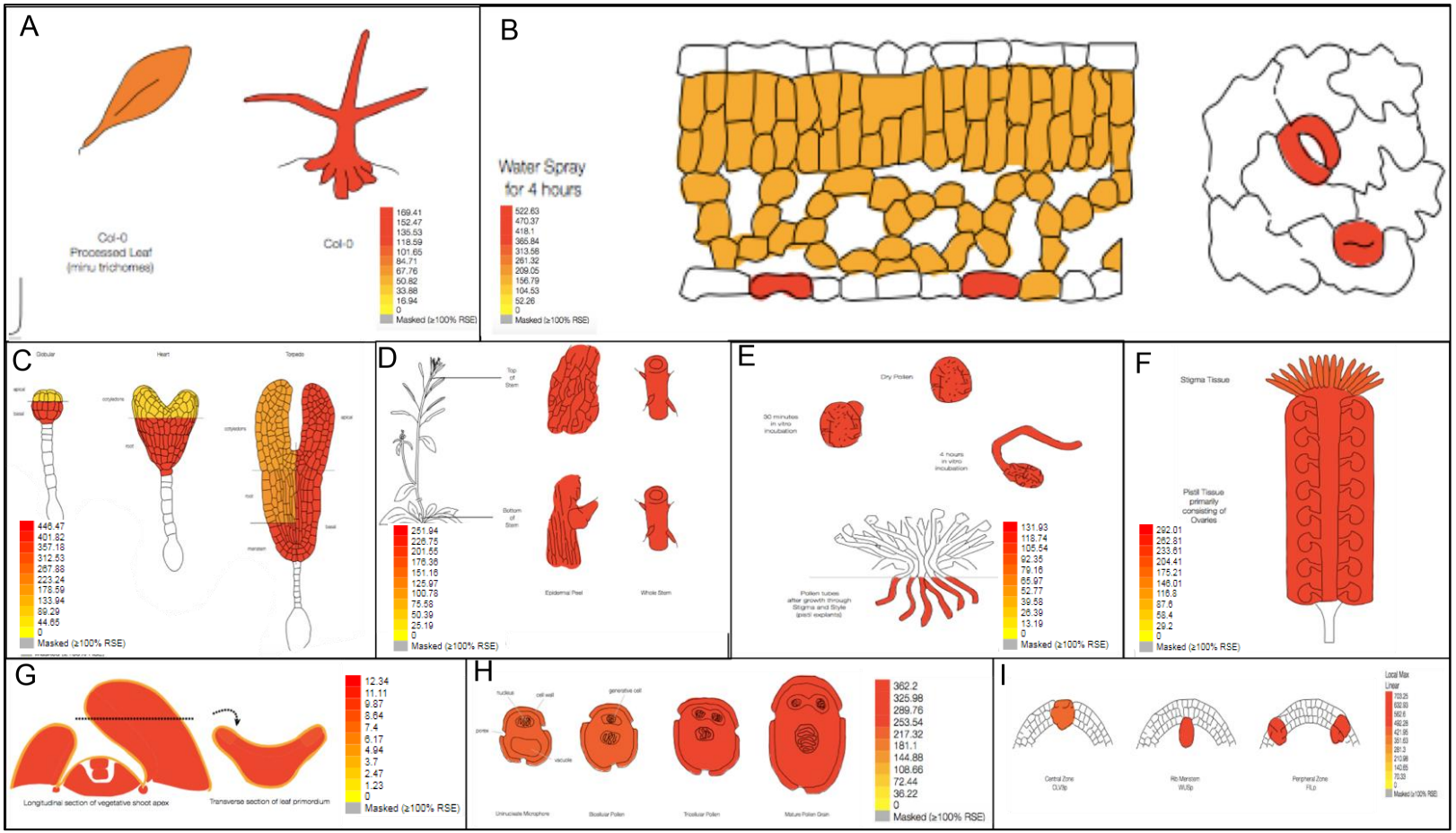

Figure 3.2: Expression of *PRT1* in public tissue specific transcriptome datasets. Images adapted from tissue specific browsers at ePlant showing *PRT1* (At3g24800) expression: (A) trichomes, (B) stomata and leaf mesophyll, (C) developing embryos, (D) stem, (E) pollen germination, (F) stigma and ovaries, (G) shoot apex, (H) micro gametogenesis, and (I) shoot apical meristem. (https://bar.toronto.ca/eplant/; accessed August 2018).

3.3 Analysis of *PRT1* promoter activity

To complement the information obtained from eFP browsers, a promoter-reporter line was developed to identify tissues in which the PRT1 promoter is active, and to determine how environmental cues influence the activity of the promoter. *prt1-1* plants were transformed with a construct containing the 1.1 kbp of genomic DNA upstream of the *PRT1* ATG start codon fused to GFP bearing a nuclear localisation signal and GUS (Dr Maria Oszvald and Dr Hongtao Zhang, Rothamsted Research, unpublished data). A schematic representing the GUS-GFP promoter reporter construct (MO15) is shown in Figure 3.3 (described in more detail in Chapter 2.1). T2 lines were obtained from Dr Zhang and made homozygous during this study through selection on kanamycin.

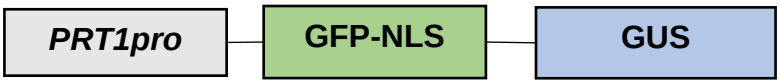

Figure 3.3: Schematic of the promoter-reporter cassette (MO15). Construct inserted into the *prt1-1* mutant background to complement the mutation which featuring GUS- and nuclear localised GFP -tagged endogenous PRT1 promoter for investigating *PRT1* promoter localisation.

Preliminary experiments by Maria Oszvald indicated that it was difficult to detect *PRT1* promoter activity under unstressed conditions. In contrast, a *PRT6* promoter-reporter construct using the same vector gave a positive signal, indicating that there were no fundamental problems with the vector backbone or reporter cassette (Hongtao Zhang, personal communication.). However, *PRT1* promoter activity was observed by Maria Oszvald in T2 lines following a combination of a cold and dark treatments of MO15 plants, which provided a starting point for studying the *PRT1* promoter. Therefore, 4 DAG seedlings were subjected to different combinations of dark/light treatment in tandem with cold stimulus to observe if the *PRT1* promoter could be observed by GUS staining (Figure 3.4). For all the conditions tested, GUS staining could not be observed in cotyledons, roots and around the shoot apical

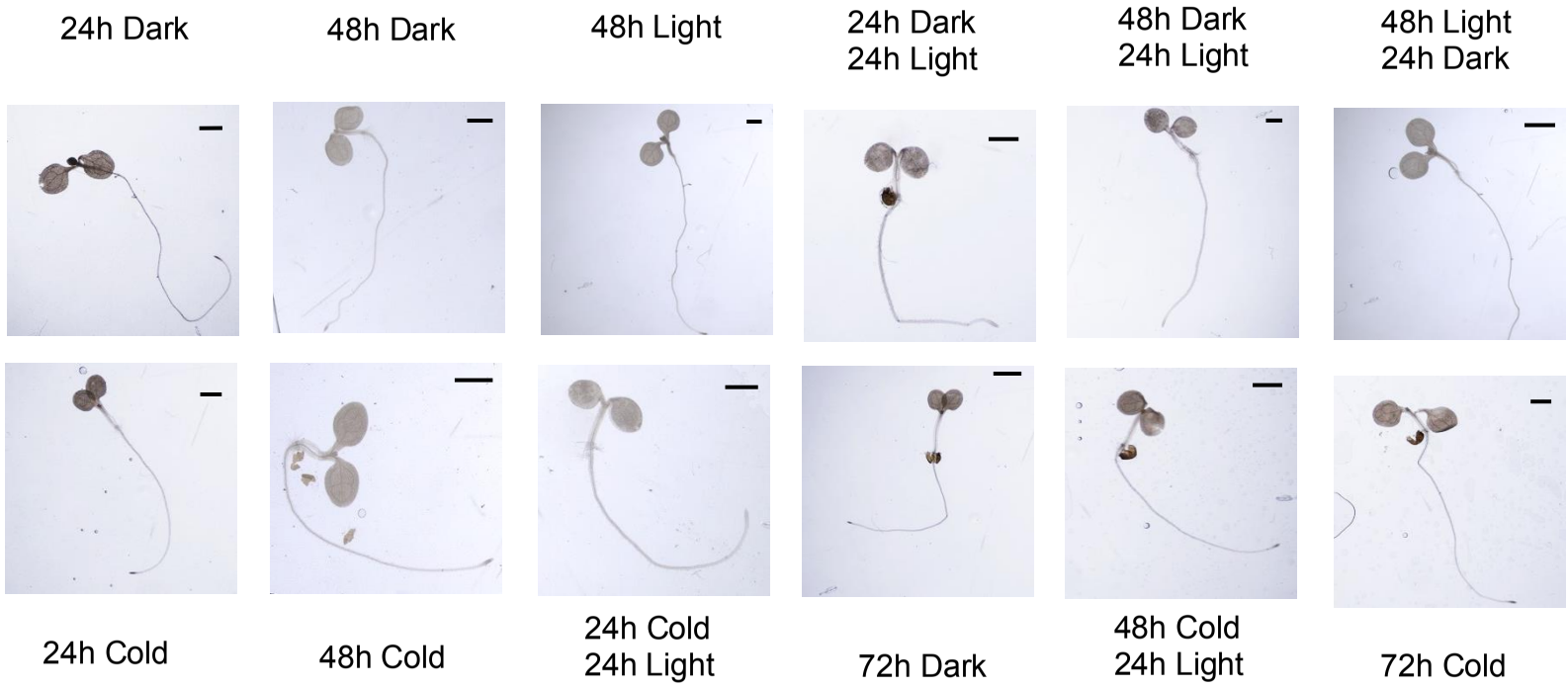

Figure 3.4: Histochemical assay of promoter GUS constructs in seedlings grown in different cold, light and dark regimes. GUS stained seedlings bearing promoter reporter constructs for the observation of PRT1 promoter activity in response to different combinations of light and cold stress. Scale bars = 1 mm.

meristems, suggesting these conditions are not sufficient to induce the *PRT1* promoter for plants at this developmental stage. As a result the expression of the PRT1 promoter as reported in the eFP browser could not be investigated and compared. This aspect of the project was not pursued as other genetic tools such as TAP tag lines were prioritised to study the PRT1 protein.

3.4 Development and use of tagged PRT1 complementation lines

Prior to this study, transgenic lines expressing tagged versions of PRT1 in the *prt1-1* background were developed in the Theodoulou laboratory, in order to study tissue and subcellular localisation and to enable affinity purification of PRT1 and potential interacting proteins. To date, no *prt1* loss of function alleles have been identified in public collections of T-DNA insertion lines, therefore it was also important to develop complementation lines to confirm that any phenotypes identified for *prt1-1* plants were associated with loss of PRT1 function.

3.4.1 Immunological detection of TAP-tagged PRT1

The genetically encoded fusion of tags such as peptides or protein domains to proteins of interest is a routine process that enables both detection with commercially-available antibodies and affinity purification. A construct was developed by Dr Maria Oszvald and Dr Hongtao Zhang (Rothamsted Research; section 2.1) to express the *PRT1* genomic sequence in frame with a tandem affinity purification (TAP) tag, comprising the streptavidin binding protein (SBP) and two copies of an immunoglobulin G binding domain, separated by a TEV protease cleavage site (Figure 3.5). The construct, driven by the native *PRT1* promoter, was introduced into the *prt1-1* background. A homozygous T3 line was available at the outset of this project and further lines were made homozygous in this study by selection on kanamycin. Line MO14-7-1 restored methotrexate sensitivity to *prt1-1* expressing F-DHFR, indicating that the fusion protein is functional and successfully complements the mutant (Figure 3.6).

Figure 3.5: Schematic showing the TAP-tag Cassette. M014-7-1 construct inserted into the *prt1-1* mutant background to complement the mutation which features allowing tandem affinity purification studies of *PRT1* interacting proteins. (*PRT1pro* = endogenous promoter; *PRT1* gDNA = full length *PRT1* genomic DNA; SBP = streptavidin binding protein; TEV= Tobacco etch virus cleavage site; IgG-BD = immunoglobulin G binding domain).

This line was chiefly developed to isolate PRT1 and study its interacting protein partners via tandem affinity purification (TAP tagging; see Appendix) but was also useful to determine the tissue localisation of PRT1. Five-day old seedlings of Col-0 and MO14-7-1 were treated for 8 h with DMSO or Bortezomib and an anti-SBP immunoblot of crude protein extracts was conducted. As expected, no bands were detected in the untransformed negative controls, Col-0 (Figure 3.7). However, a band corresponding to predicted size of the PRT1-TAP fusion (~71 kDa) was detected in MO14-7-1 roots without proteasome inhibition. No bands were detected in DMSO-treated MO14-7-1 shoots but a strong signal at ~71 kDa was apparent following inhibition of the proteasome by Bortezomib treatment. Treatment with Bortezomib, which inhibited the proteasome for 8 h, may produce a number of downstream effects manifest as the multiple banding patterns observed on the Western blot compared to MO14-7-1 root samples without PI treatment. Higher weight bands may be observed if the protein is post-translationally modified though acetylation, methylation, myristoylation, phosphorylation, glycosylation and ubiquitination are all modifications that increase the molecular weight of a protein. The presence of tagged PRT1 in flowers was tested, since *PRT1* exhibits relatively high expression in pollen, according to the eFP browser (Schmidt *et al*., 2005; Nayabayashi *et al.* 2005; see above). However, no immunoreactive bands could be detected with the anti-SBP antibody in MO14-7-1 flowers in normal conditions or heat stress conditions (Figure 3.8).

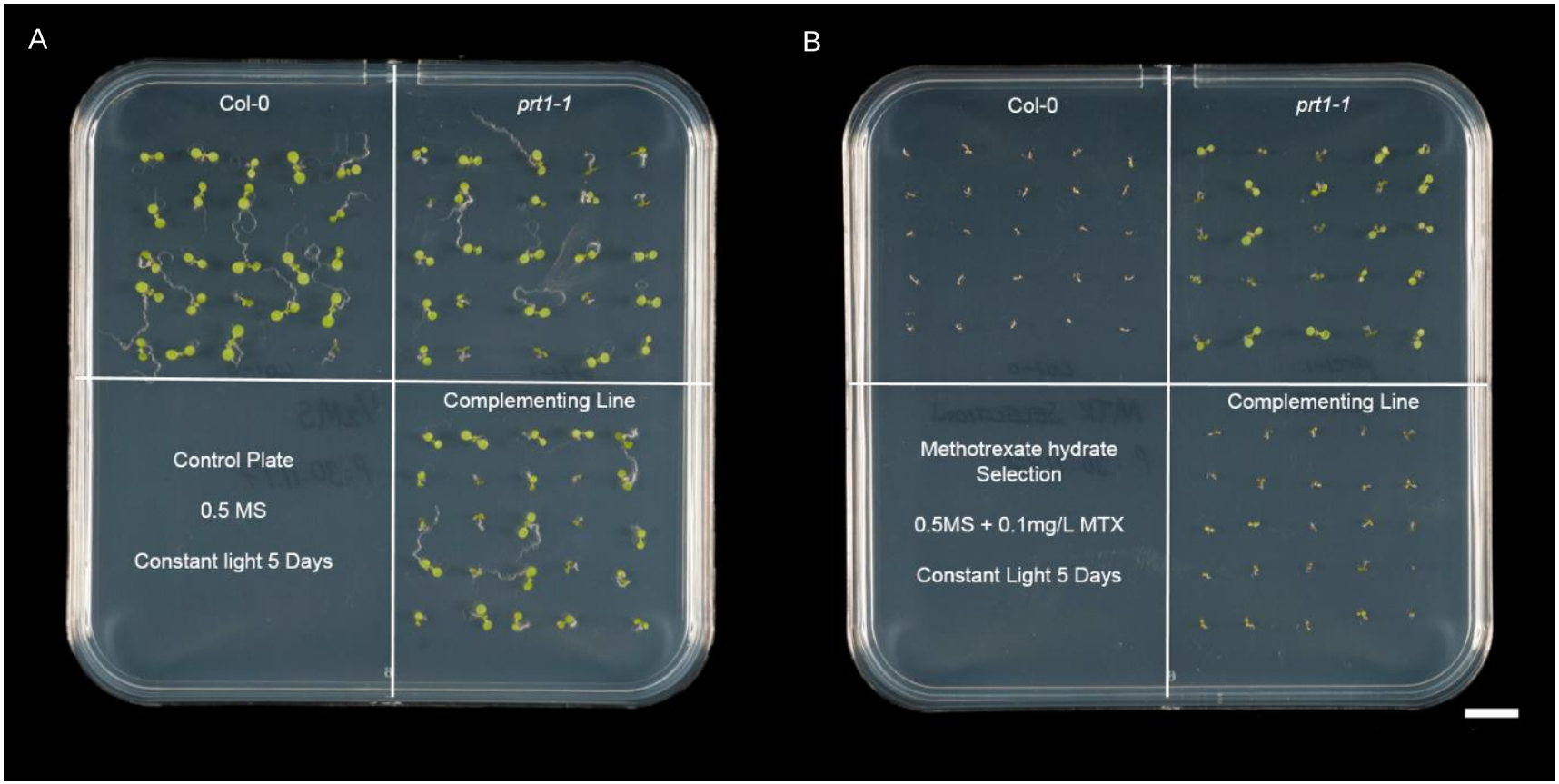

Figure 3.6: Complementation of *prt1-1* on methotrexate. Seeds of the indicated genotypes were plated on 0.5 x MS (A) and 0.5 x MS containing (0.1 mg/L) methotrexate hydrate (B), and incubated for 5 days in constant light, following 2 d stratification. Scale bar = 10 mm.

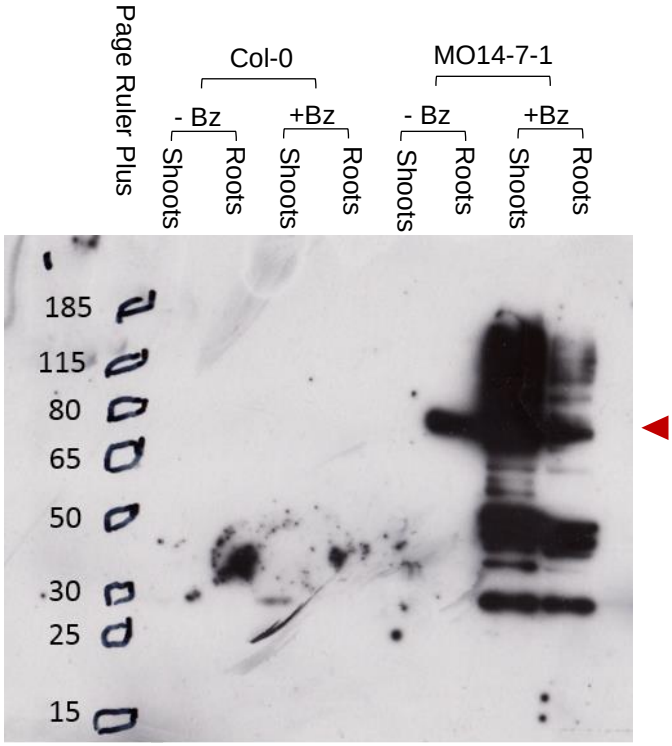

Figure 3.7: Detection of tagged PRT1 by immunoblotting. 5 d old MO14 seedlings/plants were treated with 10 μM BZ or DMSO for 8 h. Crude proteins (30 μg per lane) were separated in 4-12% denaturing polyacrylamide gels, transferred to PVDF and probed with an anti-SBP antibody. The positions of molecular weight markers (kDa) are shown to the left side of the panel. PRT1-TAP protein size is ~71 KDa (SBP ~26 kDa + PRT1~45 kDa) indicated by red arrow on the blot.

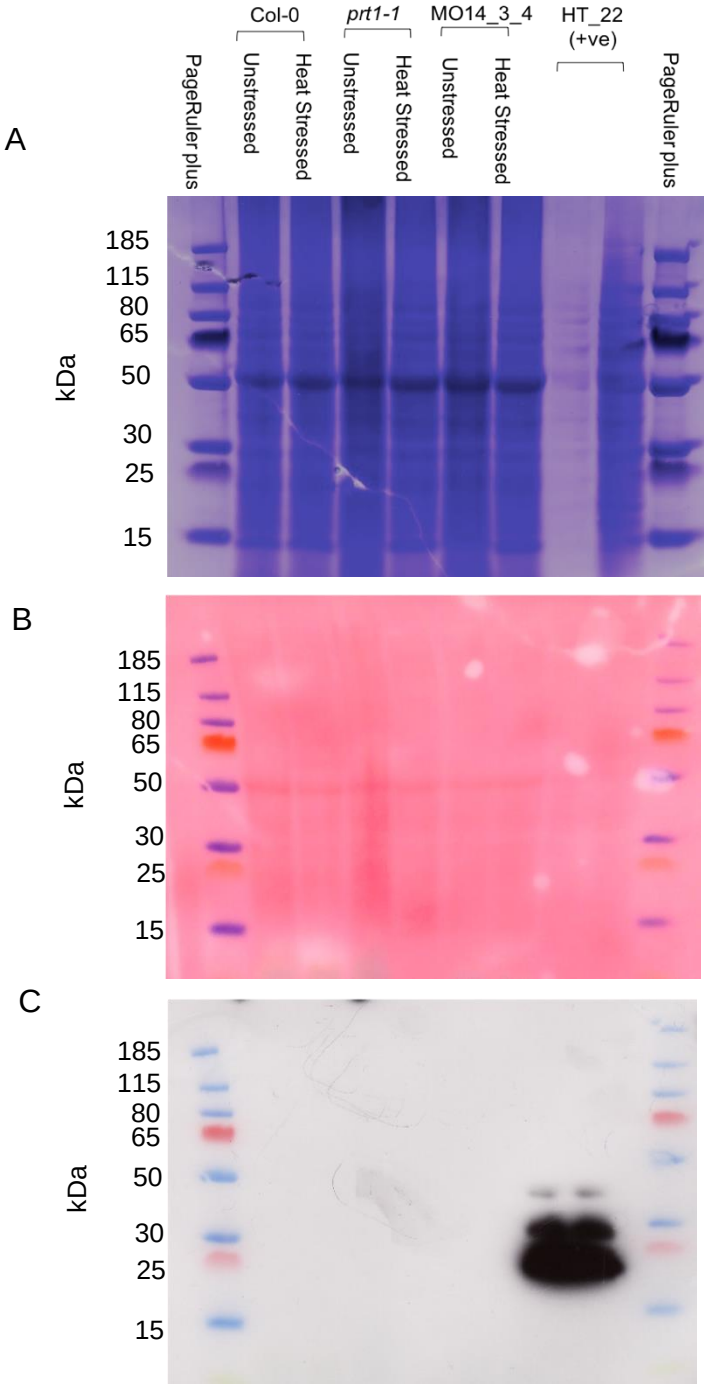

Figure 3.8: Analysis of PRT1-TAP fusion protein in flowers. Anti-SBP Western blot showing the detection of the TAP construct in unstressed and heat stressed flowers of MO14 plants: (A) Coomassie stained gel (B) Ponceau stained PVDF membrane and (C) exposed X-ray film showing no TAP detection except for the in the positive control. Expected band sizes: PRT1-TAP protein ~71 KDa (SBP ~26 kDa + PRT1~45 kDa) and HT_22/PRT6-TAP ~46 kDa (SBP ~ 26 kDa + PRT6 UBR Box ~20 kDa).

3.4.2 Subcellular localisation of PRT1-YFP

PRT1 is predicted to be localised in the nucleus: six of the algorithms integrated by the SUBcellular Arabidopsis consensus (SUBAcon) package predict a nuclear localisation for PRT1 with high confidence (Figure 3.9; Hooper *et al.,* 2014).

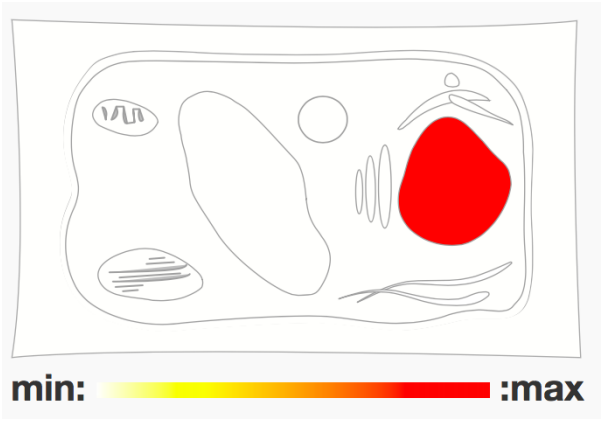

Figure 3.9: Publicly available expression data for PRT1 subcellular localisation: image showing *PRT1* (At3g24800) subcellular localisation adapted from the SUBAcon database (http://suba.live, accessed August 2018; Hooper *et al.,* 2014).

However, experimental evidence for the subcellular localisation of PRT1 has not yet been reported. In order to investigate the subcellular localisation of PRT1, a construct (MO16; *PRT1*$_{pro}$::gDNA-*PRT1*::YFP in the *prt1-1* background) was designed to express a PRT1-yellow fluorescent protein (YFP) fusion under control of the native *PRT1* promoter and used to transform *prt1-1* (Dr Maria Oszvald and Dr Hongtao Zhang, Rothamsted Research; section 2.1). A schematic of the construct is shown in Figure 3.10. In the current study, two lines (MO16-3-1 and MO16-5-1) were obtained by selecting for the construct on Basta® herbicide selection plates. The lines were shown to partially complement the *prt1-1* mutation by restoring methotrexate sensitivity.

Figure 3.10: Schematic showing the YFP fusion for subcellular localisation. Schematic showing the M016 construct inserted into the *prt1-1* mutant background to complement the mutation and study the tissue and subcellular localisation of PRT1 using YFP.

Seedlings of line MO16-3-1 were grown in constant light and imaged using confocal microscopy at 3, 5, 7 and 14 DAG. The YFP signal was detected in the root cap, columella and quiescent centre (QC) of seedlings as grainy puncta adjacent to the cell wall (Figure 3.11). No YFP signal was detected in the cortex, epidermis, endodermis, pericycle and procambium of the apical meristem, basal meristem, elongation zone differentiation zone regions of the primary root. Lateral roots also

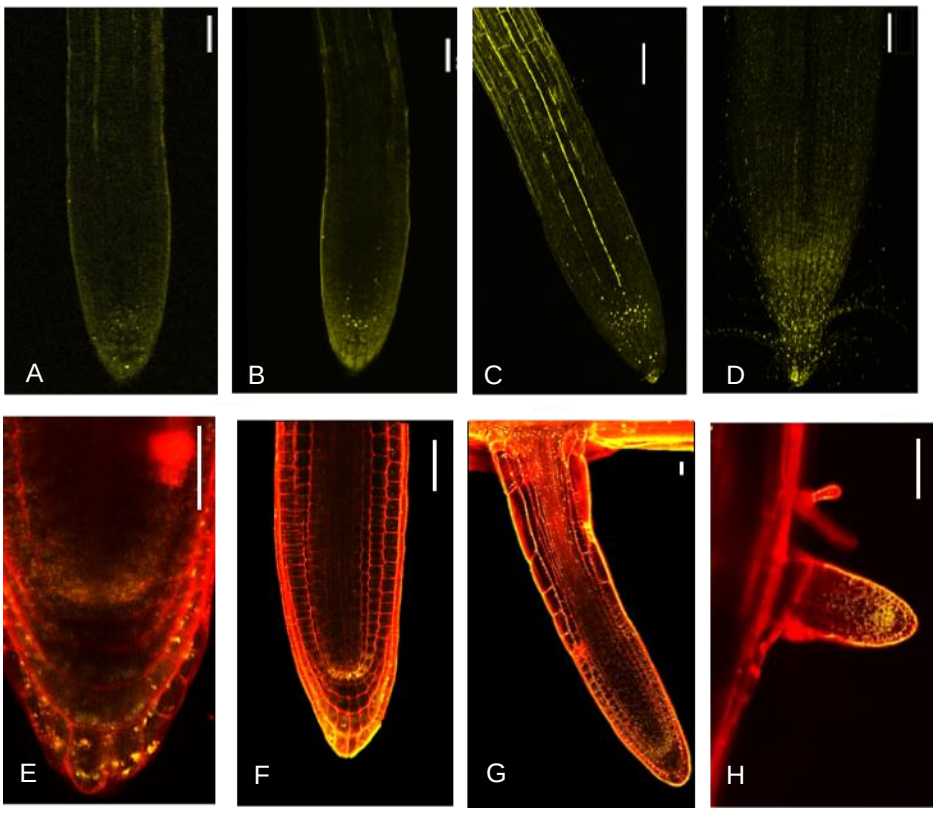

Figure 3.11 Localisation of PRT1-YFP Roots of MO16-3-1 plants were visualised by confocal microscopy. (A-D) Primary roots seedlings, 3,5,7 and 14 DAG, respectively; (E-H) primary roots of 14 DAG seedlings, counterstained with propidium iodide; (G-H) lateral roots of 14 DAG seedlings, counterstained with propidium iodide. Scale bar = 50 μm.

exhibited a similar pattern of YFP localisation in the primary root cap and quiescent centre (Figure 3.11 G-H). Counterstaining 14 DAG samples with propidium iodide was used to define the cell wall boundaries to better visualise ultrastructure (Figure 3.11 E-H). However, it was not possible to unequivocally determine the subcellular localisation of *PRT1pro*::PRT-YFP in this study. Dr Hongtao Zhang observed nuclear localisation with a GFP construct in Tobacco, however confirmation that the fusion protein is un-cleaved using Western blotting is required (personal communication, Rothamsted Research).

3.5 Protein Stability Reporter

A model ubiquitylation substrate (Garzón *et al*., 2007) was used to study the activity of PRT1 in different tissues and at different developmental stages. A *prt1-1* line containing a *DHFR-Ub-F-GUS* transgene driven by the *CaMV3S* promoter, hereafter referred to as the F-GUS reporter (Garzón *et al.,* 2007) was obtained from Professor Andreas Bachmair (University of Vienna) and crossed to Col-0 by Ms Lucy Gannon and Dr Hongtao Zhang (Rothamsted Research, unpublished data; section 2.1.1). A schematic representing the F-GUS reporter system is shown in Figure 3.12A. Dihydrofolate reductase is a metabolically stable co-translated reference protein which was fused to the Nt of ubiquitin, to which a *E. coli* beta glucuronidase (GUS) is attached. The effect of Nt destabilising residues was enhanced by extending the GUS ORF with an unstructured amino acid linker. During or immediately following translation, deubiquitinating enzymes (DUBs) recognise the Ct ubiquitin moiety and cleave the fusion protein, revealing a novel N-terminal amino acid; phenylalanine (F) for this study. The DHFR cleavage product contains one HA epitope whereas GUS cleavage products contain 3 HA epitopes. This enables detection and quantification by immunoblotting of the F-GUS test protein and the DHFR reference protein by using the same anti-HA antibody due to different product sizes.

Application of the histochemical substrate 5-bromo-4-chloro-3-indolyl glucuronide (X-Glc) in the presence of stabile *β*-Glucuronidase (GUS)

catalyses the production of a blue product which was used to analyse PRT1 localisation and activity either qualitatively or quantitatively. The artificial N-end rule substrate F-GUS is short-lived in *Arabidopsis* wild-type plants, in which an active PRT1 E3 ligase recognises the model F-substrate and, via the E1-E2-E3 cascade, facilitates poly-ubiquitin attachment to an internal lysine residue on the flexible linker. The test protein is degraded and little to no staining is observed following X-Glc application. In contrast, the F-GUS protein is stabilised and aggregates in the *prt1-1* background and in WT tissues where PRT1 is not active, meaning plantlets stain blue with the GUS substrate (Garzón *et al.,* 2007; Fig. 3.12).

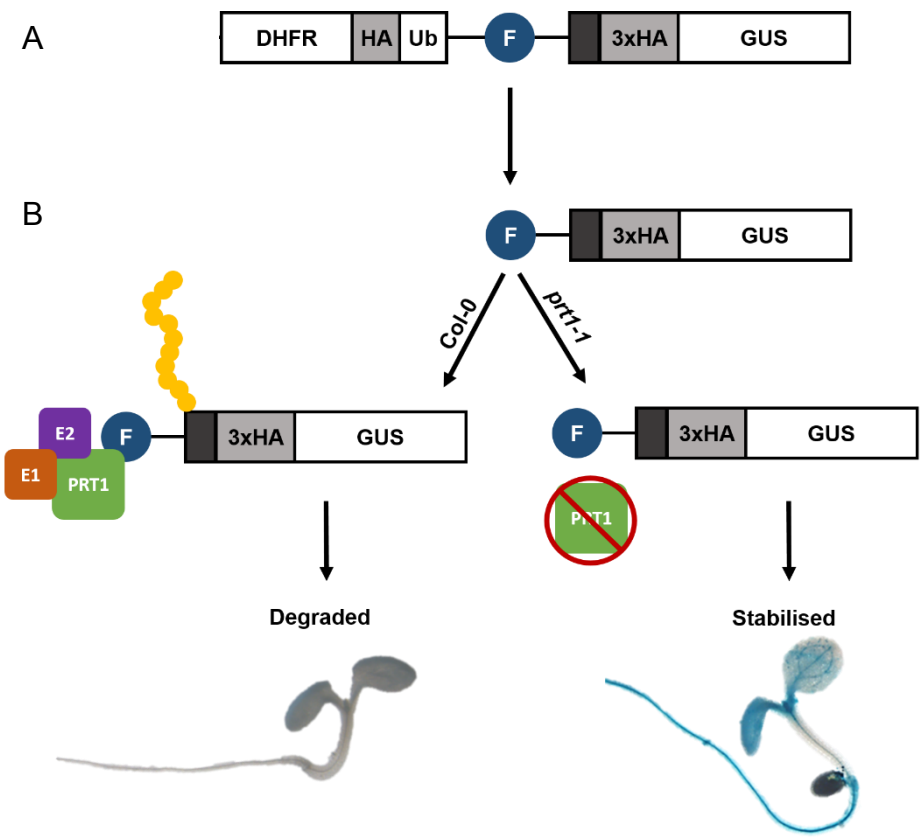

Figure 3.12: The F-GUS protein stability reporter system: (A) schematic of the F-GUS transgene transformed into Col-0 and *prt1-1* background, and (B) following fusion protein cleavage by DUBs, the F (Phenylalanine)-GUS fusion protein is degraded in Col-0 but stabilised in *prt1-1* due to non-functional PRT1. The patterns of blue staining indicate the tissues where F-GUS is stabilised. Ubiquitin is represented by yellow circles and is attached to the Lys residues of the GUS linker (dark grey). HA epitopes (light grey) enable immunological quantification through by anti-HA antibodies.

Inhibitors were tested to investigate whether PRT1-mediated degradation of F-GUS requires activity of the 26S proteasome and also to identify conditions in which PRT1 substrates could be stabilised pharmacologically. Firstly, proteasome inhibitor selection and experimental conditions were optimised. Z-Leu-Leu-Leu-Al (MG-132) is a peptide aldehyde acting on calpains and cathepsins to selectively and reversibly inhibit the proteasome (Kisselev & Goldberg *et al.,* 2001). Bortezomib (BZ) is a competitive inhibitor of the proteasome enzymes whose boron atom binds to the catalytic site of the 26S proteasome reversibly to prevent protein degradation (Bonvini *et al.,* 2007; Ruschak *et al.,* 2011).

Both the protease inhibitors were tested at 50 μM by impregnating into 0.5 x MS agar, floating seedlings in solution or spotting 0.2 μl of a stock solution onto each seedling, followed by GUS staining of F-GUS Col-0 seedlings with F-GUS *prt1-1* as a control. The spotting method for 8 h using Bortezomib was chosen as it gave GUS stabilisation in the F-GUS Col-0 background in a shorter time period than MG-132, used a significantly smaller amount of the inhibitor than the agar and liquid methods, and reduced the potential introduction of hypoxia-related effects floating the seedling (data not shown). Even application of the PIs was maintained as far as possible. In control seedlings treated with DMSO, blue colouration was only observed in the F-GUS *prt1-1* background as expected (Figure 3.13 A - B). However following BZ treatment, comparable accumulation of F-GUS product was observed in the Col-0 and *prt1-1* backgrounds, consistent with stabilisation of F-GUS (Figure 3.13 C - D).

Experiments were also conducted using the HA-tag for immunodetection of F-GUS in Col-0 and *prt1-1* with and without proteasome inhibition (Figure 3.14A). Five-day-old seedlings were treated with either DMSO or BZ for 8 h and crude protein extracts were subjected to immunoblotting with an anti-HA antibody. On the blot multiple bands are present: one HA epitope denote the stable reference protein, and three HA epitopes indicating the GUS test protein. Bands were identified by predicted size

of ~80 kDa for DHFR-GUS protein and ~30 kDa for stable DHFR. Other bands on the blot correspond to cross-reacting proteins also present in plants lack the transgene (Garzón *et al.,* 2007). Detection of the HA tags was not observed in the F-GUS Col-0 background (Figure 3.14A) and GUS staining was also absent (Figure 3.14C). Following treatment of F-GUS Col-0 seedlings with BZ, GUS staining was observed, and the HA-tag could be detected; however, the levels of HA abundance relative to those in the F-GUS *prt1-1* background were significantly reduced (Figure 3.14B). Additionally, no other bands were present in the BZ treated Col-0 samples possibly due to lower loading or due to autophagy-mediated degradation.

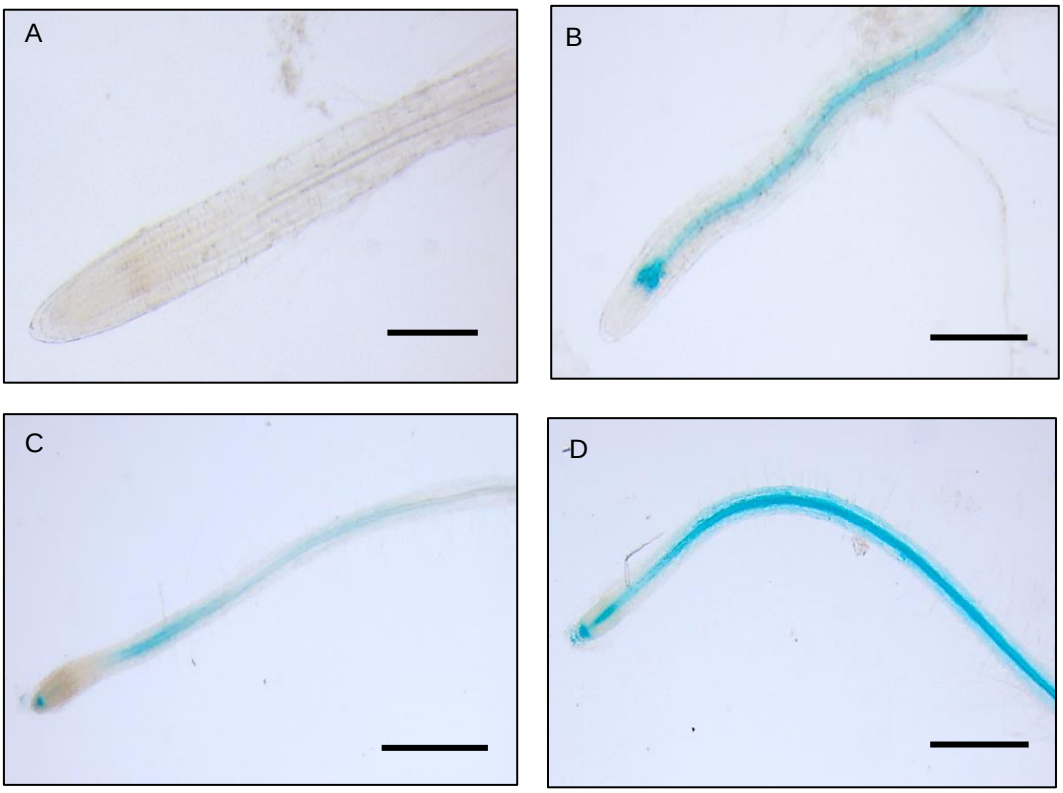

Figure 3.13: Effect of a proteasome inhibitor on stability of F-GUS reporter protein. Primary roots of 5 d old seedlings were treated for 8h with either DMSO or BZ using the spotting method and GUS activity visualised using a histochemical assay. (A) F-GUS Col-0 +DMSO (B) F-GUS *prt1-1* +DMSO (C) F-GUS Col-0 +BZ (D) F-GUS *prt1-1* +BZ. Seedlings stained for 16 hours at 37^{O}C and de-stained with 70% ethanol. Scale bars = 250 µm.

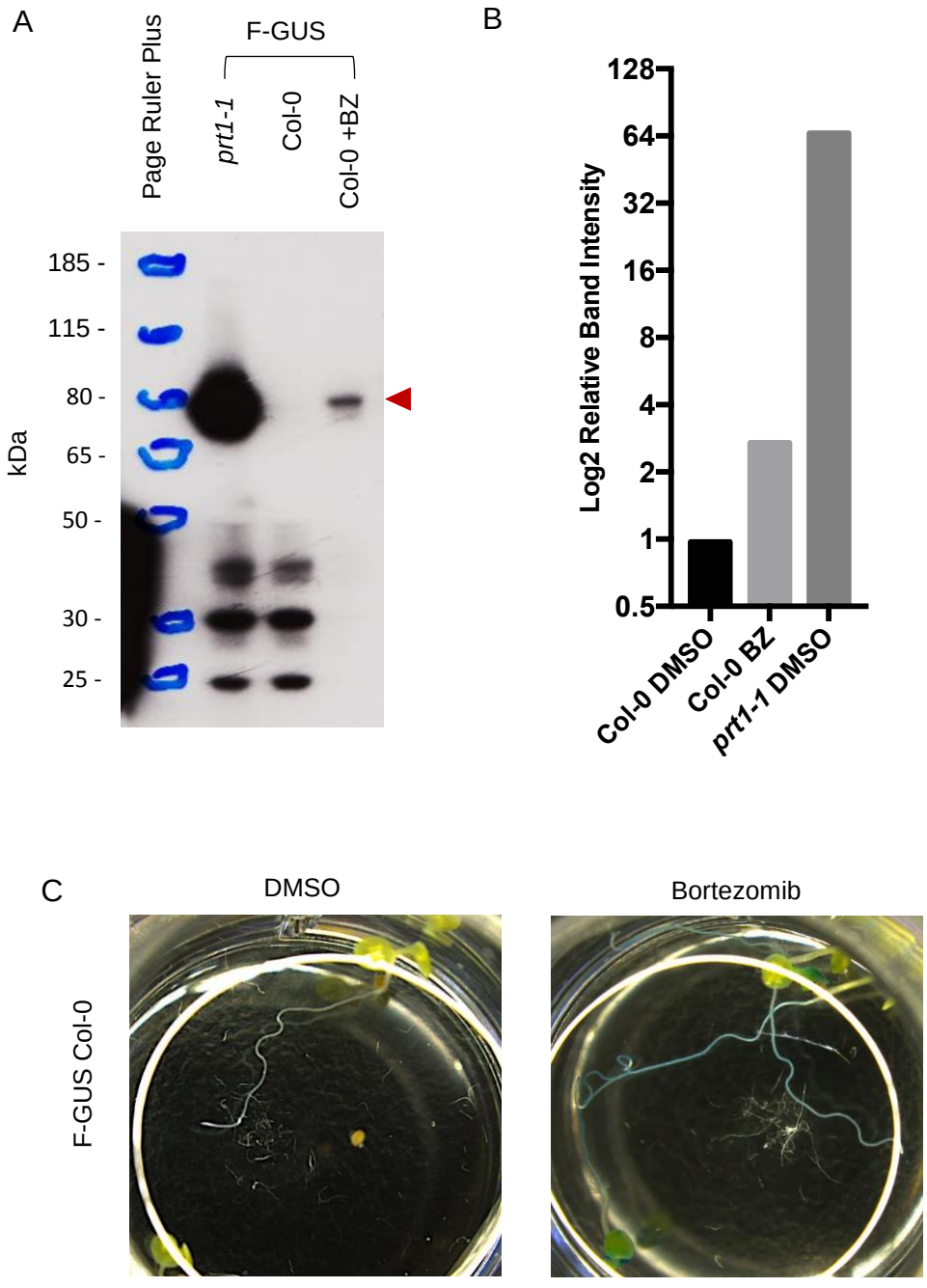

Figure 3.14: Effect of proteasome inhibitors on stability of F-GUS reporter protein. (A) Anti-HA immunoblot showing F-GUS stabilisation in the *prt1-1* background and in Col-0 background, following 8 h treatment with BZ. 30 μg protein was loaded per lane. Red arrow indicates PRT1-3xHA fusion protein. Other bands indicate cross-reacting proteins in plants lacking the transgene (Garzón *et al.,* 2007). Number on the left indicate positions of relative molecular mass markers (kDa) (B) relative band intensity of the ~80 kDa band for HA abundance in the immunoblot shown in A and (C) Histochemical GUS assay of DMSO- and BZ-treated 5 DAG F-GUS Col-0 seedlings.

3.5.1 Developmental analysis of F-GUS stabilisation

F-GUS Col-0 and F-GUS *prt1-1* plants were treated with the X-Glc substrate at different developmental stages and in response to different growth conditions to establish patterns of substrate destabilisation and stabilisation, and therefore *PRT1* activity.

From early seeding establishment (3 days after germination/DAG) to development of a mature seedling with fully expanded true leaves (8-10 DAG), no GUS stabilisation could be observed in the F-GUS Col-0 background, as judged by GUS staining (Figures 3.15 - 3.18). However, in the F-GUS *prt1-1* background, extensive staining was observed in seedlings at these developmental stages. Staining was prominently localised in the veins and stomata in true leaves and cotyledons in the F-GUS *prt1-1* background as well in the tissues in the vicinity of the shoot apical meristem. Staining was largely absent from the hypocotyl but observed extensively in the primary root system: particularly in the elongation zone, and the apical meristem and quiescent centre of the root cap. Staining diminished in the root meristems of roots however. A similar patterning of F-GUS accumulation was observed in lateral roots, with no staining observed in the F-GUS Col-0 background but staining mirroring that present in primary roots for F-GUS *prt1-1* (Figure 3.19).

Following bolting and transition to flowering, extensive staining was detected in rosettes, cauline leaves and stems in F-GUS *prt1-1* but absent from F-GUS Col-0 (Figure 3.20). Discrete staining was observed in F-GUS *prt1-1* in stomatal guard cells and veins in leaves but not in Col-0 (Figure 3.21). In the F-GUS *prt1-1* plants, staining was observed in the filament and vasculature of the anther, the stigma, style and replum of ovaries, in the inflorescence stem and staining also follows the closed reticulate venation in petals (Figure 3.22). Figure 3.23 shows localisation of F-GUS in the valves and septum of siliques in the *prt1-1* background as well as staining in the abscission zone in both the *prt1-1* and Col-0 background. No staining was observed in seeds for all lines despite being quite high in eFP browser, although seeds were not dissected.

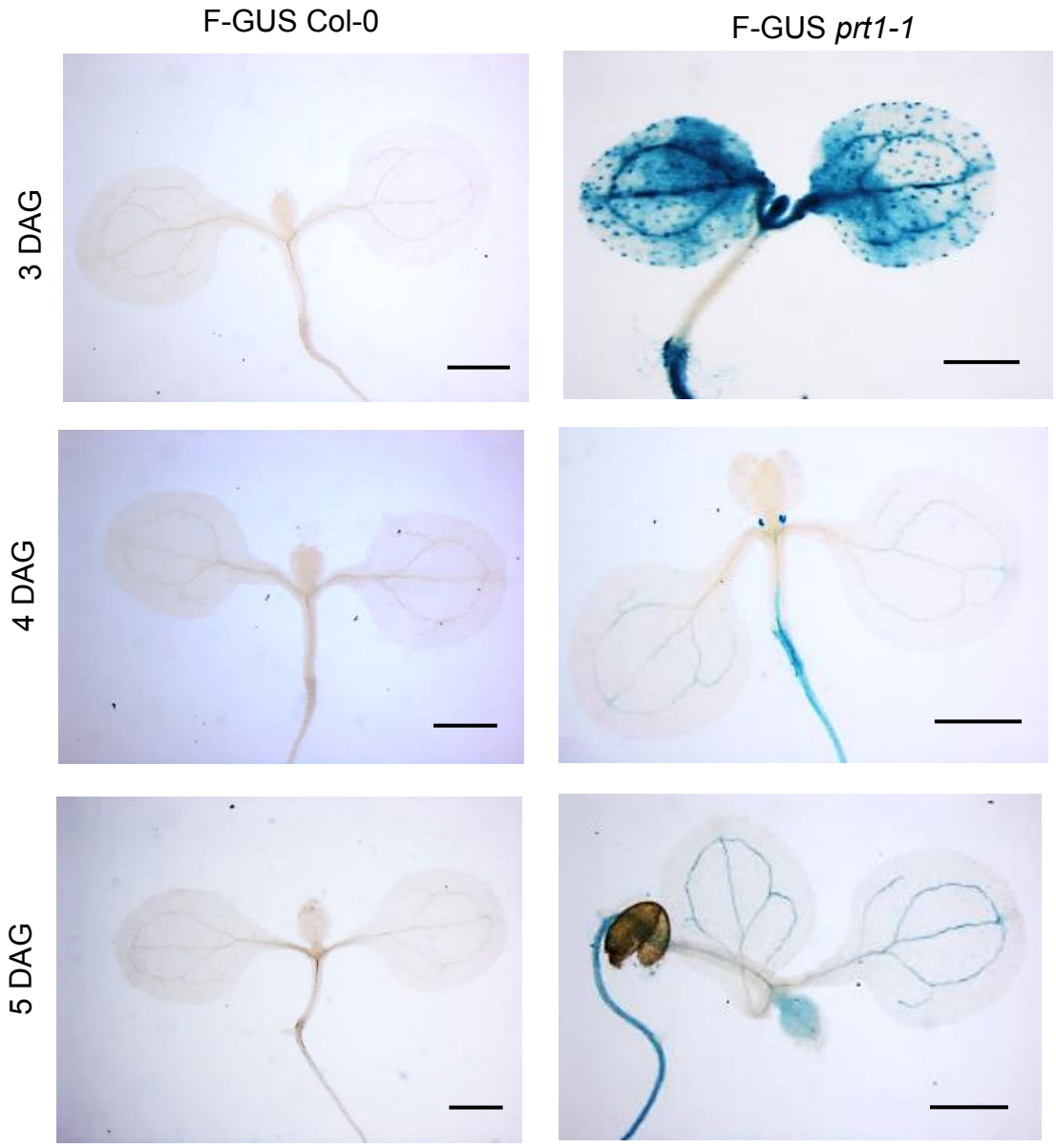

Figure 3.15: Histochemical assay of GUS reporter protein in seedlings expressing the ubiquitin fusion degradation test substrate, F-GUS: F-GUS Col-0 and F-GUS *prt1-1* seedlings were stained at 3, 4 and 5 DAG. Scale bars = 1 mm.

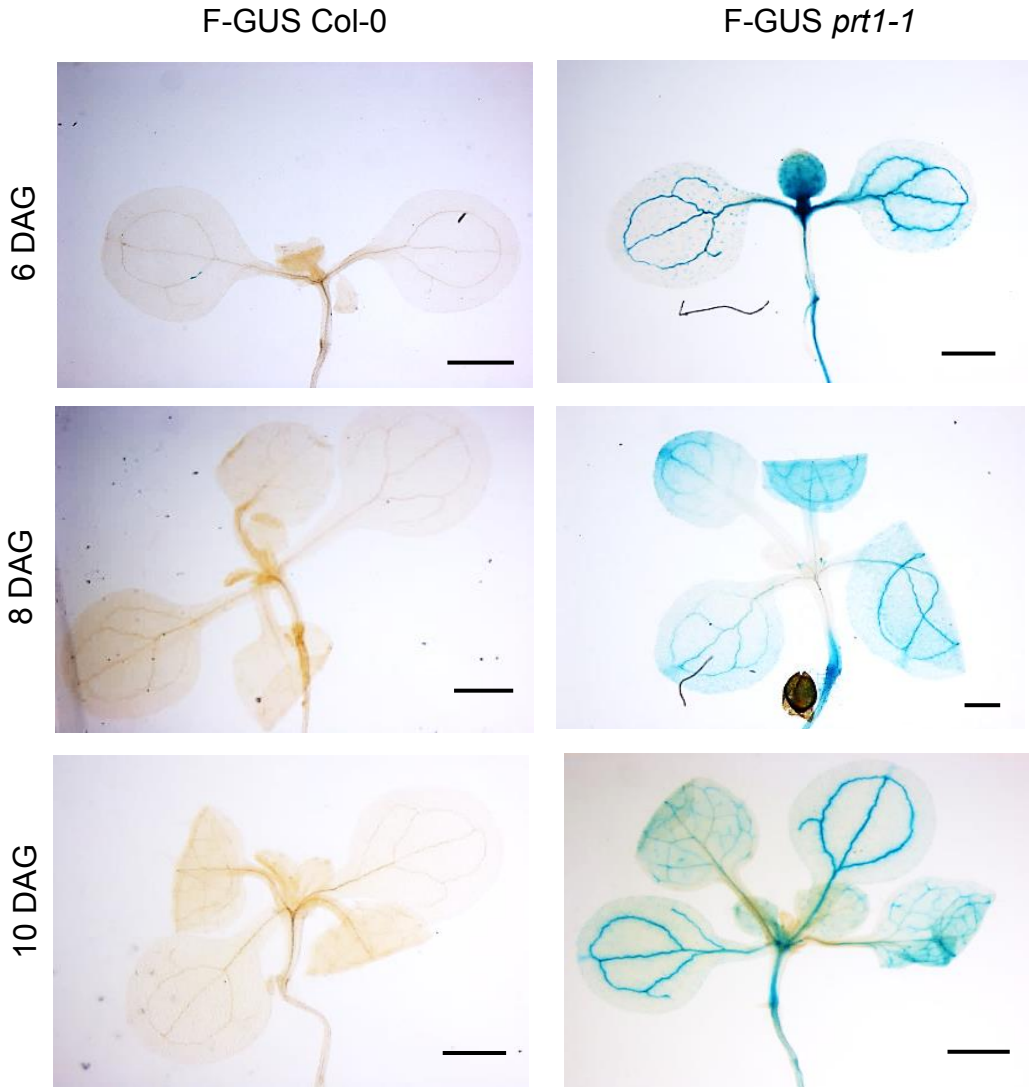

Figure 3.16: Histochemical assay of GUS reporter protein in seedlings expressing the ubiquitin fusion degradation test substrate, F-GUS: F-GUS Col-0 and F-GUS prt1-1 seedlings were stained at 6, 8 and 10 DAG. Scale bars = 1mm.

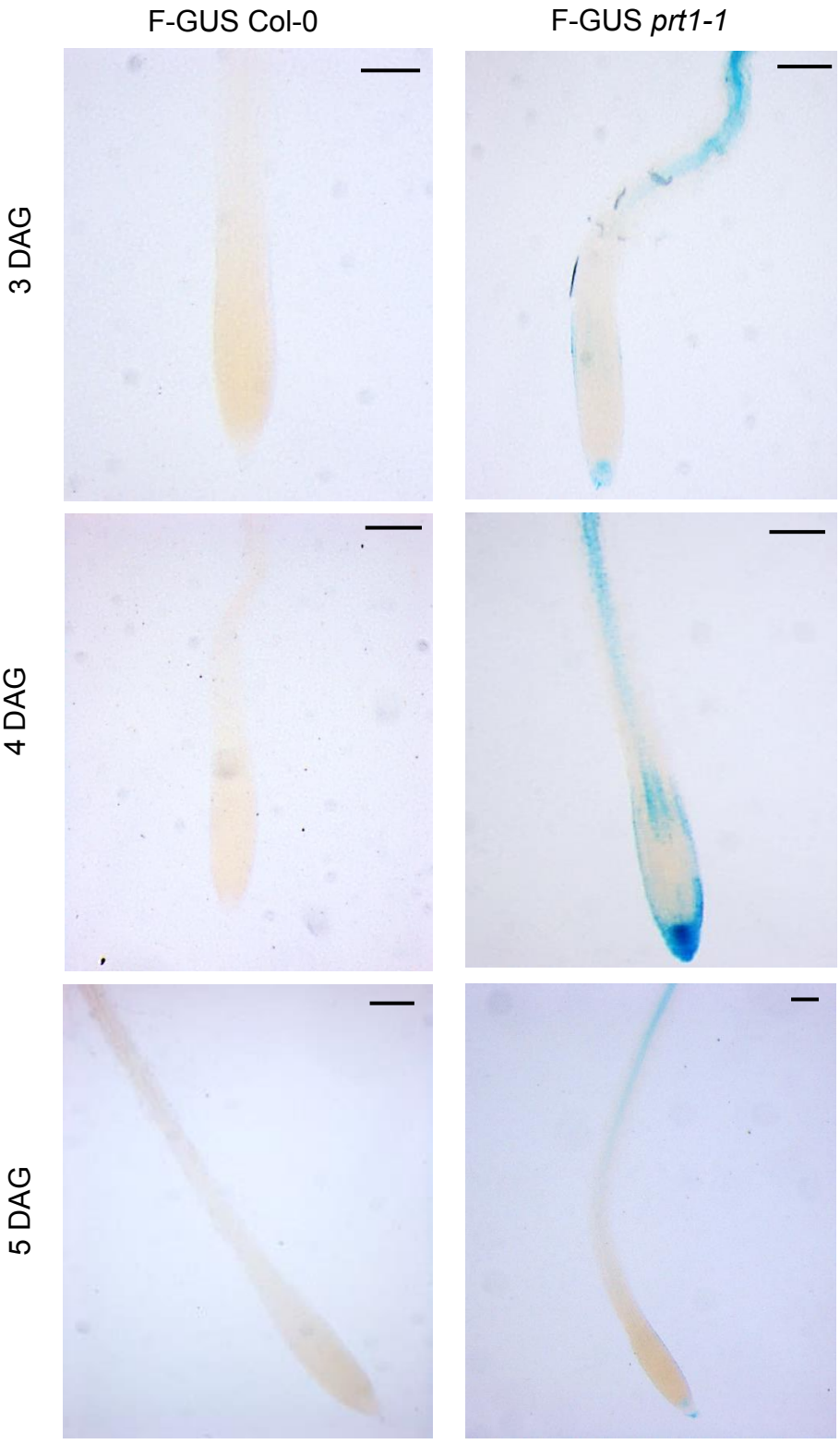

Figure 3.17: Histochemical assay of GUS reporter protein in seedlings expressing the ubiquitin fusion degradation test substrate, F-GUS: Primary roots of F-GUS Col-0 and F-GUS *prt1-1* of 3/4/5 DAG seedlings stained for 16 hours at 37^{O}C and de-stained. Scale bars = 100 µm.

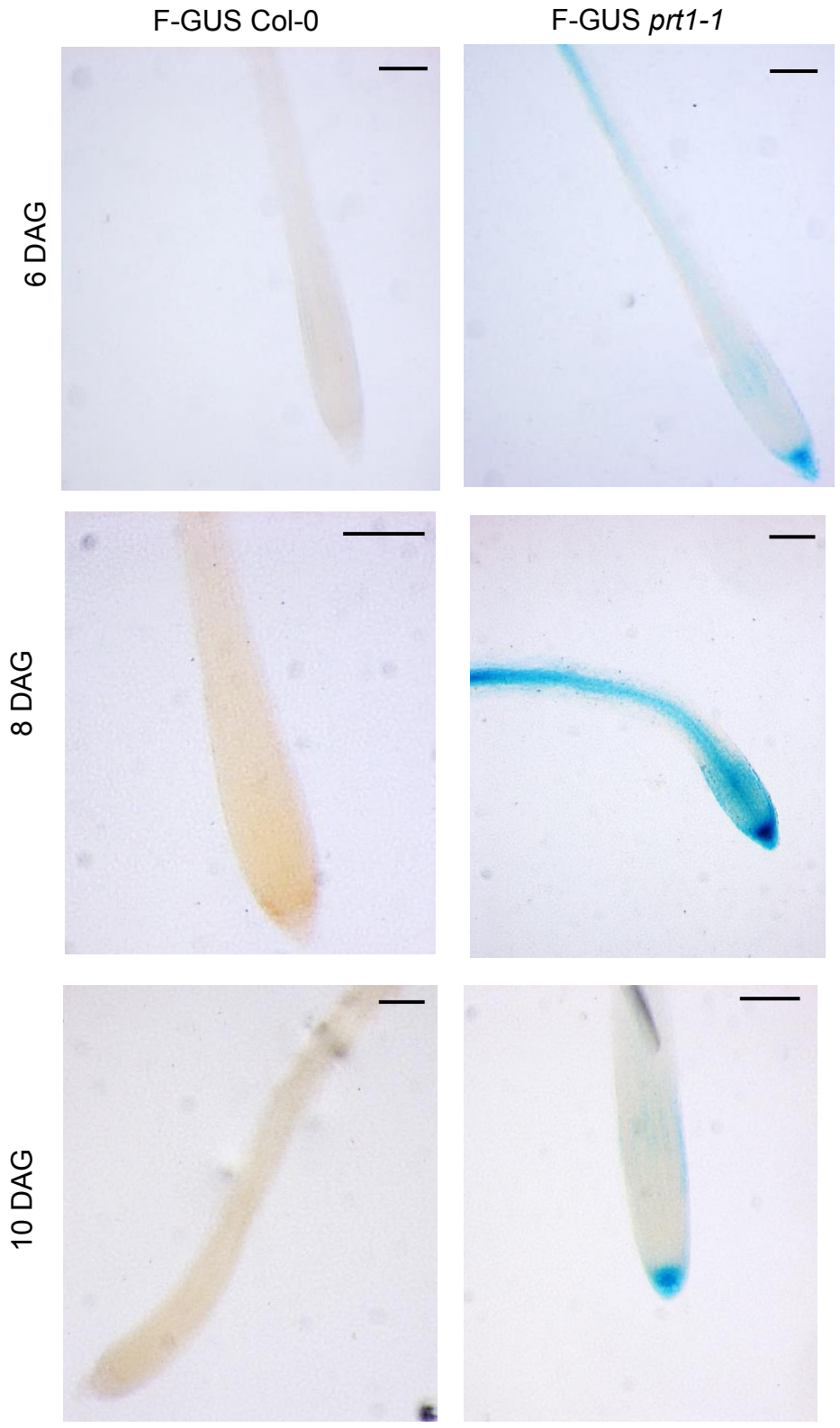

Figure 3.18: Histochemical assay of GUS reporter protein in seedlings expressing the ubiquitin fusion degradation test substrate, F-GUS: Primary roots of F-GUS Col-0 and F-GUS *prt1-1* of 6/8/10 DAG seedlings stained for 16 hours at 37^{O}C and de-stained. Scale bars = 100 µm.

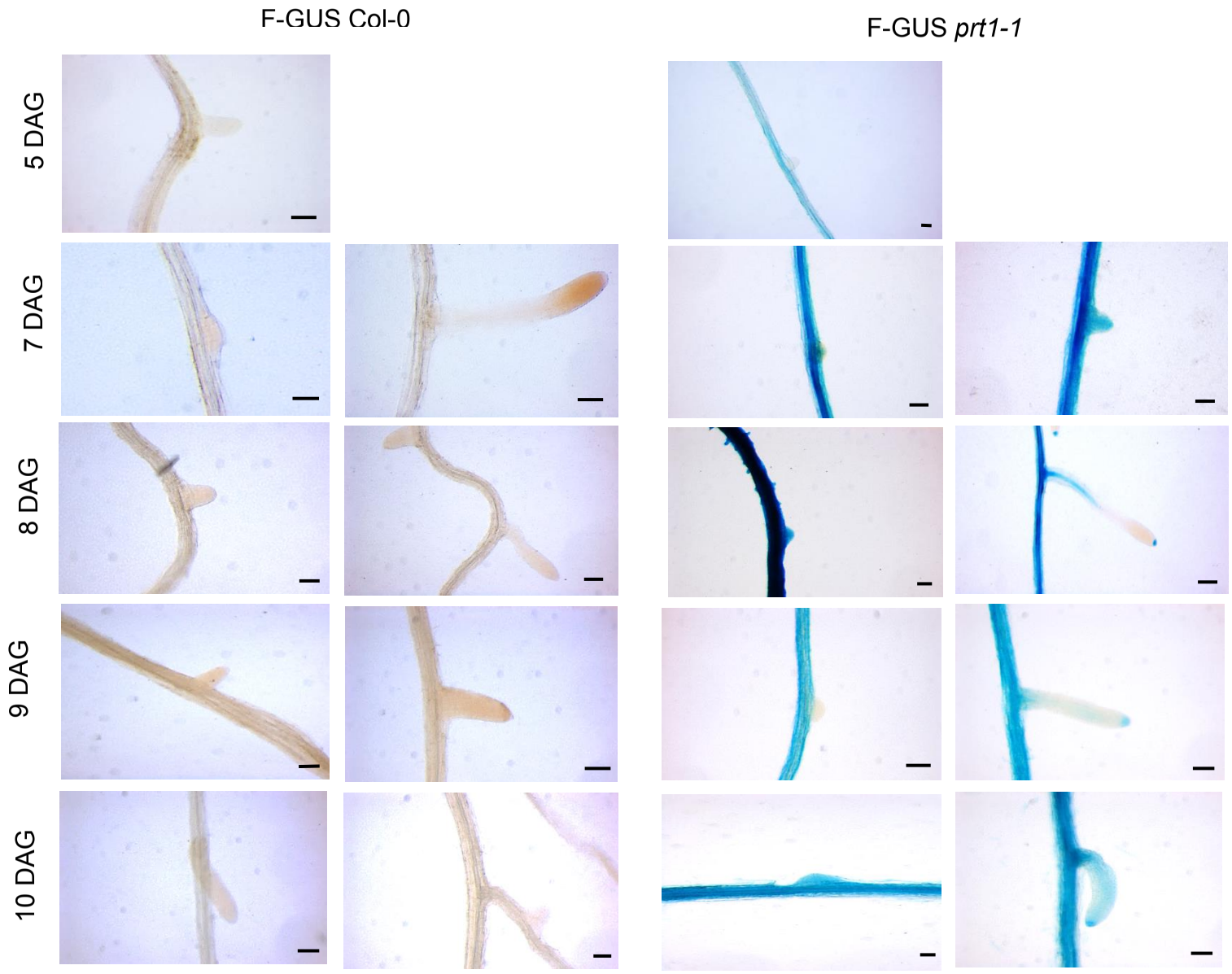

Figure 3.19: Histochemical assay of GUS reporter protein in seedlings expressing the ubiquitin fusion degradation test substrate, F-GUS: Lateral roots of F-GUS Col-0 and F-GUS *prt1-1* of 5/7/8/9/10 DAG seedlings stained for 16 hours at 37^{O}C and de-stained. Scale bars = 100 µm.

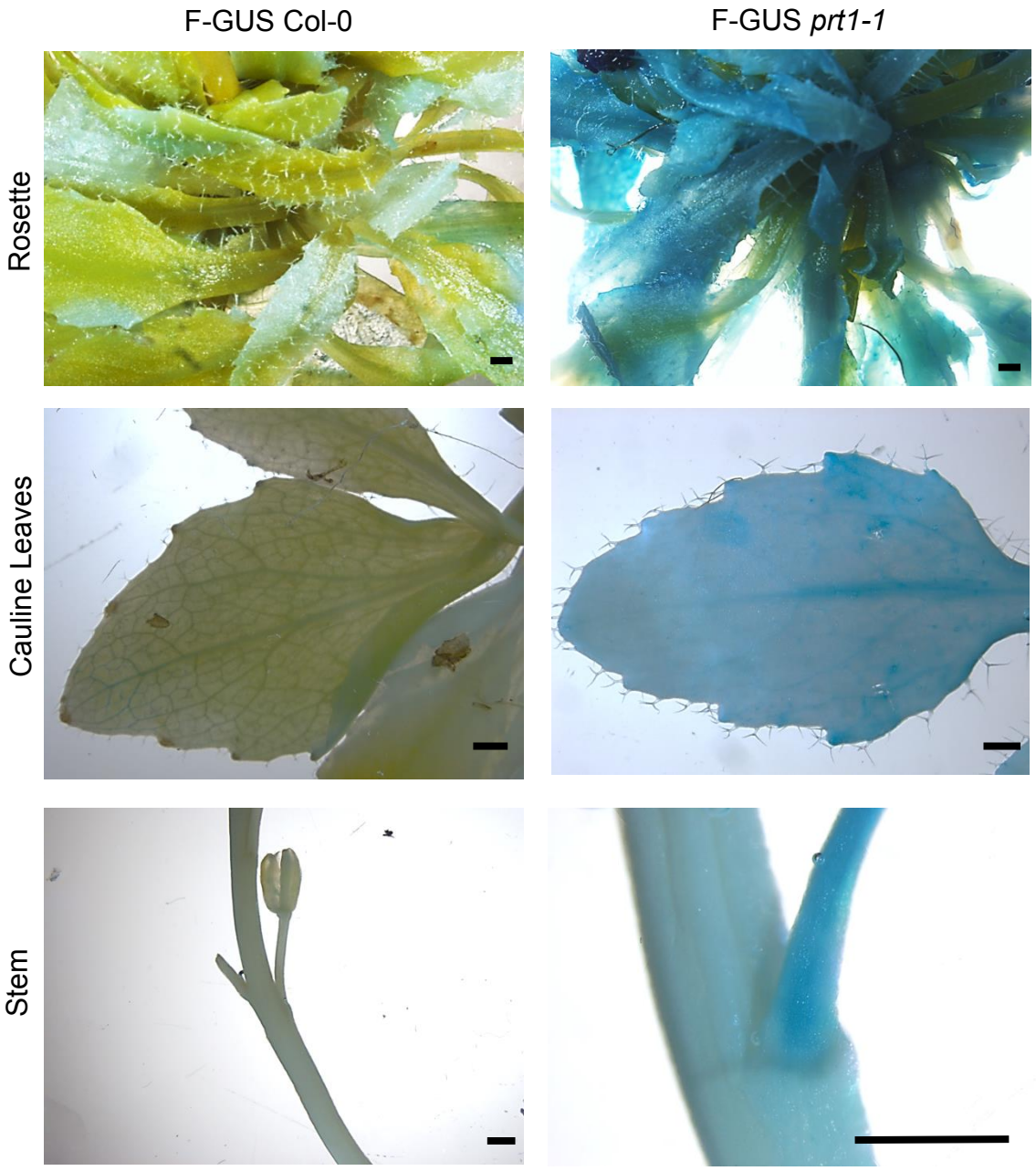

Figure 3.20: Histochemical assay of GUS reporter protein in seedlings expressing the ubiquitin fusion degradation test substrate, F-GUS: Rosettes, cauline leaves and stems of F-GUS Col-0 and F-GUS *prt1-1* at 6 weeks after germination stained for 16 h and de-stained. Scale bars = 1 mm.

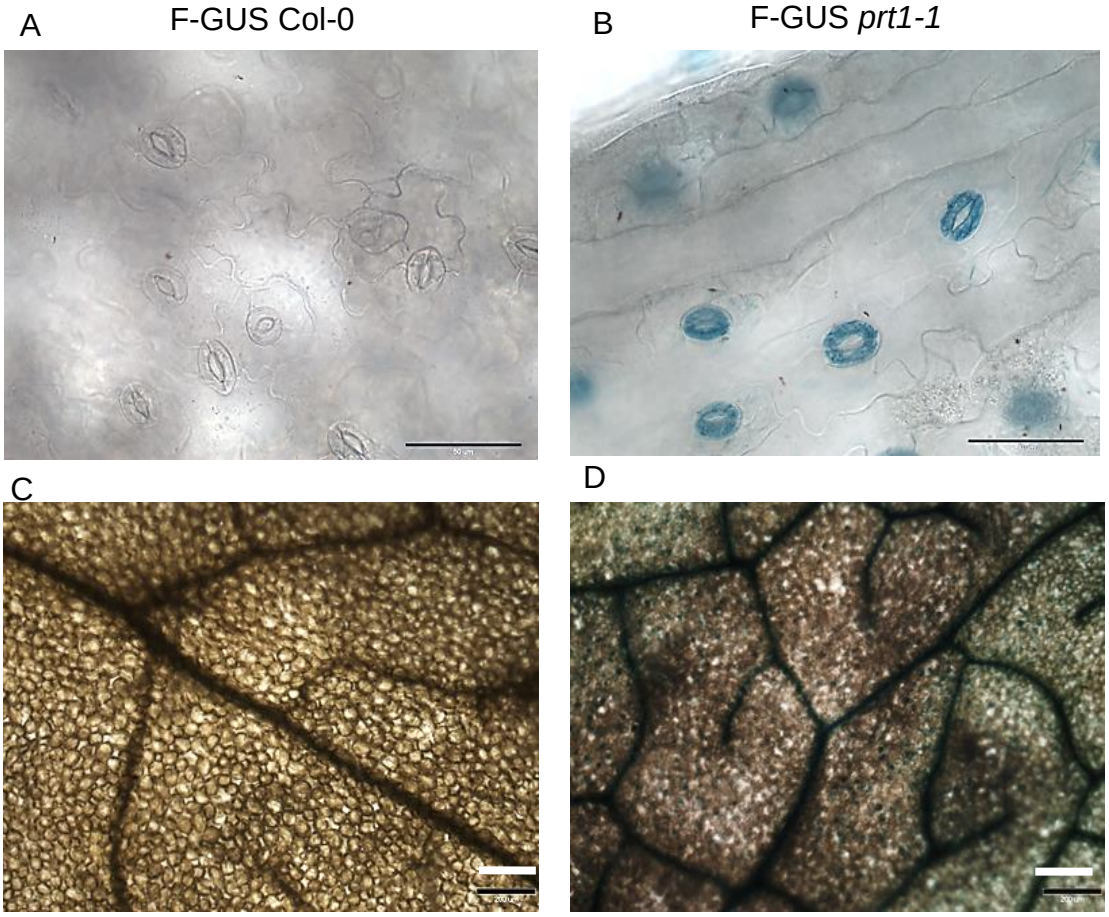

Figure 3.21: Histochemical assay of GUS reporter protein in seedlings expressing the ubiquitin fusion degradation test substrate, F-GUS: Images of GUS 16 h stained samples showing accumulation around (A-B) stomata guard cells (scale bars = 50 μm) and (C-D) veins (scale bars = 250 μm) of F-GUS constructs in the Col-0 and *prt1-1* background respectively.

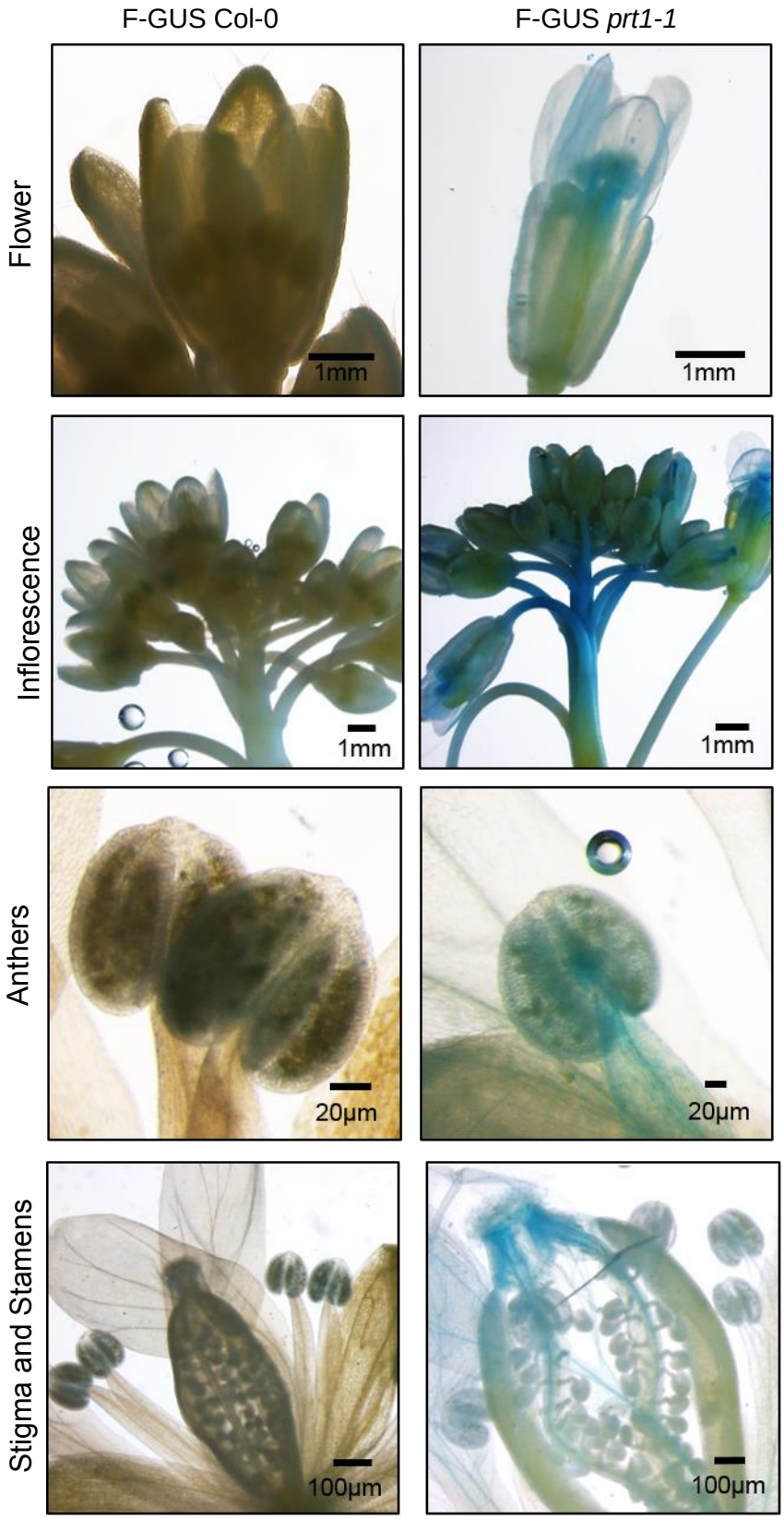

Figure 3.22: Histochemical assay of GUS reporter protein in seedlings expressing the ubiquitin fusion degradation test substrate, F-GUS: Flowers, anthers, stigma and stamen of F-GUS Col-0 and F-GUS *prt1-1* at 6 weeks at 37^{O}C after germination stained for 16 hours and de-stained.

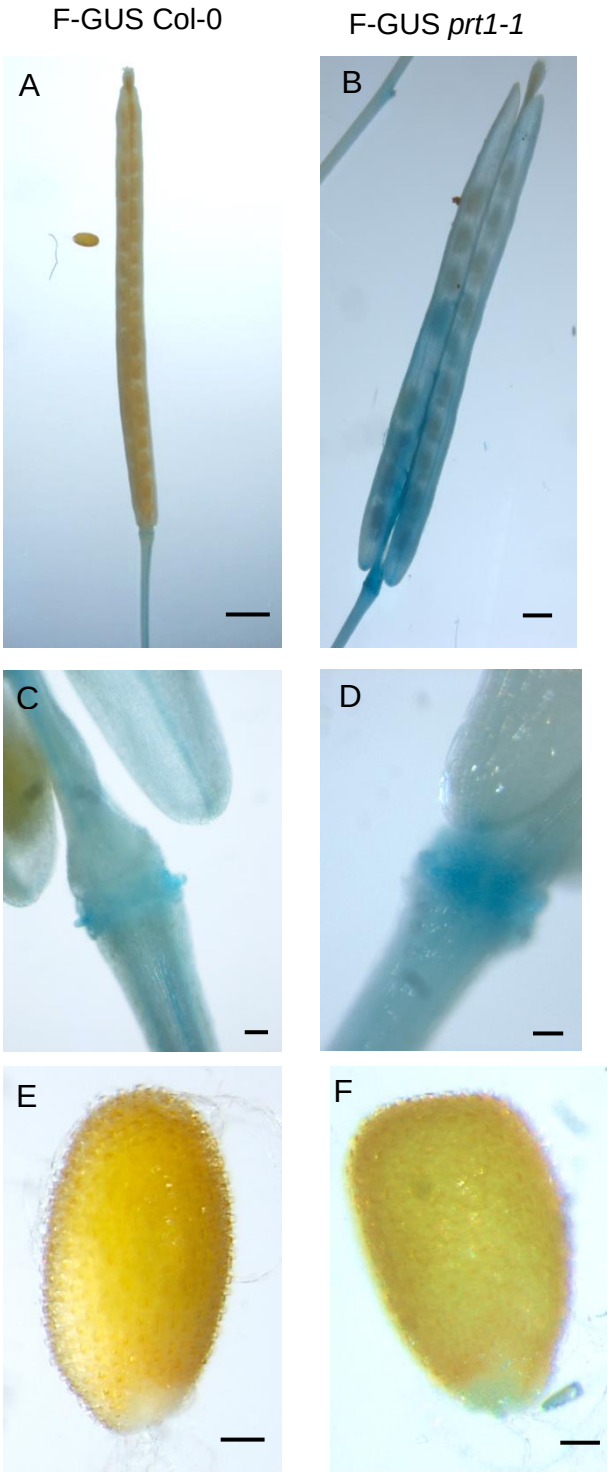

Figure 3.23: Histochemical assay of GUS reporter protein in seedlings expressing the ubiquitin fusion degradation test substrate, F-GUS: Images of GUS 16 h stained samples showing accumulation in (A-B) silique (scale bars = 100 μm), (C-D) silique internodes (scale bars = 10 μm) and (E-F) seeds (scale bars = 100 μm) of F-GUS constructs in the Col-0 and *prt1-1* background respectively.

3.6 Discussion:

This chapter aimed to identify the tissues, cells and subcellular components in which *PRT1* is localised and active as well as the localisation of *PRT1* promoter activity.

Information from publicly available array data suggests *PRT1* is expressed throughout the plant. In this study, GUS-reporter based analysis of the *PRT1* promoter provided no definitive answers regarding its activity and localisation. Dr Maria Oszvald (Rothamsted Research, UK) had previously indicated that a combination of cold stress and different light regimes was sufficient to induce *PRT1*-promoter activity as observed by GUS staining. However, for the conditions tested in this investigation, no induction of the promoter was observed. Given the presence of extensive staining in the F-GUS *prt1-1* background but inability to detect TAP in these tissues, it would be expected that PRT1 would be constantly synthesised, thus requiring a constitutively active promoter. Potentially, the MO15 construct used for *PRT1* promoter studies may need redesigning to include more promoter elements 5', and perhaps 3' DNA outside the gene region. Furthermore, other parts of the gene may be essential for its expression that were absent from this construct (Coll *et al.,* 2015). Re-designing this construct may facilitate valuable studies into the localisation and activity of the *PRT1* promoter. Further experimentation is required to identify conditions that induce the *PRT1* promoter and to observe its localisation.

Using the F-GUS activity reporter system, the localisation of PRT1 activity was investigated. In the F-GUS Col-0 background, little to no staining was observed in any of the tissues at the developmental stages investigated. This indicates that when PRT1 is active, substrates bearing phenylalanine at their N-termini are degraded throughout the plant. In contrast, F-GUS was widely stabilised in *prt1-1* plants throughout all developmental stages tested indicating that when the PRT1 E3 ligase is non-functional in this background substrates with Nt-Phe are stabilised throughout the plant.

If *PRT1* is expressed in a basal and ubiquitous manner as the eFP browser implies, it would be expected that GUS staining, driven by a *CaMV35s* promoter in the *prt1-1* background would be observed at the same level in all tissues throughout plant development. However, there were notable exceptions to this such as seedling hypocotyls, root apical meristems, true leaves and seeds. Whilst *CaMV35s* based constructs are advantageous when the gene of interest is typically constitutively expressed (as *PRT1* is predicted to be), such an approach may overlook tissue-specific characteristics of expression. Furthermore, co-expression or gene-silencing may be challenges associated with this approach (Elmayan and Vaucheret, 1996; Elmayan *et al*.,1998; Mishiba *et al*., 2005). Additionally, there may be cell type differences in expression from the *CaMV35s* promoter which may account for the differences in F-GUS expression in the *prt1-1* background. Testing a different promoter in the F-GUS construct may circumvent these issues. For instance, the Arabidopsis *ubiquitin-10* gene promoter (*UBQ10*) enables moderate expression in most tissues (Norris *et al*., 1993; Grenfen *et al.,* 2010).

Certain tissues such as seeds have a high optical density and technical issues regarding clearing of these tissues make GUS staining challenging (Stangeland & Salehian, 2002). Dark field microscopy may improve ability to visualisation of GUS activity in such tissues. Given the eFP browser implies a high expression of *PRT1* in seeds, it is possible that F-GUS is stabilised in the *prt1-1* background in these organs. Dissection of the seed into testa, endosperm and embryo, and subsequent GUS staining would be informative experiments. The absence of GUS staining in the apical meristem zone may possibly be due to the small size of these cells or because they are undergoing rapid division which drives the growth of the root (Fleming *et al.,* 1996). Finally, large cell sizes, such as epidermal and endodermal cells in the differentiation zone, might ‘dilute’ the GUS signal making it appear unstained compared to adjacent cells.

Staining of immature and mature flowers would have been an informative experiment as Sozzani *et al* (2006) demonstrate significant differences

in *PRT1* expression between these developmental stages as observed by GUS staining. Inclusion of F-GUS in the complementing line background (MO14-7-1) would have been useful to aid comparison between F-GUS Col-0 and F-GUS *prt1-1* localisation.

Stabilisation of F-GUS in the *prt1-1* background was largely restricted to stomatal guard cells, with little staining observed in the surrounding cells. Conversely, in the F-GUS Col-0 background a complete absence of staining was observed. Liu *et al* (2007) state that distinguishing clear differences using GUS staining between the mesophyll and guard cells is difficult if a gene is expressed in both these tissues, which suggests that the stronger staining in the guard cells can be misleading due to its significantly smaller volume compared to the surrounding cells. Nonetheless the F-GUS *prt1-1* staining is discrete in the guard cells and concurs with data presented in the eFP browser (Yang *et al.,* 2008; Waese *et al.,* 2017).

F-GUS was quantified in both F-GUS *prt1-1* and Col-0 backgrounds using the HA tag on the fusion proteins. No bands were present in Col-0 seedlings, but Bortezomib treatment enabled detection of HA-tagged F-GUS in this wild type background. The relative log2 levels of protein expression were 1, 2.8 and 67.6 for Col-0 DMSO, Col-0 Bortezomib and *prt1-1* Bortezomib. This demonstrates that PRT1 degrades the model F-GUS substrate completely, hence no band on the blot or staining for untreated Col-0. However, inactivation of the proteasome stabilises F-GUS observed in the anti-HA Western and GUS staining. The band intensity was significantly higher in F-GUS *prt1-1* compared to wild type levels. Furthermore, the F-GUS staining in *prt1-1* mirrors that of Col-0 treated with proteasome inhibitors, although the staining is not as intense in the latter. This suggests that another mechanism of degradation, such as autophagy, may be responsible for this disparity in F-GUS levels or that the PI is unable to completely penetrate certain tissues.

The PRT1-TAP fusion protein was readily detected in roots of the MO14-7-1 line in untreated conditions but not in shoots. The F-GUS staining in

the *prt1-1* background is observed extensively in both roots and shoots. Following proteasome inhibitor treatment however, PRT1-TAP protein could be observed in both roots and shoots of seedlings. This implies that PRT1-TAP protein half-life is shorter in leaves than roots. Degradation of E3 ligases has been demonstrated to be an integral part of their mechanism (de Bie & Ciechanover, 2011). Following potential substrate interaction in the leaves, PRT1 may be targeted for degradation which can be either self-catalysed or via an external ligase(s). Treatment with proteasome inhibitors prevents this degradation in leaves and PRT1 can therefore be observed in leaves. Given the ease of PRT1-TAP detection, it can be inferred that PRT1 does not get rapidly degraded in roots. Following an experiment investigating the potential physiological link between PRT1-mediated degradation, heat stress and fertility, an anti-SBP Western blot also demonstrated that the PRT1-TAP fusion could not be detected in flowers. Despite the F-GUS activity reporter data indicating that PRT1 is active in these tissues, the inability to detect PRT1-TAP implies that, PRT1 has a short half-life in flowers.

There is currently no PRT1-specific antibody available. Use of such an approach would be beneficial for immunological studies as it circumvents the use of fusion tags (such as those use in this study) which may produce artefacts in expression patterns that do not accurately reflect *in vivo* gene regulation of PRT1, such as disruption to folding or ubiquitination. Additionally, an anti-PRT1 antibody would enable native PRT1 abundance to be monitored. This would be a useful tool to assess PRT1 regulation following substrate interaction. Moreover, immunological studies could provide useful information regarding the cell type and subcellular localisation of the PRT1 protein.

Tandem affinity purification approaches were trialled for isolation of potential weak and strong PRT1-interacting proteins in roots however these experiments were unsuccessful due to technical issues with elution of the strong interacting proteins from the streptavidin beads. This assay should be repeated and optimised by alteration of the elution steps from

streptavidin beads by increasing time and concentration of DTT to help identify the PRT1 interacting proteins at this developmental stage. The TAP experimental design could be improved in future studies. A catalytically disabled PRT1 E3 ligase would bind to, but not release its substrate. This technique, called 'substrate trapping' allows detection of low-affinity E3–substrate interactions and low-abundance substrates (Iconomou & Saunders, 2016). Many methods for identifying the substrates of E3 ligases are insensitive to post-translational modifications of ubiquitin, E3 ligases or substrates. These possibly alter the E3 ligase activity and substrate binding and complicate E3 ligase substrate identification (Swatek & Komander, 2016; Buetow & Huang, 2016). Given that PRT1 is hypothesised to undergo auto-ubiquitination and degradation in leaf material and the TAP-PRT1 protein cannot be detected in these tissues, preventing this self-regulation would allow TAP experiments in leaf tissue. Approaches may involve treatment of leaf material with PYR-41, a cell permeable inhibitor of E1, to prevent ubiquitination (Yang *et al.,* 2007).

A more global quantitative proteomics approach such as Tandem Mass Tagging with Liquid Chromatography Mass Spectrometry (TMT-LCMS) is desirable for root tissues in order to identify proteins with altered abundance, or more targeted proteomics approaches such as terminal amine isotope labelling of substrates triple dimethyl labelling for identification and quantification of protein N-termini in Arabidopsis (Zhang *et al.,* 2015, Zhang *et al.,* 2018).

PRT1 is predicted to be nuclear localised (SUBAcon database, http://suba.live; Hooper *et al.,* 2014) however PRT-YFP confocal microscopy analysis did not provide conclusive results regarding subcellular localisation. Partially complementing lines for PRT1-YFP (MO16-3-1) construct were used in this study and therefore the mutant tagged YFP may be incorrectly targeted. Further selection of MO16 constructs on both methotrexate and kanamycin plates. Counterstaining with DAPI, a fluorescent stain with specificity for nuclei, would assist analysis of PRT1 subcellular localisation. Transient gene expression of

PRT1-YFP in Arabidopsis or tobacco may be a useful alternative to analyse PRT1 subcellular localisation. Agroinfiltration or a biolistic delivery mechanism of plasmid DNA into epidermal cells of plant leaves could enable efficient and reproducible transient expression (Sparkes et al., 2006; Li et al. 2009; Ueki *et al.,* 2013).

The data presented in this chapter provides initial starting points for the search of a physiological function for PRT1. F-GUS activity reporters imply that PRT1 is localised and expressed throughout the plant throughout development. PRT1 is readily detectable in root tissues via the PRT1—TAP tag. It is proposed that PRT1 is degraded in leaf tissue in seedlings and mature plants since the E3 ligase can only be observed in these tissues following proteasome inhibition. Taken together, these findings imply that PRT1 may be involved in root physiological responses or substrate degradation in leaves which triggers PRT1 auto-ubiquitination. The following chapter uses this information to guide experiments investigating the role of PRT1 in responses to abiotic stresses.

Chapter 4: Screening abiotic factors for a physiological function requiring PRT1-mediated protein degradation

4.1 Introduction

Due to their sessile nature, plants have to adapt to their environment, and tolerate or mitigate abiotic stresses through multiple biochemical modifications and physiological responses. Understanding the complex and integrated pathways facilitating these responses is essential. Over 30% of the proteome in *Arabidopsis thaliana* is poorly characterised, with over 13% of proteins having completely unknown function (Luhua *et al.,* 2012). Using an mRNA profiling method, Horan *et al.* (2008) annotated genes of unknown function and concluded that the transcripts of many of these genes were expressed in response to environmental stresses. Unknown or poorly characterised genes have the potential to play a fundamental role in plant responses to environmental cues; *PRT1*, whose physiological function and substrate profile remains unconfirmed, could be an example of such a gene. Environmental stresses result from unfavourable conditions for the optimal growth and development of organisms and can be categorised either as abiotic or biotic. Abiotic stresses arise due to non-optimal levels of a component of the environment, such as water deficiency or drought (Kaplan *et al.,* 2004). Survival of a plant is due to its capability to tolerate or recover from the stress due to basal or acquired tolerance mechanisms (Levitt *et al.,* 1972). Genes may be implicated in plant response to a single stress and some genes may mediate reaction to several environmental stresses (Reddy *et al.,* 2011). The latter indicates their function is reliant on stress signal transduction or may function in a concerted way with multiple or acclimation mechanisms to the stress (Mitter *et al.,* 2017).

An area of growing interest is the role of the plant N-end rule pathway in response to environmental stresses. The Cys-Arg N-end rule pathway plays a key role in the plant homeostatic response to oxygen and sending of nitric oxide through the regulation of transcription factors belonging to group VII of the ethylene response factor family (ERFVIIs) (Gibbs *et al.,*

2011; Licausi *et al.,* 2011; Gibbs *et al*., 2014). Substrates bearing N-terminal cysteine are oxidised in the presence of both these gases, arginylated by arginyl transferases (ATEs) (White *et al.,* 2017) and degradation is mediated by the PRT6 E3 ligase and the 26S proteasome. Absence of O_2 or NO causes substrate stabilisation (Gibbs *et al.* 2014). Vicente *et al* (2017) demonstrated that the Cys-Arg/N-end rule pathway is also a general sensor of abiotic stresses in *Arabidopsis thaliana* and barley (*Hordeum vulgare)*, sensing abiotic stresses either directly via oxygen sensing or indirectly through nitric oxide sensing downstream of nitrate reductase. It has been proposed that that the Cys-Arg N-end rule pathway mediates the integration of the environment and the plant response thus enhancing the survival (Vicente *et al.,* 2017).

In contrast to the important roles that PRT6 fulfils in plant responses to the environment, to date, no biological function has been assigned to PRT1-mediated protein degradation in relation to abiotic stresses. Although it is known PRT1 is an E3 ligase with specificity for proteins bearing aromatic residues at their N-terminus (Potushak *et al.,* 1998), the physiological consequences of degrading these proteins and how this N-recognin fits into the whole plant context is not understood.

Prior to this study, no physiological roles had been ascribed to PRT1. In the original publication in which the *prt1* mutant was identified, preliminary phenotyping experiments revealed no significant differences although a slight delay to germination and generally slower life cycle was suggested (Bachmair *et al.,* 1993). Building on these findings, the subsequent PRT1 publication by Potushak *et al* (1998) observed that higher temperatures, amino acid analogs, or heavy metals toxicity affected *prt1* similarly to Col-0*.* Additionally, *prt1-1* demonstrated no extreme abscisic acid (ABA) or seedling sucrose sensitivity as seen in *prt6-1* mutants (Holman *et al.,* 2009). In the Theodouolou lab, Dr Maria Ozvald and Dr Hongtao Zhang conducted preliminary physiological experiments including regreening, oil body retention, gibberellic acid treatment, sugar sensitivity, heat shock, 1-aminocyclopropane-1-

carboxylic acid (ACC) treatment and 2,4-dichlorophenoxyacetic acid. No robust phenotypic difference was observed for *prt1* compared to Col-0 (Rothamsted Research, unpublished data and personal communication).

The aim of this chapter was to attempt to identify potential physiological roles for PRT1 by screening the responses of the loss-of-function mutant *prt1-1* to a range of abiotic stresses. Complementing lines (*PRT1*$_{pro}$::gDNA-*PRT1*::TAP tag/ *PRT1*$_{pro}$::gDNA-*PRT1*::YFP in *prt1-1*) were used physiological screens in lieu of additional *prt1* mutant alleles. The general growth characteristics for Col-0, *prt1-1* and the complementing lines were initially determined for comparison to growth responses to other stresses. To facilitate the testing of many different conditions, physiological screens focused largely on root length and gross plant morphology.

4.2 Growth of *prt1-1* under non-stress conditions

The ability of plants to adapt to different environment stimuli is essential for survival. Screening mutant plant responses to different environmental influences is a strategy for identifying the potential involvement of specific genes in key physiological pathways. However, screening for a physiological function for PRT1-mediated degradation in Arabidopsis requires fundamental knowledge of the growth characteristics of lines to be used in phenotypic screens. Establishing the standard growth characteristics of *prt1-1* and Col-0 as well as the complementing line was a critical first step to establish a baseline for comparison in this study. This was particularly important for complementing lines since the induction of additional proteins to enable other studies (such as TAP tags for pull-down assays or Yellow Fluorescent Protein (YFP) fusions for protein visualisation) may place a growth burden on the plant. Initial experiments investigated whether there are significant developmental and physiological differences due to the *prt1-1* mutation.

4.2.1 Seed germination and seedling establishment

As the unit of dispersal, the seed is a critical stage of plant survival. Seeds must be capable of enduring unfavourable conditions for extended periods of time (Bentsink & Koornneef, 2008). Seed dormancy and the shift from quiescence to germination is a highly regulated and complex molecular process, requiring integration of many external environmental stimuli, hormonal cues, gene products and co-ordination of tissue responses (Holdsworth *et al.* 2008). Following germination, the growing plant relies on seed reserves including triacylglycerols, starch, and seed storage proteins which sustain the transition from germinated seeds to photoautotrophic established seedlings (Penfield *et al*., 2017). The N-end rule pathway has a well-established role in the regulation of these processes. PRT6 and ATEs have been demonstrated previously by Holman *et al.* (2009) to play a critical role in many aspects of seed germination and seedling establishment as positive regulators. *prt6* loss of function mutants have a diverse range of phenotypes related to germination and establishment. Germination of *prt6* null mutants is hypersensitive to inhibition by ABA and insensitive to nitric oxide (NO) (Holman *et al.,* 2009; Gibbs *et al.,* 2014). Establishment of *prt6* seedlings is hypersensitive to exogenous sucrose application and oil bodies are retained for several days longer in *prt6* seedlings after germination compared to Col-0 (Holman *et al.,* 2009). A recent study demonstrated that PRT6 is also involved in the complex regulation of protease activity and controls the mobilisation of seed resources through ERFVIIs (Zhang *et al.*, 2018). Overall, protein degradation via the Arg/N-end rule pathway functioning through the PRT6 E3 ligase and ATEs influences several aspects of the seed to seedling transition.

There are contrasting reports in the literature regarding a role for PRT1 in seeds. Bachmair *et al*. (1993) reported a slight delay in germination of *prt1-1* seeds but Holman *et al.* (2009) found that ABA sensitivity of *prt1-1* germination was similar to that of wild type seeds. Here, germination and establishment of *prt1-1* were re-examined.

The Arabidopsis Germination eFP browser (Waese *et al*., 2017) is a useful tool to query expression of a given gene in multiple community transcriptome datasets and provides a useful indication of *PRT1* gene expression during germination (Figure 4.1). Based on experiments conducted on freshly harvested Col-0 seeds following direct removal from siliques (H), seeds desiccated for 15 days in darkness (0 h), seeds stratified for 1, 12 and 48 hours (1/12/48 h S), and stratified seeds which were transferred to continuous light for 1, 6, 12, 24 and 48 hours (1/6/12/24/48 h SL). *PRT1* expression was greatest in dry seeds (26.07 ± 0.38), with a decline in expression observed following stratification (1h S 21.75 ± 4.9 to 12h S 19.46 ± 2.04). When seeds were stratified for 48 h and were transferred to constant light, a significant drop in expression levels was observed (48 h S = 0. 8.38 ± 0.91, 6 h SL= 9.39 ± 4.47). Finally, following germination *PRT1* expression increases (24h SL 16.86 ± 1.0 and 48h SL= = 15.47 ± 0.42. Overall, this indicates that *PRT1* is highly expressed in dormant seeds, with a decline being observed following stratification, and it is not highly expressed following transition from dormancy to germination.

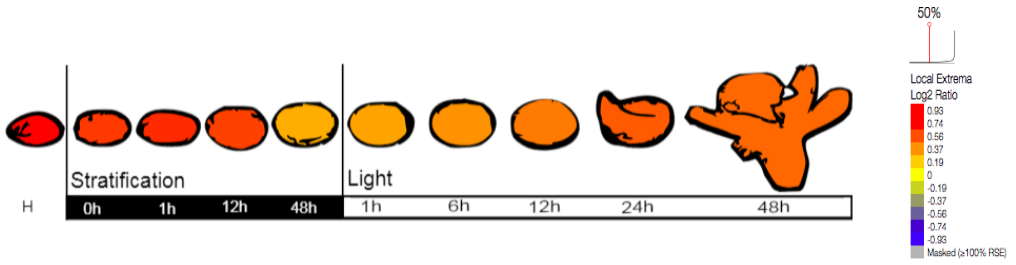

Figure 4.1: Absolute expression of *PRT1* in seed samples harvested at different time points and treatments. Adapted from the Arabidopsis Germination eFP browser at ePlant (Wassel *et al.,* 2017; https://bar.utoronto.ca/eplant/; accessed July 2018) showing the *PRT1* (At3g24800) expression in germination (Narsai *et al.,* 2011).

Germination and seedling establishment under long day conditions were scored in after-ripened, stratified seeds (Figure 4.2). There was no significant difference between Col-0, *prt1-1* and the complementing line MO16 (*PRT1*$_{pro}$::gDNA-*PRT1*::YFP in the *prt1-1* backrground) for testa rupture (A), radicle emergence (B) and establishment (C). 100% of *prt1-1* seeds had germinated by 48 h and established by 72 h after transfer to a long day cabinet.

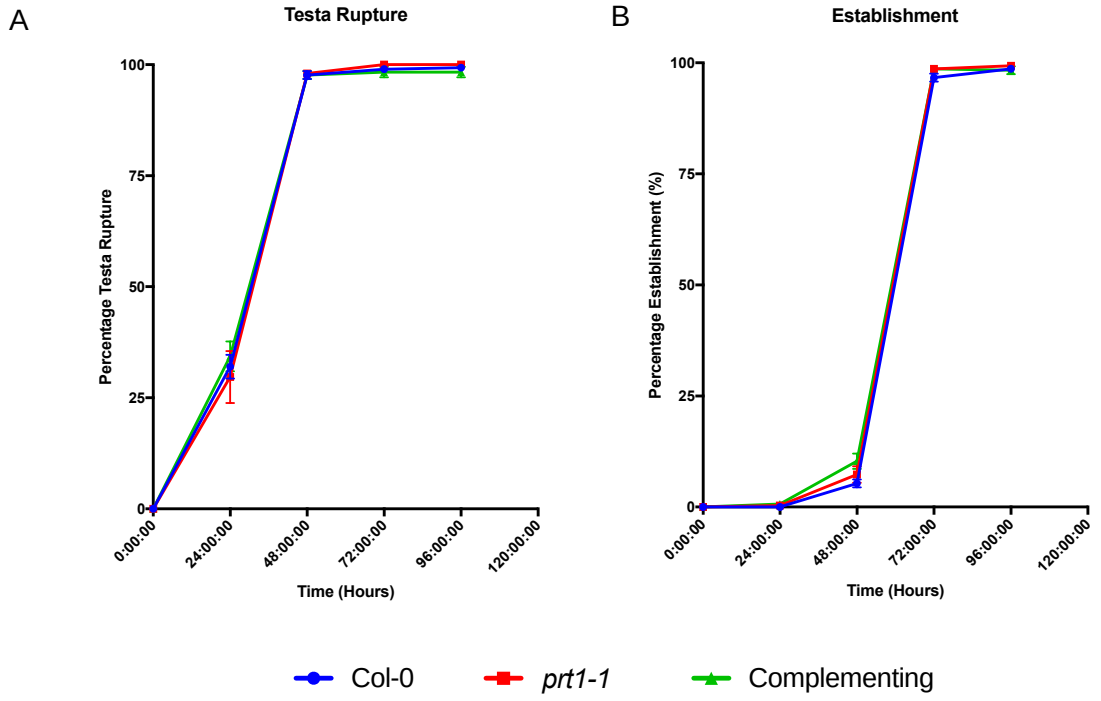

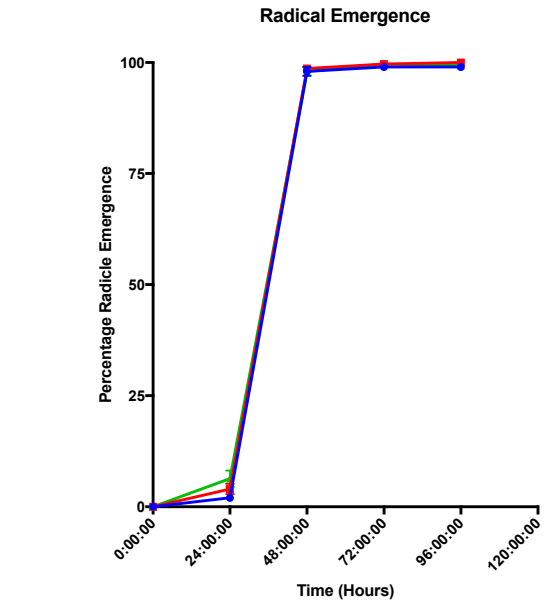

Figure 4.2: Germination and establishment rates of *prt1-1*, Col-0 and *PRT1*$_{pro}$::gDNA-*PRT1*::YFP in the *prt1-1* background as quantified by (A) testa rupture (B) radical emergence (C) Seedling establishment. Pooled data from 3 independent biological replicates (n=300; values = mean ± SEM). No significance determined by one-way ANOVA with Tukey's multiple comparisons test.

4.2.2 Root growth in constant light

The establishment of an efficient root system is fundamental to the success of a seedling as it is the means by which the plant accesses water and nutrients. Other N-end rule mutants including *prt6-1* and *ate1/2* display shorter primary root growth on 0.5 x MS media compared to Col-0. This phenotype is rescued in the presence of 0.5% sucrose (Holman *et al.,* 2009). To date, no root growth phenotype has been reported for the *prt1-1* mutant.

The tissue specific root eFP browser provides a high-resolution spatiotemporal map showing *PRT1* absolute expression data from 5-6 (radial data) and 7 (longitudinal data) day old seedlings (Cartwright *et al.* 2009; Brady *et al.,* 2007; Waese *et al.,* 2017). *PRT1* is not highly expressed in epidermal, cortex and endodermis cells in all the root zones as well as root hair cells under normal growth (Figure 4.3). The expression of *PRT1* relative to control increased in phloem, xylem and procambium cells as well as lateral root primordia. Expression was weakest in the root cap and intermediate elongation zones 9. Overall, *PRT1* is not highly expressed in roots. Contrary to this, the anti-SBP Western blot shown in chapter 3 demonstrated

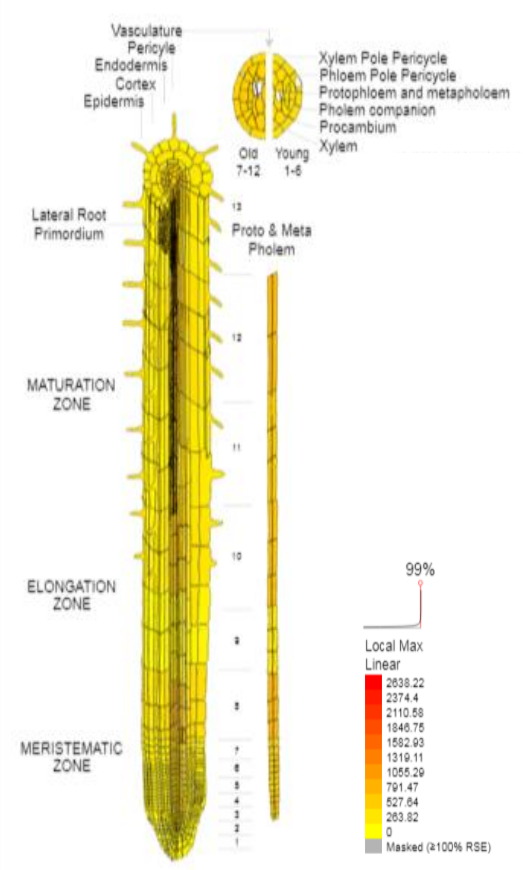

Figure 4.3: Absolute PRT1 expression in roots. Adapted from the root eFP browser at ePlant (Waese *et al.,* 2017; https://bar.utoronto.ca/eplant/; accessed July 2018) showing PRT1 expression (Cartwright *et al.*, 2009; Brady *et al*., 2007).

that, when driven by an endogenous promoter, tagged PRT1 protein is detectable in roots. Baseline phenotyping experiments tested root growth of *prt1-1,* Col-0 and the MO16 complementing line (*PRT1*$_{pro}$::gDNA-*PRT1*::YFP in the *prt1-1* background) on 0.5 x MS in constant light for 14 DAG at 24-h intervals. Images were analysed using Fiji (Schindelin *et al.,* 2012). Constant light was chosen for this starting point as it is standard in many root characterisation experiments.

A

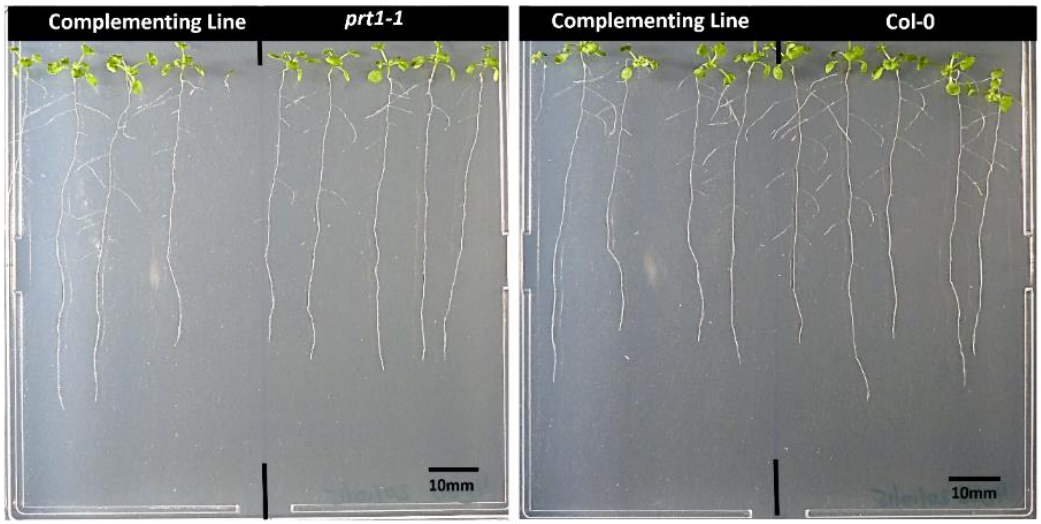

B

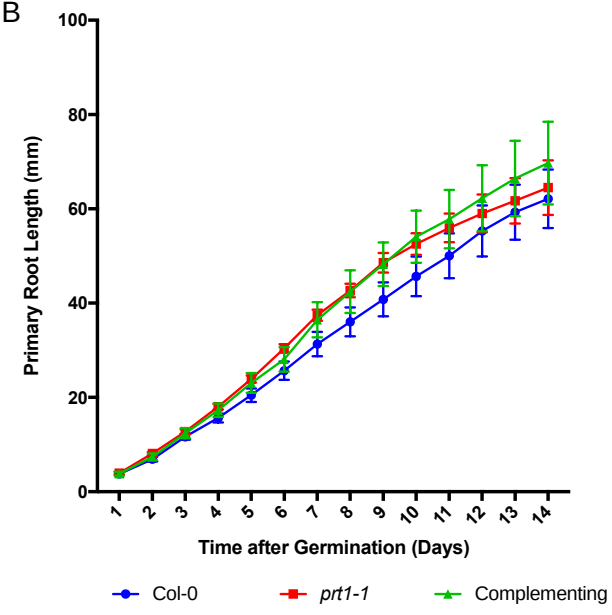

Figure 4.4: Primary root lengths quantified at 14 DAG in constant light for *prt1-1*, Col-0 and *PRT1*$_{pro}$::gDNA-*PRT1*::*YFP* in the *prt1-1* background: grown (A) representative images of primary root growth 14 days after germination in constant light and (B) quantified root kinetics plotted as mean ± SEM (n=10). No significance was determined by one-way ANOVA with Tukey's multiple comparisons test.

There was no significant difference in primary root length between Col-0, *prt1-1* and the complementing line over the initial 14 days of growth following germination (Figure 4.4). Although the growth rate of Col-0 appeared slightly slower between 3 to 12 DAG, the difference at any time point was not statistically significant, as determined by one-way ANOVA with Tukey's multiple comparison test.

After 14 DAG in constant light, plates were imaged using an infrared camera to enhance contrast between the root and plate and enable counting of emerged lateral roots (Figure 4.5A). The mean lateral number was not significantly different between for *prt1-1* (12.7 ± 0.357 mm), Col-0 (12.7 ± 0.427 mm) and the complementing line (12.0 ± 0.507 mm) (Figure 4.5B). Following imaging, seedling fresh weight was measured. Mean seedling fresh weights were 34.9 ± 2.30 mg, 38.7 ± 1.45 mg and 33.9 ± 2.66 mg for Col-0*, prt1-1* and the complementing line respectively (Figure 4.5C).

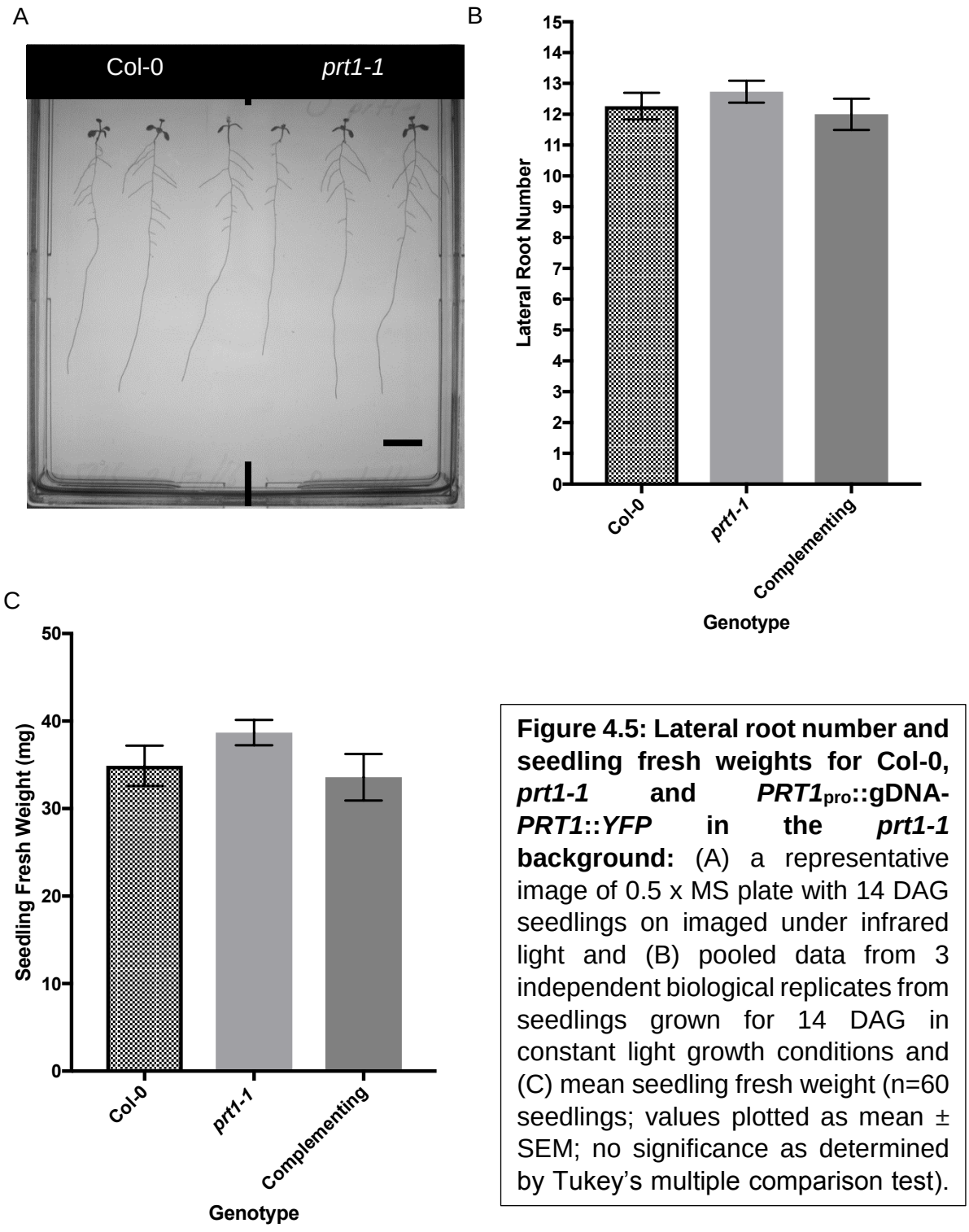

Figure 4.5: Lateral root number and seedling fresh weights for Col-0, *prt1-1* and *PRT1*$_{pro}$::gDNA-*PRT1*::*YFP* in the *prt1-1* background: (A) a representative image of 0.5 x MS plate with 14 DAG seedlings on imaged under infrared light and (B) pooled data from 3 independent biological replicates from seedlings grown for 14 DAG in constant light growth conditions and (C) mean seedling fresh weight (n=60 seedlings; values plotted as mean ± SEM; no significance as determined by Tukey's multiple comparison test).

4.2.3 Root growth under different photoperiods

Plants are autotrophic organisms that are dependent on light as a source of energy for photosynthesis. The rotation of the earth around the sun generates diurnal fluctuations in the light period or photoperiod. These photoperiods are also influenced by the seasonal proximity of the earth to the sun; the extent to which these photoperiods vary seasonally is further influenced by the latitude. Consequently, plants have to adapt to the varying photoperiod through dynamic regulation of plant metabolism in relation to the available energy (Dodd *et al.,* 2005). The net daily photosynthetic capacity and starch metabolism of a plant is governed by the photoperiod (Graf & Smith, 2011). This means that growth and flowering are influenced significantly by the circadian clock through tight molecular regulation. *Arabidopsis thaliana* is a long day plant (Hayama & Coupland, 2003; Kinmonth-Schultz, Golembeski & Imaizumi; 2015). During vegetative growth, the number, size, morphological characteristics of leaves are all determined through circadian clock-photoperiod length interaction (Baerenfaller *et al.,* 2015). The photoperiod therefore intimately links the plant growth to environmental light clues. Aberrant changes to the way light is perceived by plants can have significant and wider-spread ramifications to the plant, making it an important physiological function to characterise.

Primary root growth was compared under constant light, neutral days, short days and long days (Fig. 4.6) over a 5 d growth period. These experiments were conducted at Rothamsted Research. Following 2-way ANOVA analysis of the mean cumulative growth of primary roots over the 5 DAG period, p valves were 0.1066 and 0.2290 for constant light and long day conditions (n=12), respectively, indicating that there is no statistical significance when genotype is assessed as the source of variation (Figure 4.6A, D). For neutral day-grown plants, 2-way ANOVA analysis with post-hoc Tukey's multiple comparison test indicates that *prt1-1* grew faster than Col-0 at 4 and 5 DAG (p = 0.0123 and 0.00622 respectively), and the complementing line (MO14, *PRT1*$_{pro}$::gDNA-

PRT1::TAP tag in the *prt1-1* background) was slightly significantly longer than Col-0 at 5 DAG (p = 0.0062; Figure 4.6B). Primary roots of *prt1-1* plants grown in short days however were significantly longer over the 5-day period compared to the wild type and complementing line from 2DAG – 5DAG as demonstrated by p value <0.0001 (Figure 4.6C). Tukey's multiple comparison test indicated no statistical difference between the complementing line and Col-0 in this growth condition.

To determine the reproducibility of these results, primary root lengths were determined for these light conditions in growth cabinets at University of Nottingham (conditions 2.2.1). Over the 14 DAG period, no statistically significant difference could be determined between Col-0, *prt1-1* and *PRT1*$_{pro}$::gDNA-*PRT1*::TAP tag in the *prt1-1* background following 2-way ANOVA analysis with post-hoc Tukey's multiple comparison test for neutral days, constant light and long days (Figure 4.7A-C). The initial longer root from 2-5 DAG of *prt1-1* plants grown in short day light conditions was not observed in these conditions and no significant difference was observed for root length from 1 DAG to 19 DAG (Figure 4.7 D). At DAG 20 and 21 for neutral days grown plants, 2-way ANOVA analysis with post-hoc Tukey's multiple comparison test indicates that Col-0 primary root length was slightly longer than *prt1-1* (p = 0.0166 and 0.0406 respectively).

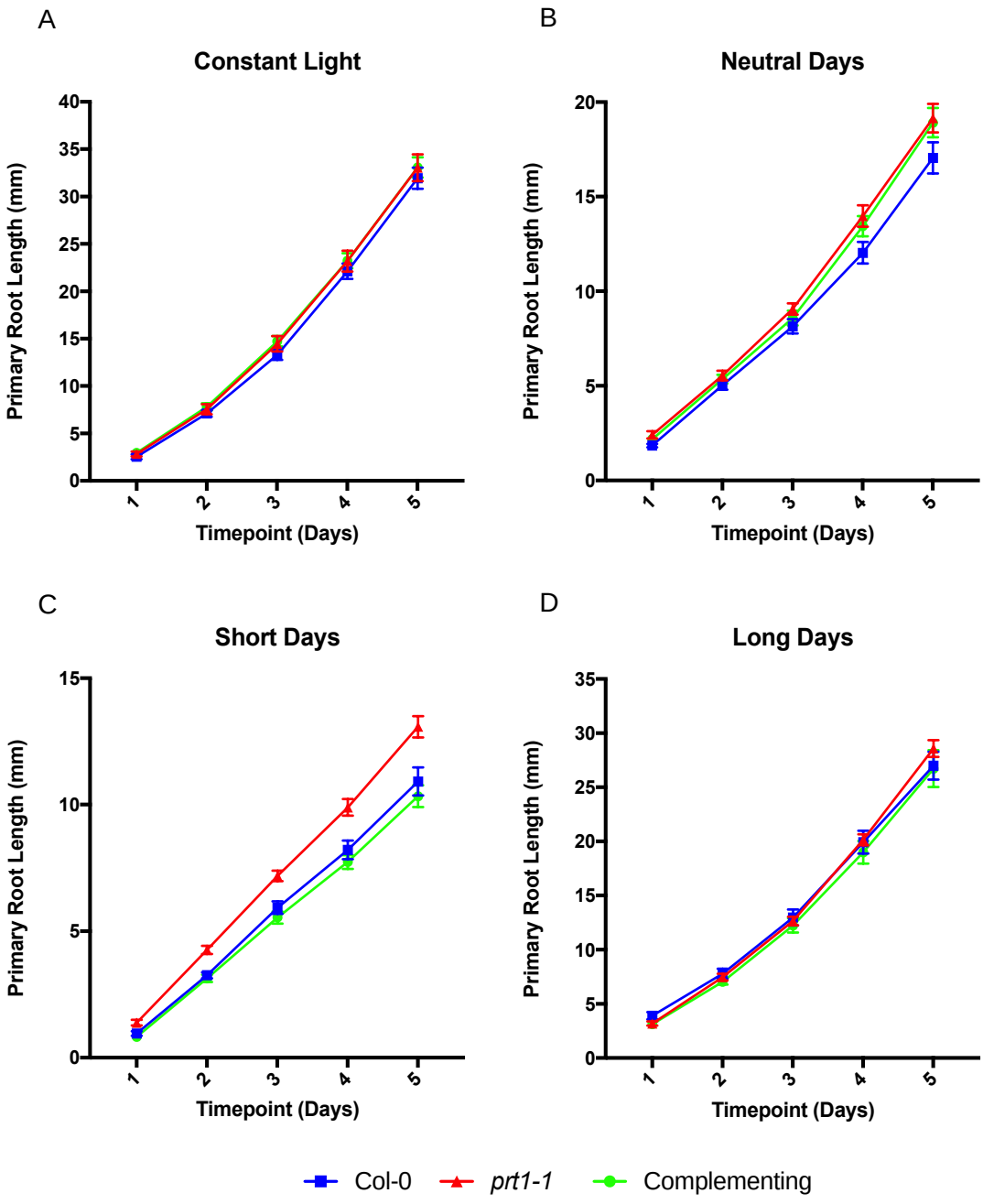

Figure 4.6: Primary root lengths over a 5-d period of Col-0, *prt1-1* and *PRT1*$_{pro}$::gDNA-*PRT1*::TAP tag in the *prt1-1* background for (A) constant light (B) neutral days (C) long days, with the exception of (D) short days. Values are mean ± SEM (n=12; no statistical significance was determined between genotypes by 2way ANOVA with Tukey's multiple comparison tests for constant light, long days and neutral days. Short days *prt1-1* primary roots were significantly longer than Col-0 and the complementing line).

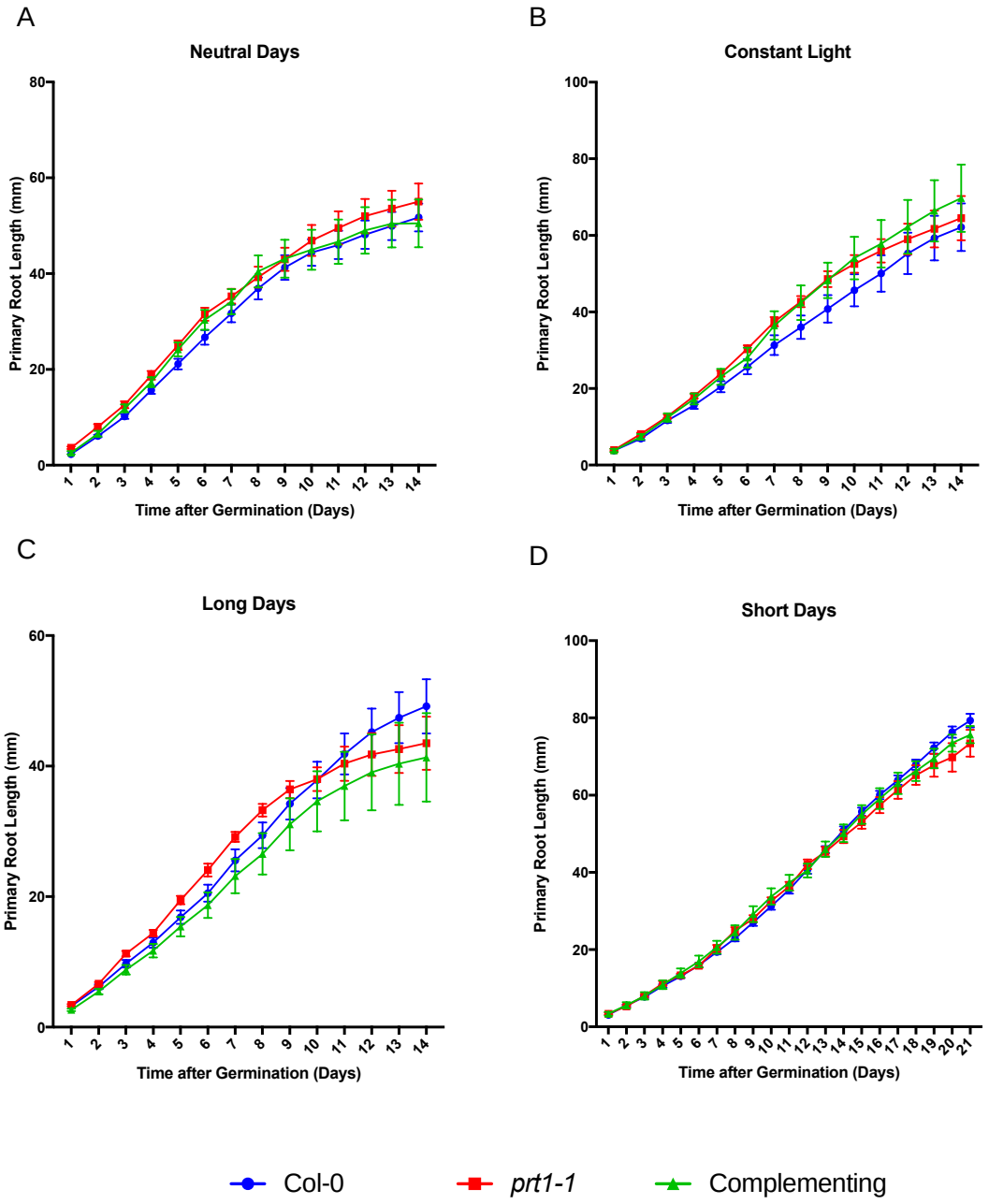

Figure 4.7: Primary root length over 14DAG of Col-0, *prt1-1* and *PRT1*$_{pro}$::gDNA-*PRT1*::TAP tag in the *prt1-1* background for (A) neutral days, (B) constant light, (C) long days and 21DAG for (D) short days. Values are mean ± SEM (n=10); no statistical significance was determined between genotypes by 2way ANOVA with Tukey's multiple comparison tests for all light conditions tested.

4.2.4 Biomass

The harvest of light energy from the sun, fixing into chemical energy and conversion of this energy into plant material is the accumulation of biomass. The conversion of this energy into biomass efficiency is considered inefficient. Very few mutants in Arabidopsis result in enhanced photochemistry, increased photosynthesis and more efficient biomass production (van Tol *et al.,* 2017). Given that the N-end Rule pathway is a proteolysis pathway, N-end rule mutants are predicted to stabilise substrates which would normally be degraded. If these stabilised substrates over-accumulate or have toxic effects on the cell, they may have a detrimental impact on plant health. Bachmair *et al* (1993) proposed that the *prt1-1* mutation may be manifest as an overall generally slower lifecycle. It is therefore important to establish whether there is a cost to the plant for the *prt1-1* mutation.

Col-0 and *prt1-1* plants were grown for 7.5 weeks on soil under long day conditions and the fresh weights were determined for rosettes and roots (Figure 4.8). The mean shoot weight for Col-0 was 459.2 ± 7.1 mg and 467.0 ± 12.9 mg for *prt1-1.* The mean fresh weights of roots were 145.3 ± 9.3 mg and 149.8 ± 7.5 mg for Col-0 and *prt1-1*, respectively. P values as determined by one-way ANOVA were 0.9775 for root and 0.8545 for shoot biomass, indicating no statistical significance. Thus, stabilisation of PRT1 substrates there does not appear to result in a trade-off in terms of plant root or shoot biomass.

A

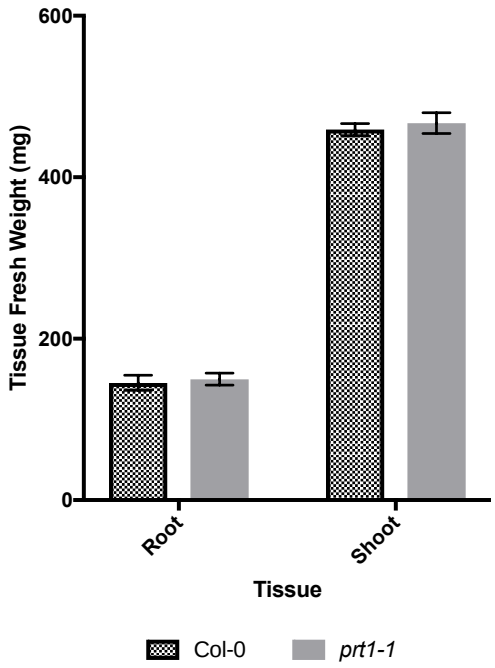

Figure 4.8: Fresh weight of roots and shoots (A) fresh weights taken from 8-week Col-0 and *prt1-1* plants grown in long day growth conditions (n=6; values = mean ± SEM; no significance as determined by one-way ANOVA with Sidak's multiple comparison test (B) a representative image of plants used to determine fresh weight of *prt1-1* and Col-0.

B

.

4.2.5 Stomatal conductance

Stomata are specialised pores found extensively on the abaxial and adaxial leaf surfaces which facilitate gaseous exchange with the leaf exterior and regulate transpirational losses. Stomatal aperture is tightly regulated through turgor pressure and allows rapid fine-tuning of gas exchange to a changing external environment while maintaining photosynthetic capacity (Damour *et al.,* 2010). Stomatal conductance is an estimate of the rate of gas exchange between the plant and the external environment. It is a function of the size, density and aperture of stomata present (Lawson, Pijut & Michler. 2014). Changes from normal stomatal conductance can have dramatic ramifications for plant yield due to changes to photosynthetic capacity and water loss (Wang *et al.,* 2014), thus making it an important avenue for investigation.

Guard cell gene expression data are available through eFP browser (Yang *et al*., 2008; Waese *et al.,* 2017). Absolute expression of *PRT1* is high (445.52 AU) in untreated guard cells compared to surrounding mesophyll cells (169.41 AU) and increases only modestly in response to ABA treatment (217.64 AU; Figure 4.9), suggesting that *PRT1* is not significantly induced during ABA-mediated stomatal closure. The strong expression of *PRT1* transcripts in guard cells concurs with the results of F-GUS staining in chapter 3.

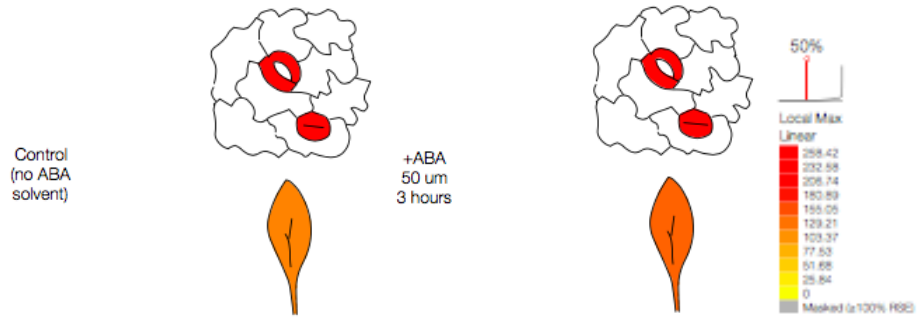

Figure 4.9: Absolute expression of *PRT1* in stomata guard cells Adapted from the Arabidopsis the guard cell mutant and wild type guard cell ABA response eFP browser at ePlant (Wassel *et al.* 2017; https://bar.utoronto.ca/eplant/; accessed July 2018) in ethanol control and ABA treated samples.

As a preliminary indication of stomatal conductance, water loss from detached rosettes was estimated by reduction in fresh weight over a 7-h period. No significant difference could be observed between Col-0, *prt1-1* and *PRT1*$_{pro}$::gDNA-*PRT1*::TAP tag in the *prt1-1* background at any time point during the experimental period (Figure 4.10). Since this method only permits a crude estimation of transpiration, stomatal apertures were measured by Joanna Landymore (group of Professor Julie Grey, University of Sheffield). No significant difference was observed between apertures of Col-0, *prt1-1* and the complementing line in control conditions or in response to ABA (data not shown, personal communication). Consequently, stomatal conductance was not pursued further.

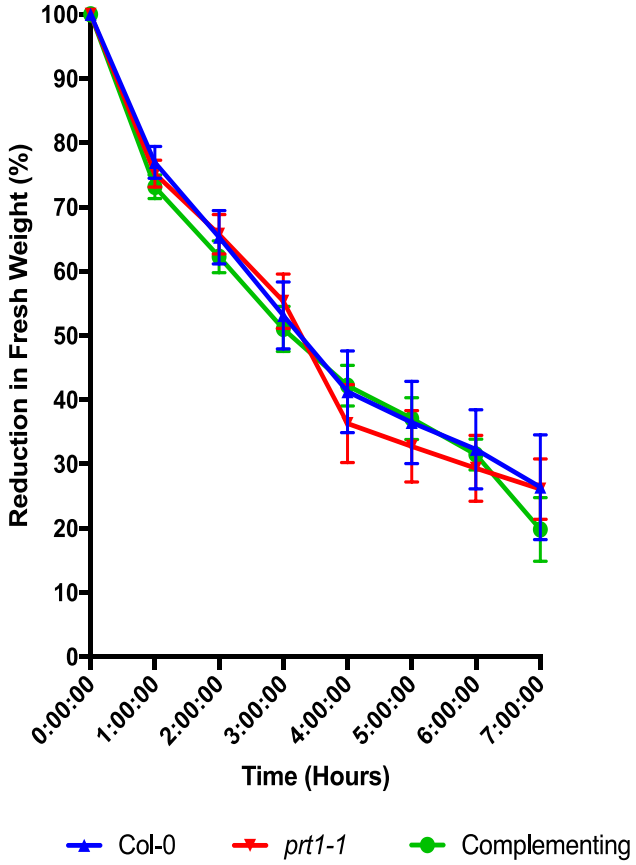

Figure 4.10: Preliminary experiments showing reduction in fresh weight over a 7 h period for Col-0, *prt1-1* and *PRT1*$_{pro}$::gDNA-*PRT1*::TAP tag in the *prt1-1* background. (n=6; values = means ± SEM; no significance determined by 2way ANOVA with Tukey's multiple comparison test.

4.2.6 Seed yield

Seed yield is a critical factor in all plants for reproductive success and is agronomically paramount for maximising profit from crop species. Seed yield is determined by the total number of seeds and the size of seeds. Large seeds are advantageous as they contain more nutrients to sustain the emerging plant following germination and the transition to establishment as well as increased tolerance to abiotic stresses. Conversely, smaller seeds are more efficiently dispersed and colonise faster (Westoby *et al*., 2002; Moles *et al*., 2005), meaning there is an optimum middle ground for both these factors, depending on species and ecological niche. Seed size is genetically controlled and tightly regulated. Final seed size is governed by the seed zygotic tissues, triploid endosperm and the seed coat (Van Daele *et al.,* 2012). The number of seeds is negatively correlated with seed size (Alonso-Blanco *et al*., 1999). F-GUS staining experiments (Chapter 3) demonstrated an accumulation of F-GUS in flowers, anthers, stigma and stamen in the *prt1-1* background (Figure 3.11) indicating that PRT1 is active in these reproductive tissues and might influence seed filling.

Preliminary observations suggested that *prt1-1* plants may have altered seed yield (Hongtao Zhang and Maria Oszvald, personal communication). As a crude determination of seed yield, the total seed weight per plant was measured for *prt1-1* and Col-0 at 8 weeks growth in long day conditions. Total seed weight for Col-0 was slightly lower (172.487 ± 10.07 mg per plant) when compared to *prt1-1* (179.78 ± 16.131 mg per plant) but no significant difference was determined by one-way ANOVA with Sidak's multiple comparison test (p = 0.8831) (Figure 4.11A). Seed size was measured by analysing seed images with the Fiji package. A slight reduction in *prt1-1* average seed size (1.26 ± 0.017 mm^2) was observed compared to Col-0 (1.29 ± 0.013 mm^2), however this difference was not significant when data were analysed by one-way ANOVA with Sidak's multiple comparison test (n=100; p = 0.1120). Since the seed weight and seed size was not significantly

different between these lines, it is logical that the seed number is unlikely to be different between these genotypes.

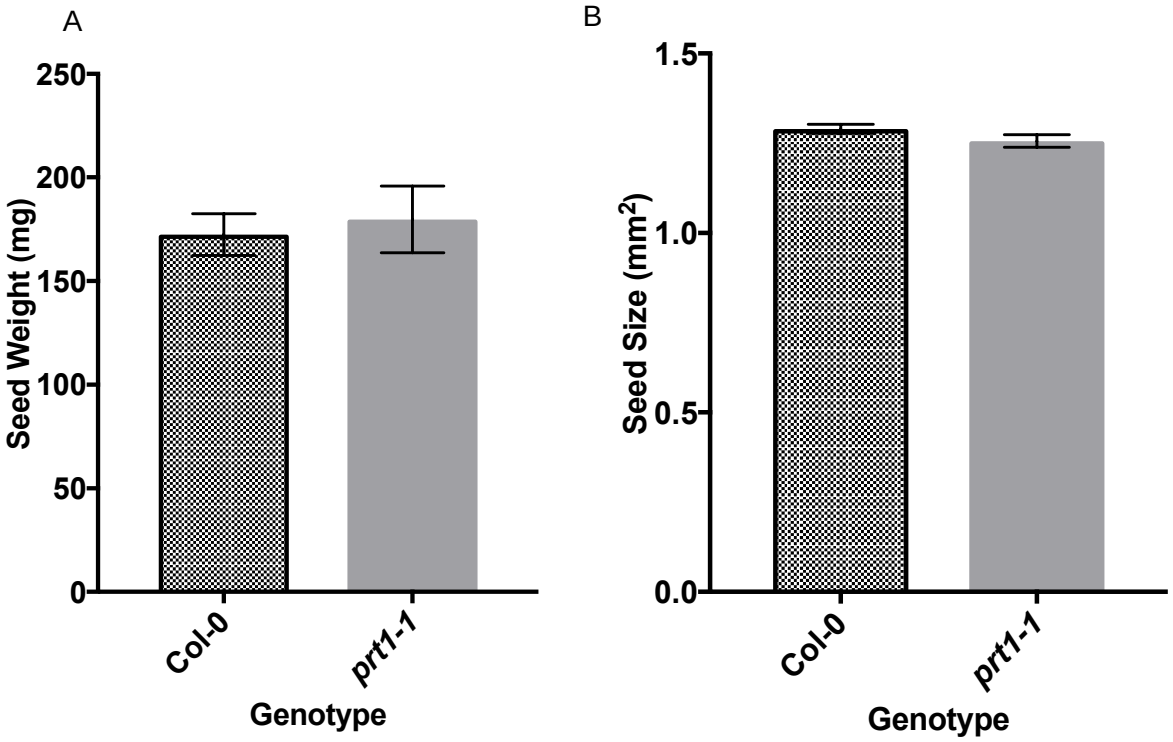

Figure 4.11: Seed yield for Col-0 and *prt1-1* (A) Seed weight (n=15) (B) seed size (n=100). Values are means ± SEM. No significance was determined by one-way ANOVA with Sidak's multiple comparison test.

4.3 Plant responses to abiotic stresses

Following general characterisation of *prt1-1,* Col-0 and the complementing lines, none of the experimental lines appeared significantly different to each other. The remainder of this chapter details experiments conducted to establish whether there are any differences between these lines in response to abiotic stresses. The eFP browser (Figure 4.12) indicates that *PRT1* expression is not significantly induced in response to a multitude of abiotic stresses compared to untreated plants.

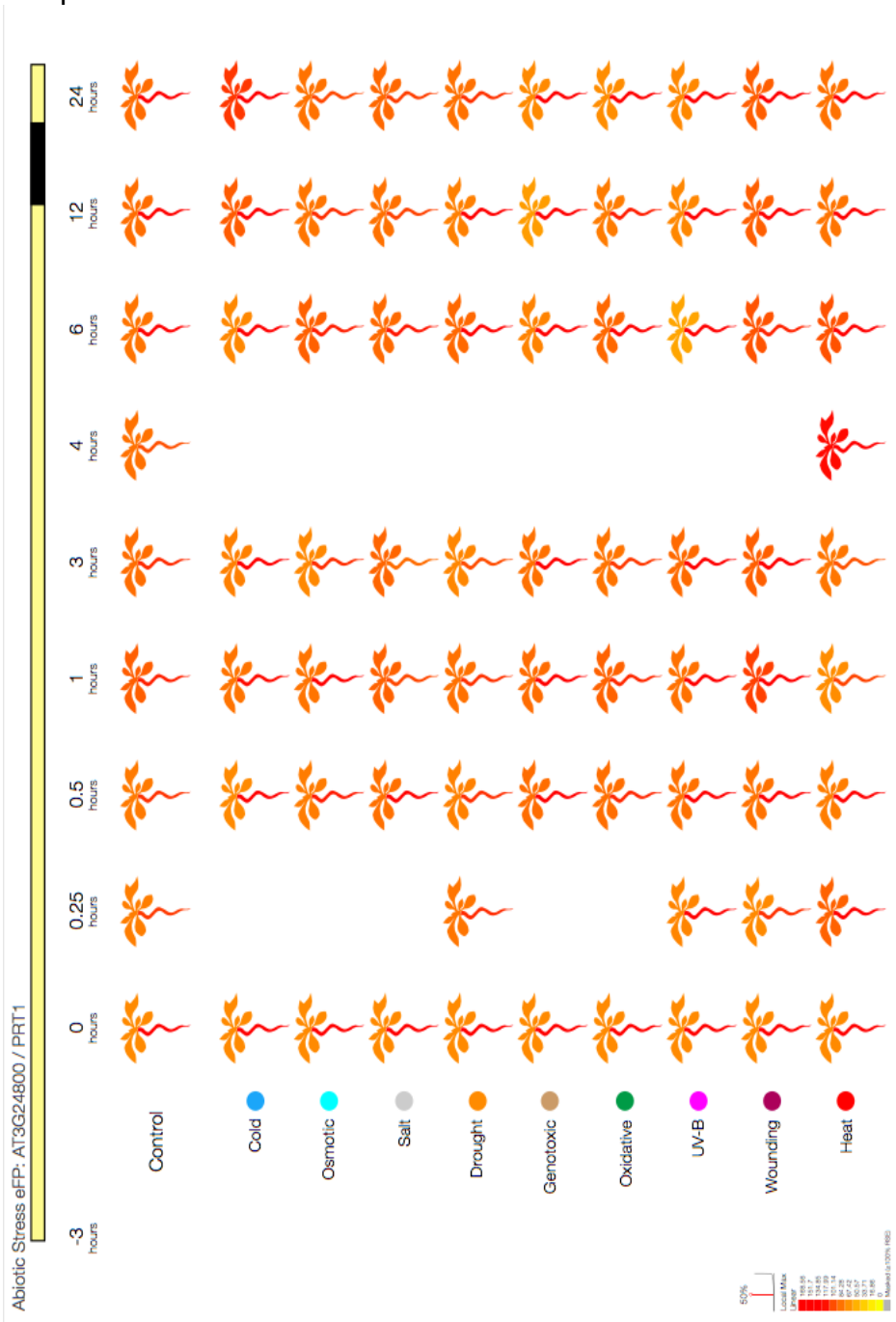

Figure 4.12: Expression of *PRT1* in public transcriptome datasets in control and plants stressed by various abiotic stressors. Adapted from the ePlant (Waese *et al.*, 2017; https://bar.utoronto.ca/eplant/; accessed July 2018) showing mapped *PRT1* (At3g24800) absolute expression profiles of the Affymetrix ATH1 array data (Kilian *et al.*, 2007) in response to different abiotic stresses.

4.3.1 Heat Stress

As with all organisms, plants have an optimum range of growth conditions in which they perform best. A small shift above or below these optimum conditions is characterised by a slight penalty to the organism's fitness. A dramatic shift outside this dynamic range however can lead to a huge fitness penalty or even have lethal consequences. Temperature is perhaps one of the best characterised environmental conditions studied in *Arabidopsis thaliana* (Liu *et al.,* 2015). Furthermore, fluctuation in water deficiency and temperature are intimately linked stresses that plants experience on an annual, seasonal, daily and even hourly timescale. Summer is generally characterised by high temperatures and lower water availability.

High temperatures have a significant impact on the plant yield and crop quality. Moving Arabidopsis seedlings to temperatures 5 °C or more above their optimum growth temperature is linked with the induction of heat shock proteins (HSP) and repression of normal protein synthesis (Vierling, 1991) in a short time frame. Heat stress overall has a negative impact on the fitness of plant, and the timing of the stress is especially critical. Heat in excess during seed production can have an extremely detrimental effect on the fitness of the plant. Additionally, if the temperature is too high during germination, a seedling may never establish. However, during vegetative growth stages, a less severe impact of the same stress may be observed. Experimentally accessible tissues including roots and leaves have been the main focus of heat stress studies (Iba *et al.,* 2002; Yamaguchi-Shinozaki & Shinozaki, 2006; Chunnusamy *et al.,* 2007; Kotak *et al.,* 2007; Wahid *et al.,* 2007), whilst reproductive tissues have been neglected due to their complexity, inaccessibility and activity within a narrow timeframe (Zinn, Tunc-Ozdemir & Harper, 2010; De Storme & Geelen, 2014).

Plants were grown for 3 weeks under long day conditions. Half of the plants were kept in this condition for 2 and 3-week time points (untreated

or U/T) and the remainder of the sample set were transferred to a long day growth chamber (16 h light/28^{o}C, 8 h Dark/28^{o}C) for this same period (Heat Stressed or HS). For heat stressed plants, wilting to stems, fewer rosette leaves and floral buds, and silique lengths were smaller with fewer seeds per silique than control treatments, indicating the heat stress was having a significant impact on plant growth and fertility. However, the rosette appearance, stem and floral bud number of these plants were indistinguishable between genotypes for each treatment type (data not shown). There were no obvious morphological differences observed between Col-0, *prt1-1* and *PRT1*$_{pro}$::gDNA-*PRT1*::TAP tag in the *prt1-1* background were stressed for 2 or 3 weeks at 28^{o}C in terms of floral morphology (Figure 4.13), pollen morphology (Figure 4.14) and siliques (Figure 4.15).

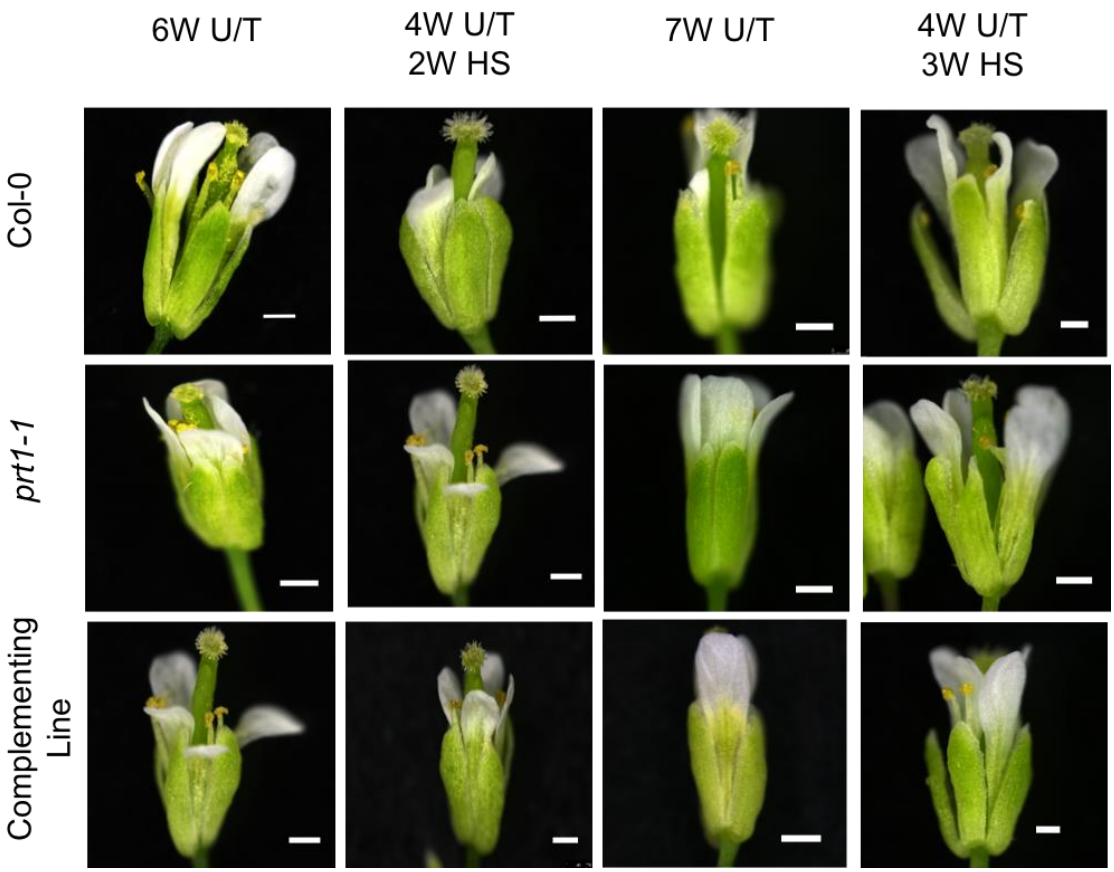

Figure 4.13 Floral morphology in unstressed and heat stressed growth conditions: Representative images showing 6 and 7-week-old (W) flowers of Col-0, *prt1-1* and *PRT1*$_{pro}$::gDNA-*PRT1*::TAP tag in the *prt1-1* background were heat stressed (HS) for 2 weeks and 3 weeks alongside unstressed controls (U/T) (scale bar = 100 μm).

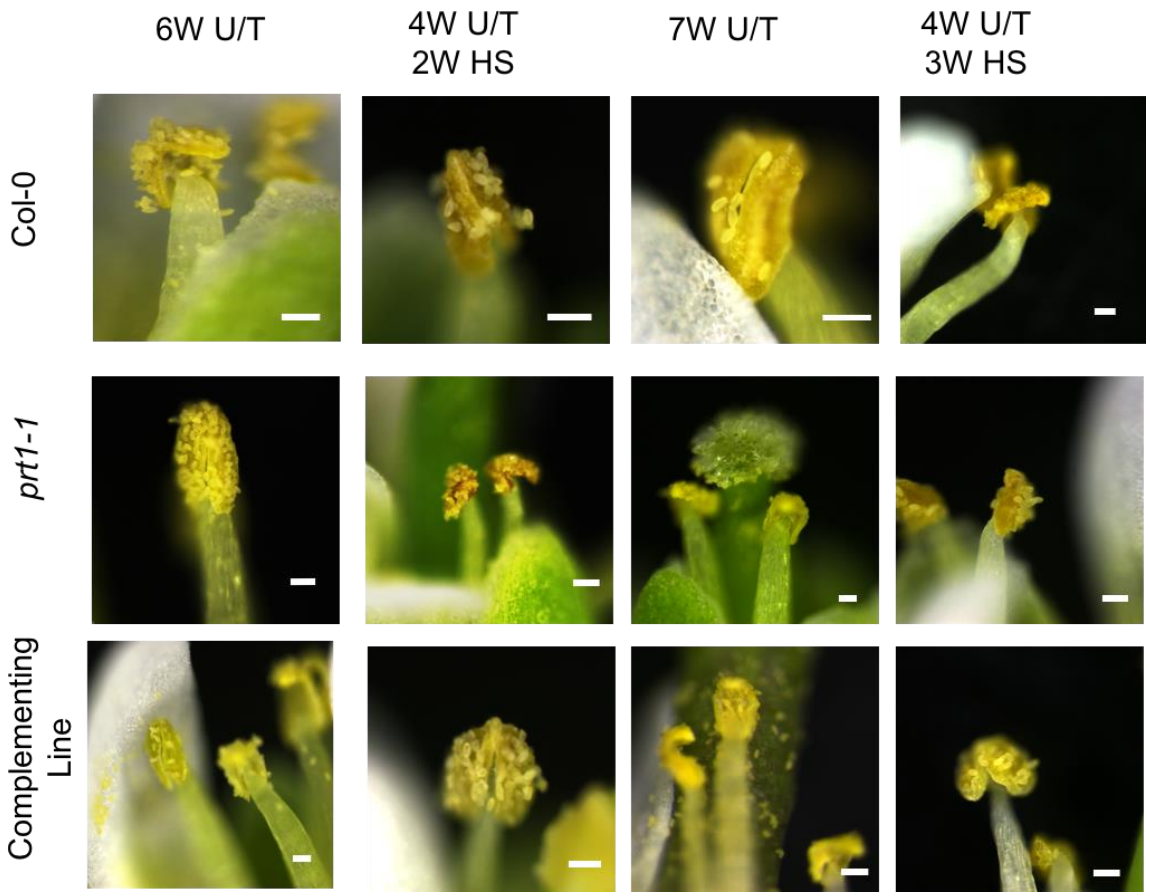

Figure 4.14: Anther and pollen morphology following heat stress. Representative images showing 6 and 7-week-old flowers of Col-0, *prt1-1* and *PRT1*$_{pro}$::gDNA-*PRT1*::TAP tag in the *prt1-1* background were heat stressed (HS) for 2 weeks and 3 weeks alongside unstressed controls (U/T) (scale bar = 75 μm).

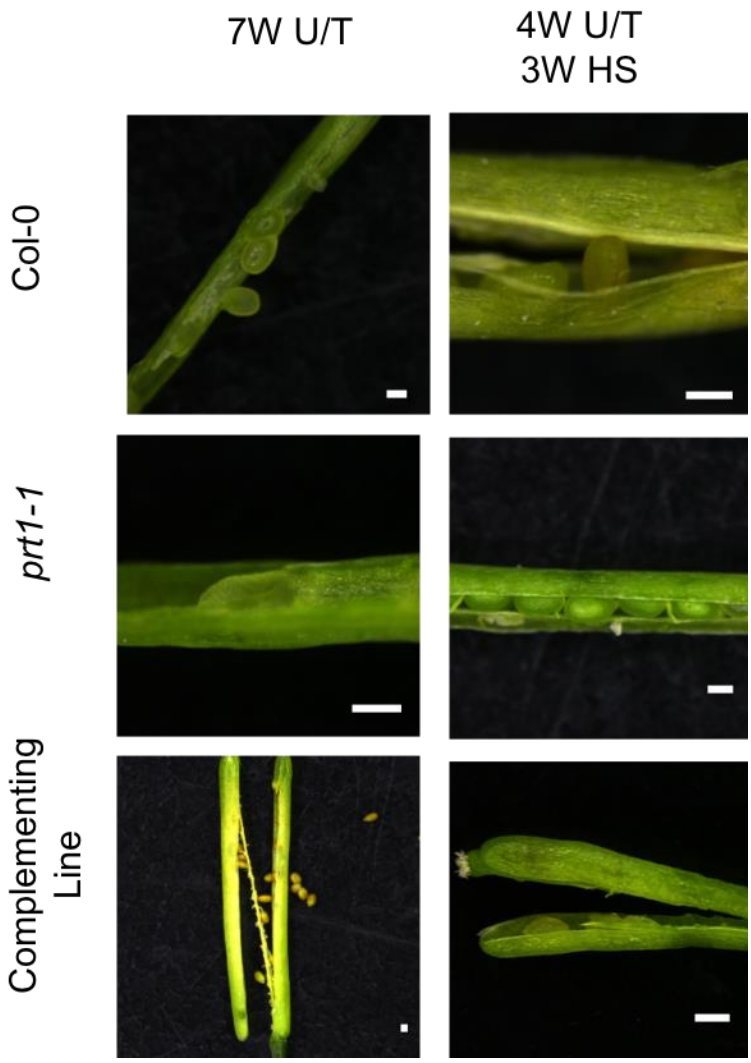

Figure 4.15: Silique filling following heat stress. Representative images showing 7-week-old (W) flowers of Col-0, *prt1-1* and *PRT1*$_{pro}$::gDNA-*PRT1*::TAP tag in the *prt1-1* background were heat stressed (HS) for 2 W and 3 W alongside unstressed controls (U/T) (scale bar = 200 μm).

4.3.2 Salt Stress

Salinisation is the increasing concentration of salt within soils and is a problem for approximately 20% of irrigated farmed land worldwide, predicted to get worse due to climate change, population expansion and intensive agriculture (Liu *et al.,* 2007). The development of crops that are able to tolerate salt stress would help address some of these challenges: one route to understanding and manipulating salt tolerance begins with dissecting salt signalling in a model species such as Arabidopsis. Plant species differ dramatically in their ability to tolerate salt. Although *Arabidopsis thaliana* is a typical glycophyte, and does not tolerate high salinity, studies by Shinozaki and Yamaguchi-Shinozaki (2000), Zhu (2000) and Shinozaki *et al* (2003) reveal that the Arabidopsis genome contains the majority of the genes for salt tolerance present in Arabidopsis-related halophytes. *Thellungiella halophila* (salt cress) is a halophyte related to Arabidopsis, whose complex developmental, physiological and biochemical mechanisms enable this plant to respond to high salinity. Taji *et al.* (2004) compared the gene expression profiles of *Thellungiella halophila* and Arabidopsis. Under salt stress, simulated by 250mM NaCl-supplemented half strength Murashige and Skoog media, comparatively few genes were induced in salt cress when compared to Arabidopsis. Conversely, biotic- and abiotic-stress inducible genes were induced in salt cress in the absence of a saline stress. Interestingly in normal conditions, the gene encoding the *Thellungiella halophila PRT1* homologue was up-regulated by a $\log_2$ ratio of 1.96 compared to Arabidopsis.

When grown on high salt media, null mutants in the Arabidopsis PRT6 E3 ligase exhibits enhanced survival rates and a hypersensitive germination response is also observed (Vicente *et al.,* 2017). This presents an interesting question as to whether PRT1 also plays a role in the adaptation of the plant to salt stress.

Data from the Arabidopsis eFP browser (Winter *et al.,* 2007; Bassel *et al.,* 2008) indicates that there is no significant induction in *PRT1* expression following treatment with 150 mM NaCl (Figure 4.16) over a 24 h treatment period. Since such findings are based on normalised microarray data they should be viewed tentatively, and transcriptional regulation may not be needed for *PRT1* to play a role, therefore plant responses to salt shouldn't be dismissed as a line of enquiry for a physiological role for PRT1.

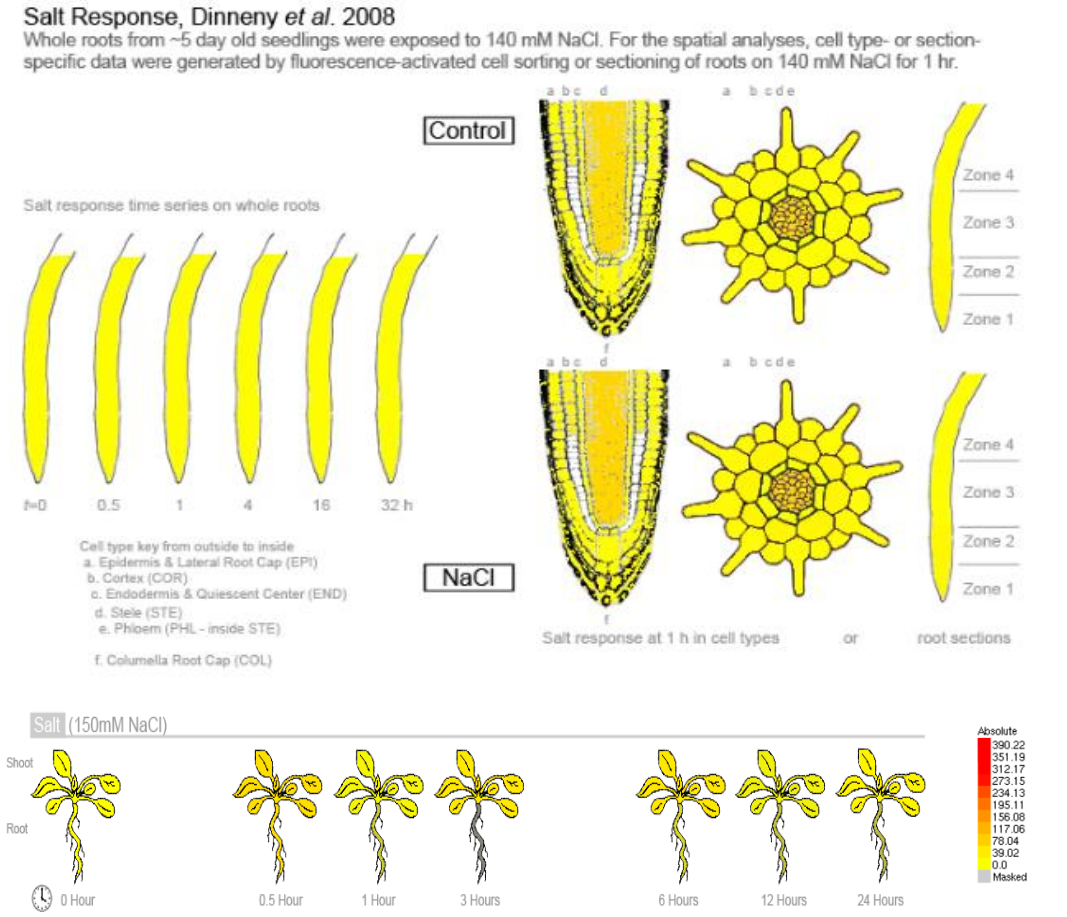

Figure 4.16: Expression of *PRT1* in response to salt stress in public transcriptome datasets: Image adapted from the Arabidopsis eFP browser (Winter *et al.,* 2007; https://bar.utoronto.ca/eplant/; accessed July 2018) demonstrating the absolute expression of *PRT1* (At3g24800) in Arabidopsis 5-day old roots with and without 1-hour exposure to 140mM NaCl (Bassel *et al.,* 2008).

To test whether PRT1 plays a role in the response to salt, germination, establishment and root length were quantified under different salt concentrations. There was negligible difference observed between Col-0, *prt1-1* and *PRT1pro*::gDNA-*PRT1*::YFP in the *prt1-1* background during the 96-h period for testa rupture (Figure 4.17), radicle emergence (Figure 4.18) and establishment (Figure 4.19) on 0.5 x MS media supplemented with 0 mM, 75 mM,100 mM and 120 mM NaCl. Overall this indicates there is no dramatic impact on germination and establishment in plants bearing the *prt1-1*.

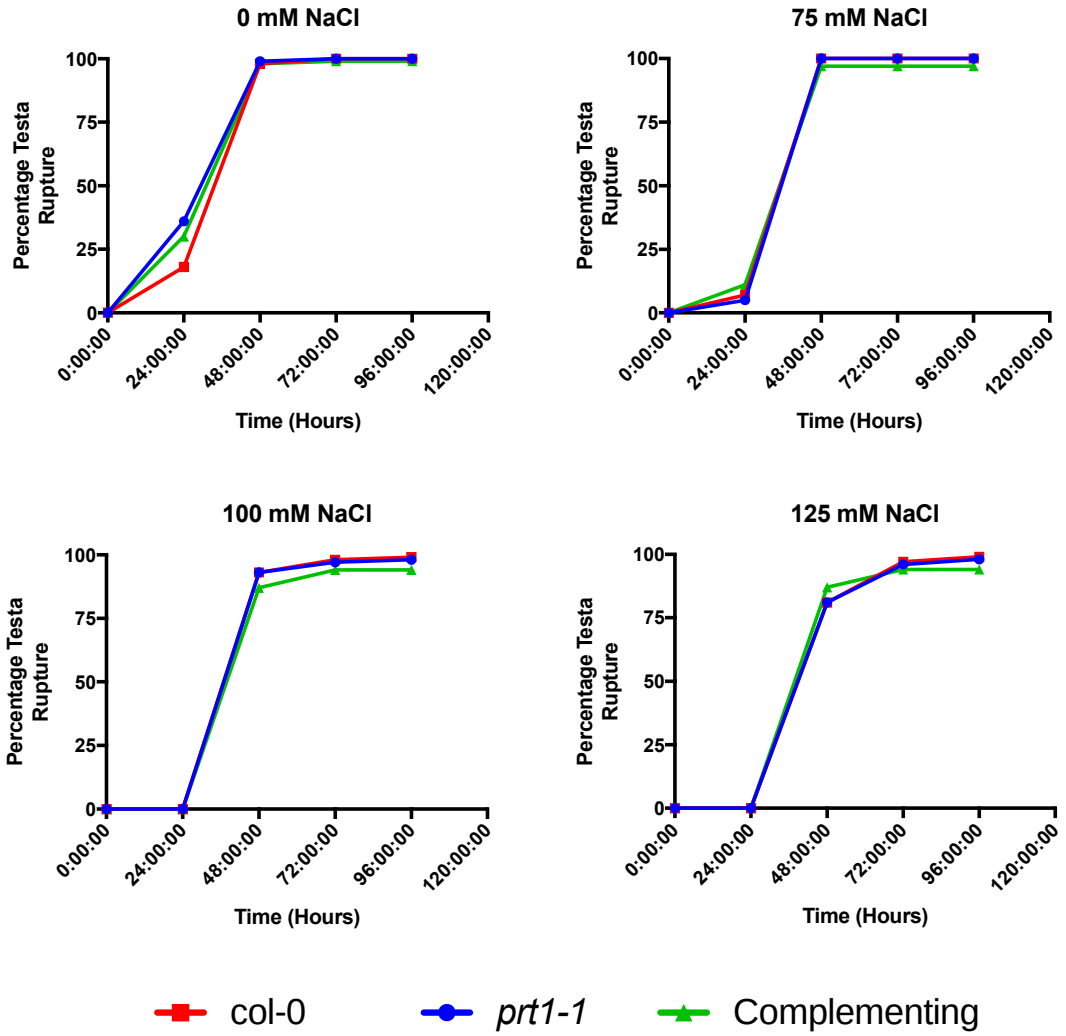

Figure 4.17: Effect of salt stress on testa rupture. Testa rupture rates for Col-0, *prt1-1* and *PRT1*$_{pro}$::gDNA-*PRT1*::YFP in the *prt1-1* background on different salt supplemented media (values are mean ± SEM; n=100) in long day growth conditions.

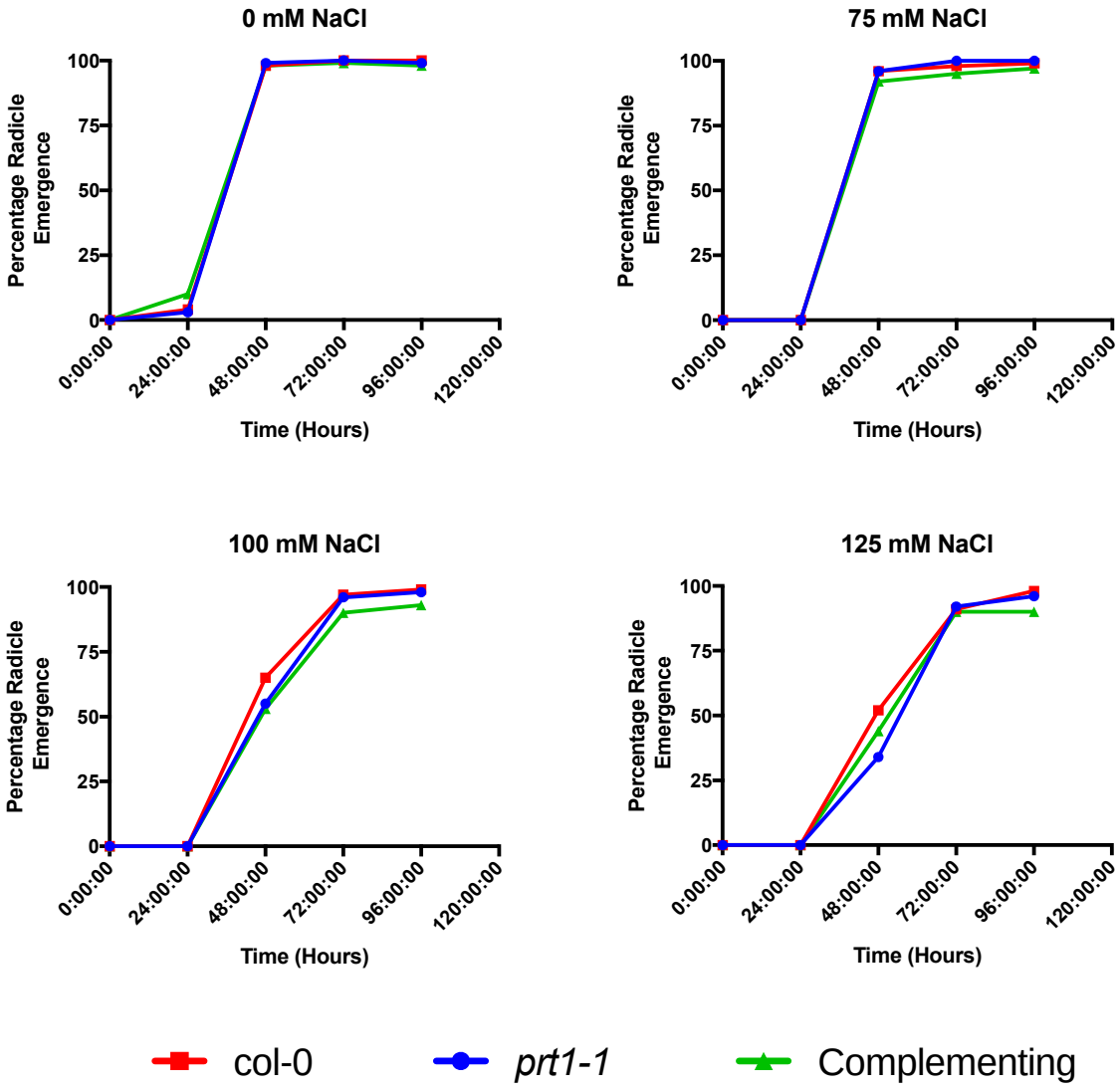

Figure 4.18: **Effect of salt stress on radicle emergence.** Radicle emergence rates for experimental genotypes at different concentrations of salt supplementation in terms of radicle emergence (values are mean ± SEM; n=100) in long day growth conditions.

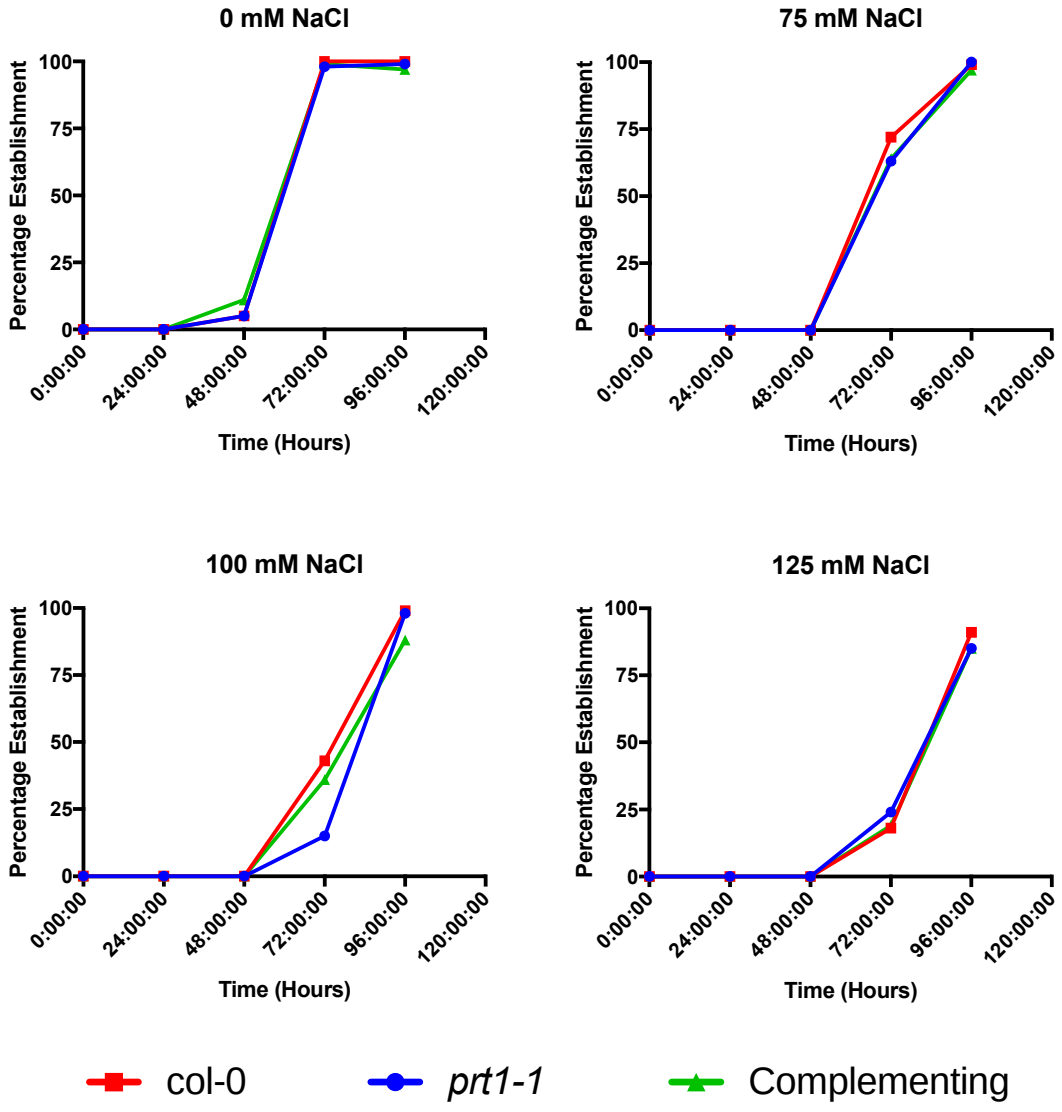

Figure 4.19: Effect of salt stress on establishment. Increasing NaCl and establishment rates between Col-0, *prt1-1* and *PRT1*$_{pro}$::gDNA-*PRT1*::YFP in the *prt1-1* background over a 96 h period (values are mean ± SEM; n=100) in long day growth conditions.

Root responses to salt were determined for Col-0, the complementing line and *prt1-1* (Figure 14.20 A). As a baseline for comparison, 0.5 x MS media supplemented with no NaCl was used. Following 7 DAG growth in long days on 0.5 x MS media, mean primary root lengths were 17.4 ± 0.98 mm, 16.9 ± 0.127 mm and 16.8 ± 0.59 mm for Col-0, *prt1-1* and the complementing line, respectively (Figure 14.10 B). Primary root growth was significantly reduced by salt supplementation as demonstrated by 2-way ANOVA with Tukey's multiple comparison test as *p* values were <0.0001 when compared to the 0.5 x MS control. At 100 mM NaCl, mean root lengths were 7.21 ± 0.98 mm for Col-0, 8.45 ± 1.27 mm for *prt1-1* and 7.47 ± 1.09 mm for the complementing line. Increasing salt concentration to 150 mM further reduced primary root length to 2.25 ± 0.43 mm for Col-0, 2.67± 0.47 mm for *prt1-1* and 2.87 ± 0.36 mm for the complementing line. At 200 mM NaCl, seedling growth was severely impacted, with many seeds failing to germinate. Following 2-way ANOVA with Tukey's multiple comparison analysis, no significant difference was observed between the tested genotypes at any of the salt supplementations. Taken together, salt supplementation assays indicate that there is no obvious role for PRT1 in response to salt in *Arabidopsis thaliana*.

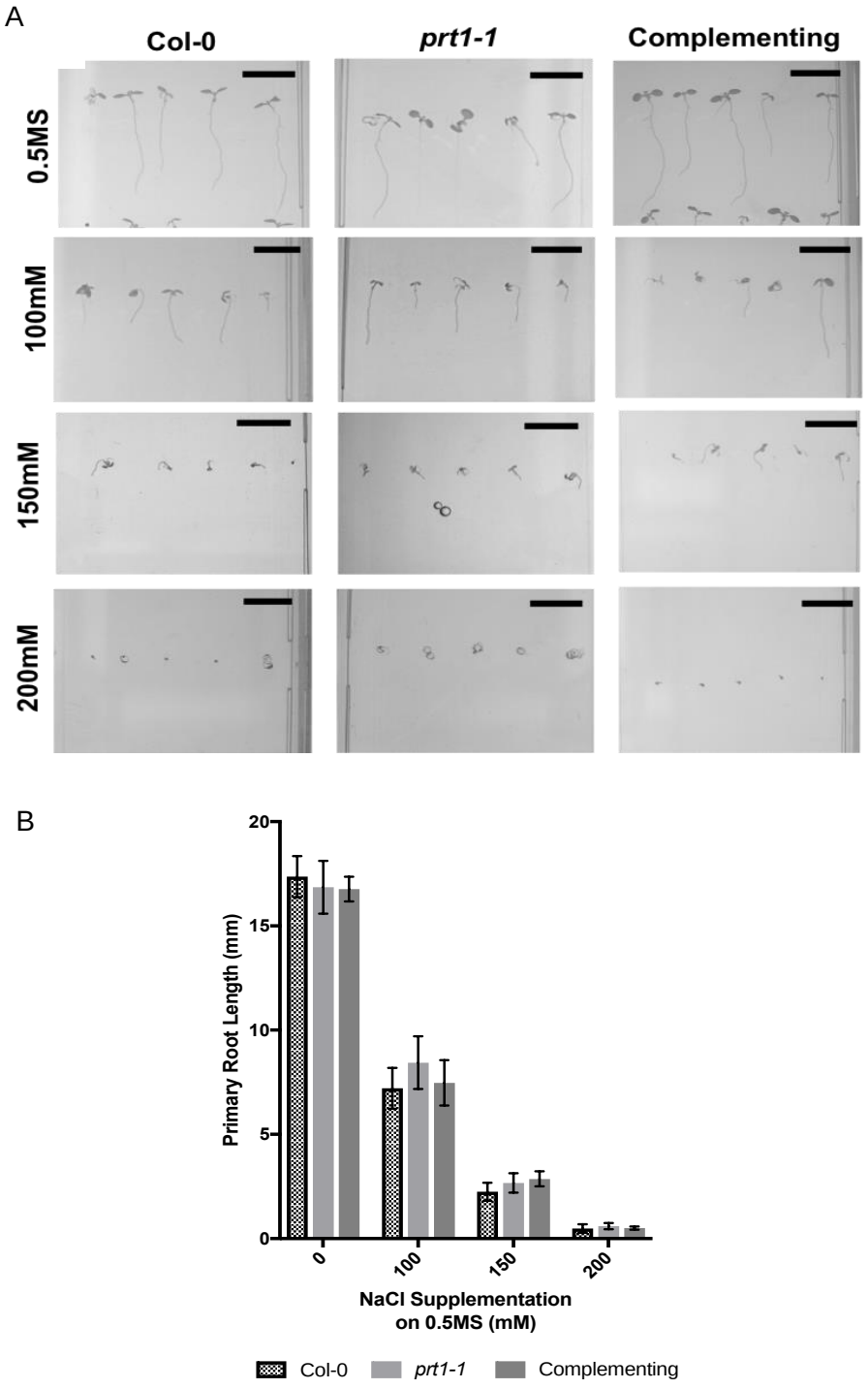

Figure 4.20: Root primary root growth on salt supplemented media for all experimental genotypes (A) representative images of primary roots grown on 0.5 x MS supplemented with different (scale bars = 10 mm) and (B) a graph showing average primary root length at 7 DAG in long days (values are mean ± SEM; n=10; no significant determined by 2way ANOVA with Tukey's multiple comparison analysis).

4.3.3 Nutrient Deficiency assays

4.3.3.1 Nitrogen deficiency

Nitrogen, and other essential nutrient deficiencies, were investigated to see if the additional burden placed on the plant system would amply the potential root phenotype that was seen under non-stressed conditions.

Being a constituent of most integral cellular components including nucleic acids, lipids, amino acids and proteins, nitrogen is an essential nutrient on which plants are fundamentally reliant (Lemaître *et al.,* 2008). Plants acquire nitrogen either in inorganic universally available forms such as nitrate or ammonium, or organically as urea, amino acids or peptides (Kiba & Krapp, 2016). In general, the abundance of nitrogen in soils is low, however, the diverse worldwide composition of soils, incidence of leaching and microbial activity means nitrogen availability is highly variable (Jackson & Caldwell, 1993). When nitrogen levels are sub-optimal for plants, this deficiency can have widespread and profound ramifications, such as chlorosis characterised by a yellowing of leaves, reduction in leaf, flower, fruit and stem growth resulting reduced photosynthetic capacity, plant biomass and seed yield. Consequently, nitrogen deficiency is a significant abiotic stress (Kiba & Krapp, 2016). In areas of low-nutrient availability, nitrogen is applied to soils as inorganic nitrogenous fertiliser at great cost to the producer and the environment. This problem is compounded by worldwide soil quality deterioration due to intense farming practices, climatic change or leaching from the soil.

The root specific eFP browser (Winter *et al.,* 2007) shows *PRT1* expression data from long-day grown 12-day old seedlings under low nitrogen conditions (control) and following 2 hours exposure to 5 mM KNO_3 (Figure 14.21). Data were obtained by fluorescence cell sorting of untreated and treated plants (Gifford *et al.* 2008). *PRT1* was weakly expressed in the lateral root cap, epidermis, cortex, endodermis and pericycle and higher in the vasculature. These findings are consistent with root eFP browser data presented in figure 4.21 (Cartwright *et al.,* 2009; Brady *et al.,* 2007; Waese *et al.,* 2017). The expression of *PRT1*

in response to KNO_3 addition is unchanged in all tissues. Overall, no significant expression increase or decrease is observed in *in silico* data following addition of NO_3 indicating that *PRT1* is unlikely to be transcriptionally active in nitrogen assimilation.

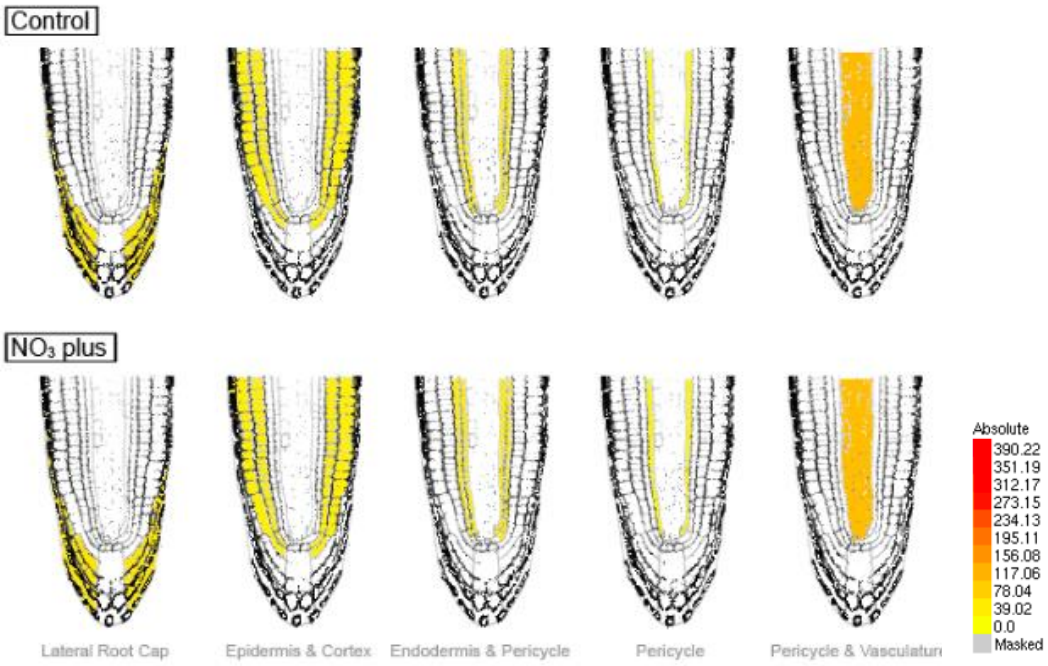

Figure 4.21: **Expression of *PRT1* in response to nitrogen deficiency in public transcriptome datasets**: Data taken from 12 DAG roots grown under long days in a low control and treated for 2-h in high nitrogen conditions for *PRT1* absolute expression (Gifford *et al.,* 2007; Winter *et al.,* 2008; https://bar.utoronto.ca/eplant/; accessed July 2018).

To establish whether PRT1 plays a role in assimilation of nitrogen or in response to nitrogen deficiency, primary root lengths were measured under different nitrogen conditions. Basic Murashige and Skoog media without nitrogen (Phytotech labs) was prepared to half strength by the same method described previously as normal MS agar and standard 0.5 x MS was prepared as a control for 'normal' Arabidopsis growth in the experimental conditions. Based on the ammonium nitrate and potassium nitrate content of MS basal salt media (Sigma Aldrich); 25 %, 50 %, 75 % and 100 % of the nitrate contents was re-supplemented to N-free 0.5 x MS media. Initially, seeds were plated on nitrate deficient media by the same method as the salt supplementation experiments, however the

number was reduced to 4 of each seed types per plate to reduce instances of overlapping roots. Plates were stratified for 3 d and put into short day light conditions for 14 DAG. The growth was measured by marking the position of the root cap every 24 h and measuring using Fiji. Mean primary root lengths at 14 DAG were 43.9 ± 3.2 mm and 45.9 ± 3.5 mm for Col-0 and *prt1-1* respectively on 0.5MS control plates, and 43.3 ± 5.7 mm and 42.2 ± 4.2 mm for Col-0 and *prt1-1* respectively on nitrate free 0.5MS plates re-supplemented with 100 % N (Figure 4.22); indicating there is no significant difference in growth due to the MS media (n=12). A similar finding was also observed for nitrate-free 0.5 x MS plates re-supplemented with 75 % N with Col-0 14 DAG primary root lengths being 53.7 ± 6.6 mm and *prt1-1* roots measuring 55.66 ± 11.2 mm. Following 2-way ANOVA analysis of Col-0 and *prt1-1* on 0.5MS, 100%N and 75%N media, *p* values were calculated as 0.1588, 0.197 and 0.0973 respectively indicating there is no statistical difference between the genotypes at higher media N contents. However, a significant genotype variation was observed at 50% N, 25% N and 0% N with calculated *p* values of <0.0001 calculated for these media types, with *prt1-1* primary roots growing significantly longer than Col-0. Final primary root lengths determined at 14 DAG were 47.2 ± 5.4 mm for Col-0 and 60.3 ± 7.8 mm for *prt1-1* at 50% N; 38.4 ± 2.6 mm for Col-0 and 52.6 ± 7.0 mm for *prt1-1* at 25% N; and, 23.1 ± 2.5 mm and 37.7 ± 4.5 mm for Col-0 and *prt1-1* respectively at 0% N content (Figure 4.23).

A similar but less pronounced effect is observed when *prt1-1* and Col-0 are grown on N deficient media under long day light condition for 14DAG (Figure 4.24). However, following 2way ANOVA with Sidak's multiple comparison analysis, no statistical difference between Col-0 and *prt1-1* primary root lengths could be determined at any time point for all N media types investigated; with the exception of 14 DAG on 0 % N media (*p*=0.0494).

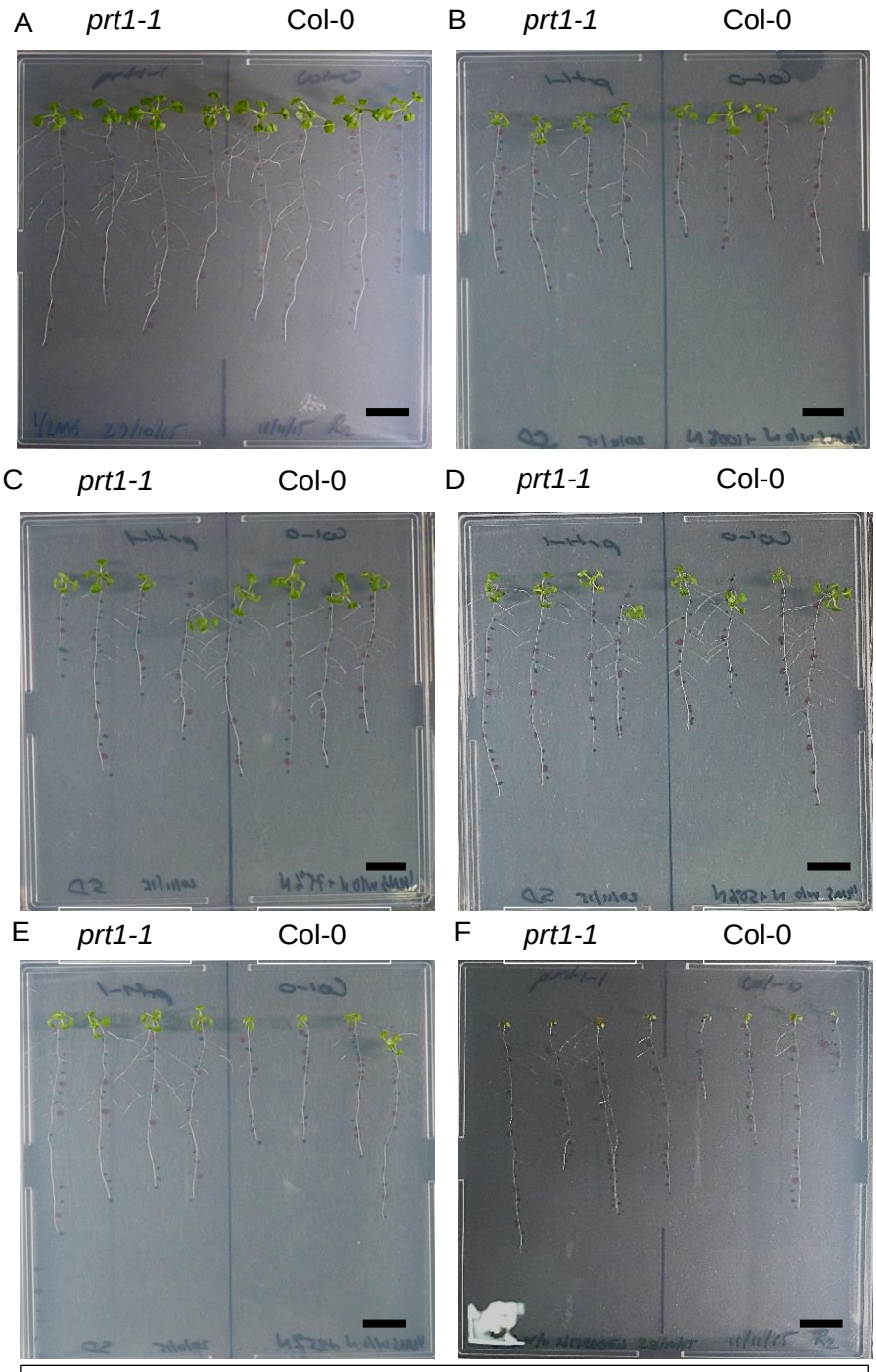

Figure 4.22: Root growth rates in response to nitrogen deficiency for Col-0 and *prt1-1* in short days. Representative images showing the root architectures of *prt1-1* and Col-0 seedlings grown for 14DAG on (A) 0.5 x MS control plates; and 0.5 x Ms nitrogen deficient media plates supplemented with (B) 100% N (C) 75% N (D) 50% N (E) 25% N and (F) 0% N content of standard 0.5MS media.

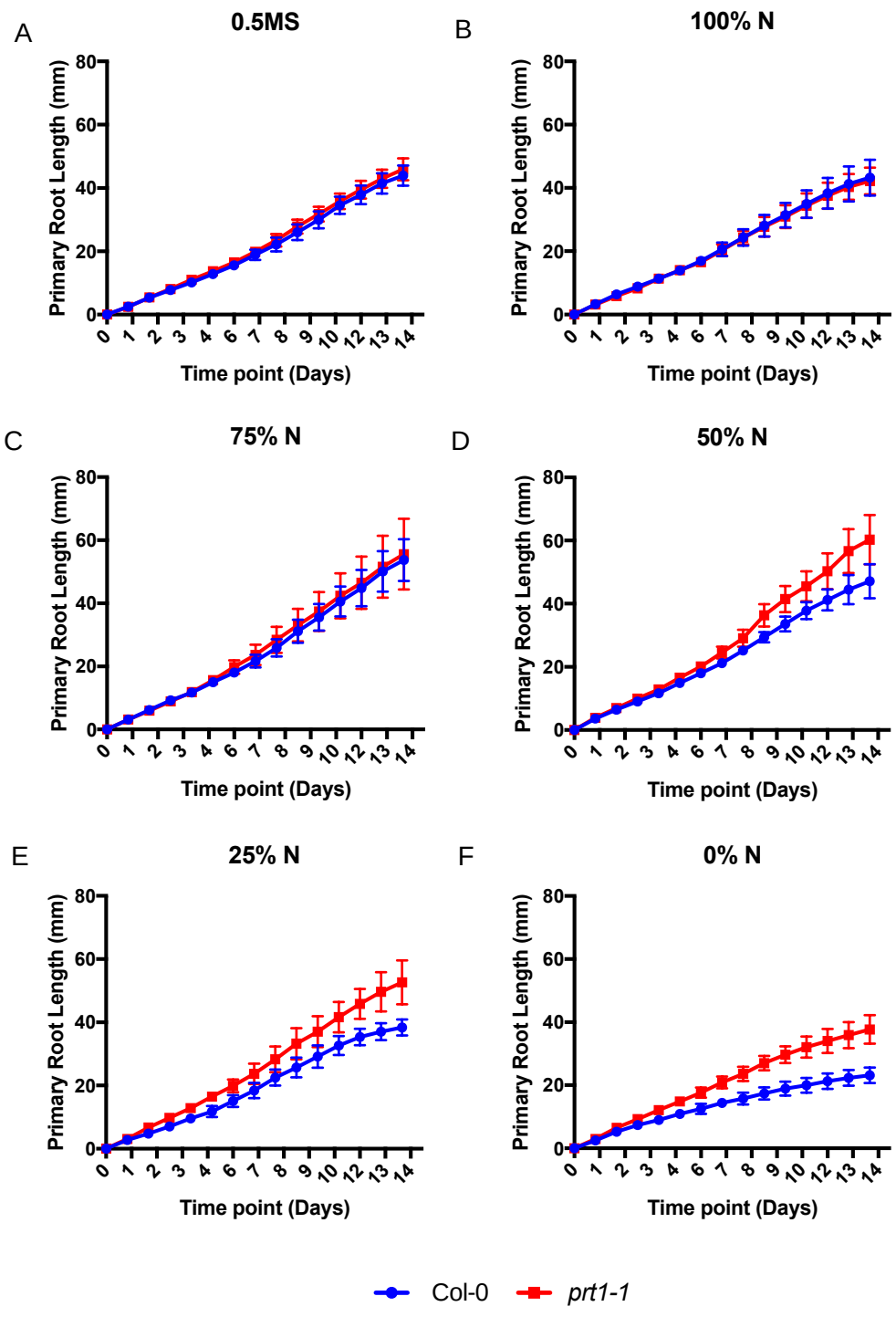

Figure 4.23: Primary roots of *prt1-1* and Col-0 on low nitrogen media in short days. Graphs showing primary root lengths of *prt1-1* and Col-0 seedlings grown for 14DAG on (A) 0.5 x MS control plates; and 0.5 x MS nitrogen deficient media plates supplemented with (B) 100% N (C) 75% N (D) 50% N (E) 25% N and (F) 0% N. Data is the pooled means of three independent biological replicates ±SEM (n=12; significance determined by 2way ANOVA with Tukey's multiple comparison test).

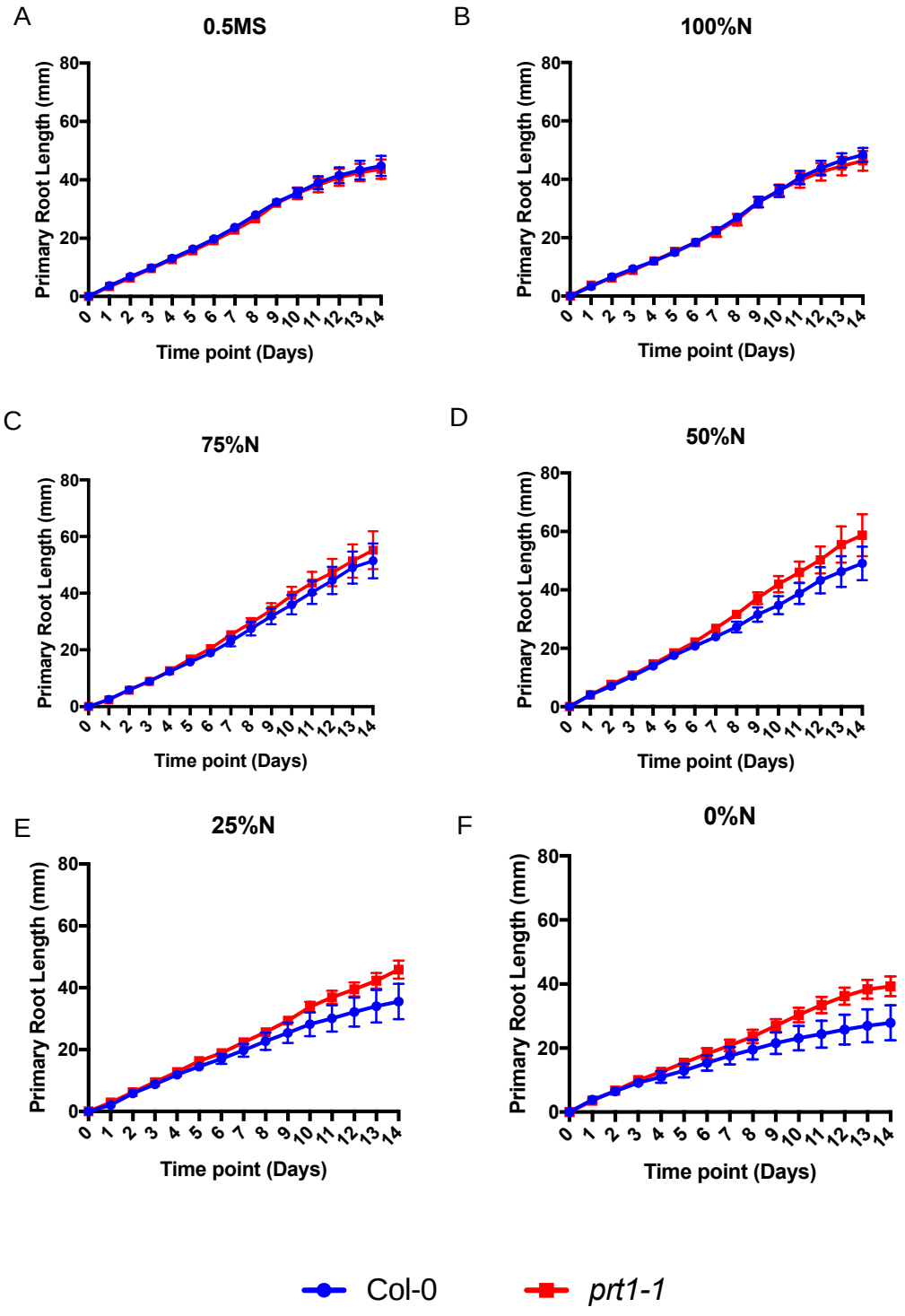

Figure 4.24: Primary root lengths compared to Col-0 and *prt1-1* on nitrogen deficient media under long days. Graphs showing primary root lengths of *prt1-1* and Col-0 seedlings grown for 14DAG on (a) 0.5 x MS control plates; and 0.5 x MS nitrogen deficient media plates supplemented with (b) 100% N (c) 75% N (d) 50% N (e) 25% N and (f) 0% N. Data is the pooled means of two independent biological replicates ±SEM (n=8; significance determined by 2way ANOVA with Tukey's multiple comparison test).

Additional experiments were also conducted to determine whether the difference observed in response of Col-0 and *prt1-1* nitrogen deficiency are seen across the life span of the plant. Shoot and root fresh weights of well-watered plants were quantified at 8-week-old plants (Figure 4.25 and 4.26). No statistically significant difference was observed between *prt1-1* and Col-0 grown on soils with different N content for plant biomass (n=6). Shoot fresh weights were 459.2 ± 7.4 mg and 467.0 ± 12.9 mg on high nutrient M3 soil for Col-0 and *prt1-1* respectively (*p*=0.8545)*;* 90.1 ± 9.6 mg for Col-0 and 92.7 ± 4.9 mg on lower nutrient traysubstrat soil (TS) (Chapter 2.1.11) (*p*=0.9940); and a further reduction to 48.4 ± 2.7 mg and 47.5. ± 2.1 mg on 50% traysubstrat with 50% sharp sand medium (TS + S) (*p*=0.9997) for Col-0 and *prt1-1* respectively. Fresh weights were 145.3 ± 9.3 mg and 149.8 ± 7.4 mg on M3 soil (*p*=0.9775); 84.8 ± 9.6 mg and 88.2 ± 2.7 mg on TS (*p*=0.9940); and finally, 53.8 ± 11.1 mg and 55.8 ± 9.6 mg on 50% traysubstrat with 50% sharp sand (*p*=0.9979) for Col-0 and *prt1-1* for roots. The reduction in nitrogen content of the growth medium overall has the greatest impact on the shoot biomass accumulation: reducing fresh weight by 89.5% and 89.8% compared to a 63.0% and 62.8% reduction in root biomass for Col-0 and *prt1-1* respectively.

Experiments were also conducted to investigate whether low N content affects the seed yield of Col-0 and *prt1-1* (Figure 4.27). Plants were grown for 8 weeks in Aracon base and tubes (Arasystem, BETATECJ, Belgium) to prevent seed loss and the mean seed weight per plant was determined (n=10). In the highest nutrient soils, Col-0 seed weights were 190.2 ± 19.1 mg and for *prt1-1* 198.7 ± 17.7 mg. In the lower nitrogen traysubstrat soil, seed weights were 47.0 ± 7.9 mg and 42.8 ± 4.3 mg for Col-0 and *prt1-1* respectively. On the lowest nitrogen soil medium tested, Col-0 seed weights were 32.5 ± 2.9 mg and for *prt1-1* 37.5 ± 2.7 mg. No significant effect was observed between genotypes for seed yield on different N content soils however $p<0.001$ indicates a strong statistical influence due to the medium type (analysed 2way ANOVA with Sidak's multiple comparison test).

A

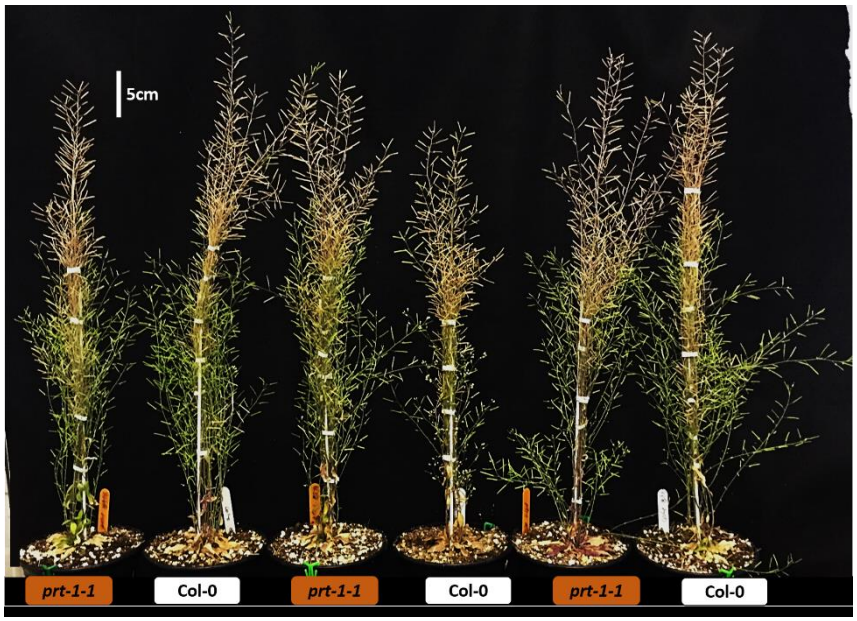

B

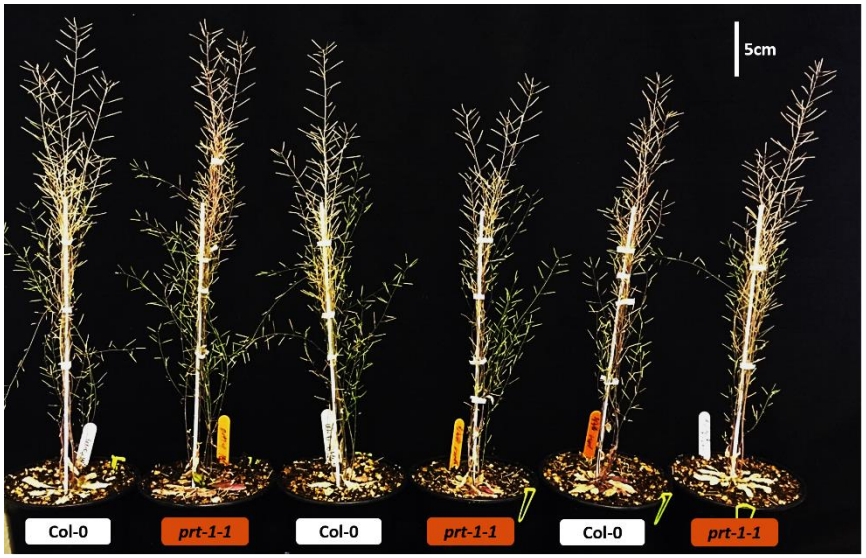

C

Figure 4.25: Representative images showing whole plant growth on soils with different nitrogen levels (A) nutrient rich M3 Levington soil (B) low nitrate Klasmann & Deilmann Traysubstrat (C) 50% Klasmann & Deilmann Traysubstrat with 50% sharp sand.

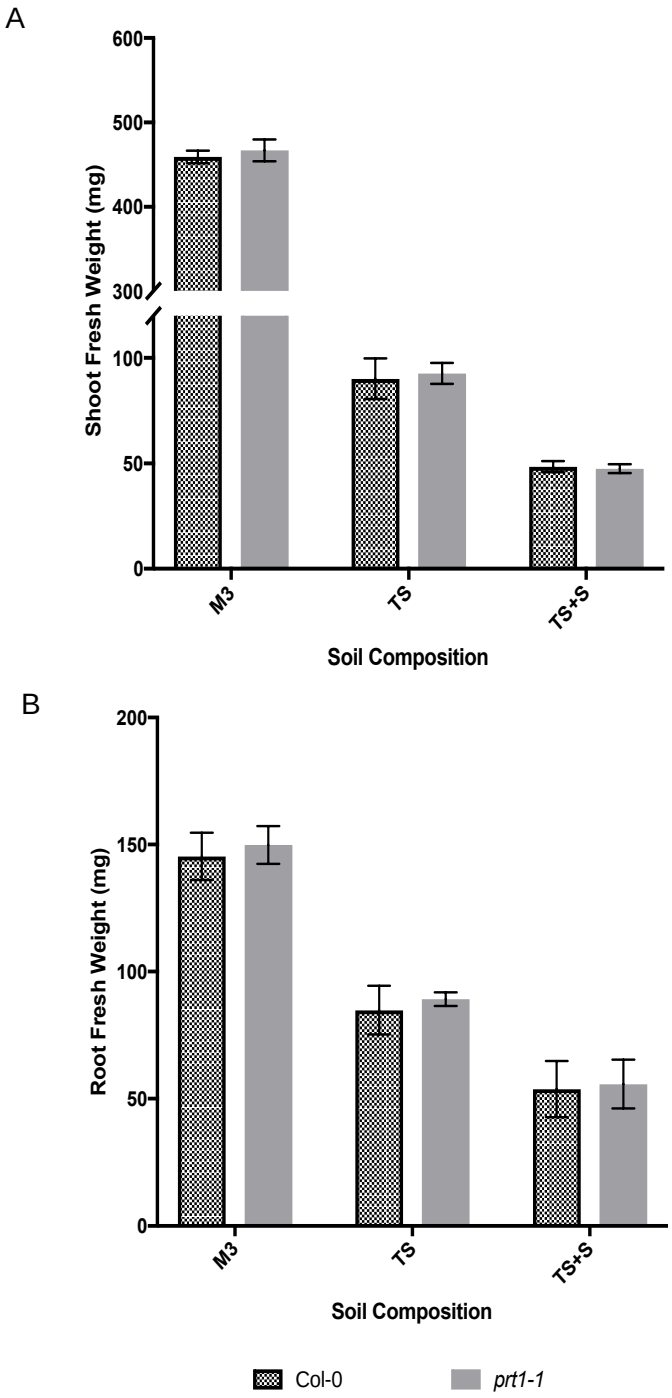

Figure 4.26: Growth on soils with different nitrate contents for Col-0 and *prt1-1*. M3 indicates high nutrient soil, TS indicates lower nutrient traysubstrat soil and TS+S is 50% traysubstrat with 50% sharp sand. Fresh root and shoot weights are plotted as means ± SEM (n=6; no significance as determined by 2way ANOVA with Sidak's multiple comparison tests).

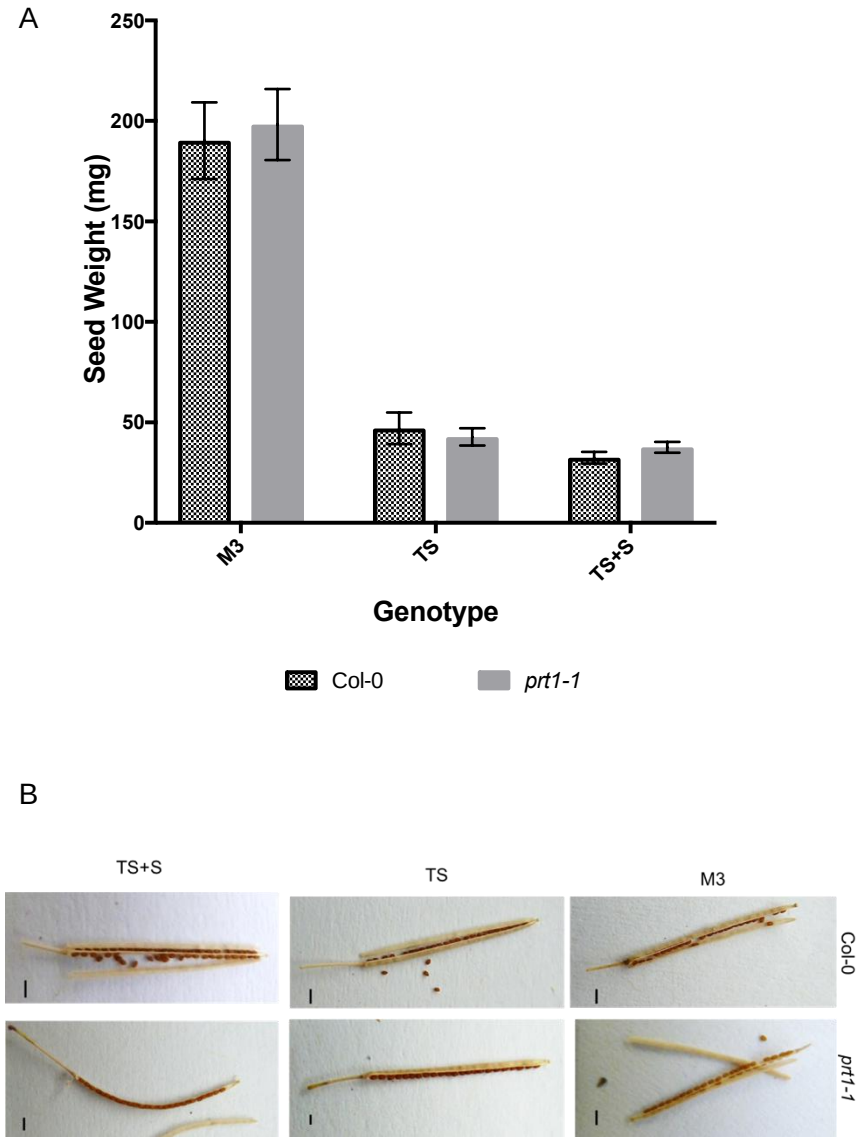

Figure 4.27 Silique filling and seed yield for Col-0 and *prt1-1* on low nitrogen soils at 8 weeks: (a) seed weights are plotted as means ± SEM (n=10; no significance as determined by 2way ANOVA with Sidak's multiple comparison tests) (b) Representative Images showing siliques from plants grown on soils with different nitrogen levels.

4.3.3.2 Iron deficiency

Plants are the primary source of human dietary iron; however, it is one of the most prevalent micronutrient deficiencies. Improvement of the iron content of plants is a double-edged sword as iron is both essential for plant health but also toxic. Regulation of uptake is therefore critical. Understanding the molecular mechanism of iron uptake in plants is essential for research to improve crop quality. Iron is mobilised from insoluble forms present in soil and from internal stores in the plant. When deficient, iron has a range of physiological effect on plants, chiefly a reduction in chlorophyll content characterised by chlorosis and re-arranging of the photosynthetic apparatus in the chloroplasts. A change in preference of metal ion uptake to zinc and copper from iron (Vert *et al.,* 2002) is observed following iron deficiency on plant roots, and alteration to carbon and nitrogen metabolism (Perea-Garcia *et al.,* 2013). Given iron deficiency has major consequences for plant nutrition, it has the potential to exacerbate the possible difference in root growth. Therefore, screening for differential growth responses for Col-0 and *prt1-1* to iron deficiency was conducted.

Transcriptome data was searched to determine whether *PRT1* expression is responsive to iron deprivation and no significant induction of *PRT1* expression was observed in 5 DAG following treatment iron deficiency over 24 h treatment period (Figure 4.28) (Dinneny *et al.,* 2008; Winter *et al.,* 2007). Col-0 and *prt1-1* plants were grown for 10 d on Hoagland's media with and without addition of iron. Mean primary root lengths were 32.57 ± 1.08 mm and 32.87 ±1.00 mm for Col-0 and *prt1-1* respectively on Fe-sufficient Hoagland's media (Figure 4.29). Primary root lengths were severely affected by iron deficiency as demonstrated by *p* values of <0.0001 following 2-way ANOVA with post hoc Sidak's multiple comparison for both Col-0 and *prt1-1* between treatments. Such statistical tests however revealed no significant differences between Col-0 (14.43 ± 0.73 mm) and *prt1-1* (13.8 ± 0.60 mm) when grown on iron deficient media (p=0.9630).

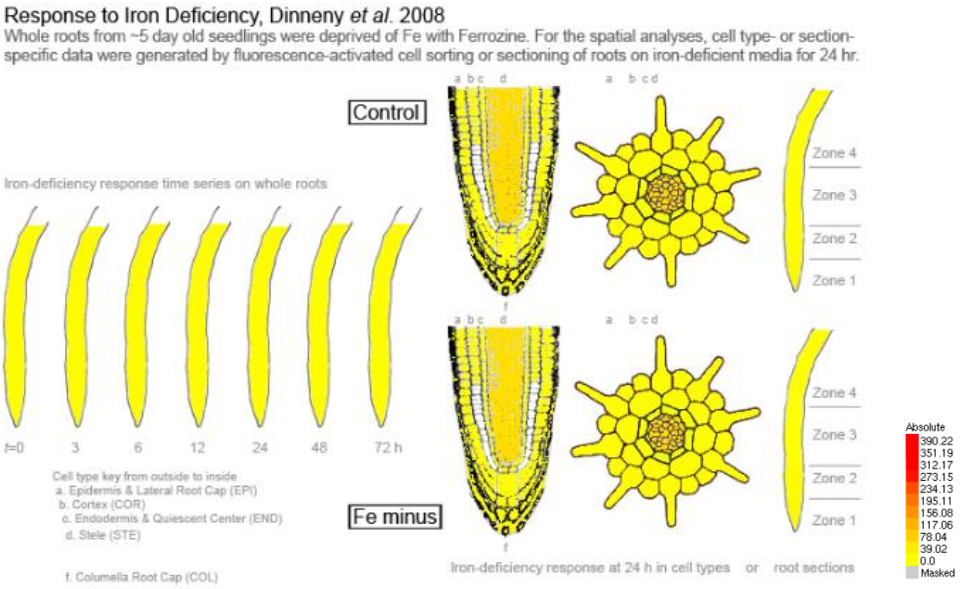

Figure 4.28: Expression of *PRT1* in response to iron deficiency in public transcriptome datasets. Image adapted from the Arabidopsis eFP browser demonstrating the expression of *PRT1* (At3g24800) in Arabidopsis 5-day old roots following 24 h exposure to iron deficient media compared to a control plate (Winter *et al.,* 2007; Dinneny *et al.,* 2008).

A

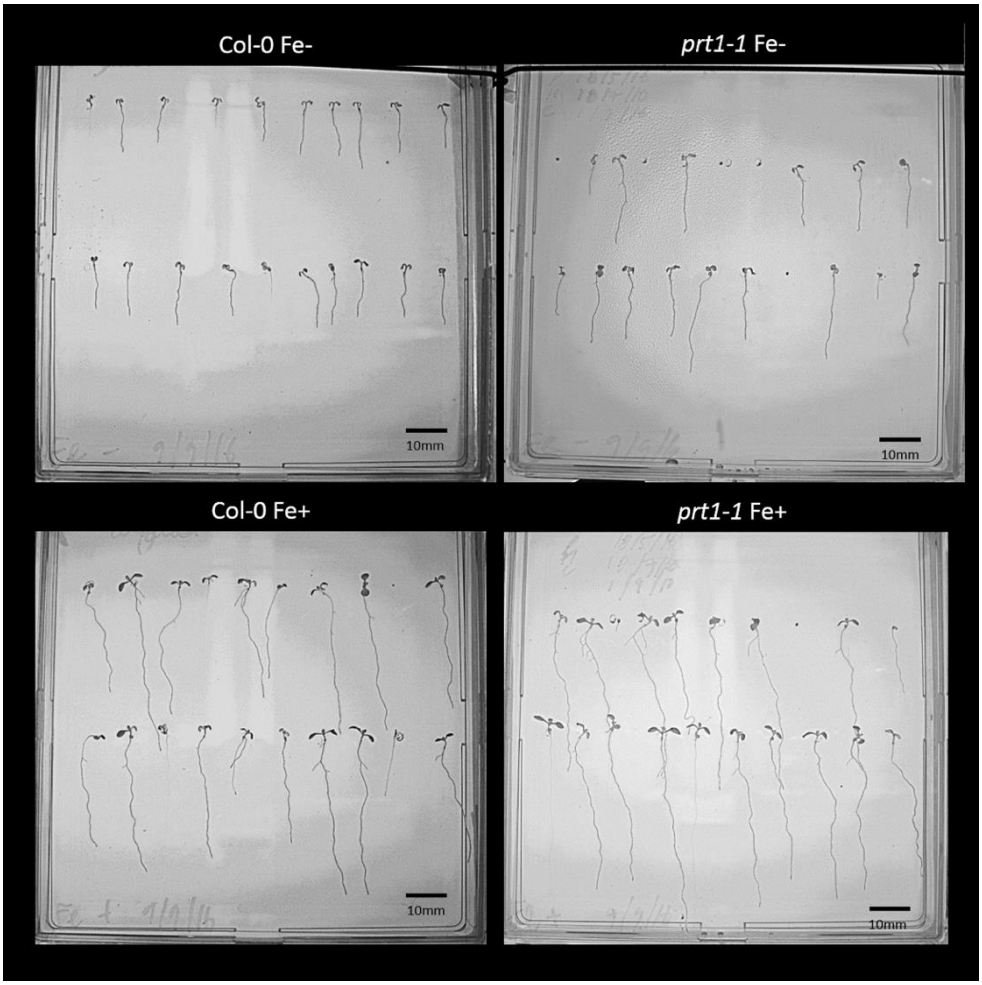

B

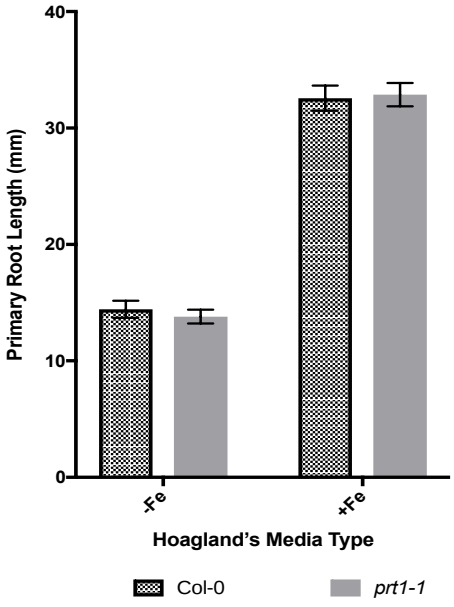

Figure 4.29 Primary root length of Col-0 and *prt1-1* seedlings on iron deficient media: (A) representative images of primary roots grown on iron sufficient and iron deficient Hoagland's media plates (scale bars = 10mm) and (B) a graph showing average primary root length at 10 DAG in long days. Values are mean ± SEM; n=60 (pooled data from three independent experiments; no significant determined by 2way ANOVA with Sidak's multiple comparison analysis.

4.3.3.3 Phosphate Deficiency

Phosphate (Pi) deficiency, like other essential nutrient insufficiencies, is commonplace due to poor bio-availability and mobility in soils. Deficiency places a huge burden on plants due to inhibition of cell division in meristematic tissues and premature root tip differentiation, culminating in primary root suppression (Chacón-López *et al.,* 2011). The PHOSPHATE DEFICIENCY RESPONSE2 (*PDR2)* (Ticconi *et al.,* 2009, phospholipase Ds *zeta1/2 (PLDζ1,2)*, PHOSPHATE ROOT DEVELOPMENT (*PRD)* genes and *low phosphate root 1/2c* (LPR1/2) are key regulators involved root growth during phosphate deficiency. These work in concert to achieve Pi deficiency-induced remodelling of root development triggered following low Pi perception in the locale around the root cap (Svistoonoff *et al.,* 2007; Ticconi *et al.,* 2004; Ticconi *et al.,* 2009; Thibaud *et al.,* 2010) and is a genetically programmed active cellular response rather than a consequence of nutrient shortage and subsequent reduction in growth (Péret *et al.,* 2014). Iron plays a fundamental role in primary root growth inhibition in response to Pi deficiency: with high iron levels accumulating in Pi starved roots. Since Pi deficiency is pervasive throughout the world (Zhang *et al.,* 2016), understanding plant adaptation to Pi deficiency is a valuable pursuit.

Data from the eFP browser (Winter *et al.,* 2007) indicates that *PRT1* is moderately expressed in 30-day old roots grown in media containing 1.5 mM Pi (Figure 4.30). Expression did not change upon transfer to Pi-replete media, indicating that *PRT1* expression is not induced or repressed in response to Pi deficiency for the conditions tested by Lin *et al* (2011).

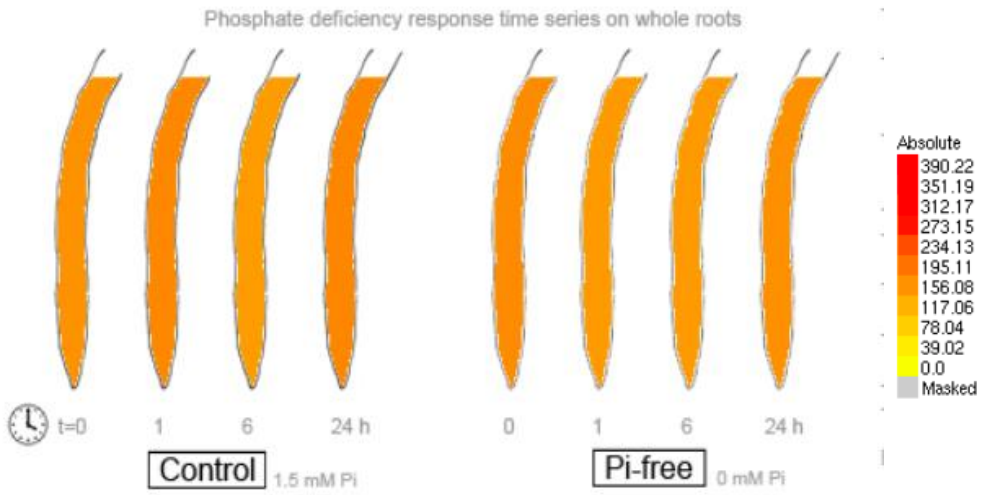

Figure 4.30: Expression of *PRT1* in response to phosphate deficiency in public transcriptome datasets. Image adapted from the Arabidopsis eFP browser (Winter *et al.,* 2007; https://bar.utoronto.ca/eplant/; accessed July 2018) demonstrating the expression of *PRT1* (At3g24800) in Arabidopsis 30-day old roots following 0/1/6/24 h exposure to Pi replete media compared to a control (Lin *et al.,* 2011).

Responses of roots to phosphate deficiency were determined for Col-0, the complementing line and *prt1-1* (Figure 4.31A). 0.5 x MS media was used as a control for comparison. Following 10 DAG growth in long days on 0.5 x MS media, mean primary root lengths were determined as 32.6 ± 0.98 mm and 30.9 ± 1.4 mm for Col-0 and *prt1-1* respectively (n=12) (Figure 4.31B). Growth on phosphate deficient 0.5 x MS re-supplemented with 100 % Pi was comparable for Col-0 (30.2 ± 1.0 mm) and *prt1-1* (31.3 ± 1.6 mm) primary root growth, indicating negligible influence of this media compared to the control. Phosphate deficient media however as an interaction factor significantly reduced the growth of primary roots (p<0.0001; 2way ANOVA with Sidak's multiple comparison): with roots being measured as 15.4 ± 0.3 mm and 14.9 ± 0.4 mm for Col-0 and *prt1-1* respectively. Following one-way ANOVA analysis between genotypes for each treatment, no statistical significance could be determined (p = 0.6175, p = 0.8709, p = 0.982 for 0.5 x MS, Pi sufficient and Pi deficient media respectively. This indicates that PRT1 is unlikely to play a role in plant responses to phosphate deficiency.

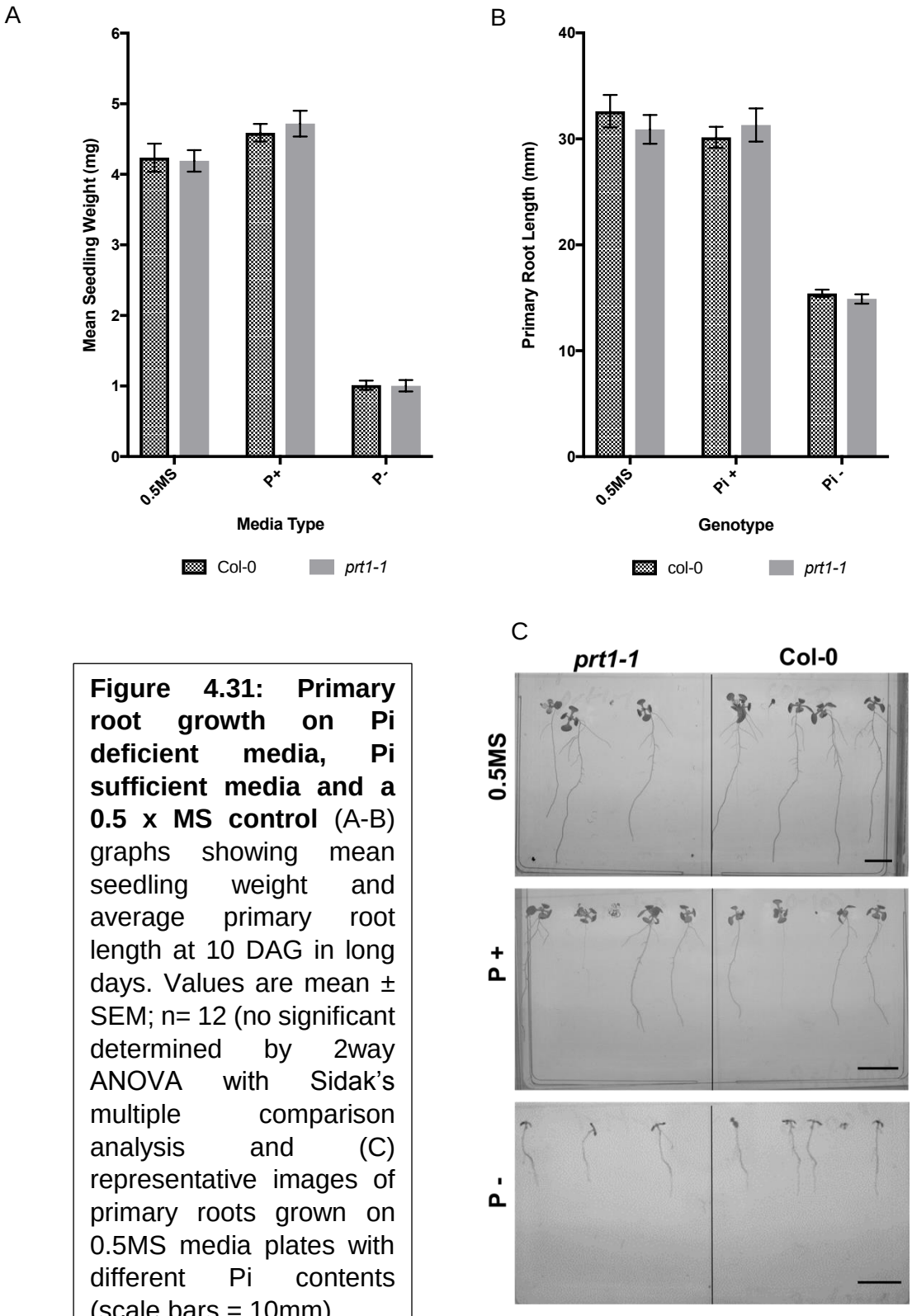

Figure 4.31: Primary root growth on Pi deficient media, Pi sufficient media and a 0.5 x MS control (A-B) graphs showing mean seedling weight and average primary root length at 10 DAG in long days. Values are mean ± SEM; n= 12 (no significant determined by 2way ANOVA with Sidak's multiple comparison analysis and (C) representative images of primary roots grown on 0.5MS media plates with different Pi contents (scale bars = 10mm).

4.4 Discussion

The plant N-end rule pathway is undergoing a renaissance, with the importance of targeted proteolysis emerging in a plethora of critical processes. The roles of PRT6 are diverse and include physiological functions in germination (Holman *et al.,* 2009; Gibbs *et al.,* 2014a), leaf development and senescence (Yoshida *et al*., 2002; Graciet *et al*., 2009), latency during submergence (Riber *et al*., 2015), plant responses to pathogens (Gravot *et al*., 2016; de Marchi *et al*., 2016) and photomorphogenesis (Abbas *et al*., 2015). Most of these physiological functions have been shown to be underpinned by ERFVIIs (Gibbs *et al.,* 2015).

In contrast, at the outset of this study, no confirmed physiological function had been found for the PRT1 N-recognin. The biochemical functions of PRT1 and PRT6 are fulfilled by a single N-recognin in yeast (ScUbr1), which raises the question of why separation of these functions on two different proteins has evolved in plants. It could reasonably be hypothesised that PRT1 and PRT6 physiological functions are very different, or similar but regulated differently. The aim of this chapter was to test these hypothesises.

Little published literature exists describing the general growth characteristics of *prt1* mutants and the initial aim this chapter was to define these for Col-0, *prt1-1* and the complementing lines. These were then used for reference when screening plant responses to abiotic stresses in this remainder of the chapter. Data from the eFP Browser was used extensively as a guide to investigate the involvement of *PRT1* in general growth of plants and in response to various abiotic stresses. Whilst informative for initial physiological screens, data generated for the eFP browser is obtained from transcriptomics not designed to directly assign a function to PRT1 and experimental parameters are potentially insufficient to demonstrate the context in which PRT1 involved (i.e. abiotic stimulus is too low to elicit a response). However, PRT1 may be

involved in a physiological process without being transcriptionally up-regulated. Nonetheless it has been used tentatively as a guide for experiments.

Physiological screens of the general growth characteristics for these complementing lines suggest they behave similarly to the wild type indicating there is no obvious growth penalty to which would have limited application in further physiological screens.

Bachmair *et al* (1993) suggested that *prt1* mutants may have a slight delay in germination. Data from the germination eFP browser (Narsai *et al.,* 2011; Waese *et al.,* 2017) indicates that *PRT1* expression is high in fresh seeds harvested directly from siliques and also in dry seeds (Schmid *et al.,* 2005; Nakabayashi *et al.*, 2005). A decline in *PRT1* expression is observed during stratification and expression is lowest following 48 h of cold imbibition. Following transition to light, *PRT1* expression increases again (Narsai *et al.,* 2011). This change in *PRT1* expression from high to low during the transition from dry quiescent seed to germination may suggest a potential role for PRT1 in germination. Large sets of differentially expressed genes are present in dormant and after-ripened seeds however information regarding temporal and spatial transcriptional changes during seed imbibition are lacking (Dekkers *et al.,* 2016). Potentially, PRT1 could facilitate the turnover of or stabilisation of germination-promoting proteins potentially through degron shielding until dormancy is broken by cold imbibition, whereby PRT1 is no longer required and thus expression declines. If this were the case, an alteration in germination behaviour would be expected in *prt1* mutants. However, in this study, no significant difference could be observed in between any of these lines in terms of germination or establishment; with negligible difference being observed between the experimental lines for testa rupture, radicle emergence or expansion of two cotyledons, over a 96 h period. This was also the case with seed germination in response to saline media, with no obvious differences being observed between genotypes. A slight delay in germination could possibly have remained unobserved in the experimental design in this study as time points were

at 24 h intervals. Following 1-3 h of imbibition, temporal expression analysis by Holdsworth *et al* (2008b) demonstrated there is a rapid increase in RNAs encoding proteins involved in cell wall modification, RNA translation and protein degradation. Furthermore, the majority of testa rupture and radicle emergence events have been reported to occur between 24-36 h and 29-43 h after imbibition respectively for Col-0 (Holdsworth *et al.,* 2008a). Overall these studies may indicate that once in motion, germination is a rapid process and such large time interval may miss such events. However, the characterisation of germination and establishment in this study is typical of many in published literature and if there were a physiologically significant role, these differences would have been expected to have been observed between Col-0 and *prt1-1* under these experimental conditions.

In support of observations presented in this thesis, Holman *et al* (2009) also reported no influence of the *prt1* mutation on ABA or sucrose sensitivity in imbibed seeds. In contrast, mutant *prt6* plants exhibit germination phenotypes such as hypersensitivity to ABA inhibition and NO insensitivity (Gibbs *et al*., 2014). Furthermore, establishment of *prt6* seedlings is sucrose hypersensitive and oil body retention is observed several days post-germination in these plants compared to the wild type (Holman *et al.,* 2009; Gibbs *et al.,* 2014a). Taken together, it appears that PRT1 plays no obvious role in the transition from dormancy to germination and establishment in plants. This ensures that any potential phenotype is not due to differences in germination or establishment which could potentially have significant ramifications very early on in plant development.

Following germination studies, other growth characteristics of Col-0, *prt1-1* and the complementing line were investigated. Roots are critical organs for water and nutrient acquisition as well as anchorage in plants. Rapid establishment of an efficient root architecture is paramount for overall success of the plant; therefore, root growth of all experimental lines was assessed during the initial 14 or 21 days after germination. In this study, no significant differences in root length were observed between

experimental lines grown on standard 0.5 x MS media under constant light. This indicates that, unlike *prt6* mutants which are unable to mobilise oil bodies and require addition of sucrose to media, *prt1-1* seedlings behave as wild type on sucrose-free media. This is advantageous for further experiments as it removes the potential for complex interactions between sugar signalling and abiotic stresses responses that may suppress or exaggerate any potential effect observed.

Following testing of light regimes, no difference between genotypes could be observed for plants grown in constant light and long days over 5 DAG at Rothamsted Research (Harpenden, UK) and over 14 DAG at the University of Nottingham (Sutton Bonington Campus, Leicestershire, UK). Furthermore, over the whole plant life cycle, there was no significant difference between the fresh weight of Col-0 and *prt1-1* roots and rosettes grown under long days. Thus, no evidence was found to support a slower life cycle for *prt1-1* plants, as suggested by Bachmair *et al* (1993), at least under unstressed conditions. This was also the case for seed yield in these genotypes.

prt1-1 primary root lengths were significantly longer at 2-5 DAG and 4-5 DAG in short and neutral day conditions, respectively, when measured at Rothamsted Research, but this phenotype could not be reproduced at University of Nottingham. The photoperiods for these conditions were comparable at both locations, however the day and night time temperatures were 2^{o}C and 3^{o}C hotter at Rothamsted research. This being a shared facility, the temperature could not be altered and may have in hindsight amplified the difference between Col-0 and *prt1-1.* Future experiments might investigate whether this growth differential is due to temperature, although from the abiotic stress eFP browser *PRT1* does not appear to be transcriptionally upregulated in response to heat stress (Figure 4.12). Furthermore, the light intensity of these facilities was not compared and may present an important source of the variation. The light intensity at Rothamsted is predicted to be higher than the facilities at the University of Nottingham, which may have exacerbated

the root phenotypes. As a result, future experiments should be conducted using comparable light intensity conditions to those at Rothamsted to establish whether this factor is responsible for the potential root phenotype.

The majority of subsequent abiotic stress screens were conducted in the long day conditions, since Col-0, *prt1-1* and complementing line plants behave similarly and predictably in unstressed conditions. Furthermore, *Arabidopsis thaliana* is a facultative long day flowering plant (Mockler *et al.,* 2003) mainly this a more physiologically relevant growth condition. If a difference was observed in such a screen, it could then be attributed to the treatment and be a physiologically relevant phenotype. In retrospect, given the potential of increased root growth in the *prt1-1* background under short days, using this growth condition may have potentially amplified the root phenotypes, if any.

The primary roots of *prt1-1* grown in nitrogen deficient conditions under long days were slightly longer than Col-0 over a 14 DAG period, but this effect was not statistically significant. Furthermore, no differences in biomass accumulation and fertility were found between Col-0 and *prt1-1* grown in low nitrogen conditions over 8 weeks. In contrast, *prt1-1* primary roots were significantly longer than Col-0 grown under nitrogen deficiency in short day conditions. Thus, there is a subtle root phenotype for *prt1-1* in short day conditions, which is amplified under nitrogen stress. Further physiological screens are required to confirm this phenotype but due to other promising leads for a physiological function in this study (see Chapter 5), these were not pursued. Given unstressed SD and ND conditions at Rothamsted research revealed a potential root phenotype for *prt1-1* as well, conducting nitrogen deficiency assays in these conditions would be useful to investigate the interplay between the stress and environmental factors such as light intensity and temperature. It is hypothesised that due to the hotter temperatures and higher light intensity of the facilities at Rothamsted, a stronger root phenotype may be observed. The ability to detect tagged PRT1 driven by the

endogenous promoter and also F-GUS stabilisation in the *prt1-1* background (Chapter 3) indicate that the PRT1 protein is located and active in roots under the experimental conditions tested.

The majority of the experiments used in this chapter to screen for difference between Col-0 and *prt1-1* responses to abiotic used the traditional agar plate culture system, in which both roots and shoots of plants are exposed to light. For roots, illumination is not a natural environment stimulus (Xu *et al.,* 2013) and potentially could introduce growth artefacts into the system. However, the plate system used throughout the physiological screens in this study is a standard technique and unlikely to influence experimental outcomes dramatically.

The Nitrate fresh weight determination experiments conducted, whilst demonstrating no major differences in root or shoot weights for *prt1-1* and Col-0, are not very informative especially for roots as they provide no information regarding the architecture of the rooting system such as rooting depth, lateral root number and length, convex hull or span.

Despite the efforts to screen the broad range of abiotic stresses plants must endure, gaps still remain in knowledge regarding *prt1-1* responses to some significant growth burdens. These include UV-B, wounding and hypoxia, the latter of which PRT6 has been shown to play an important role. Additionally, some physiological screens are technically more challenging. For instance, studying water deficiency in Arabidopsis remains difficult since controlling the water status in a quantitative way with a high degree to reproducibility is challenging. Additionally, due to the thin nature of Arabidopsis roots, imaging them in soil or vermiculite remains arduous. The experiments performed in this study to investigate stomatal conductance were also very basic and should be viewed tentatively. Comprehensive and reproducible stomatal counts and conductance measures are very technically challenging. A more rigorous testing of heat stress would have been desirable in this study also. Plants were subjected to a heat stress of 28 ^{o}C, which is considered to be a

moderate heat stress, but still elicited wilting and reduction in plant overall health. For the purposes of a high-throughput screen this was sufficient but fully investigating plant response to this stress would require a time course of plants at different temperatures, durations and recovery times, with and without pre-exposure to heat stress for heat tolerance. This remains a limitation of many of the high-throughput physiological screens presented in this study which may miss subtle phenotypes. However, given time constraints and limited published literature regarding *PRT1*, such a broad-brush approach was necessary at this point.

Recently, the plant PRT6/N-end rule pathway has been demonstrated to play a key role in the perception and response to a range of abiotic stresses, being dubbed a "general sensor" (Vicente *et al.,* 2017) alongside its well-established role in the hypoxia sensing (Licausi *et al.,* 2011, Gibbs *et al.,* 2011). Constitutive stabilisation of ERFVII substrates in *prt6-1* leads to enhanced survival under abiotic stresses compared to wild type (Riber *et al.,* 2015; Vicente *et al.,* 2017). In the current study, following guidance from the eFP browser, no statistically significant differences were observed under long days between *prt1-1* and Col-0 in response to major abiotic stresses including salinity; phosphate, nitrogen deficiency, iron deficiency and heat stress. It therefore seems likely that rather than functioning as general sensor of abiotic stresses like PRT6*,* PRT1 either plays no role, functions in a redundant manner or plays such a subtle role in response to abiotic stresses as to be unperceivable.

Overall, for the experimental conditions tested in this study, no obvious developmental defects were apparent for the *prt1-1* mutant compared to Col-0. Upon numerous abiotic stress screens, a reproducible difference between these genotypes was also not established. Given that *PRT1* was identified 20 years ago it is apt that no physiological role could be identified in such major abiotic stresses implying PRT1 is involved in a more specific physiological function. Chapter 5 investigates the role of *PRT1* in plant-pathogen interactions.

Chapter 5: The role of PRT1 in plant immunity

5.1 Introduction:

As with all kingdoms of life, plants are challenged by many pathogenic microorganisms. These pathogens exploit plants for resources or to fulfil stages of their life cycles. The terrestrial plant phyllosphere (above-ground tissues) serves as an important biological niche for such microbial survival and proliferation: with many human and plant pathogens living epiphytically for their entire lifecycle or prior to entering the plant, whereby a shift to an endophytic lifestyle is observed (Melotto *et al*., 2006). To combat this, plants have evolved complex molecular mechanisms to defend themselves against pathogen invasion. These can be basal or inducible, passive or active, localised or systemic. Molecules such as secondary metabolites, anti-microbial and cell wall polymers enable plants defend against pathogenesis. The initiation time and extent of these mechanisms determine whether a pathogen will successfully infect the plant (Seo *et al*., 2008).

A successful infection leading to disease is termed a compatible reaction whereas an unsuccessful reaction is known as an incompatible reaction (Ponzio *et al.,* 2016). A major distinction between pathogenic organisms is their lifecycle. A saprotroph is an organism which exists in the vicinity of a plant such as on the leaves (phylloplane) and causes no damage to the plant. These organisms may live off the dead plant tissue but play no active role in damage/death of the plant. Other classifications of plant pathogens do elicit damage to the plant to obtain nutrients or fulfil their lifecycle, and include biotrophs, necrotrophs and hemi-biotrophs (Spanu & Panstruga, 2017). Biotrophy requires the plant to remain alive during nutrient acquisition, and biotroph-plant interactions can be symbiotic in nature, where both plant and microbe benefit, or parasitic, where only the microbe gains from the interaction (Spanu & Kämper, 2010). Necrotrophs on the other hand, actively damage their host and use necrotic tissue as a nutrient source. Some pathogens are classified as hemi-biotrophs, in which they fulfil a biotrophic lifestyle initially but then transition into

necrotrophy. Temporal and/or spatial changes dictate this shift in lifestyle (Spanu & Panstruga, 2017).

5.2 Plant Immunity:

Plant immune response comprises the mechanisms activated upon recognition of the pathogen and can be classified in basal and induced.

5.2.1 Basal resistance (PAMP-triggered Immunity)

The basal resistance is triggered following recognition of pathogen associated molecular patterns (PAMPS) by surface localised pattern recognition receptors (PRRs) (Tsuda *et al.,* 2008). PAMPs are structurally conserved molecules that are usually essential for the pathogen development. PAMPs are not expressed by all pathogens and not all PAMPS are recognised by all plants (Zipfel & Robatzek, 2010). Damage associated molecular patterns (DAMPS) are compounds which are released by the host plant in response to wounding or pathogen infection that are also able to elicit host-plant immune responses (Arnaud & Hwang, 2015). PAMP-triggered immunity (PTI) is characterised by the induction of mitogen activated protein kinases (MAPK), an increase of calcium influx and alkalinisation of extracellular space, production of nitric oxide (NO) and reactive oxygen species (ROS), called oxidative burst, stomatal closure, callose deposition, enhancement of defense gene expression and activation of signalling pathways regulated by hormones including ethylene, salicylic acid (SA) or jasmonic acid (JA) (Boller & Felix, 2009).

5.2.2 Induced resistance (Effector Triggered Immunity)

Whilst PTI is sufficient to prevent most non-pathogenic micro-organisms from successfully infecting plants, in some cases pathogens are able to elude or suppress PTI-induced mechanisms by secretion of effector proteins, termed virulence factors (Preston, 2000). To counter pathogen-mediated suppression of PTI, plants have an additional layer of defence called effector mediated immunity (ETI). This highly specific mechanism

is mediated by the interaction of resistance genes (*R*), usually localized into the cell, with the virulence effectors. Nucleotide-binding (NB) and/or leucine-rich repeat (LRRs) domains are common features of these *R* genes. The proteins encoded by *R* gene can either directly or indirectly recognise pathogen effectors or host-proteins which have been altered by the pathogen proteins (Tsuda *et al.,* 2008). ETI is usually characterized by the activation of localized Programmed Cell Death (PCD) events, in the sites of infection that generate necrotic lesions. This process, named as Hypersensitive Response (HR), may limit the spread of the pathogen and restrict the access of nutrients and water to the pathogen. The cellular reprograming processes activated in ETI are similar to those described for PTI, although there are major differences in the first stages as well as in the intensity and induction time of the response (Jones & Dangl, 2006; Tsuda & Katagiri, 2010).

5.2.3 Systemic Acquired Resistance

Plant resistance initiates downstream signalling cascades which radiate out from the initial site of infection to distal parts of the plant. This is known as systemic acquired resistance (SAR) and primes distant tissues against secondary infections by restricting pathogenic growth (Gao *et al.,* 2015). Systemic defense can be activated by both biotrophs and necrotrophs. SAR is associated with increased levels of the hormone salicylic acid in both local site of infection and systemic tissues (Glazebrook *et al.,* 2005). Although it has been widely assumed that SAR activation is part of the ETI, there are examples that demonstrate that some PAMPs, as flagellin, can activate both a basal defense response in the site of infection and a SAR in systemic tissues.

5.2.4 Signalling pathways regulated by phytohormones

Phytohormones are essential small molecules in plants which direct and regulate a vast array of physiological processes. In plant defence, major phytohormones include salicylic acid (SA) and jasmonic acid (JA) which act in an antagonistic manner. Auxiliary phytohormones include ethylene

(ET), abscisic acid (ABA), gibberellin (GAs), brassinosteroids (BRs) and cytokinins (CKs), which act either synergistically or antagonistically with either SA or JA to elicit plant immune responses. The complexity of phytohormone signalling in plant defence emphasises the importance of the correct timing and magnitude of mounting a defence response. This is also reflected by the myriad of pathogen effectors designed to subvert and interfere with hormone signalling crosstalk or increase virulence through hormone production (Berens *et al.,* 2017).

5.2.4.1 Salicylic Acid Synthesis

In Arabidopsis there are two pathways for SA biosynthesis called the isochorismate synthase (ICS) and the phenylalanine ammonia lyase (PAL) pathway, which both initiate from the common precursor of chorismate (from the Shikimic acid pathway) (Chen *et al.* 2009). In the ICS pathway, chorismate is converted to isochorosimate through the action of ICS, which is then converted to SA by isochormismate pyruvate lyase. In the PAL pathway, chorismate is converted first to prephenate by chorismate mutase and then to phenylalanine or tyrosine. Phenylalanine is then converted to cinnamic acid by PAL and processed through a series of reactions to form SA.

The ICS pathway has been demonstrated to be critical for SA synthesis. There are two ICS genes in Arabidopsis: *ICS1* (also known as *SA INDUCTION DEFICIENT-2/SID2*) and *ICS2* (Strawn *et al., 2007;* Wildermuth *et al.,* 2001). The *ICS1* mutants *sid2-1* and *sid2-2* result in a dramatic reduction in SA levels. Following pathogen challenge by avirulent *Pseudomonas syringae* pv. *maculicola* (*Psm*) or the virulent fungal biotroph *Golovinomyces (Erysiphe) orontii*, the SA accumulation in *sid2/ICS1* mutants was reduced by 90-95% compared to the wild type (Garcion *et al.,* 2008). This resulted in a greatly reduced expression in *sid2* plants (1-10% of WT levels) for *PR-1* genes which are present downstream of SA accumulation and consequent lack of SAR. This suggests that SA synthesised through the ICS pathway is necessary for

mounting a successful SAR in Arabidopsis (Wildermuth *et al*., 2001). Mutation in *ICS1* does not completely block SA accumulation; indicating that *ICS2* may act in a functionally redundant fashion (Garcion *et al.,* 2008).

NON-EXPRESSOR OF PATHOGENESIS-RELATED1 (NPR1) is a positive regulator of systemic acquired resistance which functions downstream of SA. Upon SA accumulation, NPR1 is reduced from its disulphide oligomer form located in the cytosol to its active form which is translocated into the nucleus whereupon NPR1 interacts as a co-factor with the domain/leucine zipper transcription factor TGA (Despres *et al.* 2003; Grant & Lamb, 2006).

5.2.4.2 Jasmonates

Jasmonates, which include jasmonic acid and derivatives, are lipid-derived compounds found ubiquitously in plants. They play a significant role in signalling events during plant growth, development and responses to biotic and abiotic stress (Wasternack, 2007). JAs are synthesised through the octadecanoid biosynthetic pathway from α-linolenic acid. This fatty acid is converted to (13S)-hydroperoxyoctadecatrienoic acid (13-HPOT) in plastids by 13-lipoxygenase (LOX), which is then converted to 2,13(S)-epoxyoctadecatrienoic acid (12,13-EOT) by allene oxide synthase (AOS). AOS is in turn converted into (9S,13S)-12-oxo-phytodienoic acid (OPDA) by allene oxide cyclase (AOC) prior to transport to peroxisomes, where it is reduced, activated and shortened by three rounds of β-oxidation catalysed by three different enzymes to form jasmonic acid. Jasmonic acid is conjugated with isoleucine to form bioactive (+)-7-*iso*-JA-Ile in the cytoplasm (Wasternack & Hause, 2013; Huang *et al.,* 2017; Wasternack and Strnad, 2016).

When JA is not perceived, the transcription factors of JA-responsive gene expression are repressed through JA ZIM-DOMAIN protein interaction with the adaptor NOVEL INTERACTOR OF JAZ (NINJA) and

the co-repressor TOPLESS (TPL) (Chini *et al.*, 2007; Thines *et al*., 2007; Yan *et al.,* 2007). Bioactive JA is perceived by the CORONATINE INSENSITIVE (COI1) receptor. COI1 forms part of the SKP1/CULLIN-based SCFCOI1 E3 ligase which co-ordinates the ubiquitylation and subsequent degradation of JAZ proteins to alleviate the repression on JA-responsive gene transcription factors. This enables JA responses to occur (Yan *et al.,* 2009; Huang *et al.,* 2017).

Jasmonate and signalling through the JA-pathway confers host resistance to pathogens chiefly with necrotrophic lifestyles including *Botrytis cinerea* (Abu Qamar, Moustafa, and Tran, 2017)*, Alternaria brassicicola* and *Fusarium oxysporum* (Lyons *et al.,* 2015). Pathogens exploit this pathway or the antagonism of JA-signalling of SA to achieve compatible interactions.

5.2.4.3 Ethylene

Ethylene (ET) is a gaseous hormone which serves a critical function in a diverse range of plant physiological processes, including plant immunity. ET is implicated in plant responses to necrotrophy as well as SAR and acts in an antagonistic fashion to SA and synergistically with JA (Zhang *et al.,* 2006). PAMP recognition by PRRs triggers ET, SA and JA production and consequent PTI. ET is proposed to help sustain PTI through an amplification loop. Signals from JA and ET are integrated by *ERF1*, as expression requires JA, ET, COI1 and EIN2 (Lorenzo *et al.,* 2003). *ERF1* acts downstream from COI1 to activate gene expression of JA-responsive genes (Glazebrook, 2005).

5.2.4.4 Auxiliary Phytohormones

Phytohormones that act in an auxiliary manner to these major hormone pathways include ABA, GA, BRs and CKs. ABA is primarily involved in abiotic stress signalling but plays complex roles in plant-microbe interactions. ABA frequently suppresses host immune responses and is

exploited by pathogens as an effector molecule. ABA is also implicated in compatible mutualistic interactions including rhizosphere bacteria association with plants and stomatal closure (Lievens *et al.,* 2017; Melotto *et al.,* 2006). BRs and GAs regulate many plant developmental processes throughout its life cycle. The role of these phytohormones in microbe-plant interactions is not clear and depends to a large extent on the pathogen lifecycle, infection strategy and timing of infection (De Bruyne, Höfte, and De Vleesschauwer, 2014). CKs are hormones that promote plant growth but also play roles in pathogenesis and nodulation. Plant derived CKs are implicated in systemic induction of resistance through interplay with SA. Conversely microbe derived CKs augment sink activity in infected tissue by eliciting abnormal hypersensitivity in the plant (Choi *et al.,* 2011).

5.2.5 PRs proteins

Pathogenesis related proteins, and related homologues, are plant encoded proteins which enable them to combat invading pathogens. The biochemical and biological properties classify PR proteins into 17 families (PR-1 to PR-17) (van Loon *et al.,* 2006). The physiological functions of many of the PR proteins is known and summarised in table 5.1 (van Loon *et al.,* 2006).

PR are chiefly induced by phytohormones including SA, JA and ethylene (Seo *et al.,* 2008). The concentration of the defense hormones increases during pathogen infection, leading to expression of *PR* genes in response to infection (Durrent & Dong, 2004). In the absence of pathogen stress, these *PR* genes are expressed at a low basal level, but *PR* gene are temporally and spatially regulated. Seo *et al*. (2008) examined the tissue expression patterns of Arabidopsis *PR* genes using reverse-transcription PCR (RT-PCR) under standard, unstressed growth conditions. It was shown that *PR-1, PR-2 & PR-5* are relatively higher expressed in leaf and stem tissues compared to the reproductive tissues and roots. The opposite was observed with *PR-3* & *PR-4*, where greatest transcript

expression was in the roots, although detection was also observed in the flowers, stems and leaves.

Figure 5.1: A summary of the known function of pathogenesis related proteins (van Loon *et al.,* 2006).

PR Protein	Activity
PR-1	Unknown
PR-2	β-1,3-glucanase
PR-3	Chitinase
PR-4	Chitinase
PR-5	Thaumatin-like protein
PR-6	Proteasome Inhibitor
PR-7	Endoproteinase
PR-8	Chitinase
PR-9	Peroxidase
PR-10	Ribonuclease-like
PR-11	Chitinase
PR-12	Defensin
PR-13	Thionin
PR-14	Lipid-transfer protein
PR-15	Oxalate oxidase
PR-16	Oxalate oxidase-like
PR-17	Unknown

In Arabidopsis, salicylic acid induces *PR-1, PR-2 and PR-5*, whereas jasmonic acid acts in an antagonistic manner, activating *PR-3 and PR-4* (Seo *et al*., 2008). Signalling cross-talk involving abscisic acid has also been observed with *PR-3* being induced by ABA although *PR-2* is repressed by this hormone (Hillwig *et al.,* 2016). PR proteins may play

essential roles in plant development that go beyond defence against pathogens. For instance, PR-2 in tobacco has been implicated in seed germination (Leubner-Metzger, 2005). *PR* genes are also differentially regulated during development: transcripts of all *PR* genes are relatively low up to 7 days after germination (DAG) but a significant increase in expression is observed and maintained thereafter for *PR-1, PR-2 and PR-5.* In contrast, a gradual increase in relative expression of *PR-3 and PR-4* is observed until these levels plateau about 28 DAG (Seo *et al*., 2008). This emphasises the multifaceted nature of *PR* gene products aside from defence purposes and the clear distinction between the two groups of *PR* genes is consistent with their regulation by JA and SA.

5.2.6 Function of Plant Stomata in Pathogen Defence

Entry of microorganisms into the plant interior is a critical first step for pathogenesis. Many natural openings exist on the surface of leaves that can be exploited by microorganisms, such as stomata, hydathodes and wounds. Stomata consist of a pair of specialised guard cells (Figure 5.1) located on the leaf epidermis which maintain a constant leaf internal environment through gaseous exchange with the environment due to the impermeability of the leaf cuticle (Kim *et al.,* 2010). Stomata play an integral role in gas exchange and limitation of transpirational water loss (Arnaud & Hwang, 2015; Haworth *et al.*, 2011). Stomatal aperture is regulated in response to light, carbon dioxide, humidity and microbes (Melotto *et al*., 2006).

The opening and closure mechanism of stomata is a highly regulated and dynamic process in which complex environmental and hormonal cues are integrated to enable gas exchange but compensate for water loss. The activity of anion channels present in the stomata plasma membranes is reduced during light-induced stomata opening whereas H^+-ATPase activity is increased which results in H^+ extrusion and causes acidification of extracellular spaces (Sirichandra *et al*., 2009). Increased H^+-ATPase activity also causes membrane potential hyperpolarisation which

activates inward-rectifying K^+in channels that drive the influx and accumulation of K^+, Cl^- and $NO3^-$ anions. Additionally, osmotically inactivate starch is converted to malate, the result of which increases the turgor pressure inside the guard cells, changes their internal volume and shape, thus creating a pore in which gases can be exchanged (Kim *et al.,* 2010). Downregulation of K^+ in channels and H^+-ATPases by ABA has inhibitory effect on stomatal opening (Kim *et al*., 2010).

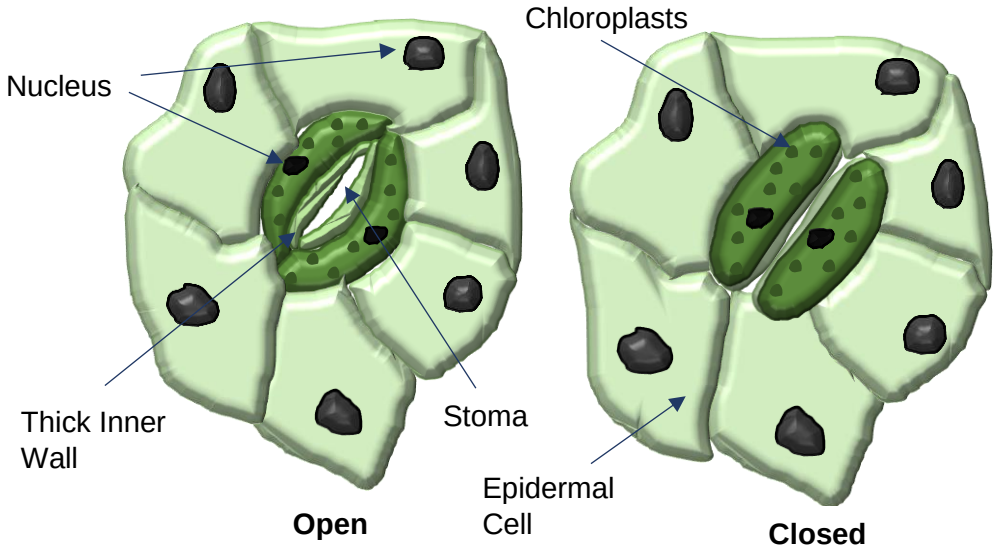

Figure 5.2: A diagram showing the opening and closure of stomata pores. The ability of plants to alter their stomatal aperture allows the regulation of gaseous exchange to be balanced with limitation to water loss, heat exchange and restriction of phytopathogens in the leaf interior. (Diagram based on Mäser, Leonhardt & Schroeder, 2003)

Abiotic stress perception results in signal transduction cascades that close stomata. The phytohormone ABA was demonstrated by Mittelheuser and van Stevenick (1969) to be a key regulator of this following observations that ABA has a pronounced anti-transpirant effect when applied to detached leaves. Cross-talk with other plant hormones, including JA, brassinosteroids, ethylene and cytokinins is also implicated in abiotic stress-induced closure of stomata (Daszkowska-Golec & Szarejko, 2013; Lee & Luan, 2012).

Stomata also have an involvement in the plant immunity against micro-organisms, which is logical since these pores are the primary route to pathogenesis of many phytopathogens such as bacteria *Pseudomonas syrinage* pv *tomato* DC3000 (*Pst* DC3000) on tomato and *Escherichia coli* O157:H7 (*E. coli)* on *Arabidopsis*, as well as the parasitic fungi *Fusiococcum amygdali* (Turner & Graniti, 1969). The microbial community normally present on the leaf phylloplane may be insufficient to elicit stomatal closure (Gudesblat, Torres & Vojnov, 2009) but higher concentrations have been reported to induce this response in the *Arabidopsis-Pst* DC3000 pathosystem. This is a mechanism to limit bacterial invasion (Melotto *et al.,* 2006).

Stomatal closure or inhibition of opening are active mechanisms of plant innate immunity, via the phytohormone ABA, limiting microbe invasion into apoplast (Arnaud & Hwang, 2015). Detection of the bacterial flagellin-derived peptide flg22 and lipopolysaccharide (LPS) are sufficient to elicit PAMP-mediated stomatal closure, indicating this is a facet of PTI (Melotto *et al*., 2006). The pathogen is then able to re-open stomata through compounds use as the toxin coronatine in *Pseudomonas syringae.* The plant then able to re-close the stomata to limit microbial invasion (Zheng *et al.,* 2012).

.

5.3 *Pseudomonas syringae* - a model foliar phytopathogenic bacterium

Pseudomonas syringae is a rod shaped, Gram negative bacterium that is an important model for studying plant-pathogen interactions. The *Pseudomonas syringae* species contains many strains responsible for a plethora of economically important plant diseases. It is grouped into pathovars based on their host specificity and further divided into races based on their mechanism of interactions amongst cultivars (Xe & He, 2013). For instance, *Pseudomonas syringae* pv. *actinidiae (Psa)* is implicated in bleeding canker disease which severely damaged the kiwifruit industry in New Zealand (Vanneste, 2017). Also, *Pseudomonas syringae* pv. *tomato* is associated with bacterial speck in *Brassica oleracea* var. *botrytis* (cauliflower) and *Solanum lycopersicum* (tomato) which affect the yield and the market value of these crops due to the presence of necrotrophic lesions surrounded by chlorotic halos (Cuppels, 1986; Preston, 2000).

Pseudomonas syringae pv. tomato (*Pst*) DC3000 is a rifampicin resistant derivative of the *Pst* DC52 strain generated by Cuppels (1986) initially for cloning purposes. Work by Whalen *et al* (1991) demonstrated the ability of this bacteria to infect tomato and *Arabidopsis thialiana*. *Pst* DC3000 is an easily culturable strain, with a well-defined and typical lifestyle for hemi-biotrophic phytobacteria. Consequently, it is suited to studying host-pathogen compatible and incompatible interactions (Preston, 2000).

5.3.1 Lifestyle and Infection cycles:

P. syringae species have an infection cycle typical for a foliar bacterium with two distinct life cycles: an epiphytic phase, in which the bacteria survive on the surface of the plant, and an endophytic phase upon entry into the apoplastic space in the plant. Despite the ability of the pathogen to live in both lifestyles, within the *Pseudomonas syringae* species there is great variation in preference at the strain level as to which lifestyle

predominates. *P. syringae* pv. *syringae* (B728a) is able to thrive epiphytically without causing host disease. Conversely, the *P. syrinage* pv. tomato (DC3000) strain is a weak epiphyte as it dies within ~48 hours on the phylloplane (leaf surface) of spray-treated tomato plants but is a very aggressive pathogen once it enters the host plant (Xin & He, 2013; Hirano & Upper, 2000).

Generally, the phyllosphere of plants represents a hostile niche for microbes, owing to large fluctuations of temperature, UV and humidity within small timescales, competition with other micro-organisms living epiphytically, and a dearth of nutrients on the plant surface (Beattie and Lindow, 1999). However, due to the heterogeneous nature of the plant surface, nutrient-rich pockets sheltered from harsh abiotic stresses exist, and it is these areas in which micro-organisms aggregate. The phyllosphere should therefore be considered as a series of micro-scale environments (Melotto *et al*., 2008). Areas surrounding stomata, trichomes and vasculature have been noted as more desirable environments for epiphytes (Hirano & Upper, 2000). Furthermore, it has been demonstrated that certain strains of *Pseudomonas* spp can manipulate the phylloplane to create more favourable conditions. For instance, Bunster *et al* (1989) demonstrated that the surface-active *Pseudomonas putida* (WCS358RR) elicited a significant increase in leaf surface wettability which positively alter the availability of water and nutrients to the microbe. These epiphytic resources are limited and as their availability dwindles, the drive to enter the nutrient-rich plant interior increases and the epiphytic community on the leaf surface are the inoculum for endophytic infection (Xin & He, 2013).

Whilst the plant interior may shelter the bacteria from abiotic stresses of the phyllosphere, it may also pose a different type of stress to the microorganism. Increased concentration of defence compounds that differ to those on the exterior of the plant are present in the plant apoplast. These may present a harsh environment for non-pathogenic and saprophytic micro-organisms (Beattie & Lindow, 1995), However,

phytopathogenic foliar bacteria such as *Pseudomonas syringae* have evolved mechanisms such as virulence factors that enable them to mitigate the effect of these plant defence compounds which may be specific to certain hosts (Lee, Jelenska & Greenberg, 2008).

5.3.2 Bacterial Entry into the host plant

The evolution and maintenance of distinct epiphytic and endophytic lifestyles in foliar bacteria suggest that entry into the plant apoplast is not a straightforward process. Many foliar bacteria exploit wounding sites and natural openings such as stomata to enter the plant apoplast (Arnaud & Hwang, 2015). Stomata make up approximately 2% of the total leaf surface. Stomatal aperture is heavily influenced by environmental conditions such as time of day, humidity and CO_2 concentration. Closure of the pores in response to these external factors is an additional barrier to pathogen entry into the plant. Stomatal density is higher on the abaxial side of the leaf, whereas foliar pathogens are most likely to land on the adaxial aspect of the leaf meaning *Pseudomonas*-stomata interactions are even less probable (Melotto, Underwood & He, 2008). Furthermore, favourable conditions aside from open stomata must be present to facilitate entry of the pathogen into the plant. Leaf surface moisture may be required for adhesion and movement of bacteria, which is highlighted by the increased incidence of plant infection by foliar bacteria after prolonged periods of high humidity and rainfall (Hirano & Upper, 2000). Consequently, being able to live epiphytically prior to endophytically can be advantageous for foliar bacteria.

5.3.3 *Pst* DC3000 Endophytic Lifestyle

Upon entry into the apoplastic space, *Pst* DC3000 lives as a hemibiotrophic pathogen, Initially, *Pst* DC3000 behaves as a biotrophic pathogen, acquiring nutrients from host tissues without causing host cell death. However, a shift to a necrotrophic lifestyle is observed in late stage pathogenesis, characterised by peak population in infected plant tissues,

host cell death and extensive necrosis (Xin & He, 2013). Establishment of an aqueous living space may be crucial for virulence. This is called the 'water soaking' phenomena and is indicative of very aggressive infection by *Pst* DC3000 during the first day of infection, although the role in pathogenesis is not fully understood (Katagiri, Thimony &, He, 2003). Generally, water soaking disappears as the onset of late stage disease symptoms begins, suggesting that it may play a role in promoting the flow of nutrients and facilitate the spread of bacteria during its biotrophic growth period and may help suppress host defence mechanisms in the apoplast (Xin *et al.,* 2016). Bacterial mulitplication has been positively correlated with air humidity during pathogen infection, with increased humidity giving greatest multiplication (Xin *et al*., 2016).

5.3.4 *Pst* DC3000 Virulence factors: Protein secretion Systems

Pst DC3000 has a high genetic potential to make it a successful plant pathogen (Xin & He, 2013), with approximately 5% of its genome dedicated to virulence-related genes (Buell *et al.,* 2003). Type I-VI and twin arginine transporter (Tat) secretion systems are encoded by the *Pst* DC3000 genome (Lindeburg *et al.,* 2008), with type II, III and Tat secretion systems being particularly pertinent for virulence. The *Tat* secretion systems export folded proteins into the periplasmic space and mutants lacking *Tat* components have reduced virulence (Bronstein *et al.,* 2005).

The Type III secretion system (Figure 5.3) resembles a syringe-like complex facilitating the delivery of type III effectors across the bacterial envelop to the plant interior and is encoded by *HRP* (hypersensitive response and pathogenesis) and *HRC* (*HRP* conserved) genes (Galan & Collmer, 1999; Buttner *et al.,* 2009). Delivery of these key virulence factors is essential for successful colonisation of plants by interfering with the plant defense mechanisms. Removal of certain individual effectors is not detrimental for virulence, due to the high degree of functional redundancy of the repertoire of pathogen effectors (Kvitko *et al.,* 2009).

Effector deletion series are useful tools for studying plant-pathogen interactions when a protein function is unknown in the plant.

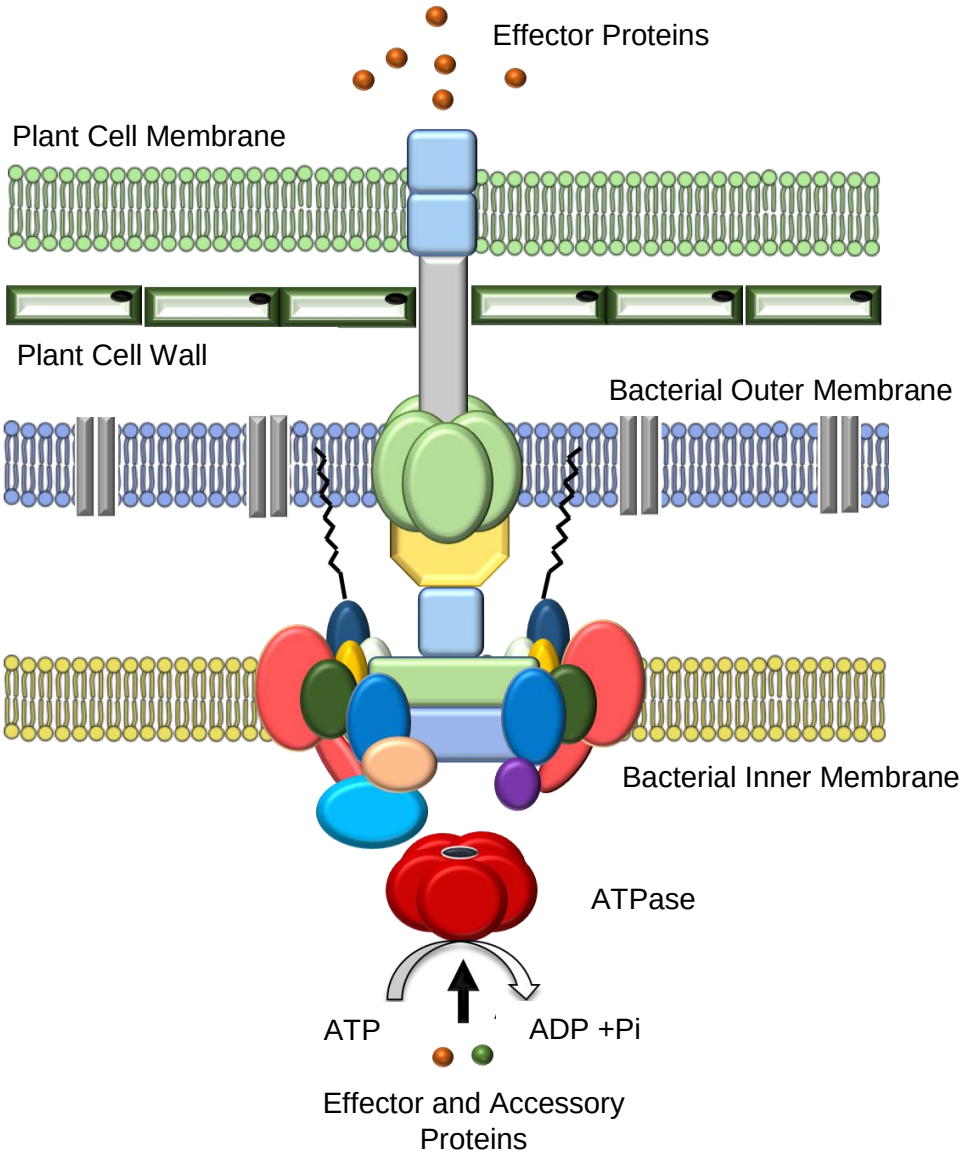

Figure 5.3: A diagram showing the structure of type III secretion systems involved in the delivery of effectors into the host organism to assist colonisation (Diagram based on Büttner *et al.,* 2012).

5.3.5 The virulence effector coronatine

Coronatine (COR) is a polyketide toxin secreted by *Pst* DC3000 and by other *P. syringae* pathovars including *maculicola, porri, glycinea, atropurpurea and alisalensis.* Toxins analogous to COR are also produced by *Xanthomonas campesteris* pv*. phormiicolai* (Geng *et al*., 2014). COR producing bacteria are more aggressive compared to COR-deficient counterparts (Panchal *et al*., 2016). COR is a non-host specific toxin compromised of coronafaric acid (CFA) and coronamic acid (CMA) structural components which are synthesised independently. The operons for producing both these structural components are separated on *Pst* DC3000 plasmids by a 26Kb intergenic region. COR production is regulated in response to environmental cues, such as temperature in *Pseudomonas syringae pv. glycinea* 4180, in a two-component system involving corR in concert with corS and corP (Xin & He, 2013). Functional COR is produced following amide linkage formation between CMA and CFA by coronfacate ligase (Bender *et al*., 1999).

Coronatine is structurally analogous to jasmonic acid and mimics JA in the plant. Once coronatine is sensed by the plant, it interferes with the salicylic acid signalling pathway through JA antagonism. This suppresses SA-dependent defence responses by hijacking the COI1-JAZ-MYC signalling pathway, leaving the plants more susceptible to pathogenesis by biotrophic pathogens such as *Pst* DC3000 (Zheng *et al.,* 2015). HOPXI and HOPZ1a *P. syringae* effectors deplete JAZ protein reserves and prevent stomatal closure to facilitate bacterial entry into the plant apoplast (Wasternack, 2017).

5.4 Aims:

Given the wealth of published literature and utility of the Arabidopsis-*Pst* DC3000 pathosystem, plant responses to biotic stresses were analysed for *prt1-1,* Col-0 and the complementing line (*PRT1pro*::gDNA-TAP in the *prt1-1* background) to assess differential responses to the bacteria. During this study, two papers were published regarding the role of the plant N-end rule pathway presenting opposite phenotypes for N-end rule mutants. This chapter also sought to establish an independent dataset to determine which result is reproducible and explore in detail molecular mechanisms underpinning any potential phenotype.

5.5 Results:

5.5.1 Publicly available expression data

As with experiments searching for a role for PRT1 in abiotic stresses, the Arabidopsis eFP browser was used initially to reveal if there is any significant transcriptional upregulation of *PRT1* following stress by pathogens. The Arabidopsis eFP browser (Figure 5.4) hints there may be a role for PRT1 mediated degradation in plant responses to biotic stresses.

Pst DC3000 (10^8 cfu/ml) direct infiltration experiments on 5-week-old rosettes suggest an increase in *PRT1* expression relative to 10mM $MgCl_2$ of 1.25, 1.12 and 2.0 at 2 h, 6 h and 24 h respectively. Treatment with avirulent *Pst* DC3000 avrRpm1 produced a similar gene expression profile to mock treatment, with an induction of *PRT1* expression observed only at 24hpi (Nürnberger lab). Treatment of 4-week-old Col-0 rosettes (ND) with the necrotroph *Botrytis cinerea* condiospores produced fold changes of 0.75 at 18 hpi and 1.08 48 hpi relative to potato dextrose broth controls (0.99 & 1.0 respectively) (data produced by the Ausubel lab). *PRT1* expression declines in response to an array of pathogens including *Golovinomyces orontii* (Chandran *et al.,* 2010), *Hyaloperonospora arabidopsidis* (Wang *et al.,* 2011), *Myzus persicae* (Couldridge *et al.,* 2007), *Phytophthora infestans* (Sheel lab) and *Eryshiphe orontii* (Aushel lab).

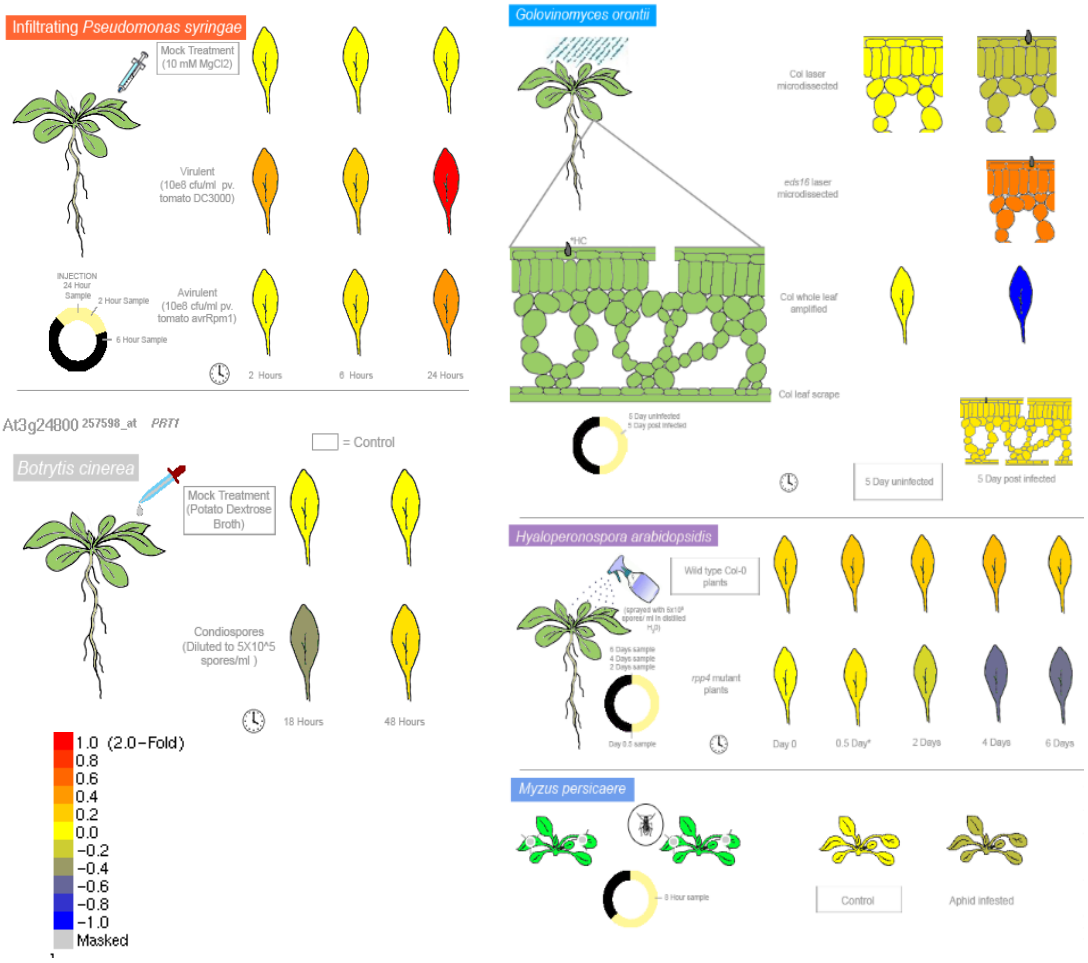

Figure 5.4: Expression of *PRT1* in public transcript data: Effect of different pathogens on expression of *PRT1* (At3g24800). Adapted from the Arabidopsis biotic stress eFP browser (Winter *et al,* 2007) showing the relative expression of *PRT1* following treatment with pathogens and pests relative to control treatments.

5.5.2 Morphological analysis of plant material

To address whether PRT1 is implicated in plant defense, 28 DAG *Arabidopsis thaliana* plants grown in soil were challenged with *Pseudomonas syringae* pv tomato strains then the bacterial load in the plant quantified 4 days post infection. Initial experiments focused on Col-0, *prt1-1* and a complementing line (*PRT1*$_{pro}$::gDNA-*PRT1*::TAP tag in *prt1-1* background), with the inclusion of *prt6-1* and *prt1-1prt6-1* lines in later experiments. Initial experiments determined whether there is any physiological difference between genotypes at the time of growth where bacterial infections were carried out.

Rosettes were removed from plants and weighed immediately for fresh weight determination (Figure 5.5A). At 28DAG rosette fresh weights were 290.06 ± 18.1 mg, 288.0 ± 10.3 mg, 286.8 ± 17.2 mg, 280.7 ± 20.7 mg and 277.7 ± 23.1 mg for Col-0, *prt1-1* the complementing line, *prt6-1* and *prt1-1 prt6-1* respectively (Figure 5.5B). Following 3 days drying of these samples at 70^{O}C, dry weights were 24.1 ± 1.4 mg for col-0*, prt1-1* was 24.2.0 ± 1.1 mg, and the complementing line was 24.3 ± 1.3 mg, *prt6-1* for 24.1 ± 1.5 mg and 23.6 ± 1.5 mg for *prt1-1prt6-1* (Figure 5.5C). At the point of bacterial quantification (32DAG), rosette fresh weights were also statistically indistinguishable as demonstrated by p=0.9526 following one-way ANOVA analysis. Overall, at the time of inoculation and quantification *prt1-1,* Col-0 and the complementing line are morphologically indistinguishable, avoiding potential artefacts due to different developmental stages. The *prt6-1* mutant and the *prt1-1 prt6-1* double mutants are slightly smaller compared to Col-0 and the other lines at 28DAG and 32DAG but not significantly (Figure 5.5 A-D as demonstrated by one-way ANOVA analysis (p = 0.9882 and 0.9526).

.

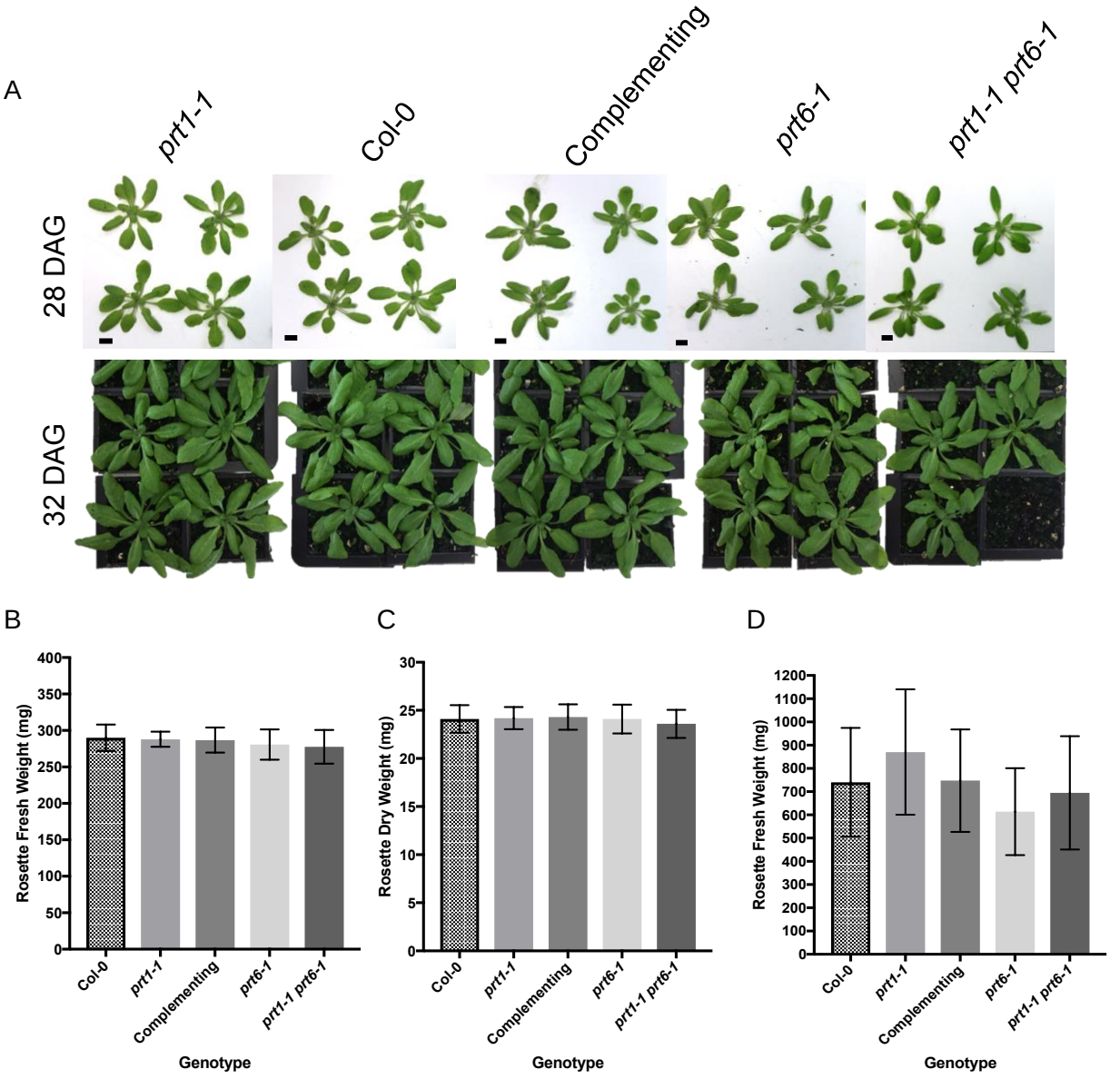

Figure 5.5 Morphological analysis of plant material at the point of bacterial inoculation and quantification: (A) representative images of rosettes of all genotypes grown for 28DAG and 32DAG in neutral day light conditions. Mean biomass accumulation measured at 28 DAG (B) fresh weight (n=16) at 28 DAG (C) dry weight at 28 DAG (n=8) and (D) fresh weight at 32 DAG (n=8). Values are means ± SEM and results of no significance were confirmed by one-way ANOVA with Tukey multiple comparison tests.

5.5.3 Quantification of bacterial load following inoculation

5.5.3.1 Quantification of Virulent *Pst* DC3000

Initial experiments involved the direct infiltration and spray treatments of 28DAG leaves 6, 7 and 8 (described in chapter 2.2.12) of virulent *Pseudomonas syringae* pv *tomato* DC3000 culture. The bacteria, following overnight culture, was resuspended in $MgCl_2$ and either injected (10^6 cfu/ml) into the abaxial side of leaves 6, 7 and 8, or sprayed on to the adaxial rosette (10^8 cfu/ml). Four days post infection the bacterial load inside the leaf was determined. Visually at the time of bacteria

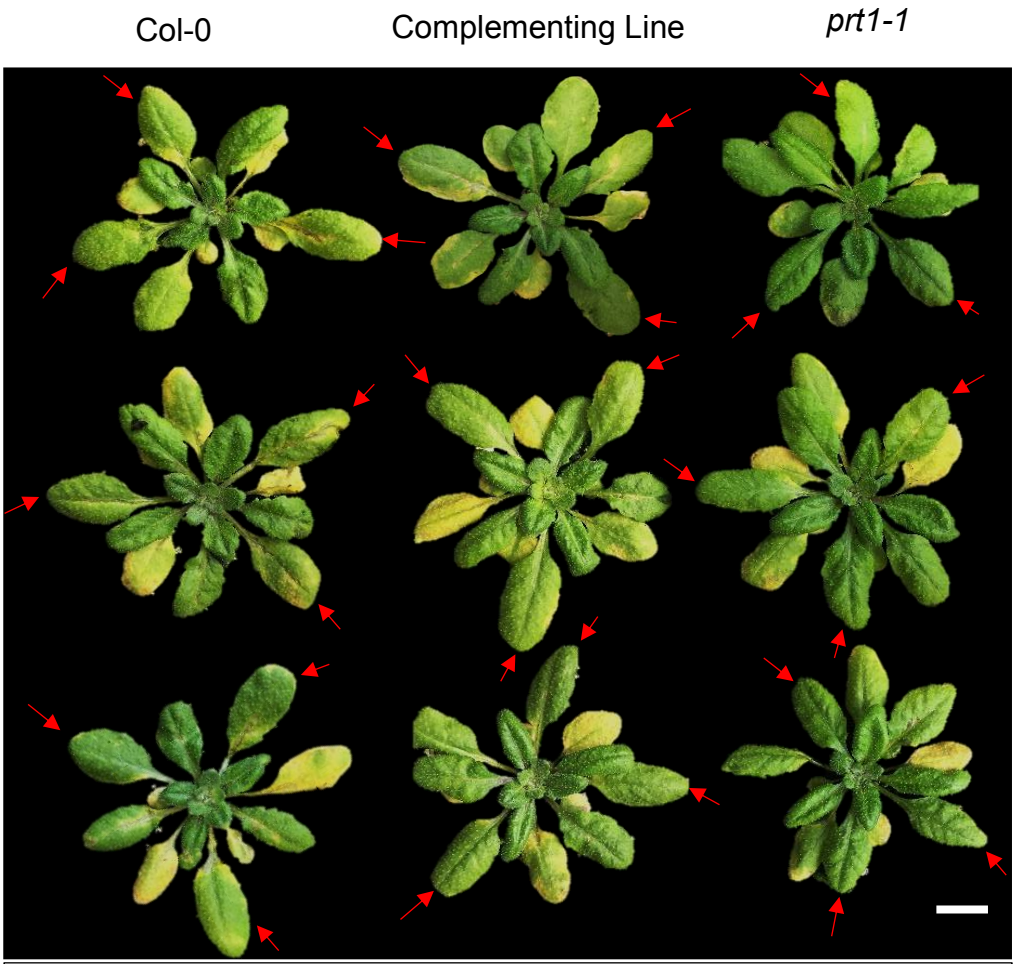

Figure 5.6 The symptoms of Col-0, *prt1-1* and *PRT1*$_{pro}$::gDNA-*PRT1*::TAP tag in *prt1-1* background following pathogen spray treatment: representative images showing an *Arabidopsis* rosette at the point of pathogen quantification (32DAG in neutral day growth conditions). Plants were treated by virulent *Pst* DC3000 spray on the adaxial rosette. Arrows in red indicate leaves 6, 7 & 8 used for quantification of bacterial load inside the plant and scale bar is 1cm.

quantification, the leaves of Col-0 and complementing line plants bore stronger symptoms of pathogen infection for both spray (Figure 5.6) and direct infiltration assays.

For both the direct infiltration and spray treatment pathogen assays for virulent *Pst* DC3000, a reproducible difference in plant resistance is observed for mutants of both plant E3 ligases functioning through the N-end rule pathway (taken from pooled data from four independent biological replicates; Figure 5.7). Following direct infiltration experiments, bacterial load was determined. A reduction in bacterial load was observed for *prt1-1, prt6-1* and *prt1-1prt6-1* mutants respectively compared to Col-0 and the complementing line. Following ordinary one-way ANOVA analysis with Tukey's multiple comparison test no significance could be determined between Col-0 and the complementing line ($p = 0.9852$) or N-end rule mutants (*prt1-1* vs *prt6-1* $p = 0.7961$; *prt1-1* vs *prt1-1prt6-1* $p = 0.9988$; *prt6-1* vs *prt1-1prt6-1* $p = 0.6329$). However, statistical significance was determined between Col-0 vs *prt1-1* ($p<0.0001$), Col-0 vs *prt6-1* ($p<0.0001$) and Col-0 vs *prt1-1prt6-1* ($p=0.0003$). The bacterial loads following spray treatment (Figure 5.7 B) were quantified and similar patterns of resistance were observed between N-end rule mutants compared to Col-0 and the complementing line as direct infiltration experiments. Compared to the wild type, all N-end rule mutant lines were statistically more resistant ($p < 0.0001$) whereas the complementing line behaved analogously ($p = 0.6832$) compared to Col-0.

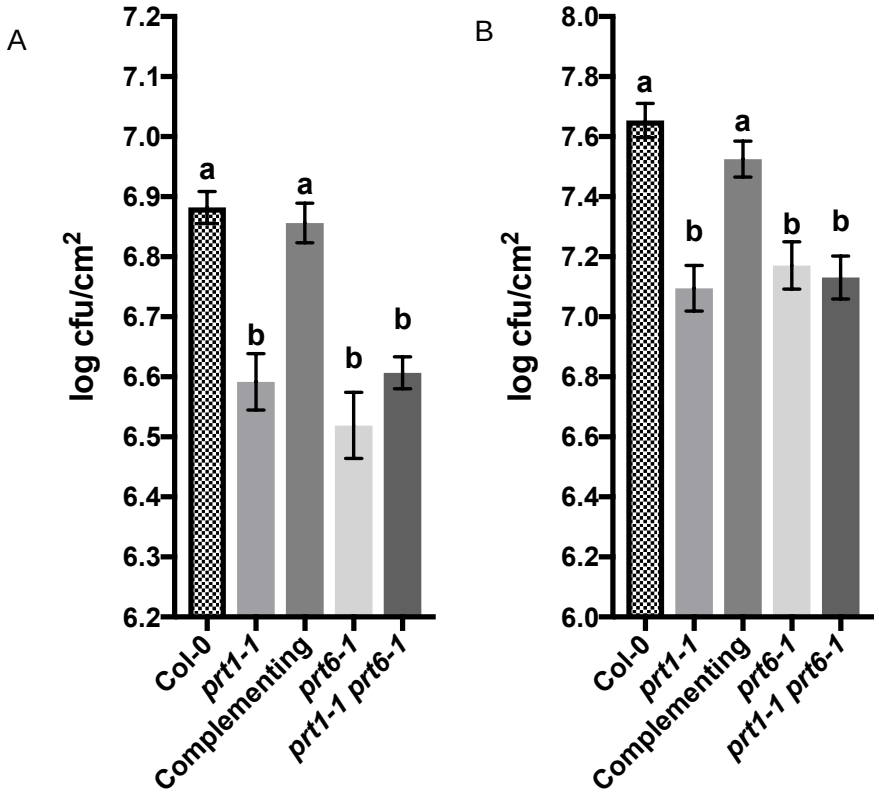

Figure 5.7 Quantification of the bacterial load in plants following direct injection and spray treatment with *Pst* DC3000*:* results of susceptibility assays with virulent *Pseudomonas syringae* pv *tomato* DC3000 on *Arabidopsis* plants grown for 28DAG in neutral day growth conditions 4dpi for (A) direct infiltration (n=18) and (B) spray treatments (n=48). Pooled data plotted as mean log cfu/cm^2 ± SEM from 4 independent biological replicates and significance determined by one-way ANOVA with Tukey's multiple comparison analysis. Means are grouped according to 'a', 'b', 'c' etc.

5.5.3.2 Quantification of Avirulent *Pst* DC3000 *AvrRpm1*

Experimental lines were then subjected to direct infiltration with the ETI-inducing avirulent strain of *Pst* DC3000 (*AvrRpm1*). The bacterial load following direct infiltration with *Pst* DC3000 *AvrRpm1* (Figure 5.8) was slightly in lower in N-end rule mutants (n=6): 5.51 ± 0.053 log cfu/cm^2 for *prt1-1*, 5.48 ± 0.051 log cfu/cm^2 for *prt6-1* and 5.51 ± 0.049 log cfu/cm^2 for *prt1-1prt6-1,* compared with 5.66 ± 0.047 log cfu/cm^2 and 5.65 ± 0.055 log cfu/cm^2 for Col-0 and the complementing line respectively. Following statistical analysis by one-way ANOVA with Tukey's multiple comparison analysis, no significance could be demonstrated however between genotypes in response to *Pst* DC3000 *AvrRpm1* infection.

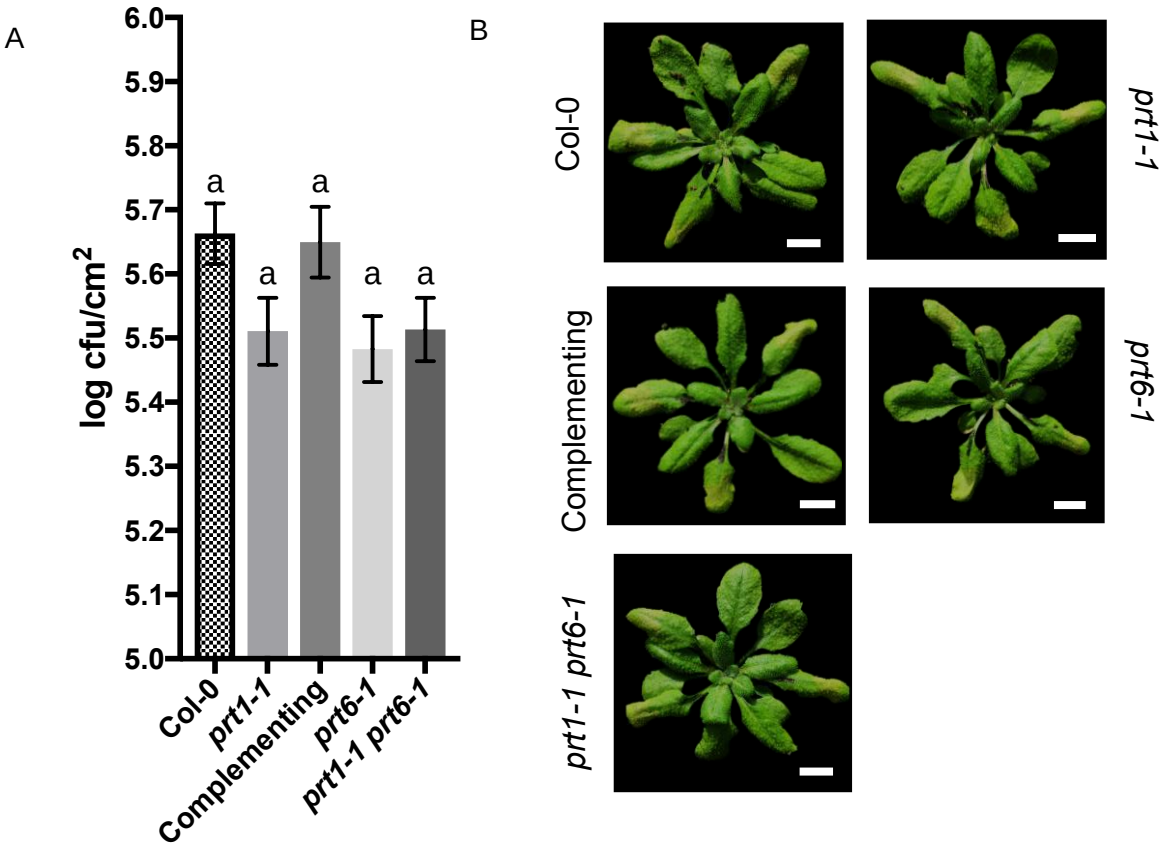

Figure 5.8 Quantification of the bacterial load in plants following direct injection with *Pst* DC3000 *AvrRpm1:* (A) quantified bacterial counts 4dpi plotted as mean log cfu/cm^2 ± SEM (n=6) and (B) representative images of rosettes. Significance determined by one-way ANOVA with Tukey's multiple comparison analysis. Means are grouped according to 'a', 'b', 'c' etc. Scale bars = 10mm.

5.5.3.3 Quantification of *Pst* DC3000 *hrpA-*

Further dissection of the Arabidopsis-*Pst* DC3000 pathosystem involved pathogen susceptibility assays conducted with *Pst* DC3000 *hrpA-:* a mutant strain with a deletion in the HrpA component of the type III secretion system which is unable to deliver effectors required for full virulence. No significant difference is observed between any of the genotypes tested in relation to susceptibility to Pst DC3000 *hrpA*- for three independent biological replicates (n=18) (Figure 5.9).

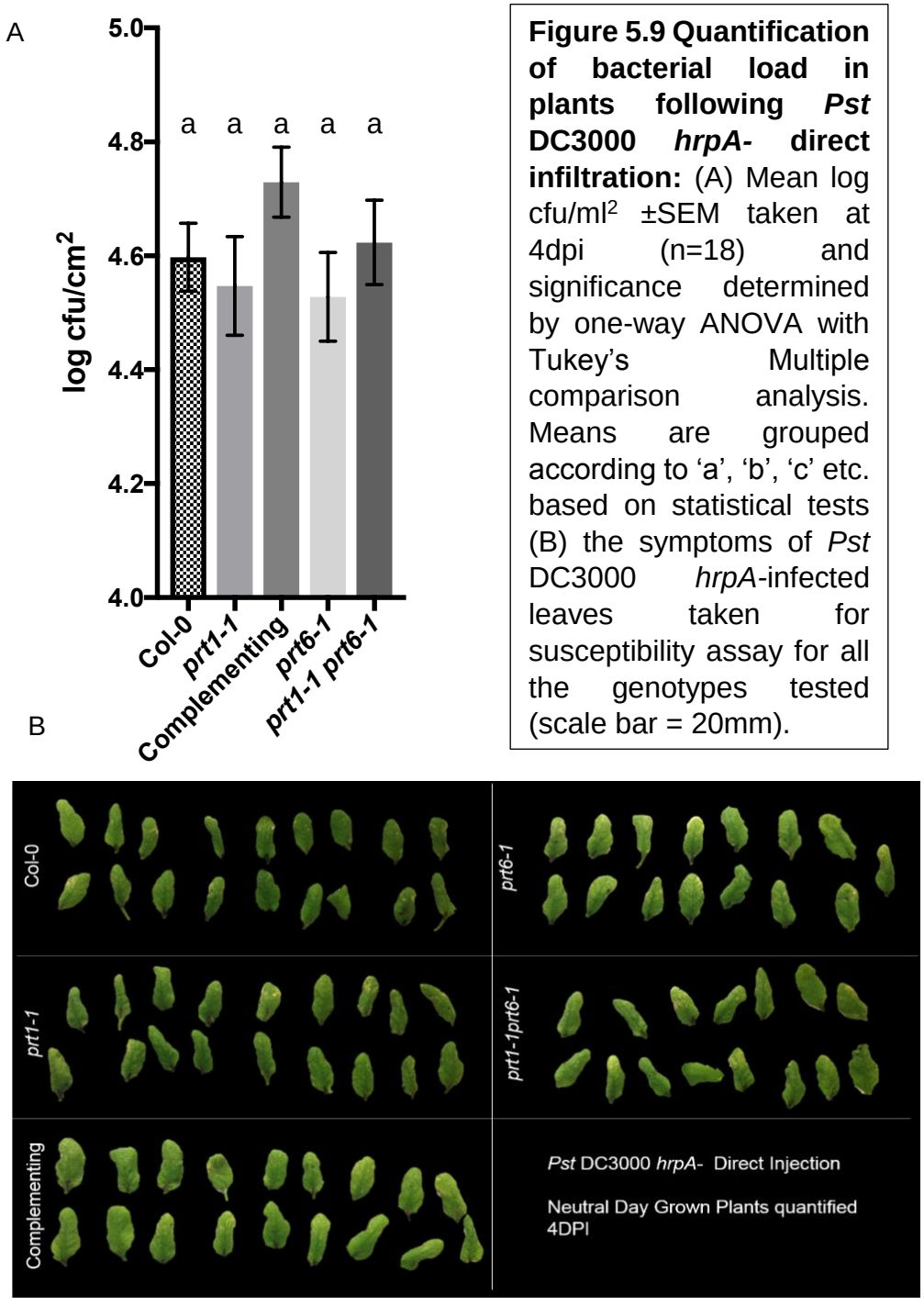

Figure 5.9 Quantification of bacterial load in plants following *Pst* DC3000 *hrpA-* direct infiltration: (A) Mean log cfu/ml^2 ±SEM taken at 4dpi (n=18) and significance determined by one-way ANOVA with Tukey's Multiple comparison analysis. Means are grouped according to 'a', 'b', 'c' etc. based on statistical tests (B) the symptoms of *Pst* DC3000 *hrpA*-infected leaves taken for susceptibility assay for all the genotypes tested (scale bar = 20mm).

5.5.3.4 Assessment of Systemic acquired resistance responses

To test whether there is any involvement of PRT1 in systemic acquired resistance, 30 DAG plants were first pre-treated with the SAR-inducing strain *Pst* DC3000 *AvrRpm*1, followed, after two days, by injection of the virulent *Pst* DC3000, which was quantified four days post inoculation. Non-pre-treated plants were challenged with *Pst* DC3000 and quantified 4dpi as a control for the assay (Figure 5.10). No significant difference was observed in susceptibility of all genotypes pre-treated with avirulent strain and subsequently infected with the virulent strain. The control assay of *Pst* DC3000 only gave the same patterns of susceptibility with *prt1-1, prt6-1* and *prt1-1 prt6-1* all showing reduced susceptibility when compared to Col-0 and the complementing line.

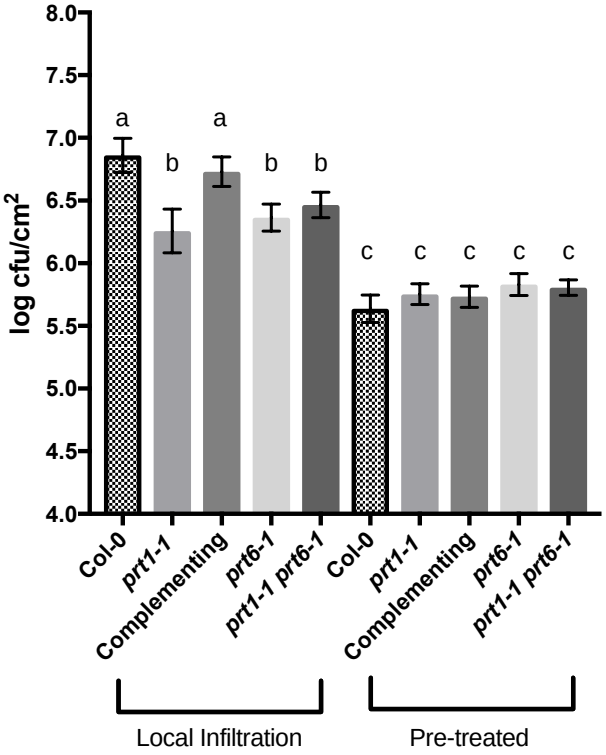

Figure 5.10: Quantified pre-treated plants and local direct infiltration experiments for assessment of systemic acquired resistance responses. A control local direct infiltration *Pst* DC3000 assay was conducted on 32 DAG leaves for comparison with pre-treated plants. Both assays are quantified at the same time. N=18 leaves taken from the rosettes of infected plants (Mean log cfu/cm^2 was determined from 3 independent biological replicates and pooled data. Error bars plotted as SEM and significance determined by one-way ANOVA with Tukey's multiple comparison analysis. Means are grouped according to 'a', 'b', 'c' etc. based on statistical tests

5.6 Transcript analysis of pathogenesis related genes

PR proteins are integral components of the *Arabidopsis* response to pathogens. *Pst* DC3000 elicits defence responses chiefly through the SA-signalling pathway such as PR-1, PR-2 and PR-5, and camalexin biosynthesis. Transcriptomic approaches were taken to reveal whether *Pathogenesis Related* genes and camalexin biosynthesis related genes are increased in abundance prior to infection which may prime the plant for infection. Total RNA was extracted from 3 biological replicates of untreated leaf material and cDNA made prior to qRT-PCR experiments, with primers for *PR* genes and *GSTF6* and *GSTF7* designed from NCBI primer blast. The wild type and *prt1-1* mutants were assessed for differential gene expression (Figure 5.11). Relative to Col-0, *PR1, PR4, PR5, GSFT6* and *GSTF7* genes transcripts in the *prt1-1* background were increased in expression in 28DAG untreated material.

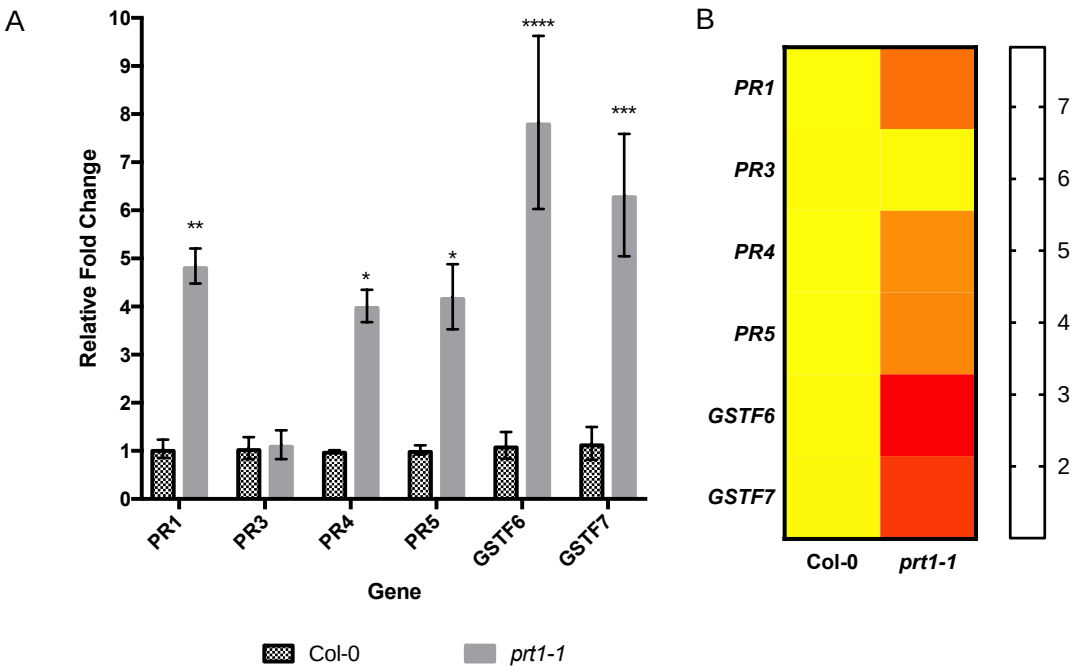

Figure 5.11 Transcript analysis of pathogenesis associated genes: (A) qRT-PCR analysis and (B) heat map showing relative gene expression in untreated leaf material grown for 28DAG in neutral days light conditions for *Pathogenesis Related* and camalexin biosynthetic genes. Values are mean of three biological replicates ± SEM; Significance was determined by 2way ANOVA with Sidak's Multiple Comparison analysis (* $p \leq 0.05$ **$p \leq 0.01$ ***$p \leq 0.001$ **** $p \leq 0.0001$).

5.7 Quantitative proteomic analysis of *prt1-1* leaves

The phenotype of increased resistance to virulent *Pst* DC3000 conferred by the *prt1-1* mutation in *Arabidopsis thaliana* has assigned a long sought-after physiological function for the PRT1 branch of the plant N-end rule pathway in regulation of plant-responses to pathogens. Given this is a facet of targeted proteolysis, it is hypothesised that the *prt1-1* mutation stabilises as yet unknown proteins, the increased abundance of which, enable the plants to better cope with the biotic stress compared to the wild type. Quantitative proteomic approaches allow the proteome of plants to be analysed to reveal why *prt1* mutants are better able to responds to pathogenesis.

5.7.1 Tandem Mass Tagging with mass spectrometry

Given previous qRT-PCR data which demonstrates that a number of *Pathogenesis Related* and camalexin biosynthesis genes are more highly expressed in *prt1-1* relative to Col-0 in untreated plant material, this tissue type was chosen for qualitative proteomics. Consequently, the leaf proteome was compared for Col-0 and *prt1-1* mutant plants through ten-plex Tandem Mass Tagging with mass spectrometry. A single mass spectrometry run identified and quantified 819 proteins, of which 15 were 1.5-fold or more increased in abundance in prt1-1 relative to Col-0, with a p-value of 0.05 or below (Table 5.1). Seven proteins exhibited reduced abundance in prt1-1, according to the same criteria (Table 5.2). The 10-plex TMT labelling was conducted by C. Till, sample clean-up and fractionation steps were performed by H. Zhang (Rothamsted Research), and MS/MS analysis was conducted by M. Deery (Cambridge centre for proteomics, University of Cambridge). Statistical analysis was performed by H. Zhang and K. Hasall (Rothamsted research).

Figure 5.1: Proteins with increased abundance in leaves of the *Arabidopsis thaliana prt1-1* mutant compared to Col-0 with >1.5-fold increased, with $p < 0.05$. The start and finish amino acid positions are defined with respect to TAIR10 gene models.

AGI code	Description	Synonyms	Log2 fold change	P-value	Score	Coverage	# proteins	# unique peptides	# PSMs
AT2G43570.1	chitinase, putative	CHITINASE, PUTATIVE, CHI, AED15	2.324498229	0.022325629	28.27	3.61	1	1	1
AT3G57260.1	beta-1,3-glucanase 2	ATBG2, ATPR2, BETA-1,3-GLUCANASE 2, BG2, BGL2, PATHOGENESIS-RELATED PROTEIN 2, PR-2, PR2	2.236801734	0.000122735	36.70	10.32	1	2	2
AT1G75040.1	pathogenesis-related gene 5	PATHOGENESIS-RELATED GENE 5, PR-5, PR5	1.943225505	0.000373418	75.31	15.90	1	3	3
AT1G02920.1	glutathione S-transferase 7	ARABIDOPSIS GLUTATHIONE S-TRANSFERASE 11, ATGST11, ATGSTF7, ATGSTF8, GLUTATHIONE S-TRANSFERASE 11, GLUTATHIONE S-TRANSFERASE 7, GST11, GSTF7	1.54839952	0.000963343	96.83	30.14	1	3	5
AT1G02930.1	glutathione S-transferase 6	ARABIDOPSIS GLUTATHIONE S-TRANSFERASE 1, ARABIDOPSIS THALIANA GLUATIONE S-TRANSFERASE F3, ATGST1, ATGSTF3, ATGSTF6, EARLY RESPONSIVE TO DEHYDRATION 11, ERD11, GLUTATHIONE S-TRANSFERASE, GLUTATHIONE S-TRANSFERASE 1, GLUTATHIONE S-TRANSFERASE 6, GST1, GSTF6	1.37072391	0.00101683	68.60	13.46	1	1	3
AT3G48090.1	alpha/beta-Hydrolases superfamily protein	ATEDS1, EDS1, ENHANCED DISEASE SUSCEPTIBILITY 1	1.160861575	0.001218747	40.64	1.44	1	1	1
AT1G08450.1	calreticulin 3	CALRETICULIN 3, CRT3, EBS2, EMS-MUTAGENIZED BRI1 SUPPRESSOR 2, PRIORITY IN SWEET LIFE 1, PSL1	1.144436214	0.00084514	22.91	1.65	1	1	1

AT5G03350.1	Legume lectin family protein	Legume lectin-like protein1, LLP1, AED9, Salicylic acid-induced lectin-like protein SAI-LLP1	1.071065443	0.001536471	47.58	11.68	1	2	2
AT2G42530.1	cold regulated 15b	COLD REGULATED 15B, COR15B	0.826496763	0.042311784	38.43	9.22	1	1	1
AT4G02520.1	glutathione S-transferase PHI 2	TGSTF2, ATPM24, ATPM24.1, GLUTATHIONE S-TRANSFERASE PHI 2, GST2, GSTF2	0.800386754	0.026521971	92.64	16.98	2	2	3
AT3G49120.1	peroxidase CB	ATPCB, ATPERX34, PEROXIDASE 34, PEROXIDASE CB, PERX34, PRX34, PRXCB	0.731792368	0.002575548	45.48	9.63	4	3	3
AT1G21750.1	PDI-like 1-1	ARABIDOPSIS THALIANA PROTEIN DISULFIDE ISOMERASE 5, ATPDI5, ATPDIL1-1, PDI-LIKE 1-1, PDI5, PDIL1-1, PROTEIN DISULFIDE ISOMERASE 5	0.698083327	0.001544599	112.85	11.98	2	6	6
AT3G07390.1	auxin-responsive family protein	AIR12, AUXIN-INDUCED IN ROOT CULTURES 12	0.679018908	0.000278073	45.82	3.66	1	1	1
AT5G16880.1	Target of Myb protein 1	Target of Myb protein 1	0.612977976	0.000692194	32.35	1.97	1	1	1
AT4G24190.1	Chaperone protein htpG family protein	THSP90-7, ATHSP90.7, HEAT SHOCK PROTEIN 90-7, HEAT SHOCK PROTEIN 90.7, HSP90.7, SHD, SHEPHERD	0.611536183	0.007498635	153.30	9.60	1	8	8

Table 5.2: Proteins with decreased abundance in leaves of the *Arabidopsis thaliana prt1-1* mutant compared to Col-0 with >1.5-fold decreased, with $p < 0.05$. The start and finish amino acid positions are defined with respect to TAIR10 gene models. PSMs= Protein Spectrum Matches

AGI code	Description	Synonyms	Log2 fold change	P-value	Score	Coverage	# proteins	# unique peptides	# PSMs
AT1G66100.1	Plant thionin	PR (pathogenesis-related) protein. Belongs to the plant thionin (PR-13) family	-1.090164536	0.007040833	44.77	10.45	1	1	1
ATCG01060.1	iron-sulfur cluster binding;electron carriers;4 iron, 4 sulfur cluster binding	PSAC	-0.97563863	0.048896401	75.26	40.74	1	3	3
AT3G25760.1	allene oxide cyclase 1	ALLENE OXIDE CYCLASE 1, AOC1, EARLY-RESPONSIVE TO DEHYDRATION 12, ERD12	-0.800935032	0.017134724	52.80	7.09	1	1	2
AT2G10940.1	Bifunctional inhibitor/lipid-transfer protein/seed storage 2S albumin superfamily protein		-0.683619878	0.028187466	111.45	11.00	1	3	3
AT1G22530.1	PATELLIN 2	PATELLIN 2, PATL2	-0.644867123	5.07611E-05	64.84	4.54	1	2	2
AT1G72150.1	PATELLIN 1	PATELLIN 1, PATL1	-0.617540721	9.42671E-05	103.04	10.12	1	6	6
AT3G25770.1	allene oxide cyclase 2	ALLENE OXIDE CYCLASE 2, AOC2	-0.591834121	0.005083734	56.81	7.11	1	1	2

5.7.2 Validation of differentially abundant peptides

Following TMT-MS analysis, qRT-PCR and Western blotting techniques were used to validate differentially regulated peptides identified. Previous qRT-PCR analysis in untreated plant material demonstrated *PR1, PR4, PR5, GSFT6* and *GSTF7* gene expression was relatively higher in *prt1-1* compared to Col-0. These results corroborate peptides increased in abundance following TMT-MS analysis: for *PR5* log2 fold change (FC) = 6.05 and 1.94; for *GSFT6* log2 FC = 4.23 and 1.55; for *GSTF7* log2 FC = 3.66 and 1.37 following initial qRT-PCR (Chapter 5.6) and TMT-MS analysis respectively.

5.7.2.1 Transcript validation of TMT-upregulated proteins by qRT-PCR

Further qRT-PCR experiments were conducted to confirm whether the transcript levels were higher in *prt1-1* for proteins indicated by TMT labelling experiments to be in increased abundance prior to infection compared to Col-0. Total RNA was extracted from 3 biological replicates of untreated leaf material and cDNA made prior to qRT-PCR experiments. Primers were designed from NCBI primer blast. Data shown in Figure 5.12 is representative of three independent experiments showing the relative fold change of gene transcripts in the Col-0 background compared to N-end rule mutants and the complementing line. Transcript analysis demonstrated that *PR-2, EDS1* and *CRT3* were all significantly transcriptionally upregulated in *prt1-1* compared to Col-0 in untreated material, substantiating TMT results. The *prt1-1prt6-1* mutant showed similar patterns of transcriptional upregulation as *prt1-1,* with the exception of *PR-2* relative expression. *PR-2* expression is also upregulated in *prt6-1* and an additive effect is observed for mutant upon both plant N-end rule mutants. The complementing line demonstrated similar gene transcription patterns to Col-0.

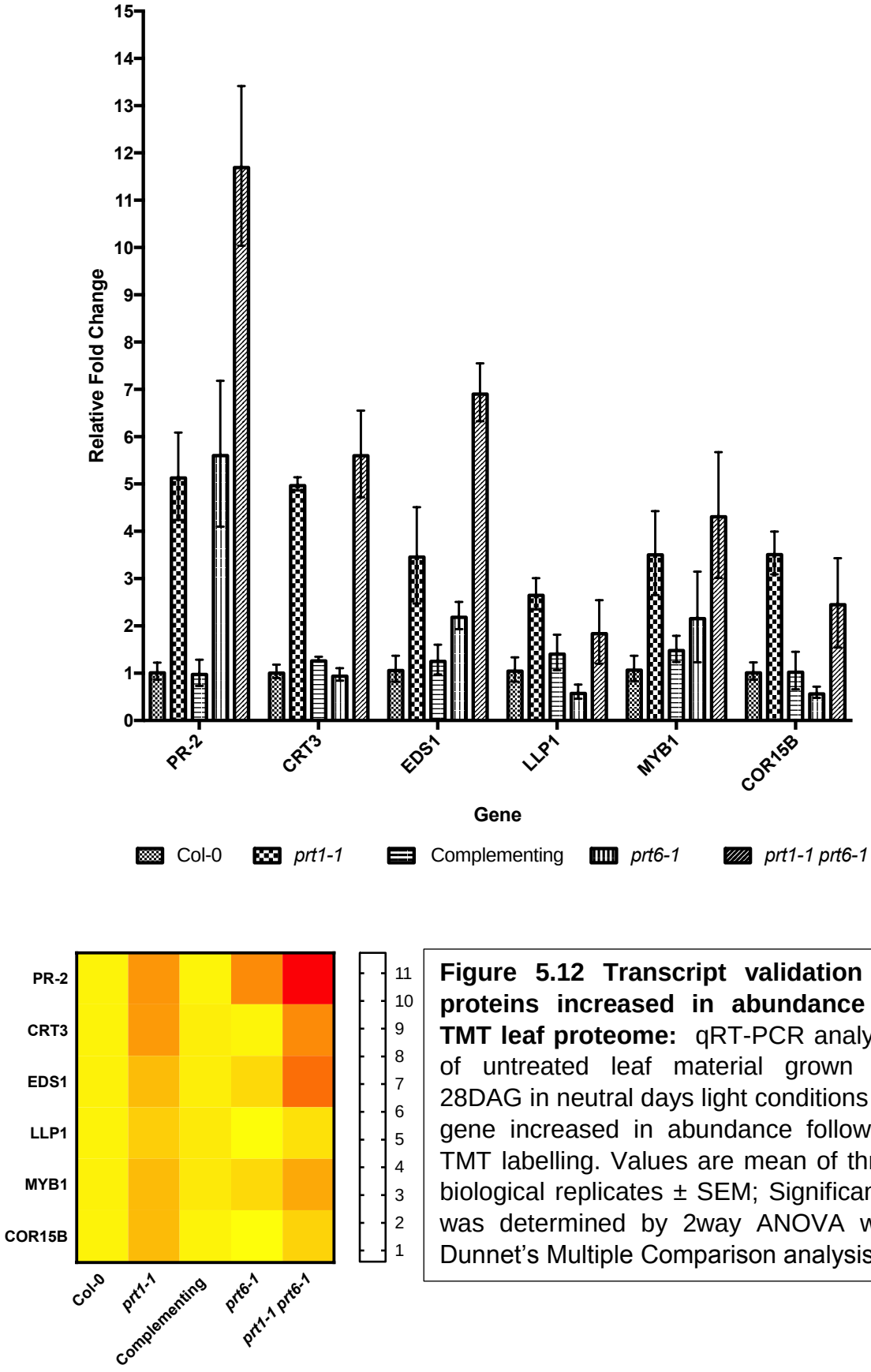

Figure 5.12 Transcript validation of proteins increased in abundance in TMT leaf proteome: qRT-PCR analysis of untreated leaf material grown for 28DAG in neutral days light conditions for gene increased in abundance following TMT labelling. Values are mean of three biological replicates ± SEM; Significance was determined by 2way ANOVA with Dunnet's Multiple Comparison analysis.

5.7.2.2 Validation of proteins increased in abundance following TMT analysis by Western blotting

Building on the transcriptomic data, immunoblotting studies were conducted on untreated leaves 6, 7 and 8 of 28DAG (ND) of experimental lines to confirm TMT-labelling results at the protein level. For *PR-2* protein abundance, as quantified by band intensity, was 4.47-, 6.72- and 11.32-fold more abundant than Col-0 for *prt1-1, prt6-1* and *prt1-1prt6-1* respectively (Figure 5.13). The complementing line displayed slightly elevated PR-2 protein abundance compared to Col-0 (1.66-fold) but not statistically significant.

In the anti-*EDS1* Western blot (Figure 5.14), the level of EDS1 in untreated *prt1-1* samples is significantly higher than in Col-0. Following 1dpi with virulent *Pst* DC3000, an increase in EDS1 levels similar to that of *prt1-1* untreated samples is observed in the Col-0. The levels of EDS1 are maintained at all-time points tested for *prt1-1.*

The anti-CRT3 Western (Figure 5.15) in untreated material is higher in *prt1-1* compared to WT. CRT3 abundance in *prt1-1* declines at 4 hpi. Following 4hpi, the protein abundance in Col-0 significantly increases to levels comparable to untreated *prt1-1*. This abundance declines at 1dpi. This is comparable to *prt6-1* mutant. However, the double *prt1-1prt6-1* mutant demonstrates similar patterning to *prt1-1* in terms of the high relative abundance in untreated material, but also Col-0 and *prt6-1* for the high relative abundance at 4hpi and decline at 1 dpi.

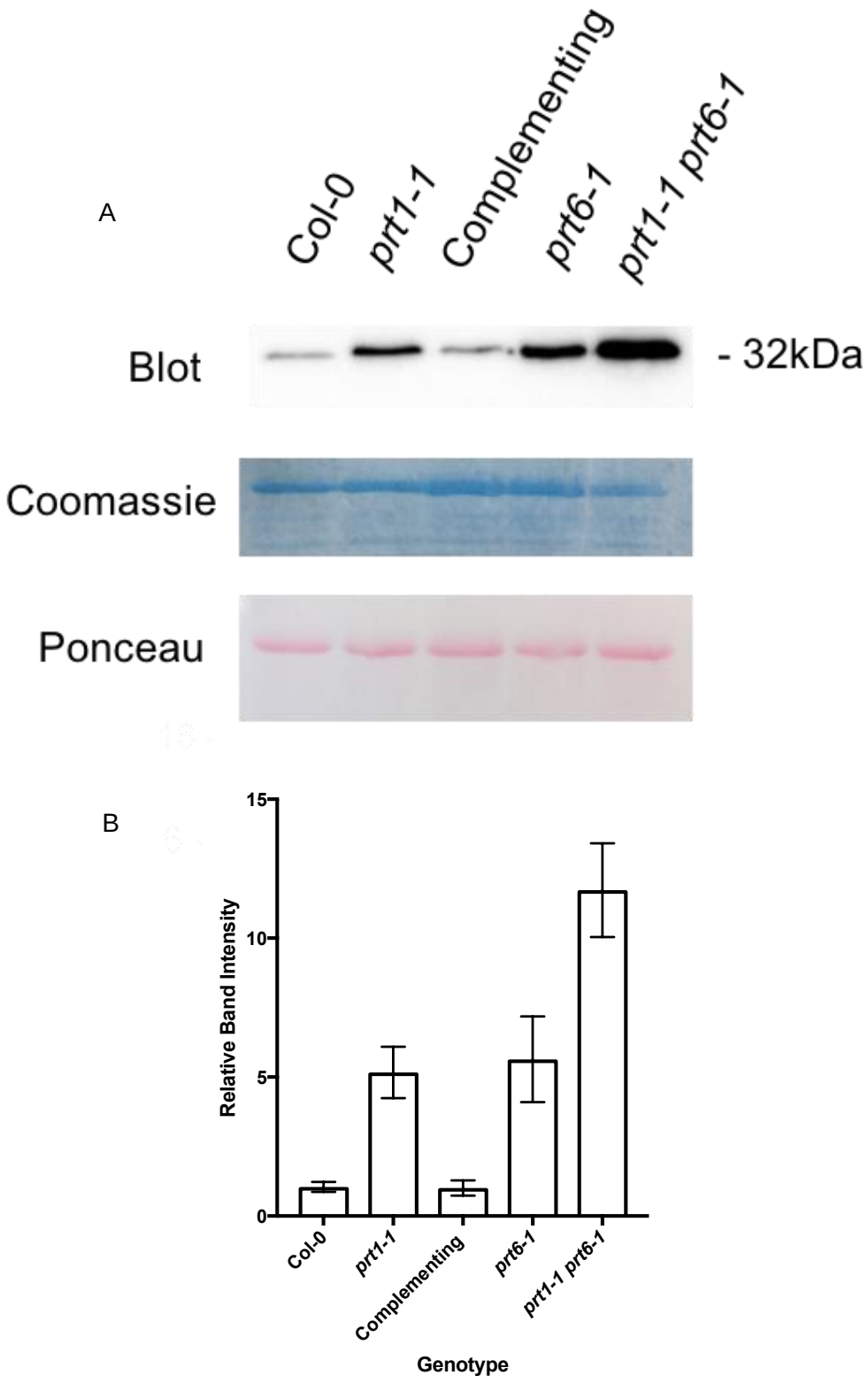

Figure 5.13: PR-2 Protein abundance in Col-0 and *prt1-1:* Anti-*PR2* Western blot on 28 DAG untreated leaf material for all N-end rule mutants (A) representative Western blot showing *PR-2* protein abundance with Coomassie stained gel and Ponceau stained PVDF membrane to show equal loading and transfer; (B) a graph relative band intensity for *PR-2* quantified using Fiji (mean ± SD; n=3). Expected band size is ~32 kDa.

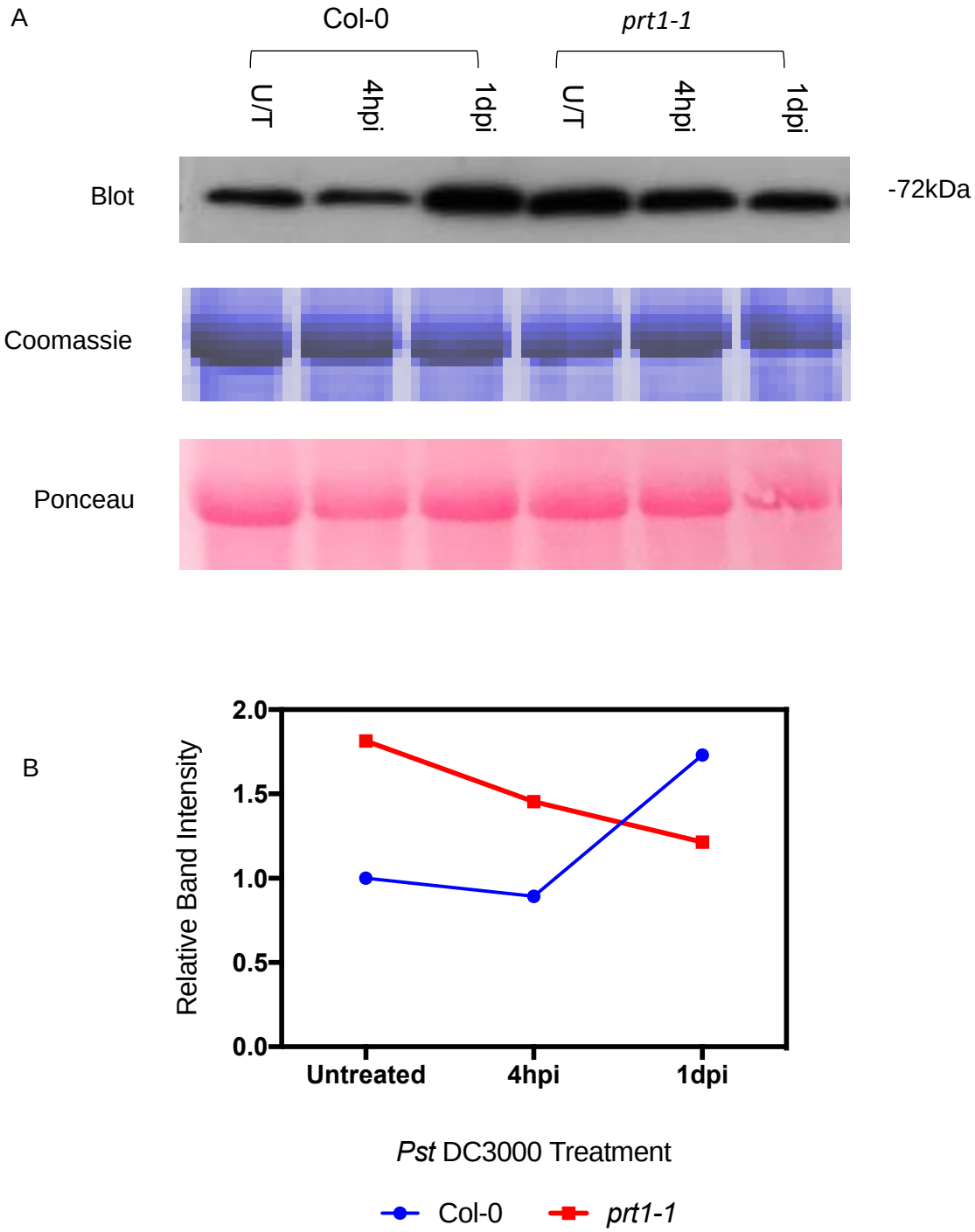

Figure 5.14: EDS1 Protein abundance in Col-0 and *prt1-1:* Anti-EDS1 Western blot on Col-0 and *prt1-1* untreated, 4 hpi and 1 dpi with virulent *Pst* DC3000 leaf material (A) Representative Western blot film shows protein abundance with Coomassie stained gel and Ponceau stained PVDF membrane to show equal loading and transfer; (B) a graph relative band intensity for EDS1 quantified using Fiji. Expected band size is ~72kDa.

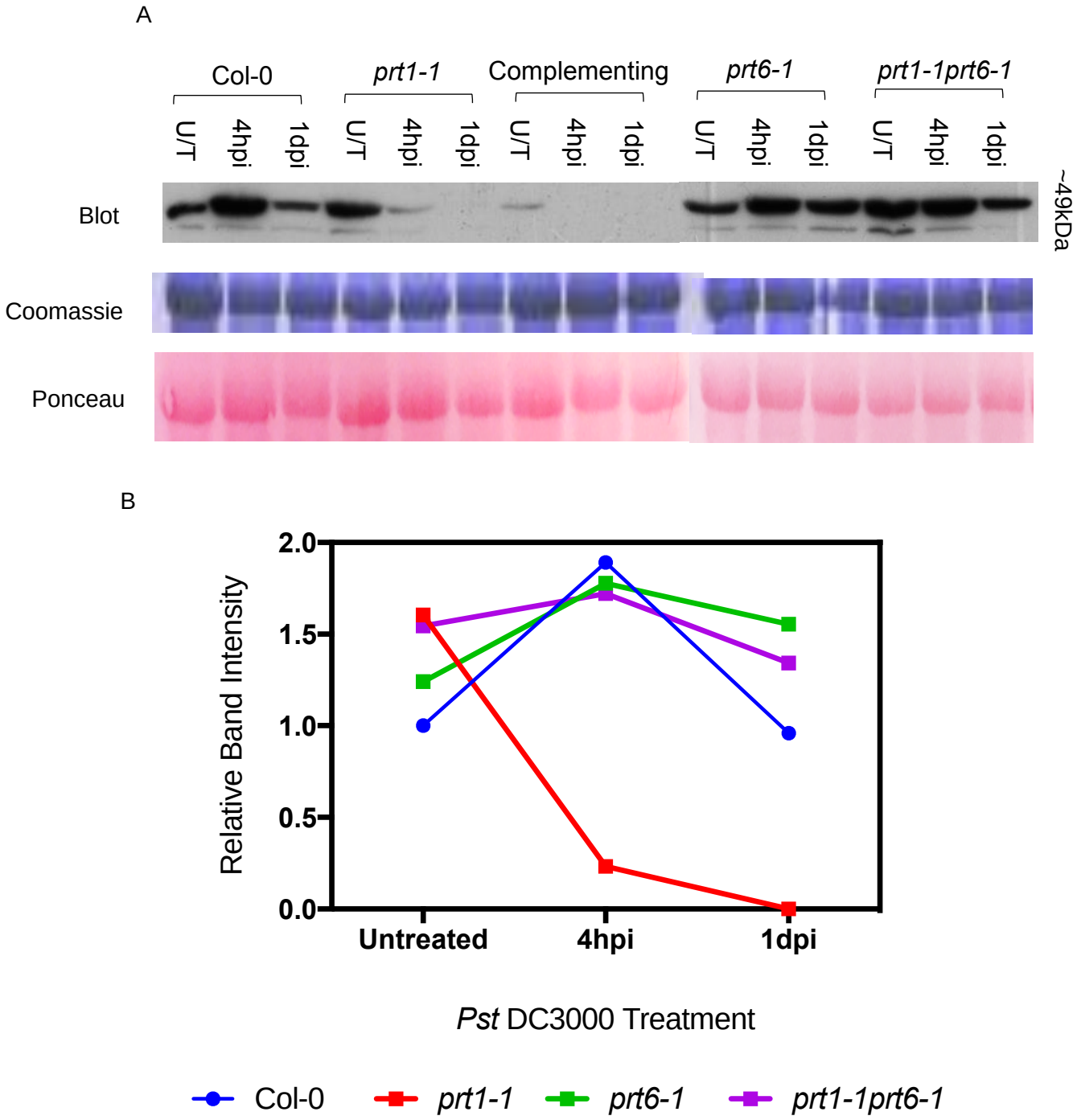

Figure 5.15: CRT3 Protein abundance in Col-0 and *prt1-1:* Anti-CRT3a Western blot on N-end rule mutant untreated, 4 hpi and 1 dpi with virulent *Pst* DC3000 leaf material (a) Representative Western blot film shows protein abundance with Coomassie stained gel and ponceau stained PVDF membrane; (B) a graph relative band intensity for EDS1 quantified using Fiji. Expected band size is ~49kDa.

5.8 Discussion

Plant response to pathogens relies on the induction of several tightly regulated layers of immunity including PAMP-triggered immunity, effector triggered immunity and systemic acquired resistance. Experiments conducted in this chapter demonstrate a role for PRT1 in regulation of plant responses to biotic stresses, specifically to *Pseudomonas syringae* pv tomato DC3000. During this study, two important papers were published ascribing functions to N-end rule mutants in relation to biotic stresses which will be explored in relation to these findings.

5.8.1 Infection assays:

Mutant *prt1-1* plants are reproducibly more resistant to both infiltration and spray treatments with *Pst* DC3000. Given a similar reduction in susceptibility is observed upon pathogen challenge for the *prt6-1* and no additive resistance was observed in the *prt1-1prt6-1* double mutant, this suggests that these two E3 ligases share the regulation of the stability of an undetermined number of protein substrates. The complementing line used in these studies behaves as the WT Col-0, restoring the susceptibility to *Pst*.

A publication by de Marchi *et al* (2016) indicated that mutants of the plant N-end rule pathway, including *ate1ate2, prt6-1* and *prt1-1,* show increase susceptibility to pathogens, including the hemi-biotrophic pathogen *Pseudomonas syringae* pv tomato DC3000. For the conditions present in this work, the opposite effect was found, with the *prt1-1* mutation producing a greater resistance to *Pst* DC3000.

There are a number of key differences in the experimental design which may account for the contradictory results. The plant material for infection in de Marchi *et al* (2016) was grown for 4 weeks in short days conditions (8h light / 16h dark) compared to the ~3.5 weeks in neutral days used in this study. It is arguable that neither of these conditions is particular

physiologically relevant since *Arabidopsis* is a facultative long plant (Andrés & Coupland, 2012). The vegetative to floral transition is accelerated in plants grown in longer photoperiods (Hayama & Coupland, 2003) characterised by increased single leaf size and a reduction overall in rosette leaf number compared to plants grown under short photoperiods. For the conditions described in de Marchi *et al* (2016) the plants are possibly smaller. The photoperiod and interaction with the circadian clock itself may have an impact. Plant material prior to infection was also prepared differently in these studies. Plants were germinated and grown initially for 7 d on 0.5 x MS plates supplemented with 0.5% sucrose prior to transfer to soil in de Marchi *et al*, whereas in this study plants were sown directly to soil following 3 d cold imbibition. The number of leaves injected per plant (3 vs 4 in this study), grinding tissue in water rather than $MgCl_2$ and day of quantification (3 dpi vs 4 dpi) are also sources for variation. Taken together, whilst in isolation these differences may not have significant ramification for the assays, their additive effect may have produced the discrepancies between these studies.

However, for comparable ND conditions to those used in this study and SD conditions as used in de Marchi et al (2006), a recent publication by Vicente *et al* (2018) (also from the Holdsworth group, University of Nottingham) demonstrated an increased resistance to challenge by *Pst* DC3000 for Cys-Arg/N-end rule mutants. These results are consistent with the findings presented in this independent study for *prt6-1* and *prt1-1prt6-1* mutants (and the opposite to the decreased resistance presented in de Marchi *et al*).

Experiments challenging plants with *Pst* DC3000 with deletions in the HrpA- component of the type III secretion system, in which the pathogen is unable to deliver effectors required for full virulence, demonstrated no significant difference between any of the genotypes. This suggests that PRT1 is not directly involved in PAMP-triggered immunity and more likely to be implicated in effector triggered immunity. However, these two processes share several features, ETI being described as a stronger,

faster version of PTI (Thomma, Nürnberger and Joostena, 2011), meaning that differences may only be observed once the stronger response ETI is elicited.

Pst DC3000 avrRpm1 acts as a SAR inducer. Following 2 days of pre-treatment of plants with the avirulent strain and 4 days of infection of virulent *Pst* DC3000, there was negligible difference between genotypes. However, quantification of the control virulent only direct infiltration gave the same results as previous (i.e. N-end rule mutants are more resistant compared with Col-0 and the complementing line). This confirms that the substrates stabilised in the untreated *prt1-1* background prime it for infection, and no differences are observed been *prt1-1* and Col-0 once primed by SAR.

Given the data that clearly indicates a role for PRT1 in the immune response against *Pst*, a deep analysis was conducted through expression analysis of defense marker genes, specifically the study of *PATHOGENESIS RELATED* gene expression prior to pathogen infection: potentially enabling *prt1-1* plants to better respond to the biotic stress. Additionally, *GSTF6* and *GSTF7*, which are involved in camalexin synthesis, a phytoalexin involved in pathogen resistance, were upregulated. Analysis of gene expression by qRT-PCR using untreated material demonstrated increased relative transcript abundance for *PR1/2/4/5* as well as the *GSTF6/7.* Given the apparent upregulation of *PR* and camalexin biosynthesis genes in untreated *prt1-1* plants, it was hypothesised that constitutive stabilisation of substrates in *prt1-1* primes *Arabidopsis* against infection of *Pst* DC3000. *PR-1, PR-2 and PR-5* in *Arabidopsis* are induced through the SA-signalling pathway whereas *PR-3 and PR-4* are induced by JA-signalling. SA and JA hormones act in an antagonistic manner: with SA positively regulating *Arabidopsis* responses to *Pst* DC3000, and JA negatively regulating responses. Therefore, *PR-4* transcriptional upregulation in uninfected material alongside SA-upregulated *PR* genes appears an anomalous result. However, a publication by Liu *et al.* (2016) hypothesised that a partial

non-canonical activation of JA-signalling via SA receptors may prevent excessive antagonism between the pathways to promote ETI.

5.8.2 Leaf proteome analysis

5.8.2.1 Proteins with increased abundance in *prt1-1*

Proteomic analysis was conducted on leaf material grown for 28DAG in neutral days light conditions through a TMT10plex with MS/MS single run experiment in Col-0 and *prt1-1* backgrounds. Peptides increased in abundance in the *prt1-1* background following 10plex TMT-MS analysis included proteins involved in major aspects of plant defence against pathogens including PAMP-triggered immunity, effector trigger immunity and systemic acquired resistance. This demonstrates that the leaf proteome in untreated *prt1-1* plants are consistent with the phenotype of resistance to *Pst* DC3000 and supports the hypothesis of a priming effect conferred by the mutation. These proteins can be categorised into several functional groups.

5.8.2.1.1 Endoplasmic reticulum quality control

A group of peptides associated with vesicle traffic, protein secretion and Endoplasmic Reticulum (ER) protein quality control (ER-QC): Calreticulin-3, chaperone protein htpG family protein, protein disulfide isomerase 5 and target of Myb protein 1.

5.8.2.1.1.1 Calreticulin-3

Calreticulins (CRT) are lectin chaperones localised to the ER where they facilitate glycoprotein folding and retention of protein folding intermediates to prevent their transit via the secretary pathway. CRTs are present in many plant species and groups into CRT1/2/3 based on the domain sequence at their C-terminal (Del Bem, 2011; Vu *et al.,* 2017). Mutations in all three plant CRTs (T123 mutant) is manifest as an increased susceptibility to water stress (Kim *et al.,* 2013). CRT3 is a plant specific isoform that plays an essential role in ER-QC in concert with

UDP-glucose glycoprotein glucosyl transferase (UGGT) and an HDEL receptor family member (ERD2b) for the proper function and accumulation of the pattern recognition receptor EFR for recognition of the EF-Tu derived peptide elf18 (Zipfel *et al.,* 2006). Mutants of *crt3* are more susceptible to *Pst* DC3000 than mutant of the EFR PRR indicating that CRT3 is involved in the accumulation of as yet unidentified PRRs and a lack of CRT3-UGGT generates a misfolded EFR protein which is degraded in the ER (Li *et al.,* 2009). BRI1-associatied kinase 1 (BAK1) is a central regulator of PTI through complex formations when ligands bind to PRRs, which has proposed to not require CRT3 for BAK1 functionality (Li *et al.,* 2009; Kørner *et al.,* 2013). Plant responses mediated by FLS2 are not however impaired in *crt3, uggt* or *erd2b* mutants (Li *et al.* 2009). Similarly, a screen for *priority in sweet life (psl)* mutants that show de-repressed anthocyanin accumulation in the presence of elf18 identified *crt3* alleles (Saijo *et al*., 2009). As part of this role in ER-QC, *CRT3* interacts with *bril-9* which encodes a defective brassinosteroid receptor in a mono-glucosylation dependent manner. CRT3 then retains bril-9 in the ER leading to its degradation. *bril-9* mutants exhibit dwarfism which is complemented with *CRT3* loss of function (Jin *et al.,* 2009).

5.8.2.1.1.2 HSP90-1

Plants contain Nucleotide-binding domain and Leucine-rich Repeat containing proteins (NLR), acting as the sensors, effectors and mediators both intra- and extra-cellularly that induce defence response during innate immunity (Griebel *et al.,* 2014; Wu *et al.* 2014). These NLRs are clients of dimeric HSP90 (Giuliano, Minghao and Chrisostomos, 2018); a protein with a 0.61 log2 fold change (2 sf.; p=0.0075) in the *prt1-1* leaf proteome compared to Col-0. Seven family members of highly conserved HSP90 proteins have been identified in *Arabidopsis* ecotype Col-0 and these are compartmentalized based on their functionality (Kadota & Shirasu, 2012). With cytoplasmic co-chaperones RAR1 and SGT1, HSP90 potentially functions to regulate intracellular abundance of R

proteins containing nucleotide-binding (NB) domains and LRR-NBs that pass through the ER (Ishiguro *et al.* 2002; Shirasu, 2009; Kadota and Shirasu 2012). The complex is thought to prevent unnecessary immune receptor activation by maintaining intracellular R-protein steady state in presumed pre-recognition complexes. It is unclear whether RAR1-SGT1-HSP90 complex regulates R-protein signaling events (Saijo *et al.* 2009). Overall, these chaperone protein htpG family proteins are essential for maturation and activation of signaling proteins.

5.8.2.1.1.3 Protein Disulfide Isomerase-1

Protein Disulfide Isomerase-1, also known as PDI-5, may play a critical role in the enhancement of plant endoplasmic reticulum function enabling this organelle to better cope with the significant burden placed by the activation of systemic acquired resistance response. PDI-5 has thiodisulfide oxidoreductase activity which facilitates formation, reduction and rearrangement of intramolecular disulphide bonds in eukaryotes for folding of nascent proteins (Yuen, Matsumoto and Christopher, 2013). PDIs contain an archetypical signal peptide which consists of: two CXXC containing thioredoxin sites (a, a'), two non-catalytic thioredoxin fold domains (b, b'), an acidic (c) domain as well as an ER KDEL retention signal at its C-terminal, hence its localisation in the ER (Ondzighi *et al.*, 2008; Yuen, Masumoto and Christopher, 2013). Annotation by The Arabidopsis Information Resource (TAIR) indicate that ER-stressors such as DTT and beta-mercaptoethanol, which reduce protein disulphide bonds, induce PDI5 (Lamesh *et al.,* 2012). Besides the role in the regulation of protein folding, PDI5 also has been reported by Ondzighi *et al* (2008) to play an inhibitory role for cysteine proteases during their trafficking from the ER to the Golgi apparatus before seed endothelium programmed cell death.

5.8.2.1.1.4 Target of Myb1

A putative member of the Endosomal Sorting Complex Required for Transport (ESCRT) machinery called Target of Myb1 (TOM1) was found

to be upregulated following proteomic analysis of untreated plant material. These homologues belong to the plant ESCRT-1 complex (Winter and Hauser, 2006) where they interact with it to degrade cargo in an ESCRT-dependent manner (Nagel *et al.,* 2017). The ESCRT-1 complex is important for plant immunity and plays a role in endosomal sorting of FLS2 (Spallek *et al*., 2013).

5.8.2.1.1.5 Summary

Taken together this group of proteins increased abundance in *prt1-1* compared to Col-0 may play a significant role in plant defence against pathogens through enhancement to protein secretion and/or vesicle traffic as well as endoplasmic reticulum quality control. Enhancing these functions by increasing protein abundance potentially enables plants to better cope with/mount a pathogen response; this is appropriate as *prt1-1* plants are evidently more primed for infection.

5.8.2.1.2 ENHANCED DISEASE SUSPECTIBILITY1 and associated proteins

Another significant functional group consists of ENHANCED DISEASE SUSPECTIBILITY1 (EDS1) and its downstream associated proteins.

5.8.2.1.2.1 EDS1

EDS1 was shown to be important in the regulation of biotrophic pathogen defence through SA-dependent responses and induction of *PR* genes including *PR-1, PR-5, GST1* and *2-oxophytodienoate reductase 3 (OPR3)* (Glazebrook *et al*., 1996; Obsenbein *et al.,* 2006). EDS1 has been implicated in the HR (Feys *et al*., 2001) and the associated detrimental effect on plant growth (Ochsenbein *et al*., 2006), SA accumulation (Shah, 2003), and SA-dependent signalling (Wiermer *et al*., 2005). EDS1 is induced by β-cyclocitral, a $^1O_2$-signaling molecule, which induces SA production (Lu *et al.*, 2015), and subsequent PR-1 and PR-5 synthesis (Ochsenbein *et al*., 2006). EDS1, in concert with

PHYTOALEXIN-DEFICIENT4 (PAD4) and SENESCENCE-ASSOCIATED GENE 101 (SAG101*)*, is an upstream central regulator of salicylic acid signalling essential for basal defence signalling (Rietz *et al.,* 2011), with the PAD4-EDS1 hub being important for PTI (Makandar *et al.,* 2015). An EDS1-PAD4 complex is required for a *PAD4* positive expression feedback loop in which more PAD4 is stabilised allowing more SA to accumulate in infected tissues (Makandar *et al.,* 2015). EDS1 appears in dimeric form mainly in the cytoplasm to restrict pathogen-induced cell death at infection sites whereas the EDS1-PAD4 complex resides in the nucleus for EDS1-dependent defence genes (Czarnocka et al., 2017). The partitioning of EDS1 between the cytoplasm and nucleus is therefore essential for biotic stress responses (García *et a*l., 2010).

Plant resistance proteins (R proteins) are essential for resistance against pathogens; the majority of these R proteins contain N-terminus toll-like/interleukin 1 receptor (TIR) or coiled coil (CC) domains, and leucine-rich repeats (LRRs) at the C-terminus as well as a central nucleotide binding (NB) domain (Zhu *et al.* 2010). The downstream components of R proteins containing TIR-NB-LRR or CC-NB-LRR domains are significantly different. EDS1 is a critical component of LRR protein R gene functionality upstream of SA-dependent *PR-1* induction (Falk et al., 1999). Mutations in *EDS1, PAD4* and/or *SAG101* however only affect resistance conferred by TIR-NB-LRR containing R proteins.

CONSTITUTIVE EXPRESSOR OF PATHOGENESIS RELATED1 (CPR1) is an SCF-E3-ubiquitin ligase complex which negatively regulates the R-proteins SNC1 (Gou *et al.,* 2012) and RPS2 (Cheng et al., 2011). *cpr1-2* mutants are severely dwarfed and morphologically similar to constitutive HR mutants in the absence of biotic stress (Gou *et al.,* 2009) and constitutively express *PR* genes. EDS1 is required for CPR1 function. Constitutive SA in *cpr1* and *cpr6* requires PAD4. *NON EXPRESSOR OF PR GENES 1 (NPR1)* was identified in a genetic screen for plants unable to express *PR* genes following SAR induction

(Mou *et al.*, 2003). NPR1 serves as a dominant co-activator of SA-responsive genes and is integral for SAR (Armijo *et al.,* 2013), and SAR through SA-induction is compromised in *npr1* mutants. The *Arabidopsis thialiana* (Col-0) *Recognition of Peronospora parasitica 5 (RPP5)* gene cluster contains genes that are important for innate immunity including *suppressor of NPR1* (*snc1*). The snc1 R gene *confers* constitutive resistance to pathovars of *Pseudomonas syringae* and *Hyaloperonospora parasitica.* However, *eds1* mutation suppresses this RPP5-mediated R gene immune responses. This indicates that there are additional resistance pathways requiring SA and EDS1 but are independent of NPR1. EDS1 *and* SGT1 has been demonstrated to enhance disease in tobacco following *B. cinerea* infection (El Oirdi & Bouarab, 2007). FLAVIN-DEPENDENT MONOOXYGENASE1 (FMO1) has been demonstrated to positively regulates the EDS1 pathway (Bartsch *et al*., 2006).

5.8.2.1.2.2 Lectin-like protein 1

Breitenbach *et al* (2014) identified an apoplastic EDS1-dependent (AED) protein through proteomic approaches using *AvrRpm1*-expressing WT and *eds1* plants called Lectin-like protein 1 (LLP1). In *llp1* plants, systemic acquired resistance is compromised whereas local resistance mediated with EDS1 and SA are unaffected. Additionally, experiments involving exogenous SA application revealed negligible differences with Col-0. Taken together, these results suggest that LLP1 is a promoter of systemic acquired resistance. LLP1 is induced via a SA-dependent mechanism by inoculation with avirulent strains. Constitutive expression restrains proliferation of *Pst Avr-Rpm1* and triggers more cell death in inoculated leaves (Armijo *et al*., 2013).

5.8.2.1.2.3 PR-2

PR-2 has been proposed to degrade the cell walls of invading fungal pathogens and may also degrade endogenous substrates to generate elicitors and thereby induce defence responses. PR-2 is one of two leaf-

specific, pathogen-responsive beta-1, 3-glucanases and was shown to have callase activity *in vitro* (Oide *et al.,* 2013). PR-2 over-expression increased susceptibility of *Arabidopsis* to necrotrophs *Alternaria brassicicola*, *Botrytis cinerea* and to the hemibiotrophic *Leptosphaeria maculans.* However, it demonstrated in the *pad3* background that *PR-2* overexpression results in increased resistance to *Pst* DC3000 (Oide *et al.,* 2013). This is consistent with findings that in the *prt1-1* background there is an increase in *PR-2* transcript and protein levels in untreated material as well as increased resistance to *Pst* DC3000.

5.8.2.1.2.4 PR-5

PR-5 is a thaumatin-like protein identified as an apoplastic EDS1-dependent protein by Breitenbach *et al* (2014) with predicted anti-fungal properties. *PR-5* requires SA signalling and is commonly used as a marker for systemic acquired resistance. It is highly expressed in leaves and stems, but not in roots and reproductive tissues (Seo *et al.,* 2008)

5.8.2.1.2.5 Summary

TMT analysis revealed EDS1 and PR protein abundance were higher in untreated *prt1-1* leaves compared to WT. These were confirmed following qRT-PCR and Western blotting for EDS1, CRT3 and PR-2 (Chapters 5.7.3 and 5.7.4) in untreated material. Interestingly, for EDS1, similar levels of protein abundance were maintained throughout infection in *prt1-1* whereas CRT3 protein levels diminished after 4hpi. In the Col-0 background, protein abundance only increased following infection. PR-2 protein levels were higher in *prt1-1* and *prt6-1* compared to Col-0 and the complementing line in untreated plant material. Interestingly in *prt1-1prt6-1,* an additive effect was observed for *PR-2*. This supports the postulation that proteins are stabilised in the *prt1-1* background pre-infection rather than an enhancement of their expression.

These facets of plant defence through salicylic acid signalling pathways, the levels of this hormone should be higher in the *prt1-1* mutant

compared to Col-0. Experiments investigating the levels of SA and JA (which act antagonistically) would therefore be important to confirm if this is the case. Plants responses to exogenous SA should be pursued in order to investigate differential responses of *prt1-1* to this hormone compared to wild type. There is no evidence to suggest that *prt1-1* is a lesion mimic mutant (LMM), in which the production of discrete lesions is observed in the absence of obvious stress or environmental condition due to irregular programmed cell death. The uninhibited or unregulated PCD resembles plants that have undergone the HR and often display enhanced resistance to pathogens (Moeder and Yoshioka, 2008). These LMMs and enhanced tolerance of biotic stresses are occasionally observed (Zhang *et al.,* 2008). Therefore, the levels of SA in *prt1-1* are likely to be slightly increased but not dramatically higher when compared to Col-0.

5.8.2.1.3 GSTFs

Phytoalexins are antimicrobial compounds produced in response to biotic stress perception including a significant of group of indole alkaloids called camalexins (Hammerschmidt, 1999; Glawischnig, 2007). These antimicrobials are also induced in response to abiotic stresses including amino acid starvation, oxidative stress and fusaric acid treatment (Zhao, Williams and Last, 1998). Camalexin biosynthesis initiates with the precursor tryptophan (Hull *et al.* 2000; Glawischnig *et al.,* 2004), with the first committed step to camalexin synthesis being fulfilled by the conversion of this IAOx intermediary into indole-3-acetonitrile (IAN) by CYP71A13 (Nafisi *et al.,* 2007).

10plex TMT leaf proteome analysis revealed that glutathione-S-transferase class phi (GSTF)-2, GSTF6 and GSTF7 were all up-regulated in the *prt1-1* background compared to Col-0. These results are consistent with the qRT-PCR results untreated material (presented in Chapter 5.6). GSTF6-knockout reduced whereas overexpression increased camalexin production in *Arabidopsis.* GSTF6 is proposed to

conjugate Cys-derived glutathione with IAN during camalexin biosynthesis (Su *et al.,* 2011) and expression is induced in response to pathogen challenge by *P. syringae* (Jones *et al.* 2006). GSTF7 is a very closely related member of the phi class of glutathione-S-transferases to GSTF6*,* proposed to have developed from tandem duplication (Sappl *et al.,* 2004). *GSTF7* expression is also induced following *Pst* DC3000 infiltration (Jones *et al.,* 2006) and *Fusarium sporotrichioides* (Asano, Kimura and Nishiuchi, 2012). It is proposed to have an overlapping function with GSTF6*,* which possibly accounts for their appearance together in the proteomics data (GSTF7 log2 FC = 1.55; GSTF6 log2 FC=1.37). Studies by Lieberherr *et al* (2003) demonstrated the accumulation of GSTF2 was induced 4 h after infection with avirulent strain *Pst* DC3000, and preceded *PR-1* gene induction. GSTF2 is induced by low concentrations of SA and ethylene and is partially NPR1-independent (Lieberherr *et al.,* 2003). The biotic stress responsiveness of GSTF2 and association with membrane vesicles suggest it is involved in regulation of binding and transport of defence-related compounds (Dixon, Sellars & Edwards, 2011).

In short, the upregulation of GSTFs in untreated *prt1-1* plants compared to Col-0 suggests that an increased abundance of camalexin should be present in this background as well as an increased capacity for transporting compounds associated with defence (GSTF2). The stabilisation of these GSTFs supports the hypothesis that the increased resistance phenotype to *Pst* DC3000 is due the stabilisation of compounds prior to infection that prime *prt1-1* plants to better respond to the biotic stress.

5.8.2.1.4 Redox signalling/oxidative burst associated proteins

The plant apoplast acts as a mediator for complex interactions between cells and the environment (Preger *et al.,* 2009). The liquid phase of the apoplast, containing low concentrations of solutes, is very sensitive to change. Fluctuations from the norm are identified by the apoplast, trigger

signalling cascades and elicit responses to the fluctuations (Dietz, 1997; Foyer & Noctor, 2005). A common response is the exponential generation of reactive oxygen species (ROS) either enzymatically or non-enzymatically in the apoplast (Apel & Hirt, 2004). A dramatic increase in ROS from steady-state is used to mount a defence response called an oxidative burst (O'Brien *et al.,* 2012). In plants, such an oxidative burst is typical of pathogen defence and is generated by apoplastic peroxidases and/or NADPH oxidases (Arnaud *et al.,* 2017). ROS is however not only generated in response to stresses but also a vast range of physiological conditions, such as stomata closure and cell growth (Preger *et al.,* 2009).

5.8.2.1.4.1 AUXIN-INDUCED IN ROOT CULTURES 12

AUXIN-INDUCED IN ROOT CULTURES 12 (AIR12) is a glycosylated b-type cytochrome protein and anchored by glycosylphosphatidylinositol to the plasma membrane exterior. It potentially acts as a redox link between the cytoplasm and apoplast (Preger *et al*., 2009) and generates superoxide at the plasma membrane (Biniek *et al*., 2017). AIR12 and a NAD(P)H quinone oxidoreductase (NQR) are both attached to the plasma membrane and may interact through the quinone moiety to facilitate electron transfer from NAD(P)H located in the cytosol to a monodehydroascorbate acceptor in the apoplast. This enables apoplastic redox state to be regulated by controlling ROS production (Biniek *et al.,* 2017). No obvious phenotypes are observed for *AIR12* mutants, but overexpression generates ROS, superoxide and lipid peroxides in leaves, indicating an altered apoplast redox state. Knockout *AIR12* plants are significantly decreased susceptibility to *B. cinerea* (in the Landsberg erecta-0 background). Ler-0 wild type plants induced *AIR12* expression. Taken together, AIR12 potentially regulates the apoplastic redox state and is a negative regulator of resistance to necrotrophy (Costa *et al*., 2015). Given overexpression of *AIR12* is associated with increased ROS production, measurements of ROS in the *prt1-1* background would be useful to establish the significance of this. AIR12 is log2 0.679-fold change up regulated in *prt1-1* leaf proteome

compared to Col-0 which is not dramatic. Therefore, the ROS levels should not be dramatically higher, especially given there is no obvious morphological difference between Col-0 and *prt1-1.*

5.8.2.1.4.2 PEROXIDASE34

PEROXIDASE34 (PRX34) belongs to the class III of cell wall-associated peroxidases which have been demonstrated to be integral for extracellular/apoplastic H_2O_2 generation in *Arabidopsis* responses to pathogens (Passardi *et al.,* 2006; Daudi *et al.,* 2012). Gene expression studies reveal that transcripts of *PRX34* are mainly found in roots, but also appear in stems and leaves. Seedling expression of *PRX34* is light induced (Passardi *et al.,* 2006). Diminishing the expression of *PRX34* through T-DNA insertion techniques reduces MAMP-induced ROS production, callose deposition and Flg22-activated gene expressions following Flg22 treatment. Phenotypically *PRX34* mutants have larger leaves and show a delay in senescence compared to wild type (Daudi *et al.,* 2012). Following PAMP-perception, Cytokinin receptors HISTIDINE KINASE3 (AHK3) and RESPONSE REGULATOR2 (ARR2) promote the closure of stomata and resistance to *Pst* DC3000. PRX34 is important for cytokinin-mediated stomatal closure with ARR2, a transcriptional regulator of peroxidase genes, controlling guard cell homeostasis (Arnaud *et al.,* 2017). Furthermore, overexpression of *PRX34* has been phenotypically associated with longer root systems due to increased cell length (Passardi *et al.,* 2006). Knocking out the related *PRX33* peroxidase enhances the susceptibility to *Pst* DC3000 (Daudi *et al.,* 2012). These findings demonstrate that oxidative bursts induced by peroxidases are important for MAMP-associated basal resistance in *Arabidopsis.* Given the indication of increased root lengths observed in *prt1-1* (chapter 4) and the increased abundance of PRX34, overexpression of which is associated with longer root lengths, transcript analysis of *PRX34* over seedling development would be informative.

5.8.2.2 Proteins with decreased abundance in *prt1-1*

5.8.2.2.1 Plant thionin

At1g66100 was down-regulated in the *prt1-1* background compared to WT, predicted to encode a PR protein belonging to the plant thionin family (PR-13) according to TAIR annotation. Thionins are anti-microbial and anti-fungal proteins secreted by Arabidopsis in response to pathogen invasion. They are capable of creating pores in phytopathogen cell membranes, causing potassium and calcium release (Asano *et al.,* 2012). There are 6 putative thionin genes in *Arabidopsis*, with At1g66100 predicted to encode acidic gene products homologous to Thi2.4. The gene is expressed in leaves and induced upon MeJA treatments as well as wounding (Chen *et al*., 2006; Sels *et al*., 2008). Given functions of the SA-dependent defence response pathway are constitutively upregulated in the *prt1-1*, downregulation of a protein functioning through the antagonistic JA -dependent pathway is logical. This supports the hypothesis that *prt1-1* mutants should be more susceptible to infection by necrotrophic pathogens.

5.8.2.2.2 PsaC

PsaC is an essential component of photosystem I (Takahashi *et al*., 1991) which bind two terminal electron acceptors F_A and F_B and facilitates the transfer of electrons to ferredoxin (Yang *et al.,* 2017) at the end of the linear photosynthetic electron transfer chain. This ferredoxin transfers electrons to ferredoxin NADP(H) oxidoreductase which supports carbon assimilation through NADP+ reduction (Goss & Hanke, 2014). These are critical steps in the photosynthetic pathway and reduction of PsaC protein levels in *prt1-1* potentially is linked to a reduction in photosynthetic capability. However, phenotypical analysis presented in this thesis demonstrate no obvious affect observed for the down-regulation of *PsaC.*

5.8.2.2.3 Patellins: PATL1 and PATL2

Arabidopsis patellins are novel cell-plate-associated proteins which are sequence-related proteins involved in membrane trafficking in other eukaryotes (Peterman *et al.,* 2004). PATL1 and PATL2 are closely related, and both contain the SEC14 domain enabling them to bind and transfer phospholipids (Mousley *et al.,* 2007), during cytokinesis (Suzuki *et al.,* 2016). It is unclear how down-regulation of these patellins fit with the increased resistance to *Pst* DC3000, however there is no observable burden due to their decreased abundance.

5.8.2.2.4 Allene oxide cyclases: AOC1 (ERD5) and AOC2

The synthesis of jasmonates in *Arabidopsis* is critical given the intimate role these hormones play in plant stress response and developmental signalling. The *ALLENE OXIDE CYCLASE (AOC)* family in *Arabidopsis* contains four functional allene oxide cyclases with high redundancy (Otto *et al.* 2016). *AOCs* encode enzymes which establish the enantiomeric structure in allene oxide to form 12-oxo-PDA a pre-cursor of jasmonates (He *et al.,* 2002; Stenzel *et al.,* 2012). Following leaf proteome analysis ERD12 (synonymous with AOC1) and AOC2 are both down-regulated. Down-regulation of these potentially may reduce the capacity of *prt1-1* plants to produce jasmonates. Again, this supports the enhanced SA-signalling and increased susceptibility to necrotrophy hypothesises. However, given the high functional redundancy in *Arabidopsis AOC* genes this may not be the case, highlighting the need for hormone measurements in *prt1-1* compared to Col-0.

5.8.3 General biotic stress discussion

Taken together, the proteins up-regulated in *prt1-1* mutants compared with the WT are mainly involved in the different defense processes as systemic acquired resistance, effector-triggered immunity and PAMP-triggered immunity. This is logical given the increased resistance to *Pst* DC3000 observed in the *prt1-1* background.

Eliciting an immune response diverts plants resources away from other developmental processes including mitigation of abiotic stresses, photosynthesis, reproduction and seed production (Yasuda *et al.,* 2008). Significant ramifications may be observed in plants which initiate prolonged and/or un-regulated immune responses such as significant growth reduction, lesions due to PCD and a reduced ability to deal with environmental stressors. Given no obvious difference was observed between *prt1-1* and Col-0 (Chapter 4.2 and Figure 5.4), the hypothesised cost of priming in *prt1-1* is likely to be relatively low. Studying the whole rosette metabolome at the point of plant infection (~28DAG untreated material) would be another important step in understanding the response of *prt1-1* plants to *Pst* DC3000.

The TMT-MS and qRT-PCR data showed, respectively, higher GSTF6 and GSTF7 protein and transcript levels in *prt1-1* compared to Col-0. Similarly, Vicente *et al* (2018) recently demonstrated higher GSTF6/7 accumulation in the N-end rule pathway mutants *ntaq1* and *prt6-1* mutants in untreated plant material as well. Although it has been proved the role of GSTF6 (and proposed for GSTF7) in camalexin synthesis (Su *et al.,* 2011), an increase in the concentration of this phytoalexin in mature leaves compared to Col-0 was observed just following infection, not in untreated material (Vicente *et al.,* 2018). The group suggests that in *ntaq1* and *prt6* the increase in camalexin accumulation, from the precursor I3CA, is linked with a decrease in other metabolite interconnected pathways. Given *prt1-1* mirrors these phenotypes of increased resistance to biotic stress and GSTFs abundance, it is hypothesised that there should also be increased abundance of proteins involved in camalexin biosynthesis; however not substantially as this would impose a growth penalty on the plant. Therefore, future analysis should include quantification of accumulation of camalexin pre- and post-infection.

Previous reports have stated the different role of the N-end rule pathway depend on the lifestyle of the pathogen (Vicente *et al.,* 2018). Camalexin

is a positive regulator of plant defense against the necrotrophic fungus *Botrytis cinerea*, however no differences in the level of resistance to this pathogen were observed in *prt6-1* and *ntaq1* mutants (Vicente *et al.,* 2018); this could be due because the increased levels of this phytoalexin were not high enough to produce a visible reduction of the infection. Based on the proteomic data it is difficult to predict whether *prt1-1* is more susceptible to necrotrophs. On one side this mutant shows increased levels of the camalexin biosynthesis proteins GSTF6/7. Conversely *prt1-1* also showed several proteins linked to PCD, which could be exploited by necrotrophs. EDS1, over accumulated in *prt1-1* compared with Col-0, enhances disease progression following challenge by the necrotrophic fungus *Botrytis cinerea* (El Oirdi & Bouarab, 2007). The stabilisation of other genes may also play a role in the potential increased susceptibility to *B. cinerea* such as *PR-2* (Oide *et al.,* 2003). PR-2 levels are higher in *prt1-1 prt6-1* and, especially, *prt1-1prt6-1*, which displays an additive effect of PR-2 abundance, compared to Col-0 (Figure 5.13); this also backups an increased susceptibility of these mutants to *B. cinerea*. Another protein which abundance is higher in *prt1-1* relative to Col-0, AIR12*,* is as well implicated in greater susceptibility to necrotrophy. In general, the likelihood for increased SA levels in *prt1-1*, which would antagonize the positive role of JA signalling in defence against necrotrophic pathogens, highlighting the need for hormone measurements.

Although no significant differences in the growth of the PTI inducer strain *Pst* DC3000 *hrpA*$^{-}$ were found between *prt1-1* and Col-0 (Figure 5.5.3.3), the increased abundance of proteins involved in the synthesis of FLS2, the receptor of the PAMP flagellin, such as TOM1, in *prt1-1* compared with Col-0, suggest a positive role for PRT1 in regulating PTI*.* As discussed, the lack of differences during Pst DC3000 *hrpA*$^{-}$ infections could be due to a lack of sensitivity of the assay. Additional informative experiments would be to measure the plant responses to the flagellin peptide flg22, by analysing the expression of key responsive genes, such as WRKY29 and FRK1.

Taken together the data obtained from the analysis of growth of the different *Pst* strains, proteomic analysis via TMT-MS of untreated leaves and the transcriptomic analysis a mode of action of PRT1 can be inferred. The substrates whose stability is regulated by PRT1 are clearly involved in the plant immune response. In absence of the pathogen, these substrates would remain degraded by the action of PRT1 and once the plant senses the pathogen PRT1 activity is down regulated allowing the stabilisation of the substrates. Following this hypothesis, *prt1-1* is placed in a primed state over WT because of increased stabilisation of substrates with age. Older *prt1-1* plants yield higher accumulation of substrates compared to Col-0. A global transcriptome profiling approach as well as a metabolomics would help to improve our knowledge about PRT1 role in environmental stresses in general and in plant defense against pathogens in particular.

One hypothesis for the involvement of PRT1 in plant immunity regulation may involve a protease which is normally active in untreated tissues. In the absence of pathogen stimuli, the protease may cleave its substrate to reveal Phe/Try/Tyr at the N-terminus which are N-degrons of PRT1. This enables the substrate to be degraded and a basal SA and SA-responsive protein abundance to be maintained. Following perception of the pathogen, the protease activity could be down-regulated resulting in PRT1 substrates stabilisation. The increased abundance of these substrates then elicits SA-dependent defense responses enabling the plant to respond to the pathogen. In this way PRT1 could be seen as a negative regulator of plant immune responses in untreated material. The PRT1 substrates will be stabilised in *prt1-1* plants without pathogen perception, explaining the increased protein abundance and resistance phenotypes observed.

EDS1 may potentially be a substrate for PRT1. Following protease cleavage, PRT1 could target EDS1 for constitutive degradation in untreated Col-0 to keep the abundance of SA and SA-responsive proteins basal in absence of biotic stress perception. The basal SA and

PR proteins presence in untreated may attributed to SA-synthesised through the *ICS1* pathway. The inability to detect PRT1 in leaf tissue through the PRT1-TAP tag may be explained by a mechanism of PRT1 regulation and degradation by either self-ubiquitylation or the action of an exogenous E3 ligase (de Bie & Ciechanover, 2011). Pathogen perception possibly results in an alteration to the PRT1-EDS1 interaction, such as protease inactivation, and enables SA-responsive defence gene expression. In this way PRT1 is a negative regulator of SA-dependent defense responses, until a bacterial pathogen is perceived whereby SA-responsive defence proteins are expressed. Since EDS1 would be stabilised in the *prt1-1* background, this would increase the abundance of this core SA-signaling component, producing enhanced SA-dependent defence responses, and the priming effect pre-infection. The feasibility of EDS1 and other candidates as substrates for PRT1 is discussed in the following chapter.

Plant defence has been demonstrated to be circadian-influenced in order to marry their expression with likelihood of pathogen infection (Wang *et al.,* 2011; Zhang *et al.,* 2013 Nicaise *et al.,* 2013; Karapetyan & Dong, 2018). Studies of the *Arabidopsis- P. syringae* pathosystem have discovered that the time of infection during the diurnal cycle strongly influences the outcome of the interaction (Bhardwaj *et al.,* 2011; Zhang *et al.,* 2013). Throughout this study, the time of infection for gene expression or proteomic analysis was standardised at ~2 hours after the lights turned on in the growth chambers. This was done first to ensure enough time for plants to switch to “light-mode” and be fully photosynthetically active, and second to avoid possible variations in the response due to circadian regulation.

In summary, for the conditions presented in this study, a robust phenotype has been established for the *prt1-1* mutant of increased resistance to the hemi-biotrophic pathogen *Pst* DC3000. Transcriptomic and proteomic data revealed that *Arabidopsis* genes and proteins associated with major components of plant immunity are increased in

abundance in the mutant prior to pathogen challenge rather than an enhancement to their induction once the biotic stress has been perceived. In this way, *prt1-1* plants in a primed state are better able to deal with the pathogenic burden. This increase in resistance is subtle and appears to mirror that observed in other mutants of the N-end components *prt6-1* and *ntaq1*, suggesting a role for glutamine deamidation and cysteine oxidation branches through PRT6-mediated degradation of NTAQ1 substrates and ERFVIIs (Vicente *et al.,* 2018). Interesting, all plant N-end rule mutants display a reduction in susceptibility to similar amounts (~0.5 log cfu cm^2) and no additive effect is observed in the *prt1-1prt6-1* double mutant, implying that the different branches of the N-end rule pathway act in the same pathway upon different substrates or the same substrate which is differently regulated. Although contradictory results are presented in current scientific literature regarding N-end rule mutants and biotic stress response, the work presented in this study is independently concurs with Vicente *et al* (2018) by showing the same resistance patterns for *prt6-1*. Conservation of this role in also presented in Vicente *et al.,* with reduced *HvPRT6* expression implicated in enhance resistance to *Pseudomonas syringae* pv. *japonica* and *Blumeria graminis* f. sp. *Hordei* in barley plants with reduced PRT6 activity. The following general discussion chapter will discuss these findings in the whole plant context.

Chapter 6: General Discussion

PRT1 is an E3 ligase functioning through the plant N-end rule pathway isolated in a genetic screen in 1998 (Bachmair *et al.*) and subsequently proposed as the first *bona fide* plant E3 ligase with specificity for bulky aromatic destabilising residues including phenylalanine, tryptophan and tyrosine (Potuschak *et al*., 1998; Stary *et al*., 2003). Mot *et al* (2018) recently confirmed that PRT1 is indeed an E3 ligase involved in poly-ubiquitylation of substrate proteins depending on their N-terminal amino acids (Figure 6.1) using fluorescently labelled substrate probes. Unlike the other plant N-recognin PRT6, PRT1 has received little attention from the scientific community, emphasised by the lack of published literature.

In this thesis, the physiological function and localisation of PRT1 were the main focus. At the outset of this study, no phenotype had been associated with *prt1-1*, although a subsequent publication by de Marchi *et al* (2016) suggests that the E3 ligase is a positive regulator of plant defence responses. The work presented in this thesis fortifies the link between the N-end rule pathway and plant responses to pathogens. However, data generated during this study show the opposite effect of *prt1-1* responses to *Pst* DC3000 as reported previously (de Marchi *et al.,* 2016), with an increased resistance to the pathogen. Physiological functions and localisation data obtained during this study will be discussed together with literature to establish potential roles for PRT1 in the whole plant context.

The F-GUS activity reporter demonstrated that PRT1 is active throughout the plant at all developmental stages. The PRT1 protein is readily detected in *prt1-1* roots using a complementing line expressing a TAP-fusion under the control of the endogenous promoter. However, this is not the case in shoots and leaves expressing the same construct. Following proteasome inhibition for 8 h with bortezomib, the PRT1-TAP fusion could be detected in both roots and shoots. This implies that PRT1 is degraded in aerial tissues. The phenotype of increased resistance to hemi-biotrophic pathogens is manifest in the leaf tissue of *prt1-1* plants,

which produces a non-functional copy of the E3 ligase that cannot target its substrate(s). In this background, verified by transcript analysis and proteomics approaches, SA-dependent defence related genes and associated proteins were increased in expression/abundance prior to pathogen challenge. One potential explanation for this is self-ubiquitylation of PRT1 (Figure 6.1). If PRT1 ubiquitylates defence-related substrates in leaves to regulate their abundance, and undergoes self-ubiquitylation, this would explain in part the lower defence protein abundance in untreated wild type and inability to detect TAP-tagged PRT1 without proteasome inhibition.

Self- ubiquitylation and consequent degradation of E3 ligases occurs via three distinct mechanisms: self-ubiquitylation independent from ubiquitylation of the substrate; concomitant E3 ligase self- ubiquitylation occurs with the ubiquitylation of the substrate; or inhibition of self-ubiquitylation by the substrate (de Bie & Ciechanover, 2011). Given TAP tagged PRT1 is detectable in roots without PI treatment and SA-dependent defence proteins are not highly expressed in root tissue, PRT1 self- ubiquitylation would likely be concomitant with its substrate in leaves. If this were the case, PRT1 would be constitutively degraded. To enable proposed regulation of defence responses in absence of biotic stress, PRT1 would be constitutively synthesised meaning the PRT1 promoter should be constitutively active too. For the conditions tested in this study, PRT1 promoter activity could not be observed. The construct used to establish PRT1 promoter activity may not have included sufficient elements of the promoter or other parts of the gene that are essential for its expression may not have been included. Re-designing this construct may facilitate valuable studies into the localisation and activity of the PRT1 promoter. Additionally, the PRT1 abundance should be established pre- and post-infection (via PRT1-tag Western blotting) to determine where the E3 ligase level changes during infection.

Expression of plant defence-related proteins places a substantial burden on the plant energy status, and over accumulation of such pathogenesis related proteins may have significant ramifications on the plant in terms

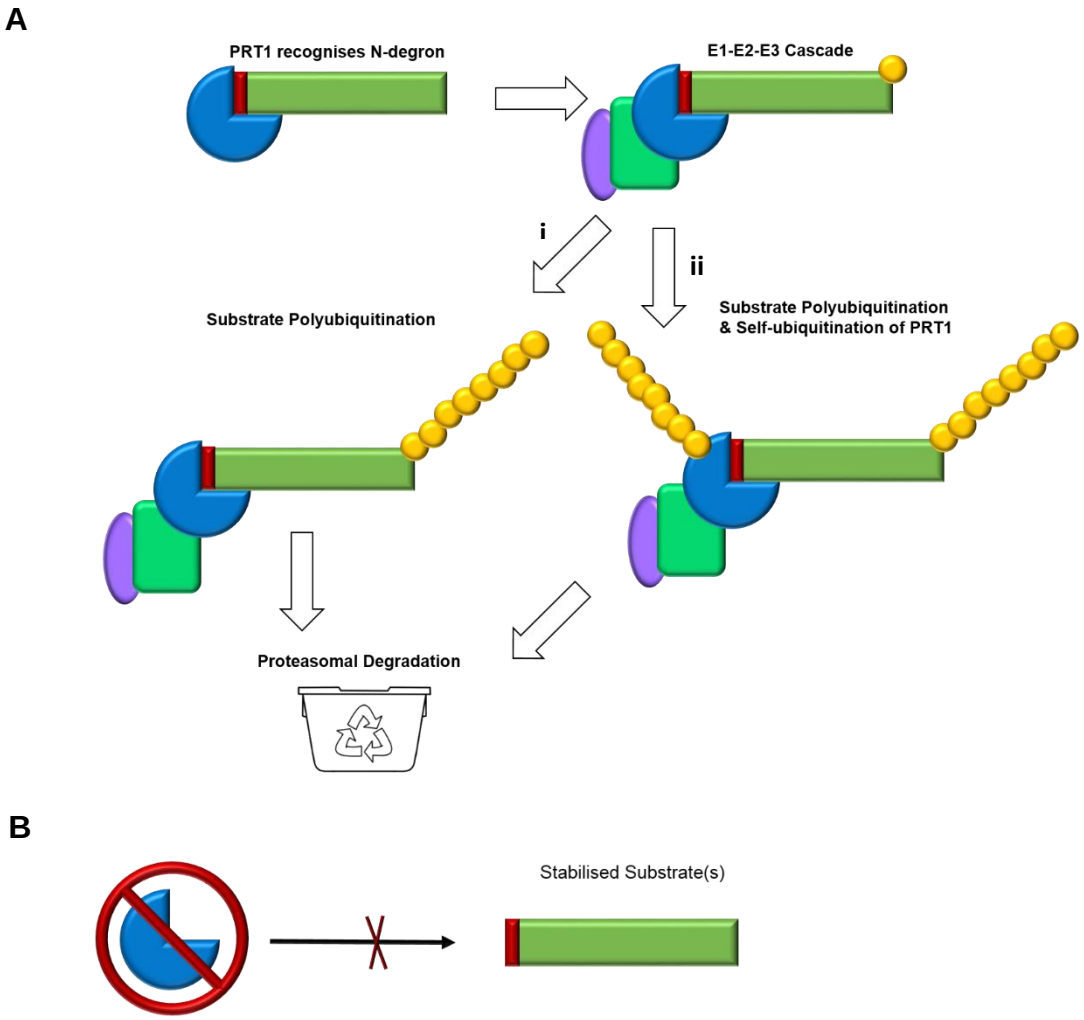

Figure 6.1: Mechanism of PRT1-mediated substrate degradation. (A) In untreated material, WT PRT1 recognises its N-degron and initiates an E1-E2-E3 cascade. Successive rounds of E1-E2-E3 cascades form (i) polyubiquitin chains with (ii) PRT1 self-ubiquitylation, (B) substrate degradation is prevented in the *prt1-1* background due to non-functional E3 ligase. (Blue = PRT1 E3 ligase; Red = N-degron; green = PRT1 substrate(s); yellow = ubiquitin; purple = E1; light green = E2).

of photosynthetic capacity, biomass yield, fertility and ability to mediate stress responses (Li *et al.,* 2001; Zhang *et al.,* 2003; Shirano *et al.,* 2002; Kemmerling *et al.,* 2007). This would be particularly detrimental during seedling stages as resource allocation to defence processes may impact greatly on plant development. It is logical therefore that tight regulation of their expression is necessary to prevent detrimental effects on plant health. Given no obvious morphological differences were observed between *prt1-1* and Col-0 plants in this study, this implies that stabilisation of defence associated proteins does not have such an effect. Consistent with this, the increase in defence protein abundance is not dramatic in the *prt1-1* mutant, emphasised by the slight reduction in pathogen burden compared to the WT (~0.5 log cfu/cm^2).

One hypothesis is that in the absence of pathogen perception, protease action cleaves a protein which reveals either tryptophan, tyrosine or phenylalanine at the N-terminus. These Nt residues are destabilising residues for PRT1-mediated degradation (Figure 6.2). As a result, PRT1 substrates are degraded, possibly with PRT1 self-regulation, which prevent SA-biosynthesis and SA-responsive gene expression in untreated tissues. Following pathogen perception, a pathogen triggering signalling cascade may inhibit the protease action which leads to the accumulation of a protease target/N-end rule substrate that enhances resistance. If PRT1 is autoubiquitylated during substrate degradation, it might be predicted that PRT1 itself would be stablised upon infection. Anti-SBP Western blots for the TAP-tag line following inoculation with *Pst* DC3000 would establish the fate of PRT1 following pathogen infection, however such experiments were not completed due to time constraints. In the *prt1-1* mutant background, protease activity proceeds and W/Y/F destabilising residues are revealed, but no PRT1 E3 ligase is present to mediate substrate degradation leading to constitutive SA-biosynthesis and SA-responsive gene expression. A potential future experiment might use protease inhibitors prior to infection. Col-0 treated with protease inhibitor prior to infection may accumulate SA and SA-responsive proteins at higher levels than untreated Col-0, placing these plants in a

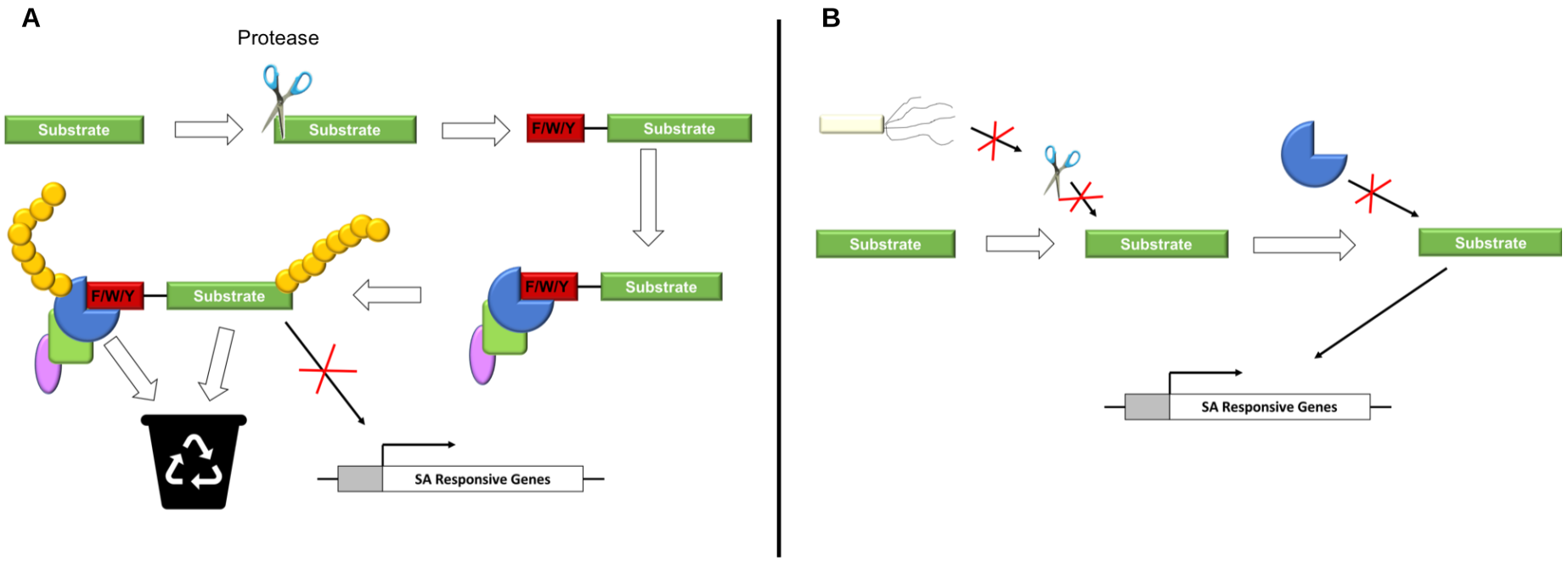

Figure 6.2 Proposed mechanisms for the role of proteases and PRT1 in plant responses to pathogens: (A) in uninfected Col-0 (B) infected Col-0. (Red indicates protease cleaved substrate with Phe, Try or Tyr at the N-terminus; Blue = PRT1 E3 ligase; green = PRT1 substrate(s); yellow = ubiquitin; purple = E1; light green = E2; Recycle bin = 26S proteasome).

primed state too. However, there are no precedents reported in literature searches for an experiment of this nature, it may be very technically challenging and produce artefacts in the response that make interpretation difficult.

Leaf proteomics data indicates that EDS1 is upregulated in uninfected *prt1-1* plants. EDS1 acts with PAD4 as central regulatory hub via NPR1 for the initiation of SA-dependent defence gene expression (Armijo *et al.,* 2013). Transcript and proteomic analysis revealed that SA-dependent response genes and proteins were higher in untreated *prt1-1* than WT. This SA-dependent pathway is antagonistic to the jasmonic acid pathway, and vice versa. JA initiates the ubiquitylation and ensuing degradation of jasmonate ZIM-domain-protein (JAZ) through the COI1 E3 ligase, lifting the repression of transcription factors of JA-dependent genes, enabling their expression. This action is repressed by NPR1 (Yan *et al.,* 2009; Huang *et al.,* 2017). Leaf proteome analysis revealed that ERD5 and AOC2 proteins are decreased in abundance in *prt1-1* which are associated with JA biosynthesis. Furthermore, the JA-associated plant thionin/PR-13 protein was decreased in abundance, suggesting that JA-responses are suppressed in *prt1-1.* Therefore, measurement of SA and JA hormone levels in the *prt1-1* background should be conducted, as these are predicted to be respectively higher and lower compared to WT. Consequently, *prt1-1* is predicted to be more susceptible to pathogens with a necrotrophic lifestyle. In support of this, *prt1-1* was demonstrated to be more susceptible to the necrotrophic fungus *Sclerotinia sclerotiorum* than Col-0 but phenotypically comparable in response to *Botrytis cinerea* (de Marchi *et al.,* 2011).

In a recent publication by Pan *et al* (2018), a receptor-like kinase (RLK) called DOES NOT MAKE INFECTIONS 2 (DMI2) is constitutively degraded by the proteasome in *Medicago truncatula*. DMI2 functions as a co-receptor which is proposed to interact with RLK Nod factor receptors (Antolín-Llovera *et al*., 2014), which perceives Nod factors secreted by rhizobia during nitrogen-fixing symbiotic events for initiation of nodulation

(Vijn *et al.,* 1993). DMI is necessary for perception of these beneficial symbiotic events in *Medicago,* and protein levels are highly regulated by the host to ensure maximum benefit in terms of nitrogen fixation and minimise any losses associated with the symbiosis. DMI2 degradation is prevented upon inoculation by rhizobia as revealed by high DMI2 protein concentration. The group do not propose a mechanism of how the DMI degradation may be prevented however. Possible reasons may be due to steric degron shielding of the N-degron following biotic stress perception, which prevents degradation (Shemorry, Hwang & Varshavsky, 2013) (Figure 6.3). Alternatively, biotic stress perception may trigger degradation by an unknown exogenous E3 ligase or non-proteolytic self-ubiquitylation which alters the E3 ligase substrate specificity (de Bie & Ciechanover, 2011). This alteration prevents the degradation of DMI2 and facilitates symbiosis when Nod factors are perceived.

A model is proposed in this thesis which involves PRT1-mediated constitutive degradation of a regulator of SA-dependent defence genes in the absence of biotic stress perception. PRT1 then potentially self-ubiquitylates which may account for the inability to detect the PRT1-TAP in leaf material (Figure 6.1). Inoculation with the pathogen may result in an alteration to the PRT1 E3-ligase interaction through a mechanism similar to those proposed for DMI2 (Figure 6.3). This acts to prevent the degradation of the upstream regulator and permits SA-dependent downstream events to occur. EDS1 therefore could be a candidate substrate for PRT1, which is targeted for degradation in untreated Col-0 to negatively regulate SA-dependent defense responses. Exogenous SA generated through the *ICS1* pathway in the plant may explain the basal levels of PR protein abundance observed in untreated Col-0. Following pathogen perception, PRT1-EDS1 interaction may be perturbed through E3 ligase regulation, leading to increased EDS1 abundance and associated SA-dependent responses. Since the *prt1-1* mutant would not be able to turnover EDS1, its increased abundance would produce

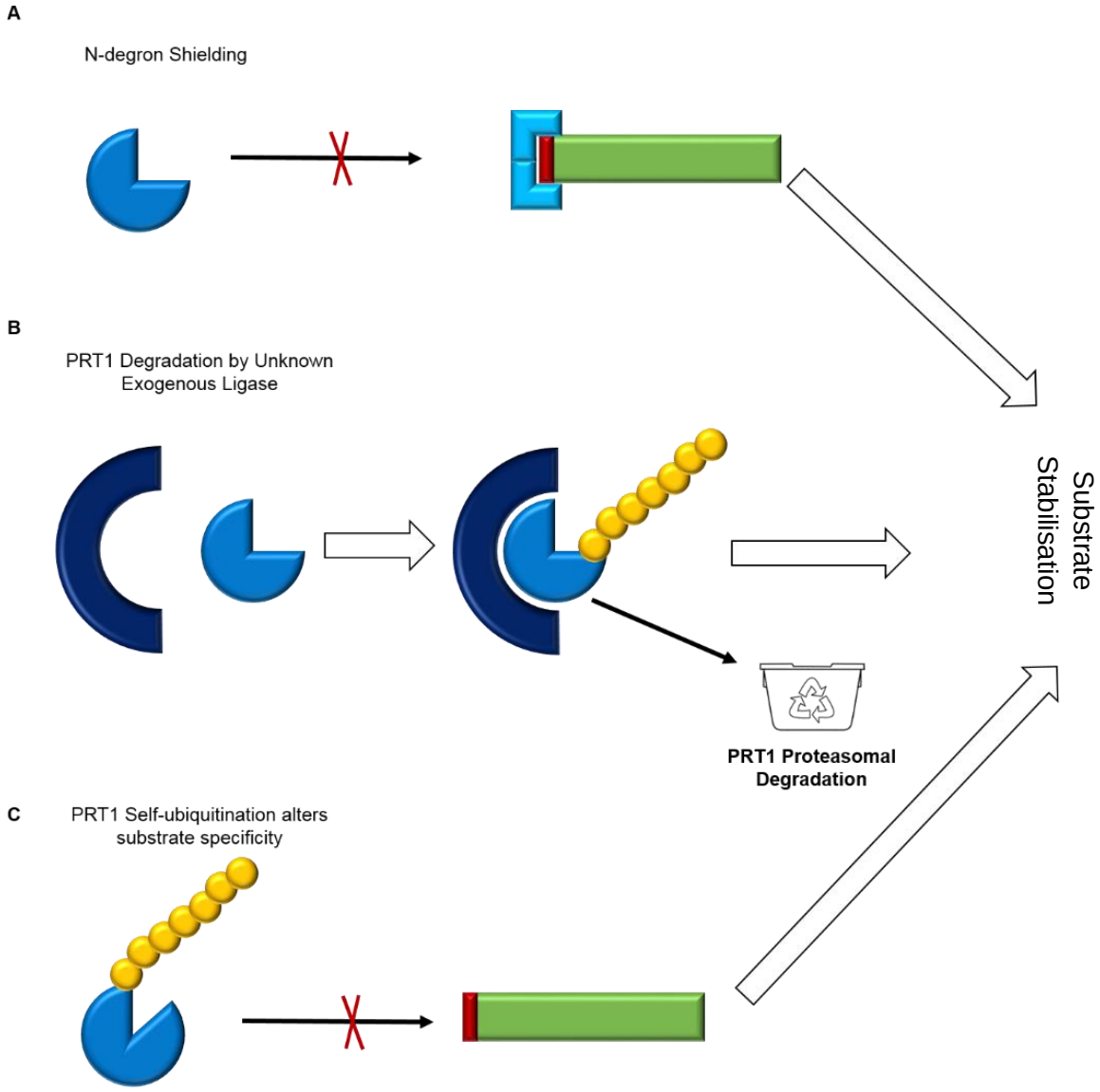

Figure 6.3: Proposed alterations to E3 ligase–substrates interaction in following stimuli such as pathogen challenge in PRT1-mediated degradation. (Blue = PRT1 E3 ligases; light blue = Degron shielding'' red = destabilising Nt residue; green = substrate; dark blue = exogenous E3 ligase; yellow = ubiquitin)

enhanced SA-dependent defence responses, placing these plants in a primed state for infection.

The proteomic data presented in this thesis was obtained following a single run of 10plex-TMT with MS/MS untreated leaf material for Col-0 and *prt1-1.* At the time of writing, analysis on the full TMT dataset with increased coverage was unavailable. Preliminary analysis of the full data set confirmed that PRT1 is increased in abundance in Col-0 but not detected in *prt1-1* showing that *prt1-1* is truly an EMS null allele of PRT1. Furthermore, proteins further upstream than EDS1 were shown to be increased in abundance in *prt1-1* compared to Col-0 (personal communication, Professor Theodoulou, Rothamsted Research), indicating that EDS1 is likely not to be a direct substrate of PRT1.

Zschiesche *et al* (2015) propose two proteins upstream of EDS1 that may regulate SA-dependent responses. HEAVY METAL-ASSOCIATED ISOPRENYLATED PLANT PROTEIN3 (HIPP3) may act as a chaperone for zinc which activates the LESION SIMULATING DISEASE RESISTANCE1 (LSD1) zinc-finger transcription factor, a negative regulator of the SA-dependent pathway (Rustérucci *et al.,* 2001). LSD1 may repress SA-dependent defence responses via EDS1. Alternatively, HIPP3 may repress NPR1 directly. Copper is essential for NPR1. HIPP3 may facilitate the replacement of copper with zinc and consequent inhibition of NPR1. This is reminiscent of the bacterial cop-operon in which the zinc requirement of the copY repressor is replaced by copper facilitated by copZ (Solioz & Stoyanov, 2003).

PRT1 may have potential to play a role in these interactions (Figure 6.4). The substrates of PRT1 in this model are predicted to repress the HPP3-LSD1 regulon. In the untreated WT, in which PRT1 substrates are degraded and are unable to repress the HPP3-LSD1 regulon, HPP3 is able to repress SA responses either via LSD1 repression of EDS1 or direct repression of NPR1. This ensures SA-responsive gene expression is basal. However, in the untreated *prt1-1* background, the non-functional E3 ligase results in accumulation of or prevents degradation of PRT1

substrate(s) which repress HPP3 or LDS1 and alleviate the repression of EDS1/NPR1. Subsequently an increased in SA-dependent defence proteins abundance would be observed which places *prt1-1* in a primed state compared to Col-0 pre-infection. Given the increase in EDS1 transcript and protein abundance in *prt1-1* untreated plants, an increase in SA and SA-dependent response is most likely to occur through increased repression of HPP3-LSD1 and subsequent reduced repression of EDS1. This upregulation of SA signalling is likely to antagonise JA signalling, which would in turn reduce the capacity of *prt1-1* to respond to necrotrophic pathogens. It is proposed that following pathogen challenge, wild type PRT1 E3 ligase-substrate interactions are perturbed (as shown in Figure 6.4) which stabilise PRT1 substrates. In this way, the HPP3-LSD1-EDS1-PAD4 regulon behaves as *prt1-1* (less repressed) and SA-responses are mediated.

Taken together, this model suggests that PRT1 could act either with HIPP3 and/or LSD1 to negatively regulate SA-dependent defence responses in the absence of pathogen stress. Following perception of bacteria, a change occurs between PRT1 and its substrate(s) preventing substrate degradation. This stabilised substrate increases the repression on HPP3-LSD1 regulon which in turn alleviates repression of EDS1-PAD4, and initiates SA-dependent defence responses. This model is entirely speculative and relies on as yet unidentified upstream PRT1 substrates and unreported mechanisms of PRT1 regulation but provides a hypothesis that incorporates upstream regulation of EDS1 and SA-dependent PR protein accumulation that would lead to increased resistance to *Pst* DC3000; all of these effects are observed in *prt1-1* compared to Col-0. Informative experiments might probe a PRT1 overexpressing (Ox) line with *Pst* DC3000. In untreated PRT1 Ox, the increased PRT1 abundance would be expected to further degrade PRT1 substrates leading to increased abundance of HIPP3/LSD1 which further repress EDS1/PAD4. This should either further reduce SA-responsive defence processes or no difference to Col-0 will be observed. This implies that PRT1 OX lines may be more susceptible to *Pst* DC3000 than

Col-0, but by reducing repression on JA-signalling pathways, more resistant to necrotrophy.

Alternately, there are other candidates that PRT1 may act on the regulation of SA-dependent responses upstream of EDS1. Microarray analyses following plant challenge by avirulent pathogens have demonstrated that a Nudix hydrolyase called NUDT7 is upregulated which acts as a negative regulator of EDS1 and associated defence responses (Bartsch *et al.,* 2006; Ge *et al.,* 2007; Adams-Phillips *et al.,* 2008). The *nudt7* mutation appears similar to other constitutive defence mutants with increased SA and expression of defence genes including *PR-1* and *PR-2* (Ge *et al.,* 2007), as well as a severely reduced growth phenotype and spontaneous leaf cell death (Bartsch *et al.,* 2006). *nudt7* mutants are reported to be hyper-resistant to virulent *Hyaloperonospora parasitica* (Bartsch *et al.,* 2006) as well as virulent *Pst* (Jambunathan & Mahalingam, 2006; Ge *et al*., 2007). However, NUDT7 as a substrate for PRT1 does not follow observations made so far. In the *prt1-1* mutant background, NUDT7 would be increased in abundance which should repress EDS1 and downstream SA-gene responses to a greater extent. However, phenotypically the results are opposite indicating that NUDT7 is unlikely to be a substrate of PRT1.

Additionally, FLAVIN-DEPENDENT MONOOXYGENASE1 (FMO1) was shown to be a positive regulator of the EDS1-PAD4 node (Bartsch *et al.*, 2006). Koch *et al* (2006) demonstrated that constitutive overexpression of *FMO1* enhances disease resistance against *P. syringae* (Koch *et al.,* 2006). FMO1 possibly initiates SAR in infected tissues, emanation to distal tissues, perception of the mobile SAR signal in distal tissues or regulation of FMO1 in systemic tissues (Mishina & Zeier, 2006). In *eds1* and *pad4* mutants, induced *FMO1* expression is attenuated, which confirms the role of FMO1 in the regulation of the EDS1/PAD4 regulatory hub (Bartsch *et al.,* 2006). In the *prt1-1* mutation, if FMO1 was a PRT1 substrate, more FMO1 would be stabilised which, through its positive regulation of EDS1, increases SA accumulation, SA-dependent responses and thus resistance to *Pst* DC3000 (Figure 6.4). In Col-0,

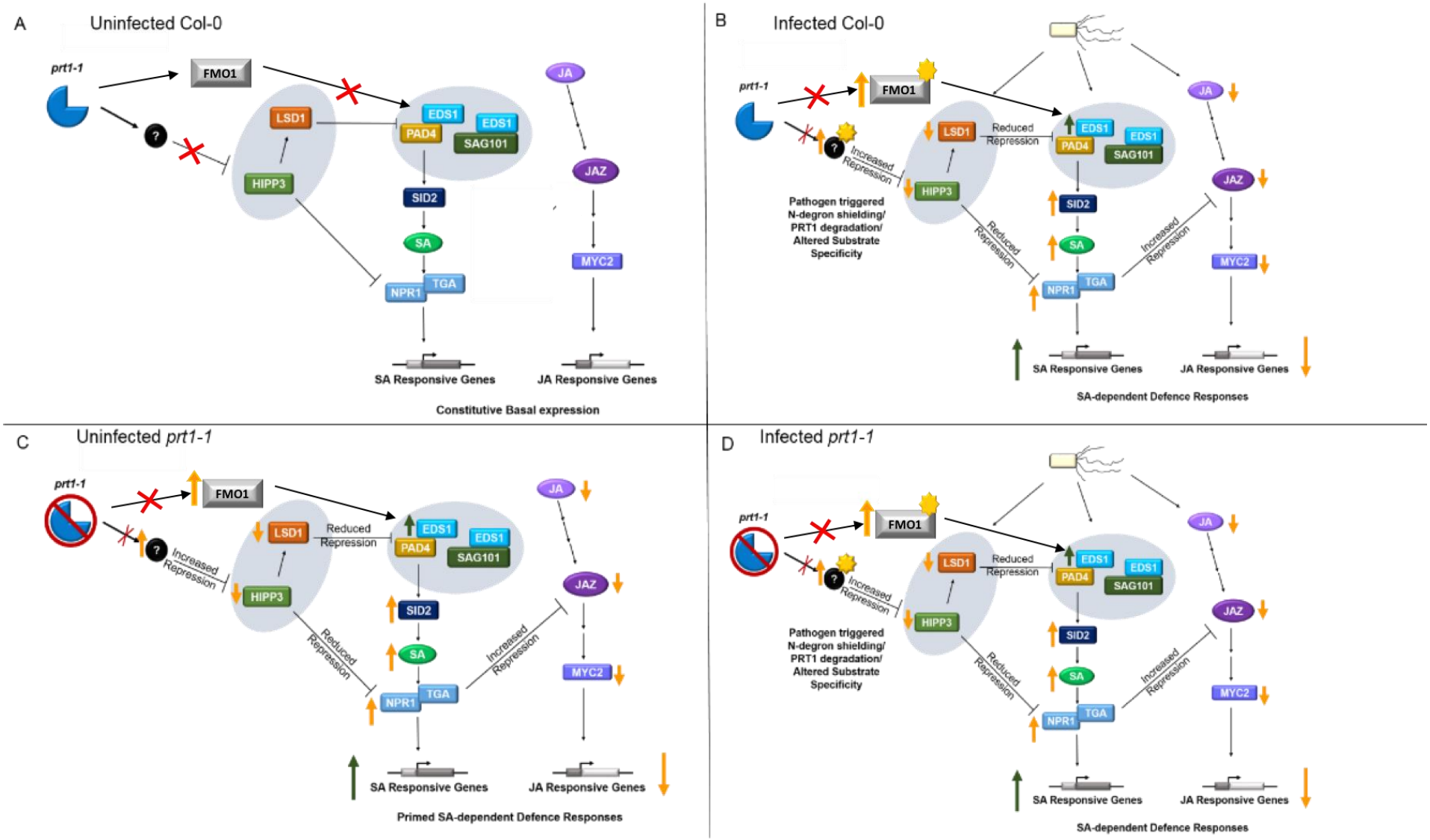

Figure 6.4 Proposed mechanism S for the role of PRT1 in plant responses to pathogens: (A) in uninfected Col-0 (B) infected Col-0 (C) uninfected *prt1-1* and (D) infected *prt1-1*.

PRT1 could degrade FMO1 to limit EDS1-PAD4 abundance thus keeping SA abundance and SA-dependent responses basal. Following *Pst* DC3000 perception, an alteration occurs between PRT1 and FMO1 which prevents PRT1-mediated FMO1 degradation. This stabilised FMO1 increases EDS1-PAD4 abundance, and initiates SA production and SA-dependent defence responses.

Again, the alteration to the PRT1-FMO1 interaction following pathogen perception and PRT1 concurrent self-ubiquitylation with FMO1 degradation are assumptions with no experimental evidence to reinforce them. Probing *fmo1* mutants would help establish if it is involved in PRT1-mediated defence regulation. *fmo1* mutants would be expected to behave as Col-0 in the absence of biotic stress, as FMO1 is degraded by PRT1 in wild type and not expressed in *fmo1.* A *prt1-1 fmo1* double mutant would also reflect untreated Col-0 and *fmo1,* meaning the *fmo1* mutation should abolish the priming effect of *prt1-1.* Mishina and Zeier (2006) reported that plant responses to local avirulent and virulent infection were comparable for Col-0 and *fmo1,* thus a *prt1-1 fmo1* may behave as Col-0 and *fmo1* upon local pathogen challenge. Overexpression of *FMO1* in the *prt1-1* background may produce hyper resistant phenotypes to *Pseudomonas syringae* but potentially severely stunted growth (van Wersch, Li & Zhang, 2016).

The ePlant Cell eFP browser (Waese *et al.,* 2017) was queried to investigate the subcellular expression of PRT1 and proposed substrates. The eFP browser uses predictions of localisation in the absence of experimental evidence meaning predictions should be viewed tentatively. However, according to the SUBAcon database (Hooper *et al.,* 2017), PRT1 is predicted to be localised primarily in the nucleus but also in the cytoplasm (Figure 6.5). FMO1 expression is predicted to be chiefly cytoplasmic whereas LSD1 and HIPP3 are predicted to be nuclear proteins. The likelihood of PRT1-HIPP3/LSD1 model is potentially higher than PRT1-FMO1 due to the predicted localisation in the nucleus of the former. The dimeric form of EDS1 is chiefly located in the cytoplasm whereas the EDS1-PAD4 complex required for the induction of SA and

SA-responsive defence gene expression, resides in the nucleus (Czarnocka *et al*., 2017). Given that all components of the proposed HIPP3-LSD1-EDS1 regulon are nuclear located where they induce SA-dependent gene expression, interaction with PRT1, via an unknown substrate, which is also nucleus-localised looks promising. However, pathogen perception is likely to occur elsewhere such as the cytoplasm, plasma membrane and apoplast, with extensive signalling cascades involved.

The models presented for PRT1-mediated regulation of plant pathogen responses do not account for the upregulation of other proteins such as GSFTs which are not influenced by the EDS1-PAD4 hub. The mitogen activated kinases MPK3 and MPK6 have been demonstrated to trigger GSTF6 and GSFT7 accumulation, leading to increased camalexin abundance (Su *et al.,* 2011). Cui *et al* (2017) demonstrated that MPK3/6 signalling is not a part of the EDS1-PAD4 mechanism for SA-dependent defence induction. How PRT1-mediated degradation of proteins related to camalexin biosynthesis fits into the proposed models is unclear and suggests that PRT1 may have specificity for more than one substrate or that substrates are further upstream of EDS1. Similarly, GSTFs are also increased in abundance in *ntaq1* and *prt6-1*, which are phenotypically similar to *prt1-1* in the response to *Pst* DC3000. Vicente *et al.* (2018) demonstrated that camalexin biosynthetic genes *GSTF6* and *GSTF7* are ectopically upregulated in untreated *prt6-1* compared to wild type, as is the case for *prt1-1*. However significant differences in camalexin abundance was only observed following pathogen inoculation. A *prt1-1 pad3* mutant should reverse the enhanced resistance phenotype of the *prt1-1* mutant to *Pst* DC3000, as demonstrated by Vicente *et al.* (2018) for *prt6-1,* if PRT1 is involved in camalexin biosynthesis regulation.

A significant unanswered question in the models proposed is how does the PRT6 E3 ligase fit into the suggested regulation of SA-dependent responses in the absence of bacterial perception? The work presented in this study demonstrated that *prt6-1* also responded similarly to *Pst*

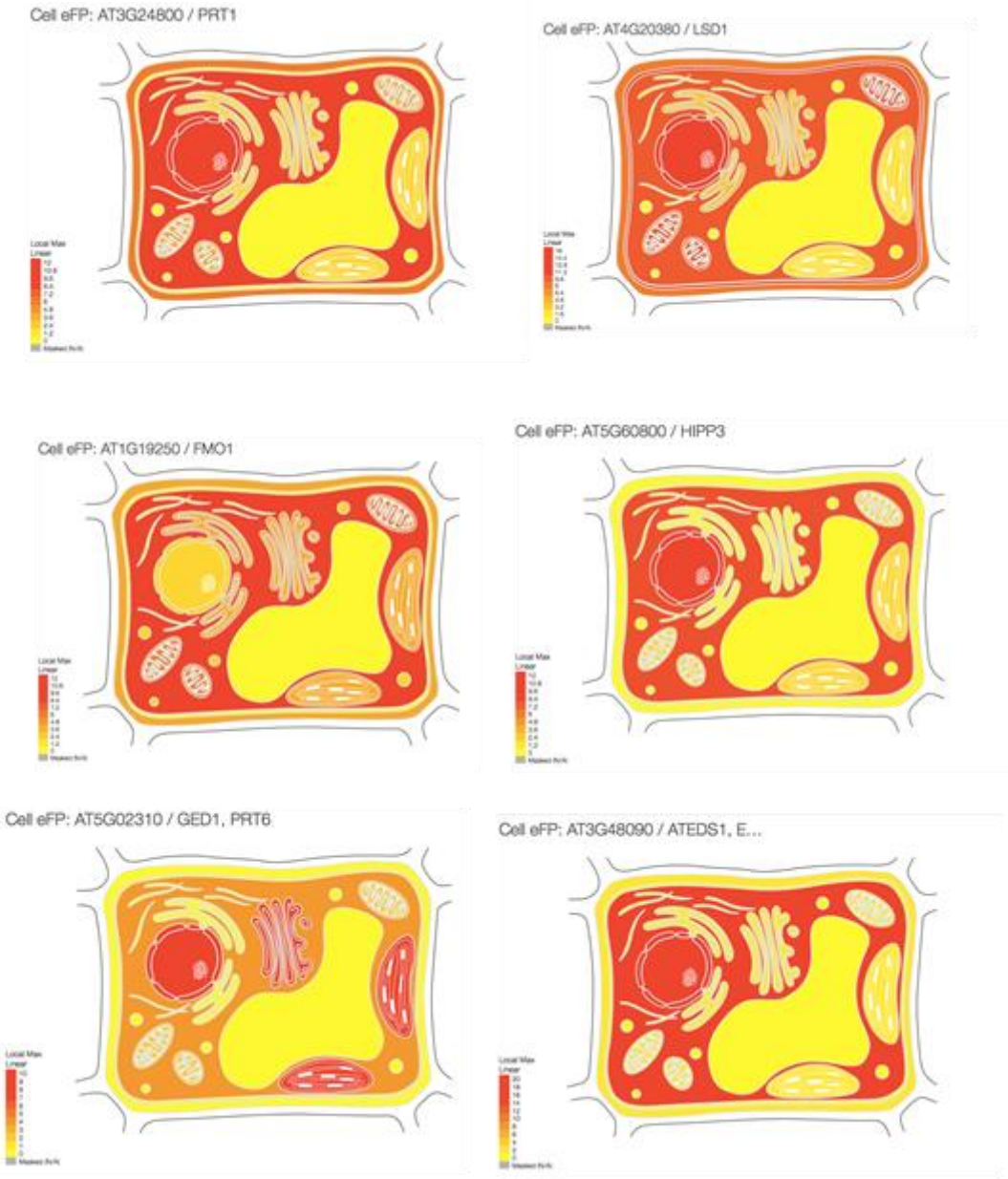

Figure 6.5: Predicted subcellular localisation of PRT1, PRT6 and proposed substrates from publicly available transcript data sources: adapted from the Arabidopsis cell eFP browser (Waese *et al.,* 2017; https://bar.utoronto.ca/eplant/; accessed August 2018) showing the absolute expression of *PRT1* (At3g24000), *PRT6* (At5g02310), *FMO1* (At1g19250), *LSD1* (At4g20380), *HIPP3* (At5g60800) and *EDS1* (At3g48090) in a subcellular context (Hooper *et al.,* 2017).

DC3000 as *prt1-1* (i.e. increased resistance). These results confirm the findings independently presented in Vicente *et al* (2018) and contradict those in de Marchi *et al* (2016). Interestingly, no additive effect was observed in the *prt1-1prt6-1* double mutant in terms of resistance to *Pst* DC3000. PRT6 is predicted to be primarily localised in the nucleus according to the SUBAcon database (Figure 6.5) and there is a significant commonality between the proteins stabilised in leaf material pre-infection such as SA-dependent PR-1 and PR-5 (Vicente *et al.,* 2018). This implies that both E3 ligases could act upon different members of the same gene family, which are cleaved to produce destabilising residues and give the overlapping phenotype of increased resistance. Alternatively, both E3 ligases may target the same protein but these are cleaved by different proteases. This may be centred on the EDS1-PAD4 regulatory hub. A global transcriptome profiling approach for Col-0, *prt1-1* and *prt6-1* may enable patterns of gene regulation to be compared between these lines and potentially establish the points in the pathway these E3 ligases act, establishing a signalling hierarchy. The proposed involvement of both these N-recognins the maintenance of basal SA-responsive gene expression in the absence of pathogens, may suggest that they act partially redundantly. The combined function of PRT1 & PRT6, i.e. the binding of both type-1 (basic; Arg, Lys, and His) and type-2 (bulky hydrophobic; Phe, Trp, Tyr) destabilising residues, is fulfilled alone by Yeast Ubr1 in *S. cerevisiae* (Tasaki e*t al.,* 2009). Separation of these functions onto two separate proteins in plants, with distinct specificities, may enable for greater fine tuning of the pathogen response. Although, PRT6 alone is homologous to Ubr1 (although it lacks ClpS). PRT1 is a novel plant E3 ligase which is not derived from Ubr1, so this may be a tenuous hypothesis.

PRT6 has been described as a general sensor of stress in plants, having been implicated in plant critical processes including: germination, development and senescence, delay during submergence, plant responses to pathogens and photomorphogenesis (Holman *et al*., 2009; Gibbs *et al*., 2014a, Yoshida *et al*., 2002; Graciet *et al*., 2009, Riber *et*

al., 2015; Gravot *et al*., 2016; de Marchi *et al*., 2016; Abbas *et al*., 2015; Vicente *et al.,* 2017; Vicente *et al.,* 2018). Group VII ethylene response factors are substrates which underpin most of these physiological functions (Gibbs *et al*., 2015). Following extensive high-throughput analysis of *prt1-1* and Col-0, with inclusion of a complementing line where possible, no significant role of PRT1-mediated degradation could be established in relation to biotic stress perception and *prt1-1* plants are morphologically indistinct from Col-0. There is indication of a root phenotype during early development in which *prt1-1* roots appear to grow faster in conditions with shorter photoperiods, and in response to nitrogen stress. In contrast, *prt6* mutants display an oil body retention phenotype, which delays root establishment in the absence of sucrose. The proven stabilisation of pathogenesis related proteins (such as EDS1, CRT3 PR-2) in the *prt1-1* is unlikely to occur during this early period of growth as the primary focus of the plant is growth and established. It may however be expected to place a growth penalty on older *prt1-1* plants, however these mutants are morphologically indistinguishable from the wild type. More rigorous testing is required to further establish this potential PRT1 root phenotype.

Recently, the RING E3 ligase BIG BROTHER (BB) was proposed to be the first physiological substrate identified for PRT1 (Dong *et al*., 2017). Big brother in concert with another RING E3 ligase called DA2 activate, via multiple ubiquitylations, a peptidase called DA1. Activated DA1 cleaves the UBP15, TEOSINTE BRANCED 1/CYCLOIDEA/PCF 15 (TCP15) and TCP22. By this action, DA1 represses cell proliferation and promotes the transition endoreduplication and differentiation in Arabidopsis leaves. (Li *et al.,* 2008; Du *et al.,* 2014; Peng *et al.,* 2015). In a feedback mechanism, DA1 also destabilises BB and DA2. Following cleavage of BB by ubiquitylated DA1, N-terminal tyrosine is revealed at residue 61 making it a substrate from PRT1-mediated degradation through the plant N-end rule pathway. This prevents BB ubiquitinating DA1 and drives the transition of leaves from cell proliferation to endoreduplication through downstream cleavage events. (Dong *et al.,*

2017). This publication showed that overexpression of *BB (35S::BB)* leads to a strong reduction in growth which could be rescued by over-expressing *DA1* in this background *(35S::BB/35S::DA1).*

DA1-cleaved BB should be stabilised in *prt1-1* mutant plants. There are no significant implications for plant growth or aberrant leaf development in the *prt1-1* background. Therefore DA1-cleaved BB should be unable to further ubiquitylate DA1. Therefore, it prompts the question what is the fate of the stabilised DA1-cleaved BB in the *prt1-1* background? There is cross-talk between the ubiquitin-proteasome system and autophagy pathways in plants (Bozhkov, 2018). Autophagy is involved in the response to many biotic or abiotic stresses, such as oxidative stress, nutrient deficiency and pathogenesis (Yang *et al.,* 2015). Macro-autophagy is a mechanism of degrading damaged cellular components or cytoplasmic contents through autophagosome formation. These engulf the offending component and directs it to the vacuole for degradation (Liu & Bassham, 2012). Given mis-folded proteins can trigger autophagy, it seems plausible that stabilised cleaved-BB could be degraded in this fashion without placing a physiological burden on the plant. This may provide a mechanism which links the plant N-end rule and autophagy-lysosome pathways, but there is currently no evidence to connect them in this way.

To conclude, the data presented in this thesis reinforces the role for both PRT1 and PRT6 of the N-end rule pathway in plant immunity. A consistent and reproducible phenotype for *prt1-1* in response to *Pst* DC3000 has been observed. Upon further dissection, genes and proteins related to pathogen immunity were increased in expression and abundance prior to challenge by *Pst* DC3000 implying these plants are “primed” for infection. Therefore, this thesis presents strong evidence that PRT1 is a mechanism of basal immune response regulation prior to biotic stress perception. Following challenge by a pathogen, PRT1 regulation is attenuated and defence responses are elicited. Furthermore, this work independently validates data presented in Vicente *et al* (2018) for the other plant N-recognin PRT6, which appears

to play a similar role in regulation of plant immunity. The findings presented in this thesis open a new line of enquiry regarding the role of PRT1 in plant responses to biotic stresses, and many questions remain especially regarding substrates of the PRT1 E3 ligase.

References

- Abbas, M., Berckhan, S., Rooney, D. J., Gibbs, D. J., Vicente Conde, J., Sousa Correia, C., Bassel, G.W., Marín-de la Rosa, N., León, J., Alabadí, D., Blázquez, M.A. and Holdsworth, M. J. (2015). Oxygen Sensing Coordinates Photomorphogenesis to Facilitate Seedling Survival. *Current Biology*, ***25***(11), 1483–1488.
- Abu Qamar, S., Moustafa, K. and Tran, L-S. (2017). Mechanisms and strategies of plant defense against Botrytis cinerea. *Critical Reviews in Biotechnology* **37**: 262-274.
- Adams-Phillips, L., Wan, J., Tan, X., Dunning, F.M., Meyers, B.C., Michelmore, R.W. and Bent, A.F. (2008) Discovery of ADP-ribosylation and other plant defense pathway elements through expression profiling of four different Arabidopsis-Pseudomonas R-avr interactions. *Molecular Plant Microbe Interactions* **21**(5):646-657.
- Aksnes H., Van Damme P., Goris M., Starheim K.K., Marie M., Stove S.I., Hoel C., Kalvik T.V., Hole K., Glomnes N., Furnes, C., Ljostveit, S., Zielger, M., Niere, M., Gevaert, K. and Arnesen, T. (2015) An organellar nalpha-acetyltransferase, naa60, acetylates cytosolic N termini of transmembrane proteins and maintains Golgi integrity. *Cell Reports* **10**(8)1362–1374.
- Alonso-Blanco, C., Blankestijn-de Vries, H., Hanhart, C.J. and Koornneef, M. (1999) Natural allelic variation at seed size loci in relation to other life history traits of Arabidopsis thaliana. *PNAS USA* **96**(8):4710-4717.
- Andème Ondzighi, C., Christopher, D. A., Cho, E. J., Chang, S.-C., & Staehelin, L. A. (2008). Arabidopsis Protein Disulfide Isomerase-5 Inhibits Cysteine Proteases during Trafficking to Vacuoles before Programmed Cell Death of the Endothelium in Developing Seeds. *The Plant Cell* **20**(8): 2205–2220.
- Andrés, F. & Coupland, G. (2012) The genetic basis of flowering responses to seasonal cues. *Nature Reviews* 13: 627 – 639.
- Antolín-Llovera, M, Petutsching, E.K., Ried, M.K., Lipka, V., Nürnberger, T., Robatzek, S. and Parniske M. (2014) Knowing your friends and foes--plant receptor-like kinases as initiators of symbiosis or defence. *New Phytologist* **204**(4):791-802.
- Apel, K. and Hirt, H. (2004) Reactive oxygen species: metabolism, oxidative stress, and signal transduction. *Annual Reviews of Plant Biology* **55**: 373-399.
- Armijo, G., Salinas, P., Monteoliva, M.I., Seguel, A., García, C., Villarroel-Candia, E., Song, W., van der Krol, A.R., Álvarez, M.E. and Holuigue, L. (2013) A salicylic acid-induced lectin-like protein plays a positive role in the effector-triggered immunity response of *Arabidopsis thaliana* to *Pseudomonas syringae Avr-Rpm1*. *Molecular Plant Microbe Interactions* **26**(12):1395-1406.
- Arnaud, D. and Hwang, I. (2015) A sophisticated network of signaling pathways regulates stomatal defenses to bacterial pathogens. *Molecular Plant* **8**(4):566-581.
- Arnaud, D., Lee, S., Takebayashi, Y., Choi, D., Choi, J., Hitoshi Sakakibara, H. and Hwang, I. (2017) Cytokinin-Mediated Regulation

of Reactive Oxygen Species Homeostasis Modulates Stomatal Immunity in Arabidopsis. *Plant Cell* **29**(3): 543–559.
- Asano, T., Kimura, M., and Nishiuchi, T. (2012) The defense response in *Arabidopsis thaliana* against *Fusarium sporotrichioides*. *Proteome Science* **10**: 61.
- Bachmair, A. and Varshavsky, A. (1989) The degradation signal in a short-lived protein. *Cell* **56**(6):1019-1032.
- Bachmair, A., Finley, D. and Varshavsky, A. (1986) *In vivo* half-life of a protein is a function of its amino-terminal residue. *Science* **234**(4773):179-186.
- Baerenfaller, K., Massonnet, C., Hennig, L., Russenberger, D., Sulpice, R., Walsh, S., Stitt, M., Granier, C. and Gruissem, W. (2015) A long photoperiod relaxes energy management in Arabidopsis leaf six. *Current Plant Biology* **2**: 34–45
- Ballar P., Ors, A.U., Yang, H. and Fang, S. (2010) Differential regulation of CFTRDeltaF508 degradation by ubiquitin ligases GP78 and HRD1. *The International Journal of Biochemistry and Cell Biology* **42**: 167–173.
- Balzi, E., Choder, M., Chen, W.N., Varshavsky, A. and Goffeau, A. (1990) Cloning and functional analysis of the arginyl-tRNA-protein transferase gene ATE1 of *Saccharomyces cerevisiae. Journal of Biological Chemistry* **265**(13):7464-7471.
- Bartel, B., Wünning, I., & Varshavsky, A. (1990). The recognition component of the N-end rule pathway. *The EMBO Journal* **9**(10), 3179–3189.
- Bartsch, M., Gobbato, E., Bednarek, P., Debey, S., Schultze, J.L., Bautor, J. and Parker, J.E. (2006) Salicylic acid-independent ENHANCED DISEASE SUSCEPTIBILITY1 signaling in Arabidopsis immunity and cell death is regulated by the monooxygenase FMO1 and the Nudix hydrolase NUDT7. *Plant Cell* **18**(4):1038-1051.
- Bassel, G. W., Fung, P., Chow, T. F., Foong, J. A., Provart, N. J., & Cutler, S. R. (2008). Elucidating the Germination Transcriptional Program Using Small Molecules. *Plant Physiology* **147**(1): 143–155.
- Beattie, G.A. and Lindow, S.E. (1999) Bacterial colonization of leaves: a spectrum of strategies. *Phytopathology* **89**(5):353-359.
- Ben-Saadon, R., Zaaroor, D., Ziv, T. and Ciechanover, A. (2006) The polycomb protein RING1B generates self-atypical mixed ubiquitin chains required for its *in vitro* histone H2A ligase activity. *Molecular Cell* **24:** 701 – 711.
- Bender, C.L., Alarcon-Chaidez, F. and Gross, D.C. (1999). Pseudomonas syringae phytotoxins: mode of action, regulation and biosynthesis by peptide and polyketide synthetases. *Microbiology and Molecular Biology Reviews* **63**: 266–292.
- Bentsink, L. and Koornneef, M. (2008) Seed Dormancy and Germination. *Arabidopsis Book* **6:** e0119
- Berens, M.L., Berry, H.M., Mine, A., Argueso, C.T. and Tsuda, K. (2017) Evolution of Hormone Signaling Networks in Plant Defense. *Annual Review of Phytopathology* 2017 **55** (1): 401-425.

- Berens, M.L., Berry, H.M., Mine, A., Argueso, C.T. and Tsuda, K. (2017) Evolution of Hormone Signaling Networks in Plant Defense. *Annual Reviews in Phytopathology* **55**:401-425.
- Bhardwaj, V., Meier, S., Petersen, L. N., Ingle, R. A., & Roden, L. C. (2011). Defence Responses of Arabidopsis thaliana to Infection by Pseudomonas syringae Are Regulated by the Circadian Clock. *PLoS ONE* **6**(10), e26968.
- Biniek, C., Heyno, E., Kruk, J., Sparla, F., Trost, P. and Krieger-Liszkay, A. (2017) Role of the NAD(P)H quinone oxidoreductase NQR and the cytochrome b AIR12 in controlling superoxide generation at the plasma membrane. *Planta* **245**(4): 807-817.
- Boller, T. and Felix, G. (2009) A renaissance of elicitors: perception of microbe-associated molecular patterns and danger signals by pattern-recognition receptors. *Annual Reviews in Plant Biology* **60**:379-406.
- Bonvini, P., Zorzi, E., Basso, G. & Rosolen, A. (2007). Bortezomib-mediated 26S proteasome inhibition causes cell-cycle arrest and induces apoptosis in CD-30+ anaplastic large cell lymphoma. *Leukemia* **21**(4): 838– 842.
- Bozhkov, P. (2018) Plant autophagy: mechanisms and functions. *Journal of Experimental Botany* **69**(6): 1281–1285.
- Brady, S.M., Zhang, L., Megraw, M., Martinez, N.J., Jiang, E., Yi, S.C., Liu, W., Zeng, A., Taylor-Teeples, M., Kim, D., Ahnert, S., Ohler, U., Ware, D., Walhout, A.J.M. and N Benfey, P.N. (2007) A stele-enriched gene regulatory network in the Arabidopsis root. *Molecular Systems Biology* **7:**459.
- Breitenbach, H.H., Wenig, M., Wittek, F., Jordá, L., Maldonado-Alconada, A.M., Sarioglu, H., Colby, T., Knappe, C., Bichlmeier, M., Pabst, E., Mackey, D., Parker, J.E. and Vlot, A.C. (2014) Contrasting Roles of the Apoplastic Aspartyl Protease APOPLASTIC, ENHANCED DISEASE SUSCEPTIBILITY1-DEPENDENT1 and LEGUME LECTIN-LIKE PROTEIN1 in Arabidopsis Systemic Acquired Resistance. *Plant Physiology* **165**(2):791-809.
- Broad, W., Ling, P. & Jarvis, P. (2016) Chapter one – new insights into roles of ubiquitin modification in regulating plastids and other endomsymbiotic organelles. *International Review of Cell and Molecular Biology* **325:** 1 -33.
- Broadley, M.R., White, P.J., Hammond, J.P., Zelko, I. and Lux, A. (2007) Zinc in plants. *New Phytologist* **173:** 677 – 702.
- Bronstein, P. A., Marrichi, M., Cartinhour, S., Schneider, D. J., & DeLisa, M. P. (2005). Identification of a Twin-Arginine Translocation System in *Pseudomonas syringae* pv. tomato DC3000 and Its Contribution to Pathogenicity and Fitness. *Journal of Bacteriology* **187**(24), 8450–8461.
- Bu, Q. Li, H., Zhao, Q., Jiang, H., Zhai, Q., Zhang, J., Wu, X., Sun, J., Xie, Q., Wang, D. and Li, C. (2009) The Arabidopsis RING Finger E3 Ligase RHA2a Is a Novel Positive Regulator of Abscisic Acid Signaling during Seed Germination and Early Seedling Development. *Plant Physiology* **150** (1) 463-481.

- Buell, C. R., Joardar, V., Lindeberg *et al* (2003). The complete genome sequence of the Arabidopsis and tomato pathogen Pseudomonas syringae pv. tomato DC3000. *Proceedings of the National Academy of Sciences of the United States of America* **100**(18): 10181–10186.
- Buetow, L. & Huang, D.T. (2016) Structural insights into the catalysis and regulation of E3 ubiquitin ligases. *Nature Reviews Molecular Cell Biology* **17**(10):626-42.
- Bunster, L., Fokkema, N.J. and Schippers, B. (1989) Effect of Surface-Active *Pseudomonas* spp. on Leaf Wettability. Applied and Environmental Microbiology **55**(6):1340-1345.
- Büttner, D., & He, S. Y. (2009). Type III Protein Secretion in Plant Pathogenic Bacteria. *Plant Physiology* **150**(4): 1656–1664.
- Byrd, C., Turner, G.C. and Varshavsky, A. (1998) The N-end rule pathway controls the import of peptides through degradation of a transcriptional repressor. *The EMBO Journal* **17**(1) 269–277.
- Cai, Y., Zhuang, X., Wang, J., Wang, H., Lam, S. K., Gao, C., Wang, X. and Jiang, L. (2012) Vacuolar Degradation of Two Integral Plasma Membrane Proteins, AtLRR84A and OsSCAMP1, Is Cargo Ubiquitination-Independent and Prevacuolar Compartment-Mediated in Plant Cells. *Traffic* **13**: 1023-1040.
- Cakmak, I. (2008) Enrichment of cereal grains with zinc: agronomic or genetic biofortification? *Plant and Soil* **302:** 1-17
- Callis, J., Carpenter, T., Sun, C.-W. and Vierstra, R.D. (1995) Structure and evolution of genes encoding polyubiquitin and ubiquitin- like proteins in Arabidopsis thaliana ecotype Columbia. *Genetics* **139** (2) 921-939.
- Cartwright, D.A., Brady, S.M., Orlando, D.A., Sturmfels, B. & Benfey, P.N. (2009) Reconstructing spatiotemporal gene expression data from partial observations. *Bioinformatics* **25**: 2581-2587.
- Casson, S., Spencer, M., Walker, K. and Lindsey, K. (2005) Laser capture microdissection for the analysis of gene expression during embryogenesis of Arabidopsis. *The Plant Journal* **42**: 111–123.
- Castro, P.H., Couto, D., Freitas, S., Verde, N., Macho, A.P., Huguet, S., Botella, M.A., Ruiz-Albert, J., Tavares, R.M., Bejarano, E.R and Azevedo, H. (2016) SUMO proteases ULP1c and ULP1d are required for development and osmotic stress responses in Arabidopsis thaliana. *Plant Molecular Biology* **92**(1-2):143-159.
- Cavalier-Smith, T. (1975) The origin of nuclei and of eukaryotic cells. *Nature* **256**: 463–468.
- Chacón-López, A., Ibarra-Laclette. E., Sánchez-Calderón, L., Gutiérrez-Alanis, D. and Herrera-Estrella, L. (2011) Global expression pattern comparison between low phosphorus insensitive 4 and WT Arabidopsis reveals an important role of reactive oxygen species and jasmonic acid in the root tip response to phosphate starvation. *Plant Signal Behaviour* **6**(3):382-392.
- Chen, H., Jones, A. D. and Howe, G. A. (2006), Constitutive activation of the jasmonate signaling pathway enhances the production of secondary metabolites in tomato. *FEBS Letters* **580.**

- Chen, L. & Hellmann, H. (2013) Plant E3 Ligases: Flexible Enzymes in a Sessile World*. Molecular Plant* **6** (5) 1388-1404
- Chen, S.-J., Wu, X., Wadas, B., Oh, J.-H., & Varshavsky, A. (2017). An N-end rule pathway that recognizes proline and destroys gluconeogenic enzymes. *Science (New York, N.Y.)*, **355**(6323), eaal3655.
- Chen, Z., Zheng, Z., Huang, J., Lai, Z., & Fan, B. (2009). Biosynthesis of salicylic acid in plants. *Plant Signaling & Behavior* **4**(6), 493–496.
- Cheng, Y.T., Li, Y., Huang, S., Huang, Y., Dong, X., Zhang, Y. and Li, X. (2011) Stability of plant immune-receptor resistance proteins is controlled by SKP1-CULLIN1-F-box (SCF)-mediated protein degradation. *PNAS* **108**(35):14694-14699.
- Chini, A., Fonseca, S., Fernández, G., Adie, B., Chico, J.M., Lorenzo, O., García-Casado, G., López-Vidriero, I., Lozano, F.M., Ponce, M.R., Micol, J.L. and Solano, R. (2007) The JAZ family of repressors is the missing link in jasmonate signalling. *Nature* **448** (7154):666-671.
- Chinnusamy, V., Zhu, J. and Zhu, J.K. (2007) Cold stress regulation of gene expression in plants. *Trends in Plant Science* **12**:444–451.
- Chinnusamy, V., Zhu, J. and Zhu, J.K. (2007) Cold stress regulation of gene expression in plants. *Trends in Plant Sciences.* **12**(10):444-451.
- Cho, S. K., Ryu, M. Y., Kim, J. H., Hong, J. S., Oh, T. R., Kim, W. T., & Yang, S. W. (2017). RING E3 ligases: key regulatory elements are involved in abiotic stress responses in plants. *BMB Reports* **50**(8): 393–400.
- Choi, J., Choi, D., Lee, S., Choong-Min Ryu, C-M. and Hwang, I. (2011) Cytokinins and plant immunity: old foes or new friends? *Trends in Plant Sciences* **16** (7): 388-394.
- Choi, W.S., Jeong, B.C., Joo, Y.J., Lee, M.R., Kim J., Eck, M.J. and Song, H.K. (2010) Structural basis for the recognition of N-end rule substrates by the UBR box of ubiquitin ligases. *Nature Structural Molecular Biology* **17**(10):1175-1181.
- Ciechanover, A. (2005). Proteolysis: from the lysosome to ubiquitin and the proteasome. *Nature Reviews: Molecular Cell Biology* **6**(1):79-87.
- Clague, M.J. and Urbé, S. (2010) Ubiquitin: same molecule, different degradation pathways. *Cell* **143**(5):682-685.
- Clough, S.J. and Bent, A.F. (1998) Floral dip: a simplified method for Agrobacterium-mediated transformation of *Arabidopsis thaliana. The Plant Journal* **16**(6):735-743.
- Cohen-Kaplan, V., Livneh, I., Avni, N., Fabre, B., Ziv, T., Kwon, Y.T. and Ciechanover, A. (2016) p62- and ubiquitin-dependent stress-induced autophagy of the mammalian 26S proteasome. *Proceedings of the National Academy of Sciences of the United States of America* **113**(47): E7490-E7499.
- Conti, L., Nelis, S., Zhang, C., Woodcock, A., Swarup, R., Galbiati, M., Tonelli, C., Napier, R., Hedden, P., Bennett, M. and Sadanandom, A. (2014) Small Ubiquitin-like Modifier protein SUMO enables plants

to control growth independently of the phytohormone gibberellin. *Developmental Cell* **28:** 102–110.
- Conti, L., Price, G., O'Donnell, E., Schwessinger, B., Dominy, P. and Sadanandom, A. (2008) Small ubiquitin-like modifier proteases OVERLY TOLERANT TO SALT1 and −2 regulate salt stress responses in *Arabidopsis*. *Plant Cell*, **20**: 2894–2908.
- Costa, A., Barbaro, M.R., Sicilia, F., Preger, V., Krieger-Liszkay, A., Sparla, F., De Lorenzo, G. and Trost, P. (2015) AIR12, a b-type cytochrome of the plasma membrane of Arabidopsis thaliana is a negative regulator of resistance against Botrytis cinerea. *Plant Science* **233:**32-43.
- Crick, F.H. (1958) On protein synthesis. *Symposia of the Society of Experimental* Biology **12**:138-13.
- Cui, H., Gobbato, E., Kracher, B., Qiu, J., Bautor, J. and Parker, J.E. (2017), A core function of EDS1 with PAD4 is to protect the salicylic acid defense sector in Arabidopsis immunity. *New Phytologist* **213**: 1802-1817.
- Cuppels, D. A. (1986). Generation and Characterization of Tn5 Insertion Mutations in *Pseudomonas syringae* pv. tomato. *Applied and Environmental Microbiology* **51**(2), 323–327.
- Czarnocka, W., Van Der Kelen, K., Willems, P, Szechyńska-Hebda, M., Shahnejat-Bushehri, S., Balazadeh, S., Rusaczonek, A., Mueller-Roeber, B., Van Breusegem, F. and Karpiński, S. (2017) The dual role of LESION SIMULATING DISEASE 1 as a condition-dependent scaffold protein and transcription regulator. *Plant Cell Environment* **40**(11):2644-2662.
- Damour, G., Simonneau, T., Cochard, H. & Urban, L. (2010) An overview of models of stomatal conductance at the leaf level. *Plant, Cell & Environment* **33** (9): 1419–1438.
- Daszkowska-Golec, A., & Szarejko, I. (2013). Open or Close the Gate – Stomata Action Under the Control of Phytohormones in Drought Stress Conditions. *Frontiers in Plant Science* **4**:138.
- Daudi, A., Cheng, Z., O'Brien, J.A., Mammarell, N., Khan, S., Ausubel, F.M. and Bolwella, G.P. (2012) The Apoplastic Oxidative Burst Peroxidase in Arabidopsis Is a Major Component of Pattern-Triggered Immunity. *Plant Cell* **24**(1): 275–287.
- de Bie, P. and Ciechanover, A. (2011) Ubiquitylation of E3 ligases: self-regulation of the ubiquitin system via a proteolytic and non-proteolytic mechanism. *Cell Death and Differentiation* **18**: 1393 – 1402.
- De Bruyne, L., Höfte, M. and De Vleesschauwer, D. (2014) Connecting Growth and Defense: The Emerging Roles of Brassinosteroids and Gibberellins in Plant Innate Immunity. *Molecular Plant* **7**(6): 943-959.
- de Marchi, R., Sorel, M., Mooney, B., Fudal, I., Goslin, K., Kwasniewska, K., Ryan, P.T., Pfalz, M., Kroymann, J., Pollmann, S., Feehan, A., Wellmer F., Rivas, S. and Graciet, E. (2016). The N-end rule pathway regulates pathogen responses in plants. *Scientific Reports* **6**: 26020.

- De Storme, N. and Geelen, D. (2014) The impact of environmental stress on male reproductive development in plants: biological processes and molecular mechanisms *Plant, Cell & Environment* **37**(1): 1–18.
- Dekkers, B. J., He, H., Hanson, J., Willems, L. A., Jamar, D. C., Cueff, G. , Rajjou, L. , Hilhorst, H. W. and Bentsink, L. (2016), The Arabidopsis *DELAY OF GERMINATION 1* gene affects *ABSCISIC ACID INSENSITIVE 5 (ABI5)* expression and genetically interacts with *ABI3* during Arabidopsis seed development. *Plant Journal* **85**: 451-465.
- Del Bem, L.E. (2011) The evolutionary history of calreticulin and calnexin genes in green plants. *Genetica*, **139**: 255–259.
- Després, C., Chubak, C., Rochon, A., Clark, R., Bethune, T., Desveaux, D. and Fobert, P.R. (2003) The *Arabidopsis* NPR1 disease resistance protein is a novel cofactor that confers redox regulation of DNA binding activity to the basic domain/leucine zipper transcription factor TGA1. *Plant Cell* **15**: 2181–2191.
- Dietz, K.J. (1997) Functional responses of the leaf apoplast under stress. *Progressive Botany* **58:** 221–254.
- Dinneny, J.R., Long, T.A., Wang, J.Y., Jung, J.W., Mace, D., Pointer, S., Barron, C., Brady, S.M., Schiefelbein, J. and Benfey, P.N. (2008) Cell identity mediates the response of Arabidopsis roots to abiotic stress. *Science* **320**: 942-945.
- Ditzel, M., Wilson, R., Tenev, T., Zachariou, A., Paul, A., Deas, E. and Meier, P. (2003) Degradation of DIAP1 by the N-end rule pathway is essential for regulating apoptosis. *Nature Cell Biology* **5**(5):467-473.
- Dixon, D.P., Sellars, J.D., Edwards, R. (2011) The Arabidopsis phi class glutathione transferase AtGSTF2: binding and regulation by biologically active heterocyclic ligands. *Biochemical Journal* **438**(1):63-70.
- Dodd, A. N., Belbin, F. E., Frank, A., & Webb, A. A. R. (2015). Interactions between circadian clocks and photosynthesis for the temporal and spatial coordination of metabolism. *Frontiers in Plant Science* **6**: 245.
- Dong, H., Dumenil, J., Lu, F.H., Na, L., Vanhaeren, H., Naumann, C., Klecker, M., Prior, R., Smith, C., McKenzie, N., Saalbach, G., Chen, L., Xia, T., Gonzalez, N., Seguela, M., Inze, D., Dissmeyer, N., Li, Y. and Bevan, M.W. (2017) Ubiquitylation activates a peptidase that promotes cleavage and destabilization of its activating E3 ligases and diverse growth regulatory proteins to limit cell proliferation in Arabidopsis. *Genes and Development* **31**(2):197-208.
- Dong, J., Piñeros, M.A., Li, X., Yang, H., Liu, Y., Murphy, A.S., Kochian, L.V. and Liu, D. (2017) An Arabidopsis ABC Transporter Mediates Phosphate Deficiency-Induced Remodeling of Root Architecture by Modulating Iron Homeostasis in Roots. *Molecular Plant* **10** (2) 244–259.
- Dörfel, M.J. and Lyon, G.J. (2015) The biological functions of Naa10 - From amino-terminal acetylation to human disease. *Gene* **567**(2):103-131.

- Dougan, D.A., Micevski, D., Truscott, K.N. (2012) The N-end rule pathway: From recognition by N-recognins, to destruction by AAA+ proteases. *Biochimica et Biophysica Acta* **1823** (1): 83-91.
- Dougan, D.A., Truscott, K.N. and Zeth, K. (2010) The bacterial N-end rule pathway: expect the unexpected **76**(3): 545 – 588.
- Dove, K.K. and Klevit, R.E. (2017) RING-Between-RING E3s ligases: Emerging themes amid the variation. *Journal of Molecular Biology* **429:** 3363 – 3375.
- Downes, B.P., Stupar, R.M., Gingerich, D.J. and Vierstra, R.D. (2003) The HECT ubiquitin-protein ligase (UPL) family in Arabidopsis: UPL3 has a specific role in trichome development. *The Plant Journal* **(6)**:729-742.
- Du, L., Li, N., Chen, L., Xu, Y., Li. Y., Zhang, Y., Li, C. and Li, Y. (2014). The ubiquitin receptor DA1 regulates seed and organ size by modulating the stability of the ubiquitin-specific protease UBP15/SOD2 in Arabidopsis. *Plant Cell* **26**: 665–67.
- Durrant, W.E. and Dong, X. (2004) Systemic acquired resistance. *Annual Reviews in Phytopathology* **42**:185-209.
- El Oirdi, M. and Bouarab, K. (2007) Plant signalling components EDS1 and SGT1 enhance disease caused by the necrotrophic pathogen Botrytis cinerea. *New Phytologist* **175**(1):131-139.
- Elmayan, T. & Vaucheret, H. 1996 Expression of single copies of a strongly expressed 35S transgene can be silenced post-transcriptionally. *The Plant Journal.* **9**: 787- 797.
- Elmayan, T., Balzergue, S., Béon, F., Bourdon, V., Daubremet, J., Guénet, Y., Mourrain, P., Palauqui, J.C., Vernhettes, S., Vialle, T., Wostrikoff, K. and Vaucheret, H. (1998) Arabidopsis mutants impaired in cosuppression. *Plant Cell* **10**(10):1747-1758.
- Erbse, A., Schmidt, R., Bornemann, T., Schneider-Mergener, J., Mogk, A., Zahn, R., Dougan, D.A. and Bukau, B. (2006) ClpS is an essential component of the N-end rule pathway in *Escherichia coli. Nature* **439**(7077):753-756.
- Falk, A., Feys, B.J., Frost, L.N., Jones, J.D., Daniels, M.J. and Parker, J.E. (1999) EDS1, an essential component of R gene-mediated disease resistance in Arabidopsis has homology to eukaryotic lipases. *PNAS USA* **96**(6):3292-3297.
- Fang S. and Weissman, A.M. (2004) A field guide to ubiquitylation. *Cell & Molecular Life Sciences* **61**(13):1546-1561.
- Fang S., Ferrone, M., Yang, C., Jensen, J.P., Tiwari, S. and Weissman, A.M. (2001) The tumor autocrine motility factor receptor, GP78, is a ubiquitin protein ligase implicated in degradation from the endoplasmic reticulum. *Proceedings of the National Academy of Sciences of the United States of America* **98**: 14422–14427.
- Ferrández-Ayela, A., Micol-Ponce, R., Sánchez-García, A.B., Alonso-Peral, M.M., Micol, J.L. and Ponce, M.R. (2013) Mutation of an Arabidopsis NatB N-alpha-terminal acetylation complex component causes pleiotropic developmental defects. *PLoS One* **8**(11): e80697.
- Feys, B. J., Moisan, L. J., Newman, M.-A., & Parker, J. E. (2001). Direct interaction between the Arabidopsis disease resistance

signaling proteins, EDS1 and PAD4. *The EMBO Journal* **20**(19): 5400–5411.
- Fleming, A. J., Manzara, T., Gruissem, W. and Kuhlemeier, C. (1996), Fluorescent imaging of GUS activity and RT-PCR analysis of gene expression in the shoot apical meristem. *The Plant Journal* **10**: 745-754.
- Flors, V., Ton, J., van Doorn, R., Jakab, G., García-Agustín, P., Mauch-Mani, B. (2008) Interplay between JA, SA and ABA signalling during basal and induced resistance against Pseudomonas syringae and Alternaria brassicicola. *Plant Jounrnal* **54** (1):81-92.
- Foyer, C.H. and Noctor, G. (2005) Redox homeostasis and antioxidant signaling: a metabolic interface between stress perception and physiological responses. *Plant Cell* **17**(7):1866-1875.
- Fukao, Y. (2012) Protein-protein interactions in plants. *Plant Cell Physiology* **53**(4):617-625.
- Galán J.E. and Collmer, A. (1999) Type III secretion machines: bacterial devices for protein delivery into host cells. *Science* **284**(5418):1322-1328.
- Gao, Q.-M., Zhu, S., Kachroo, P., & Kachroo, A. (2015). Signal regulators of systemic acquired resistance. *Frontiers in Plant Science* **6***:* 228.
- García, A.V., Blanvillain-Baufumé, S., Huibers, R.P., Wiermer, M., Li, G., Gobbato, E., Rietz, S. and Parker, J.E. (2010) Balanced nuclear and cytoplasmic activities of EDS1 are required for a complete plant innate immune response. *PLoS Pathology* **6**: e1000970.
- Garcion, C., Lohmann, A., Lamodière, E., Catinot, J., Buchala, A., Doermann, P., and Métraux, J-P. (2008) Characterization and Biological Function of the ISOCHORISMATE SYNTHASE2 Gene of Arabidopsis. *Plant Physiology* **147**(3): 1279–1287.
- Garzón M., Eifler K., Faust A., Scheel H., Hofmann K., Koncz C., Yephremov A. and Bachmair A. (2007) PRT6/At5g02310 encodes an Arabidopsis ubiquitin ligase of the N-end rule pathway with arginine specificity and is not the CER3 locus. *FEBS Letters* **581**:3189–3196.
- Garzón, M., Eifler, K., Faust, A., Scheel, H., Hofmann, K., Koncz, C., Yephremov, A. and Bachmair, A. (2007) PRT6/At5g02310 encodes an Arabidopsis ubiquitin ligase of the N-end rule pathway with arginine specificity and is not the CER3 locus. *FEBS Letters* **581**(17):3189-3196.
- Ge, X., Li, G.-J., Wang, S.-B., Zhu, H., Zhu, T., Wang, X., & Xia, Y. (2007). AtNUDT7, a Negative Regulator of Basal Immunity in Arabidopsis, Modulates Two Distinct Defense Response Pathways and Is Involved in Maintaining Redox Homeostasis. *Plant Physiology*: **145(**1), 204–215.
- Geng, X., Jin, L., Shimada, M., Kim, M. G., & Mackey, D. (2014). The phytotoxin coronatine is a multifunctional component of the virulence armament of Pseudomonas syringae. *Planta* **240**(6): 1149–1165.
- Ghandilyan, A., Kutman, U.B., Kutman, B.Y., Cakmak, I. and Aarts, M.G.M. (2012) Genetic analysis of the effect of zinc deficiency on Arabidopsis growth and mineral concentrations. *Plant and Soil* **361:** 227 – 239.

- Giardina BJ, Chiang HL. Fructose-1,6-bisphosphatase, malate dehydrogenase, isocitrate lyase, phosphoenolpyruvate carboxykinase, glyceraldehyde-3-phosphate dehydrogenase, and cyclophilin A are secreted in Saccharomyces cerevisiae grown in low glucose. *Communicative & Integrative Biology* **6**: e27216.
- Giardina, B.J. and Chiang, H.L. (2013) The key gluconeogenic enzyme fructose-1,6-bisphosphatase is secreted during prolonged glucose starvation and is internalized following glucose re-feeding via the non-classical secretory and internalizing pathways in *Saccharomyces cerevisiae. Plant Signalling & Behaviour*. **8**(8). pii: e24936.
- Gibbs, D. J., Conde, J. V., Berckhan, S., Prasad, G., Mendiondo, G. M., & Holdsworth, M. J. (2015). Group VII Ethylene Response Factors Coordinate Oxygen and Nitric Oxide Signal Transduction and Stress Responses in Plants. *Plant Physiology* **169**(1): 23–31.
- Gibbs, D.J. (2015) Emerging Functions for N-Terminal Protein Acetylation in Plants. *Trends in Plant Science* **20** (10) 599-601.
- Gibbs, D.J., Lee, S.C., Isa, N.M., Gramuglia, S., Fukao, T., Bassel, G.W., Correia, C.S., Corbineau, F., Theodoulou, F.L., Bailey-Serres, J. and Holdsworth, M.J. (2011) Homeostatic response to hypoxia is regulated by the N-end rule pathway in plants. *Nature* **479** (7373):415-418.
- Gibbs, D.J., Md Isa, N., Movahedi, M., Lozano-Juste, J., Mendiondo, G.M., Berckhan, S., Marín-de la Rosa, N., Vicente Conde, J., Sousa Correia, C., Pearce, S.P., Bassel, G.W., Hamali, B., Talloji, P., Tomé, D.F., Coego, A., Beynon, J., Alabadí, D., Bachmair, A., León, J., Gray, J.E., Theodoulou, F.L., Holdsworth, M.J. (2014a). Nitric oxide sensing in plants is mediated by proteolytic control of group VII ERF transcription factors. *Molecular Cell* **53**: 369–379.
- Gibbs, D.J., Barcardit, J., Bachmair, A. and Holdsworth, M. (2014b) The eukaryotic N-end rule pathway: conserved mechanisms and diverse functions. *Trends in Cell Biology* **24**(10): 603-611.
- Gifford, M. L., Dean, A., Gutierrez, R. A., Coruzzi, G. M., & Birnbaum, K. D. (2008). Cell-specific nitrogen responses mediate developmental plasticity. *Proceedings of the National Academy of Sciences of the United States of America* **105**(2): 803–808.
- Giglione, C., Vallon, O., & Meinnel, T. (2003). Control of protein life-span by N-terminal methionine excision. *The EMBO Journal* **22**(1), 13–23.
- Gil, P., Dewey, E., Friml, J., Zhao, Y., Snowden, K.C., Putterill, J., Palme, K., Estelle, M. and Chory, J. (2001) BIG: a calossin-like protein required for polar auxin transport in Arabidopsis. *Genes and Development* **15**(15):1985-1997.
- Giuliano, S., Minghao, Z. and Chrisostomos, P. (2018) The Stoichiometric Interaction of the Hsp90-Sgt1-Rar1 Complex by CD and SRCD Spectroscopy. *Frontiers in Molecular Biosciences* 4 :95.
- Glawischnig,E. (2007) Camalexin. *Phytochemistry* **68**: 401–406.
- Glazebrook, J. (2005) Contrasting mechanisms of defense against biotrophic and necrotrophic pathogens. *Annual Reviews in Phytopathology* **43**:205-227.

- Glazebrook, J. (2005) Contrasting mechanisms of defense against biotrophic and necrotrophic pathogens. *Annual Reviews in Phytopathology* **43**:205-227.
- Glazebrook, J., Rogers, E.E. and Ausubel, F.M. (1996) Isolation of Arabidopsis mutants with enhanced disease susceptibility by direct screening. *Genetics* **143**(2):973-982.
- Golembeski, G. S., & Imaizumi, T. (2015). Photoperiodic Regulation of Florigen Function in *Arabidopsis thaliana*. *The Arabidopsis Book / American Society of Plant Biologists* **13:** e0178.
- Gonda, D.K., Bachmair, A., Wünning, I., Tobias, J.W., Lane, W.S. and Varshavsky, A. (1989) Universality and structure of the N-end rule. *Journal of Biological Chemistry* **264**:16700-16712.
- Goss, T. and Hanke, G. (2014) The end of the line: can ferredoxin and ferredoxin NADP(H) oxidoreductase determine the fate of photosynthetic electrons? *Current Protein and Peptide Science* **15**(4):385-393.
- Gou, M., and Hua, J. (2012). Complex regulation of an *R* gene *SNC1* revealed by autoimmune mutants. *Plant Signaling & Behavior* **7**(2): 213–216.
- Gou, M., Su, N., Zheng, J., Huai, J., Wu, G., Zhao, J., He, J., Tang, D., Yang, S. and Wang, G. (2009) An F-box gene, CPR30, functions as a negative regulator of the defense response in Arabidopsis. *The Plant Journal* **60**(5):757-770.
- Graciet, E. and Wellmer, F. (2010) The plant N-end rule pathway: structure and functions. *Trends in Plant Science* **15**(8):447-453.
- Graciet, E., Hu, R.G., Piatkov, K., Rhee, J.H., Schwarz, E.M. and Varshavsky, A. (2006) Aminoacyl-transferases and the N-end rule pathway of prokaryotic/eukaryotic specificity in a human pathogen. *PNAS USA* **103**(9):3078-3083.
- Graciet, E., Walter, F., Ó'Maoiléidigh, D.S., Pollmann, S., Meyerowitz, E.M., Varshavsky, A. and Wellmer, F. (2009) The N-end rule pathway controls multiple functions during Arabidopsis shoot and leaf development. *PNAS USA* **106**(32):13618-13623.
- Graf, A. and Smith, A.M. (2011) Starch and the clock: the dark side of plant productivity. *Trends in Plant Sciences* **16**(3):169-175.
- Grant, M. and Lamb, C. (2006) Systemic immunity. *Current Opinion in Plant Biology* **9**(4):414-420.
- Gravot, A., Richard, G., Lime, T., Lemarié, S., Jubault, M., Lariagon, C., Lemoine, J., Vicente, J., Robert-Seilaniantz, A., Michael J. Holdsworth, M. J. and Manzanares-Dauleux, M. J. (2016). Hypoxia response in *Arabidopsis* roots infected by *Plasmodiophora brassicae* supports the development of clubroot. *BMC Plant Biology* **16**: 251.
- Grefen, C., Donald, N., Hashimoto, K. , Kudla, J. , Schumacher, K. and Blatt, M. R. (2010), A ubiquitin-10 promoter-based vector set for fluorescent protein tagging facilitates temporal stability and native protein distribution in transient and stable expression studies. *The Plant Journal* **64**: 355-365.

- Griebel, T., Maekawa, T. and Parker, J.E. (2014) NOD-like receptor cooperativity in effector-triggered immunity. *Trends in Immunology* **35**(11):562-570.
- Grigoryev, S., Stewart, A.E., Kwon, Y.T., Arfin, S.M., Bradshaw, R.A., Jenkins, N.A., Copeland, N.G. and Varshavsky, A. (1996) A mouse amidase specific for N-terminal asparagine. The gene, the enzyme, and their function in the N-end rule pathway. *Journal of Biological Chemistry* **271**(45):28521-28532.
- Groll, M., Ditzel, L., Löwe, J., Stock, D., Bochtler, M., Bartunik, H.D., Huber, R. (1997) Structure of 20S proteasome from yeast at 2.4 A resolution. *Nature* **386**(6624):463-471.
- Grumati, P. and Dikic, I. (2018) Ubiquitin Signaling and autophagy. *Journal of Biological Chemistry* **293**(15):5404-5413.
- Gudesblat, G.E., Torres, P.S. and Vojnov, A.A. (2008) *Xanthomonas campestris* overcomes Arabidopsis stomatal innate immunity through a DSF cell-to-cell signal-regulated virulence factor. *Plant Physiology* **149**(2):1017-1027.
- Guo, H. and Recker, J. (2004) The ethylene signaling pathway: new insights. *Current Opinion in Plant Biology* **7**(1): 40-49.
- Hammerschmidt, R. (1999). Phytoalexins: What have we learned after 60 years? *Annual Reviews of Phytopathology* **37**: 285–306.
- Hanna, J. and Finley, D. (2007) A proteasome for all occasions. *FEBS Letters* **581**(15):2854-2861.
- Haworth, M., Elliott-Kingston, C. and McElwain, J.C. (2011) Stomatal control as a driver of plant evolution. *Journal of Experimental Botany* **62**(8):2419-2423.
- Hayama, R. and Coupland, G. (2003) Shedding light on the circadian clock and the photoperiodic control of Flowering. *Current Opinion in Plant Biology* **6:** 13-19.
- He, X., Fang, J., Li, J., Qu, B., Ren, Y., Ma, W., Zhao, X., Li, B., Wang, D., Li, Z. and Tong, Y. (2014) A genotypic difference in primary root length is associated with the inhibitory role of transforming growth factor-beta receptor-interacting protein-1 on root meristem size in wheat. *The Plant Journal* **77:** 931 – 943.
- He, Y., Fukushige, H., Hildebrand, D. F., & Gan, S. (2002). Evidence Supporting a Role of Jasmonic Acid in Arabidopsis Leaf Senescence. *Plant Physiology* **128**(3): 876–884
- Hermann-Bachnsky, Y., Ryoo, H.D., Ciechanover, A. and Gonen, H. (2007) Regulation of the Drosophila ubiquitin ligase DIAP1 is mediated by several distinct ubiquitin system pathways. *Cell Death Differentiation* **14:** 861-871.
- Hillwig, M. S., Chiozza, M., Casteel, C. L., Lau, S. T., Hohenstein, J., Hernández, E. , Jander, G. and MacIntosh, G. C. (2016), ABA deficiency and increased resistance to aphids. *Molecular Plant Pathology* **17**: 225-235.
- Hirano, S.S. and Upper, C.D. (2000) Bacteria in the leaf ecosystem with emphasis on *Pseudomonas syringae*-a pathogen, ice nucleus, and epiphyte. *Microbiology and Molecular Biology Reviews* **64**(3):624-653.

- Holdsworth, M.J., Bentsink, L. and Soppe, W.J. (2008b) Molecular networks regulating Arabidopsis seed maturation, after-ripening, dormancy and germination. *New Phytology* **179**(1):33-54
- Holdsworth, M.J., Finch-Savage, W.E., Grappin, P. and Job D. (2008b) Post-genomics dissection of seed dormancy and germination. *Trends in Plant Science.* **13**(1):7-13.
- Holman, T.J., Jones, P.D., Rusell, L., Medhurst, A., Úbeda Tomás, S, Talloji, P., Marquez, J., Schmuths, H., Tung, S-A., Taylor, I., Footitt, S., Bachmair, A, Theodoulou, F.L. and Holdsworth, M.J. (2009) The N-end rule pathway promotes seed germination and establishment through removal of ABA sensitivity in *Arabidopsis*. *PNAS* **106** (11): 4549-4554.
- Hongyan, Z., Xiaoying, P., Yuxia, D., Huamao, W., Pei, L. and Xuexian, L. *(2016) AtOPR3* specifically inhibits primary root growth in Arabidopsis under phosphate deficiency. *Scientific Reports* **6:** 24778.
- Honys, D. and Twell, D. (2004) Transcriptome analysis of haploid male gametophyte development in Arabidopsis. *Genome Biology* **5:** R85.
- Hooper, C.M., Castleden, I.R., Tanz, S.K., Aryamanesh, N. and Millar, A.H. (2017). SUBA4: the interactive data analysis centre for Arabidopsis subcellular protein locations. *Nucleic Acids Research* **45**(D1): D1064-D1074.
- Hooper, C.M., Tanz,S.K., Castleden, I.R., Vacher, M.A., Small, I.D. and Millar, A.H. (2014) SUBAcon: a consensus algorithm for unifying the subcellular localization data of the Arabidopsis proteome. *Bioinformatics* **30**(23): 3356 - 3364.
- Horan, K., Jang, C., Bailey-Serres, J., Mittler, R., Shelton, C., Harper, J.F., Zhu, J.K., Cushman, J.C., Gollery, M. and Girke, T. (2008) Annotating genes of known and unknown function by large-scale coexpression analysis. *Plant Physiology* **147**(1): 41-57.
- Hotton, S.K. and Callis, J. (2008) Regulation of cullin RING ligases. *Annual Reviews of Plant Biology* **59**: 467-489.
- Hu, R-G., Wang, H., Xia, Z. and Varshavsky, A. (2008) The N-end rule pathway is a sensor of heme. *Proceedings of the National Academy of Sciences* **105** (1) 76-81.
- Hu, R.G., Sheng, J., Qi, X., Xu, Z., Takahashi, T.T. and Varshavsky, A. (2005) The N-end rule pathway as a nitric oxide sensor controlling the levels of multiple regulators. *Nature* **437**: 981–986.
- Hua, Z. and Vierstra, R.D. (2011) The cullin–RING ubiquitin–protein ligases. *Annual. Reviews of Plant Biology* 62: 299-334.
- Huang, H., Liu, B., Liu, L. and Song, S., (2017) Jasmonate action in plant growth and development. *Journal of Experimental Botany* **68** (6) 1349–1359.
- Huibregtse, J.M., Scheffner, M., Beaudenon, S. and Howley, P.M. (1995) A family of proteins structurally and functionally related to the E6-AP ubiquitin-protein ligase. *Proceedings of the National Academy of Sciences of the United States of America* **92**(7):2563-7.
- Hull, A. K., Vij, R., & Celenza, J. L. (2000). Arabidopsis cytochrome P450s that catalyze the first step of tryptophan-dependent indole-3-acetic acid biosynthesis. *PNAS USA* **97**(5): 2379–2384.

- Hwang, C.S., Shemorry, A., Auerbach, D. and Varshavsky, A. (2010) The N-end rule pathway is mediated by a complex of the RING-type Ubr1 and HECT-type Ufd4 ubiquitin ligases. *Nature Cell Biology* **12**(12):1177-1185.
- Iba, K. (2002) Acclimative response to temperature stress in higher plants: approaches of gene engineering for temperature tolerance. *Annual Review of Plant Biology* **53**: 225–245.
- Iconomou, M. and Saunders, D.N. (2016) Systematic approaches to identify E3 ligase substrates. *Biochemistry Journal* **473**(22): 4083–4101.
- Ishida, T., Yoshimura, M., Miura, K. and Sugimoto, K. (2012) MMS21/HPY2 and SIZ1, two Arabidopsis SUMO E3 ligases, have distinct functions in development. *PLoS One* **7:** e46897.
- Ishiguro, S., Watanabe, Y., Ito, N., Nonaka, H., Takeda, N., Sakai, Kanaya, H. and Okada, K. (2002). SHEPHERD is the Arabidopsis GRP94 responsible for the formation of functional CLAVATA proteins. *The EMBO Journal* **21**(5): 898–908.
- Isono, E. and Nagel, M.K. (2014) Deubiquitylating enzymes and their emerging role in plant biology. *Frontiers in Plant Science* **5**: 56.
- Jackson, R. B. and Caldwell, M. M. (1993), The Scale of Nutrient Heterogeneity Around Individual Plants and Its Quantification with Geostatistics. *Ecology* **74**: 612-614.
- Jacobson, A.D., Zhang, N.Y., Xu, P., Han, K.J., Noone, S., Peng, J. and Liu, C.W. (2009) The lysine 48 and lysine 63 ubiquitin conjugates are processed differently by the 26s proteasome. *Journal of Biological Chemistry* **284:** 35485–35494.
- Jambunathan, N. and Mahalingam, R. (2006) Analysis of Arabidopsis growth factor gene 1 (GFG1) encoding a nudix hydrolase during oxidative signaling. *Planta* **224**: 1–11.
- Jentsch, S. and Psakhye, I. (2013) Control of nuclear activities by substrate-selective and protein-group SUMOylation. *Annual Reviews in Genetics* **47**: 167–186.
- Jin, H., Hong, Zhi, Su, W., Li, J. (2009) A plant-specific calreticulin is a key retention factor for a defective brassinosteroid receptor in the endoplasmic reticulum. *Proceedings of the National Academy of Sciences* **106** (32): 13612-13617.
- Johnson, E.S. (2004) Protein modification by SUMO. *Annual Reviews in Biochemistry* **73:** 355–382.
- Jones, J.D. and Dangl, J.L. (2006) The plant immune system. *Nature* **444**(7117):323-329.
- Kadota, Y. and Shirasu, K. (2012) The HSP90 complex of plants. *Biochim Biophys Acta* **1823**(3):689-697.
- Kalvik, T.V. and Arnesen, T. (2013) Protein N-terminal acetyltransferases in cancer. *Oncogene* **32**(3):269-276.
- Kanyuka, K., Praekelt, U., Franklin, K.A., Billingham, O.E., Hooley, R., Whitelam, G.C. and Halliday, K.J. (2003) Mutations in the huge Arabidopsis gene BIG affect a range of hormone and light responses. *Plant Journal* **35**(1):57-70.

- Kaplan, F., Kopka, J., Haskell, D.W., Zhao, W., Schiller, K.C., Gatzke, N., Sung, D.Y. and Guy, C.L. (2004) Exploring the temperature-stress metabolome of Arabidopsis. *Plant Physiology* **136**(4):4159-4168.
- Karapetyan, S., & Dong, X. (2018). Redox and the circadian clock in plant immunity: A balancing act. *Free Radical Biology & Medicine* **119**: 56–61.
- Karimi, M., Depicker, A. and Hilson, P. (2007) Recombinational Cloning with Plant Gateway Vectors. *Plant Physiology* **145** (4) 1144-1154.
- Kaur, G. and Subramanian, S. (2015) The UBR box and its relationship to binuclear RING-like treble clef zinc fingers. *Biology Direct* **10**:36.
- Kaur, G., and Subramanian, S. (2015) The UBR-box and its relationship to binuclear RING-like treble clef zinc fingers. *Biology Direct* **10**:36.
- Kelderon, D (1996) De-ubiquitinate to decide your fate. *Current Biology* **6**:662–665.
- Kemmerling, B., Schwedt, A., Rodriguez, P., Mazzotta, S., Frank, M., Qamar, S. A., et al. (2007). The BRI1-associated kinase 1, BAK1, has a brassinolide-independent role in plant cell-death control. *Current Biology* **17**: 1116–1122.
- Kiba, T. and Krapp, A. (2016) Plant Nitrogen Acquisition Under Low Availability: Regulation of Uptake and Root Architecture. *Plant Cell Physiology* **57**(4):707-714.
- Kim, D.S. and Hwang, B.K. (2014) An important role of the pepper phenylalanine ammonia-lyase gene (PAL1) in salicylic acid-dependent signalling of the defence response to microbial pathogens. *Journal of Experimental Botany* **65**(9):2295-2306.
- Kim, H.T., Kim, K.P., Lledias, F., Kisselev, A.F., Scaglione, K.M., Skowyra, D., Gygi, S.P. and Goldberg, A.L. (2007) Certain pairs of ubiquitin-conjugating enzymes (E2s) and ubiquitin-protein ligases (E3s) synthesize nondegradable forked ubiquitin chains containing all possible isopeptide linkages. *Journal of Biological Chemistry* **282**: 17375-17386.
- Kim, J.H., Nguyen, N.H., Nguyen, N.T., Hong, S.W. and Lee, H. (2013) Loss of all three calreticulins, CRT1, CRT2 and CRT3, causes enhanced sensitivity to water stress in Arabidopsis. *Plant Cell Reports* **32**(12):1843-1853.
- Kim, S.H., Gao, F., Bhattacharjee, S., Adiasor, J.A., Nam, J.C. 3 and Gassmann, W. (2010) The Arabidopsis Resistance-Like Gene SNC1 Is Activated by Mutations in SRFR1 and Contributes to Resistance to the Bacterial Effector AvrRps4. *PLoS Pathology* **6**(11): e1001172.
- Kim, T.H., Böhmer, M., Hu, H., Nishimura, N. and Schroeder, J.I. (2010) Guard cell signal transduction network: advances in understanding abscisic acid, CO2, and Ca2+ signaling. *Annual Reviews in Plant Biology* **61**:561-591.
- Kinmonth-Schultz, H.A., Golembeski, G.S. and Imaizumi, T. (2013) Circadian clock-regulated physiological outputs: dynamic responses in nature. *Seminars in Cell Developmental Biology* **24**(5):407-413.

- Kisselev, A.F. & Goldberg, A.L. (2001) Proteasome inhibitors: from research to drug candidate. *Chemistry & Biology* **8:** 739 – 758.
- Klepikova, A. V., Kasianov, A. S., Gerasimov, E. S., Logacheva, M. D. and Penin, A. A. (2016), A high resolution map of the Arabidopsis thaliana developmental transcriptome based on RNA-seq profiling. *The Plant Journal* **88**: 1058-1070.
- Koch, M., Vorwerk, S., Masur, C., Sharifi-Sirchi, G., Olivieri, N. and Schlaich, N.L. (2006) A role for a flavin-containing mono-oxygenase in resistance against microbial pathogens in Arabidopsis. *The Plant Journal* **47**(4):629-639.
- Komander, D. and Rape, M. (2012) The ubiquitin code. *Annual Reviews of Biochemistry* **81**: 203-229.
- Kørner, C.J., Klauser, D., Niehl, A., Domínguez-Ferreras, A., Chinchilla, D., Boller, T., Heinlein, M. and Hann, D.R. (2013) The immunity regulator BAK1 contributes to resistance against diverse RNA viruses. *Molecular Plant Microbe Interactions* **26**(11):1271-1280
- Kotak, S., Larkindale, J., Lee, U., von Koskull-Doring, P., Vierling, E. and Scharf, K.D. (2007) Complexity of the heat stress response in plants. *Current Opinion in Plant Biology* **10**: 310–316.
- Kurepa, J., Walker, J.M., Smalle, J., Gosink, M.M., Davis, S.J., Durham, T.L., Sung, D.Y. and Vierstra, R.D. (2003) The small ubiquitin-like modifier (SUMO) protein modification system in *Arabidopsis*. Accumulation of SUMO1 and −2 conjugates is increased by stress. *J. Biol. Chem.* **278**: 6862–6872.
- Kvitko, B.H., Park, D.H., Velásquez, A.C., Wei, C.F., Russell, A.B., Martin, G.B., Schneider, D.J. and Collmer, A. (2009) Deletions in the repertoire of *Pseudomonas syringae* pv. tomato DC3000 type III secretion effector genes reveal functional overlap among effectors. *PLoS Pathology* **5**(4):e1000388.
- Kwon, Y.T. and Ciechanover, A. (2017) The Ubiquitin Code in the Ubiquitin-Proteasome System and Autophagy. *Trends in Biochemical Sciences* **42**(11):873-886.
- Lamesch, P., Berardini, T.Z., Li, D., Swarbreck, D., Wilks, C., Sasidharan, R., Muller, R., Dreher, K., Alexander, D.L., Garcia-Hernandez, M., Karthikeyan, A.S., Lee, C.H., Nelson, W.D., Ploetz, L., Singh, S., Wensel, A. and Huala, E. (2012) The Arabidopsis Information Resource (TAIR): improved gene annotation and new tools. *Nucleic Acids Research* **40:** D1202–D1210.
- Lawson, S.S., Pijut, P.M. and Michler, C.H. (2014) Comparison of arabidopsis stomatal density mutants indicates variation in water stress responses and potential epistatic effects. Journal of Plant Biology **57**:162-173.
- Lee, J., Nam, J., Park, H.C., Na, G., Miura, K., Jin, J.B., Yoo, C.Y., Baek, D., Kim, D.H., Jeong, J.C., Kim, D., Lee, S.Y., Salt, D.E., Mengiste, T., Gong, Q., Ma, S., Bohnert, H.J., Kwak, S.S., Bressan, R.A., Hasegawa, P.M. and Yun, D.J. (2007) Salicylic acid-mediated innate immunity in *Arabidopsis* is regulated by SIZ1 SUMO E3 ligase. *Plant Journal.* **49:** 79–90.

- Lee, K.E., Heo, J.E., Kim, J.M. and Hwang, C.S. (2016) N-Terminal Acetylation-Targeted N-End Rule Proteolytic System: The Ac/N-End Rule Pathway. *Molecules and Cells* **39**(3):169-178.
- Lee, M.W., Jelenska, J. and Greenberg, J.T. (2008) Arabidopsis proteins important for modulating defense responses to Pseudomonas syringae that secrete HopW1-1. *The Plant Journal* **54**(3):452-465.
- Lee, S.C. and Luan, S. (2012) ABA signal transduction at the crossroad of biotic and abiotic stress responses. *Plant Cell Environment* **35**(1):53-60.
- Lemaître, T., Gaufichon, L., Boutet-Mercey, S., Christ, A., Masclaux-Daubresse, C. (2008) Enzymatic and metabolic diagnostic of nitrogen deficiency in Arabidopsis thaliana Wassileskija accession. *Plant Cell Physiology* **49**(7):1056-1065.
- Leubner-Metzger, G. (2005) Beta-1,3-Glucanase gene expression in low-hydrated seeds as a mechanism for dormancy release during tobacco after-ripening. *The Plant Journal* **41**(1):133-145.
- Levitt J (1972) Responses of plants to environmental stresses. Academic Press, New York.
- Li, H-M., Altschmied, L. and Chory, J. (1994) *Arabidopsis* mutants define downstream branches in the phototransduction pathway. *Genes & Development* **8**: 339-349
- Li, J., Zhao-Hui, C., Batoux, M., Nekrasov, V., Roux, M., Chinchilla, D., Zipfel, C. and Jones, J.D.G. (2009) Specific ER quality control components required for biogenesis of the plant innate immune receptor EFR. *PNAS* **106** (37) 15973-15978.
- Li, J.F., Park, E., von Arnim, A.G. and Nebenführ, A. (2009) The FAST technique: a simplified Agrobacterium-based transformation method for transient gene expression analysis in seedlings of Arabidopsis and other plant species. *Plant Methods* **5**:6.
- Li, X., Clarke, J. D., Zhang, Y., and Dong, X. (2001). Activation of an EDS1-mediated R-gene pathway in the snc1 mutant leads to constitutive, NPR1-independent pathogen resistance. *Molecular Plant Microbe Interactions* **14**:1131–1139.
- Li, Y., Zheng, L., Corke, F., Smith, C. and Bevan, M.W. (2008). Control of final seed and organ size by the DA1 gene family in Arabidopsis thaliana. *Genes and Development* **22**: 1331–1336.
- Licausi, F., Giorgi, F.M., Zenoni, S., Osti, F., Pezzotti, M. and Perata, P. (2010) Genomic and transcriptomic analysis of the AP2/ERF superfamily in Vitis vinifera. *BMC Genomics* **11**:719.
- Licausi, F., Kosmacz, M., Weits, D.A., Giuntoli, B., Giorgi, F.M., Voesenek, L.A.C.J., Perata, P. and van Dongen, J.T. (2011) Oxygen sensing in plants is mediated by an N-end rule pathway for protein destabilization. *Nature* **479**: 419 – 422.
- Licausi, F., Pucciariello, C. and Perata, P. (2013) New role for an old rule: N-end rule-mediated degradation of ethylene responsive factor proteins governs low oxygen response in plants. *Journal of Integrative Plant Biology* **55**(1):31-39.
- Lieberherr, D., Wagner, U., Dubuis, P.H., Métraux, J.P. and Mauch, F. (2003) The rapid induction of glutathione S-transferases *AtGSTF2*

and *AtGSTF6* by avirulent Pseudomonas syringae is the result of combined salicylic acid and ethylene signaling. *Plant Cell Physiology* **44**(7):750-757.
- Lievens, L., Pollier, J., Goossens, A., Beyaert, R., & Staal, J. (2017). Abscisic Acid as Pathogen Effector and Immune Regulator. Frontiers in *Plant Science* **8**: 587.
- Lilienbaum, A. (2013) Relationship between the proteasomal system and autophagy. *International Journal of Biochemistry and Molecular Biology.* 2013; **4**(1): 1–26.
- Lin, W.D., Liao, Y.Y., Yang, T.J.W., Pan, C.Y., Buckhout, T.J. and Schmidt, W. (2011) Coexpression-based Clustering of Arabidopsis Root Genes Predicts Functional Modules in Early Phosphate Deficiency Signaling. *Plant Physiology* **115:** 110 – 145.
- Lindeberg, M. Myers, C.R., Collmer, A., and Schneider, D.J. (2008) Roadmap to New Virulence Determinants in *Pseudomonas syringae*: Insights from Comparative Genomics and Genome Organization. *MPMI* **21**(6):685–700.
- Liu, J., Feng, L., Li. J. and He, Z. (2015) Genetic and epigenetic control of plant heat responses. *Frontiers in Plant Science* **6:** 267**.**
- Liu, L., Sonbol, F.M., Huot, B., Gu, Y., Withers, J., Mwimba, M., Yao, J., He, S.Y. and Dong, X. (2016) Salicylic acid receptors activate jasmonic acid signalling through a non-canonical pathway to promote effector-triggered immunity. *Nature Communications* **7**:13099.
- Liu, Z., Wang, W., Zhang, C-G., Zhao, J-F. & Chen, Y-L. (2007) GUS staining of guard cells to identify localised guard cell gene expression. *Bio-protocol* **7**(14): e2446.
- Lorenzo, O., Piqueras, R., Sánchez-Serrano, J.J. and Solano, R. (2003) ETHYLENE RESPONSE FACTOR1 integrates signals from ethylene and jasmonate pathways in plant defense. *Plant Cell* **15**(1):165-178.
- Lucyshyn, D. and Wigge, P.A. (2009) Plant development: PIF4 integrates diverse environmental signals. *Current Biology* **19**: R265–R266.
- Lue, S., Zhao, H., Des Marais, D.L., Parsons, E.P., Wen, X., Xu, X., Bangarusamy, D.K., Wang, G., Rowland, O., Juenger, T., Bressan, R.A. and Jenks, M.A. (2012) Arabidopsis ECERIFERUM9 involvement in cuticle formation and maintenance of plant water status. *Plant Physiology* **159**: 930–944.
- Lv, F., Zhou, J., Zeng, L. and Xing, D. (2015) β-cyclocitral upregulates salicylic acid signalling to enhance excess light acclimation in Arabidopsis. *Journal of Experiment Botany* **66**(15):4719-4732.
- Lyons, R., Stiller, J., Powell, J., Rusu, A., Manners, J.M. and Kazan, K., (2015) Fusarium oxysporum Triggers Tissue-Specific Transcriptional Reprogramming in Arabidopsis thaliana. *PLOS ONE* **10**(4): e0121902.
- Makandar, R., Nalam, V.J., Chowdhury, Z., Sarowar, S., Klossner G., Lee, H., Burdan, D., Trick, H.N., Gobbato, E., Parker, J.E. and Shah, J. (2015) The Combined Action of ENHANCED DISEASE SUSCEPTIBILITY1, PHYTOALEXIN DEFICIENT4, and SENESCENCE-ASSOCIATED101 Promotes Salicylic Acid-Mediated

Defenses to Limit Fusarium graminearum Infection in Arabidopsis thaliana. *Molecular Plant Microbe Interactions* **28**(8):943-953.
- Marín, I. (2013) Evolution of Plant HECT Ubiquitin Ligases. *PLOS ONE* **8**(7): e68536.
- Marks, M.D., P. Wenger, J.P., Gilding, E., Jilk, R., & A. Dixon, R.A. (2009) Transcriptome Analysis of Arabidopsis Wild-Type and gl3–sst sim Trichomes Identifies Four Additional Genes Required for Trichome Development. *Molecular Plant* **2** (4): 803–822.
- Marín, I. (2013) Evolution of Plant HECT Ubiquitin Ligases. *PLoS ONE* **8**(7): e68536.
- Matta-Camacho, E., Kozlov, G., Li, F.F. and Gehring, K. (2010) Structural basis of substrate recognition and specificity in the N-end rule pathway. *Nature Structural Molecular Biology* **17**(10):1182-1187.
- Melotto, M., Underwood, W., & He, S. Y. (2008). Role of Stomata in Plant Innate Immunity and Foliar Bacterial Diseases. *Annual Review of Phytopathology* **46**: 101–122.
- Melotto, M., Underwood, W., Koczan, J., Nomura, K. and He, S.Y. (2006) Plant stomata function in innate immunity against bacterial invasion. *Cell* **126**(5):969-980.
- Merrill, J.C., Melhuish, T.A., Kagey, M.H., Yang, S.H., Sharrocks, A.D. and Wotton, D. (2010) A role for non-covalent SUMO interaction motifs in Pc2/CBX4 E3 activity. *PLoS One* **5**: e8794.
- Metzger, M.B., Pruneda, J.N., Klevit, R.E. and Weissman, A.M. (2014) RING-type E3 ligases: Master manipulators of E2 ubiquitin-conjugating enzymes and ubiquitination. *Biochimica et Biophysica Acta* **1843** (1) 47-60.
- Mishiba, K., Nishihara, M., Nakatsuka, T., Abe, Y., Hirano, H. , Yokoi, T. , Kikuchi, A. and Yamamura, S. (2005), Consistent transcriptional silencing of 35S-driven transgenes in gentian. *The Plant Journal* **44**: 541-556.
- Mishina, T.E. and Zeier, J. (2006) The Arabidopsis Flavin-Dependent Monooxygenase FMO1 Is an Essential Component of Biologically Induced Systemic Acquired Resistance. *Plant Physiology* **141** (4) 1666-1675.
- Mittelhauser, C.J. and Van Stevenick, R.F.M. (1969) *Nature* **221:** 281-282.
- Mitter, B., Pfaffenbichler, N., Flavell, R., Compant, S., Antonielli, L., Petric, A., Berninger, T., Naveed, M., Sheibani-Tezerji, R., van Maltzahn, G. and Sessitsch, A. (2017). A New Approach to Modify Plant Microbiomes and Traits by Introducing Beneficial Bacteria at Flowering into Progeny Seeds. *Frontiers in Microbiology* **8**: 11.
- Mockler, T., Yang, H. Yu, X., Parikh, D., Cheng, Y., Dolan, S. and Lin, C. (2003) Regulation of photoperiodic flowering by Arabidopsis photoreceptors. *PNAS* **100**(4): 2140 – 2145.
- Moeder, W., and Yoshioka, K. (2008) Lesion mimic mutants. *Plant Signaling & Behavior* **3:** 764 – 767.
- Mogk, A., Schmidt, R. and Bukau, B. (2007) The N-end rule pathway for regulated proteolysis: prokaryotic and eukaryotic strategies. *Trends in Cell Biology* **17**(4):165-172.

- Moles, A.T., Ackerly, D.D., Webb, C.O., Tweddle, J.C., Dickie, J.B. & Westoby, M. (2005) A brief history of seed size. *Science* **307:** 576–580.
- Morreale, F.E. and Walden, H. (2016) Types of Ubiquitin Ligases. *Cell* **165**: e241.
- Mot, A.C., Prell, E., Klecker, M., Naumann, C., Faden, F., Westermann, B. and Dissmeyer, N. (2018) Real-time detection of N-end rule-mediated ubiquitination via fluorescently labeled substrate probes. *New Phytologist* **217**(2):613-624.
- Mou, Z., Fan, W. and Dong, X. (2003) Inducers of plant systemic acquired resistance regulate NPR1 function through redox changes. *Cell* **113**(7):935-944.
- Mousley, C.J., Tyeryar, K.R., Vincent-Pope, P. and Bankaitis, V.A. (2007) The Sec14-superfamily and the regulatory interface between phospholipid metabolism and membrane trafficking. *Biochimica et Biophysica Acta* **1771**(6):727-736.
- Mudgil, Y., Shiu, S-H., Stone, S.L., Salt, J.N. and Goring, D.R. (2004) A Large Complement of the Predicted Arabidopsis ARM Repeat Proteins Are Members of the U-Box E3 Ubiquitin Ligase Family. *Plant Physiology* **134**(1): 59-66.
- Murashige, T. and Skoog, F. (1962) A Revised Medium for Rapid Growth and Bio Assays with Tobacco Tissue Cultures. *Physiologia Plantarum* **15**: 473-497.
- Murtas, G., Reeves, P.H., Fu, Y.F., Bancroft, I., Dean, C. and Coupland, G. (2003) A nuclear protease required for flowering-time regulation in *Arabidopsis* reduces the abundance of SMALL UBIQUITIN-RELATED MODIFIER conjugates. *Plant Cell* **15**: 2308–2319.
- Nafisi, M., Goregaoker, S., Botanga, C.J., Glawischnig, E., Olsen, C.E., Halkier, B.A. and Glazebrook, J. (2006) Arabidopsis Cytochrome P450 Monooxygenase 71A13 Catalyzes the Conversion of Indole-3-Acetaldoxime in Camalexin Synthesis. *The Plant Cell* **19** (6): 2039-2052.
- Nagel, M., Kalinowska, K., Vogel, K., Reynolds, G.D., Wud, Z., Anzenberger, F., Ichikawa, M., Tsutsumi, C., Sato, M.H., Kuster, B., Bednarek, S.Y. and Isono, E. (2017) Arabidopsis SH3P2 is an ubiquitin-binding protein that functions together with ESCRT-I and the deubiquitylating enzyme AMSH3. *PNAS* **114** (34) E7197-E7204.
- Nakabayashi, K., Okamoto, M., Koshiba, T., Kamiya, Y. & Nambara, E. (2005) Genome-wide profiling of stored mRNA in Arabidopsis thaliana seed germination: epigenetic and genetic regulation of transcription in seed. *The Plant Journal* **41**: 697-709.
- Nakabayashi, K., Okamoto, M., Koshiba, T., Kamiya, Y. and Nambara, E. (2005), Genome-wide profiling of stored mRNA in Arabidopsis thaliana seed germination: epigenetic and genetic regulation of transcription in seed. *The Plant Journal* **41**: 697-709.
- Nakamichi, N., Takao, S., Kudo, T., Kiba, T., Wang, Y., Kinoshita, T. & Sakakibara, H. (2016) Improvement of Arabidopsis Biomass and Cold, Drought and Salinity Stress Tolerance by Modified Circadian

Clock-Associated PSEUDO-RESPONSE REGULATORs. *Plant and Cell Physiology* **57:** 1085–1097.
- Nakano, T., Suzuki, K., Fujimura, T. and Shinshi, H. (2006) Genome-Wide Analysis of the ERF Gene Family in Arabidopsis and Rice. *Plant Physiology* **140** (2) 411-432.
- Narita, K. (1958) Isolation of acetylpeptide from enzymic digests of TMV-protein. *Biochimica et Biophysica Acta* **28**:184–191.
- Narsai, R., Law, S.R., Carrie, C., Xu, L. & Whelan, J (2011) In-Depth Temporal Transcriptome Profiling Reveals a Crucial Developmental Switch with Roles for RNA Processing and Organelle Metabolism That Are Essential for Germination in Arabidopsis. *Plant Physiology* **157**(3): 1342-1362.
- Nedelsky, N., Todd, P.K. and Taylor, J.P. (2008) Autophagy and the ubiquitin-proteasome system: collaborators in neuroprotection. *Biochimica et Biophysica Acta* **(12)**: 691–699.
- Nicaise, V., Joe, A., Jeong, B.R., Korneli, C., Boutrot, F., Westedt, I., Staiger, D., Alfano, J.R. and Zipfel, C. (2013) Pseudomonas HopU1 modulates plant immune receptor levels by blocking the interaction of their mRNAs with GRP7. *EMBO Journal* **32**(5):701-712.
- Nordgren, M., Francisco, T., Lismont, C., Hennebel, L., Brees, C., Wang, B., Van Veldhoven, P.P., Azevedo, J.E. and Fransen, M. (2015) Export-deficient monoubiquitinated PEX5 triggers peroxisome removal in SV40 large T antigen-transformed mouse embryonic fibroblasts. *Autophagy.* **11**(8):1326-1340.
- Norris, S.R., Meyer, S.E. and Callis, J. (1993) The intron of Arabidopsis thaliana polyubiquitin genes is conserved in location and is a quantitative determinant of chimeric gene expression. *Plant Molecular Biology* **21**(5):895-906.
- O'Brien, J.A., Daudi, A., Butt, V.S. and Bolwell, G.P. (2012) Reactive oxygen species and their role in plant defence and cell wall metabolism. *Planta* **236** (3) 765–779.
- Ochsenbein, C., Przybyla, D., Danon, A., Landgraf, F., Göbel, C., Imboden, A., Feussner, I. and Apel, K. (2006) The role of EDS1 (enhanced disease susceptibility) during singlet oxygen-mediated stress responses of Arabidopsis. The Plant Journal **47**(3):445-456.
- Oide, S., Bejai, S., Staal, J., Guan, N., Kaliff, M. and Dixelius, C. (2013) A novel role of PR2 in abscisic acid (ABA) mediated, pathogen-induced callose deposition in Arabidopsis thaliana. *New Phytologist* **200**(4):1187-1199.
- Okamoto, K. Taya, Y. and Nakagama, H. (2009) Mdmx enhances p53 ubiquitination by altering the substrate preference of the Mdm2 ligase. *FEBS Letters* **583:** 2710 – 2714.
- Otto, M., Naumann, C., Brandt, W., Wasternack, C. and Hause, B. (2016) Activity Regulation by Heteromerization of Arabidopsis Allene Oxide Cyclase Family Members. *Plants* (*Basel*) **5**(1): 3.
- Pan, H., Stonoha-Arther, C., & Wang, D. (2018). Medicago Plants Control Nodulation by Regulating Proteolysis of the Receptor-Like Kinase DMI2. *Plant Physiology* **177**(2): 792–802.
- Panchal, S., Roy, D., Chitrakar, R., Price, L., Breitbach, Z.S., Armstrong, D.W. and Melotto, M. (2016) Coronatine Facilitates

Pseudomonas syringae Infection of Arabidopsis Leaves at Night. *Frontiers in Plant Science* **7**:880.
- Pandey, S., Wang, R., Wilson, L., Li, S., Zhao, Z., Gookin, T.E., Assmann, S.M. & Alberta, R. (2010) Boolean modeling of transcriptome data reveals novel modes of heterotrimeric G-protein action. Molecular Systems Biology **6:** 372.
- Parisy, V., Poinssot, B., Owsianowski, L., Buchala, A., Glazebrook, J., and Mauch, F. (2006) Identification of PAD2 as a c-glutamylcysteine synthetase highlights the importance of glutathione in disease resistance of Arabidopsis. *The Plant Journal* **49**:159–172
- Park, C-W & Ryu, K-Y. (2014). Cellular Ubiquitin Pool Dynamics and Homeostasis. *BMB reports* **47.**
- Park, H.J., Kim, W.Y., Park, H.C., Lee, S.Y., Bohnert, H.J. and Yun, D.J. (2011) SUMO and SUMOylation in plants. *Molecules and Cells* **32**: 305–316.
- Park, J.-M., Jo, S.-H., Kim, M.-Y., Kim, T.-H., & Ahn, Y.-H. (2015). Role of transcription factor acetylation in the regulation of metabolic homeostasis. *Protein & Cell* **6** (11): 804–813.
- Passardi, F., Tognolli, M., De Meyer, M., Penel, C. and Dunand, C. (2006) Two cell wall associated peroxidases from *Arabidopsis* influence root length. *Planta* **223:** 965 – 974.
- Penfield, S. (2017) Seed dormancy and germination. *Current Biology* **27:** 874 – 878.
- Peng, Y., Chen, L., Lu, Y., Wu, Y., Dumenil, J., Zhu, Z., Bevan, M.W. and Li, Y. (2015) The ubiquitin receptors DA1, DAR1, and DAR2 redundantly regulate endoreduplication by modulating the stability of TCP14/15 in *Arabidopsis*. *Plant Cell* **27**: 649–662.
- Perea-García, A., Garcia-Molina, A., Andrés-Colás, N., Vera-Sirera, F., Pérez-Amador, M.A., Puig, S. and Peñarrubia, L. (2013) Arabidopsis copper transport protein COPT2 participates in the cross talk between iron deficiency responses and low-phosphate signaling. *Plant Physiology* **162**(1):180-194.
- Péret, B., Desnos, T., Jost, R., Kanno, S., Berkowitz, O., and Nussaume, L. (2014) Root architecture responses: in search of phosphate. *Plant Physiology* **166**: 1713–1723.
- Pesaresi, P., Gardner, N. A., Masiero, S., Dietzmann, A., Eichacker, L., Wickner, R., Salamini, F. and Leister, D. (2003). Cytoplasmic N-Terminal Protein Acetylation Is Required for Efficient Photosynthesis in Arabidopsis. *The Plant Cell* **15**(8), 1817–1832.
- Peterman, T.K., Ohol, Y.M., McReynolds, L.J. and Luna, E.J. (2004) Patellin1, a novel Sec14-like protein, localizes to the cell plate and binds phosphoinositides. *Plant Physiology* **136**(2):3080-3094.
- Petroski, M.D. and Deshaies, R.J. (2005) Function and regulation of Cullin-RING ubiquitin ligases. *Nature Reviews Molecular Cell Biology* **6:** 9-20.
- Piatkov, K.I., Oh, J-H., Liu, Y. and Varshavsky, A. (2014) Calpain-generated N-end rule substrates. *Proceedings of the National Academy of Sciences* **111** (9) E817-E826.

- Pieterse, C.M., Van der Does, D., Zamioudis ,C., Leon-Reyes , A. and Van Wees, S.C. (2012) Hormonal modulation of plant immunity. *Annual Reviews in Cell Developmental Biology* **28**:489-521.
- Pietro D. Spanu, P.D. and Ralph Panstruga, R. (2017) Editorial: Biotrophic Plant-Microbe Interactions. *Frontiers in Plant Science* **8**: 192.
- Polevoda, B. and Sherman, F. (2000) Nα-terminal Acetylation of Eukaryotic Proteins. *The Journal of Biological Chemistry* **275**: 36479-36482.
- Polevoda, B., Arnesen, T., & Sherman, F. (2009). A synopsis of eukaryotic N^{α}-terminal acetyltransferases: nomenclature, subunits and substrates. *BMC Proceedings* **3**(Suppl 6), S2.
- Ponzio, C., Weldegergis, B. T., Dicke, M. , Gols, R. and Rasmann, S. (2016) Compatible and incompatible pathogen–plant interactions differentially affect plant volatile emissions and the attraction of parasitoid wasps. *Functional Ecology* **30**: 1779-1789.
- Potuschak, T., Stary, S., Schlögelhofer, P., Becker, F., Nejinskaia, V. and Bachmair, A. (1998) PRT1 of Arabidopsis thaliana encodes a component of the plant N-end rule pathway. *PNAS* **95:** 790 – 7908.
- Preger, V., Tango, N., Marchand, C., Lemaire, S.D., Carbonera, D., Di Valentin, M., Costa, A., Pupillo, P. and Trost, P. (2009) Auxin-Responsive Genes AIR12 Code for a New Family of Plasma Membrane b-Type Cytochromes Specific to Flowering Plants. *Plant Physiology* **150**(2): 606–620.
- Preston, G. M. (2000) *Pseudomonas syringae* pv. tomato: the right pathogen, of the right plant, at the right time. *Molecular Plant Pathology* **1**: 263-275.
- Puig, O., Caspary, F., Rigaut, G., Rutz, B., Bouveret, E., Bragado-Nilsson, E., Wilm, M. and Séraphin, B. (2001) The tandem affinity purification (TAP) method: a general procedure of protein complex purification. *Methods* **24**(3):218-29.
- Qiao, W. and Fan, L.M. (2008) Nitric oxide signaling in plant responses to abiotic stresses. *Journal of Integrative Plant Biology* **50**(10):1238-46.
- Qin, Y., Leydon, A.R., Manziello, A., Pandey, R., Mount, D., Denic, S., Vasic, B., Johnson, M.A. and Pananivelu, R. (2016) Penetration of the Stigma and Style Elicits a Novel Transcriptome in Pollen Tubes, Pointing to Genes Critical for Growth in a Pistil. *PLOS Genetics* **12**(7): e1006210.
- Rao, H., Uhlmann, F., Nasmyth, K. and Varshavsky A. (2001) Degradation of a cohesin subunit by the N-end rule pathway is essential for chromosome stability. *Nature 410* (6831):955-999.
- Reddy, A.S., Ali, G.S., Celesnik, H. and Day, I.S. (2011) Coping with stresses: roles of calcium- and calcium/calmodulin-regulated gene expression. *Plant Cell* **23**(6):2010-2032.
- Riber, W., Müller, J. T., Visser, E. J. W., Sasidharan, R., Voesenek, L. A. C. J., & Mustroph, A. (2015). The Greening after Extended Darkness1 Is an N-End Rule Pathway Mutant with High Tolerance to Submergence and Starvation. *Plant Physiology* **167**(4): 1616–1629.

- Rietz, S., Stamm, A., Malonek, S., Wagner, S., Becker, D., Medina-Escobar, N., Vlot, A.C., Feys, B.J., Niefind, K. and Parker, J.E. (2011) Different roles of Enhanced Disease Susceptibility1 (EDS1) bound to and dissociated from Phytoalexin Deficient4 (PAD4) in Arabidopsis immunity. *New Phytologist* **191**(1):107-119.
- Rope, A.F., Wang, K., Evjenth, R., Xing, J., Johnston, J.J., Swensen, J.J., Johnson, W.E., Moore, B., Huff, C.D., Bird, L.M., Carey, J.C., Opitz, J.M., Stevens, C.A., Jiang, T., Schank, C., Fain, H.D., Robison, R., Dalley, B., Chin, S., South, S.T., Pysher, T.J., Jorde, L.B., Hakonarson, H., Lillehaug, J.R., Biesecker, L.G., Yandell, M., Arnesen, T. and Lyon, G.J. (2011) Using VAAST to identify an X-linked disorder resulting in lethality in male infants due to N-terminal acetyltransferase deficiency. *American Journal of Human Genetics* **89**(1):28-43
- Rubinsztein, D.C., Shpilka, T. and Zvulun Elazar, Z. (2012) Mechanisms of Autophagosome Biogenesis. *Current Biology* **22** (1): R29-R34.
- Rubio, V., Shen, Y., Saijo, Y., Liu, Y., Gusmaroli, G., Dinesh-Kumar, S.P. and Deng, X.W. (2005) An alternative tandem affinity purification strategy applied to Arabidopsis protein complex isolation. *The Plant Journal* **41**(5):767-778.
- Ruegger, M., Dewey, E., Hobbie, L., Brown, D., Bernasconi, P., Turner, J., Muday, G. and Estelle, M. (1997) Reduced NPA-binding in the *tir3* mutant of Arabidopsis is associated with a reduction in polar auxin transport and diverse morphological defects. *Plant Cell* **9**:745–757.
- Ruschak, A.M., Slassi, M., Kay, L.E. & Schimmer, A.D. (2011) Novel Proteasome Inhibitors To Overcome Bortezomib Resistance. *Journal of the National Cancer Institute* **103**(13): 1007 – 1017.
- Russell L., Larner V., Kurup S., Bougourd S., Holdsworth M. J. (2000) The Arabidopsis COMATOSE locus regulates germination potential. *Development*.**1276**(1):3759–3767.
- Rustérucci, C., Aviv, D.H., Holt, B.F., Dangl, J.L. and Parker, J.E. (2001) The Disease Resistance Signaling Components EDS1 and PAD4 Are Essential Regulators of the Cell Death Pathway Controlled by LSD1 in Arabidopsis. *The Plant Cell* **13** (10) 2211-2224.
- Ryan, P.E., Davies, G.C., Nau, M.M. and Lipkowitz, S. (2006) Regulating the regulator: negative regulation of CBL ubiquitin ligases. *Trends in Biochemical Sciences* **31:** 79-88.
- Sadanandom, A., Bailey, M., Ewan, R., Lee, J. and Nelis, S. (2012). The ubiquitin–proteasome system: central modifier of plant signalling. *New Phytologist* **196:** 13 -28.
- Sadnandom, A., Ádám, É., Orosa, B., Viczián, A., Klose, C., Zhang, C., Josse, E.-M., Kozma-Bognár, L. and Nagy, F. (2015) SUMOylation of phytochrome-B negatively regulates light-induced signaling in *Arabidopsis thaliana*. *Proceedings of the National Academy of Sciences of the United States of America* **112** (11): 108–111.
- Saijo, Y., Tintor, N., Lu, X., Rauf, P., Pajerowska-Mukhtar, K., Häweker, H., Dong, X., Robatzek, S. and Schulze-Lefert, P. (2009)

Receptor quality control in the endoplasmic reticulum for plant innate immunity. *EMBO Journal* **28**(21):3439-3449.
- Sappl, P.G., Oñate-Sánchez. L., Singh, K.B. and Millar, A.H. (2004) Proteomic analysis of glutathione S -transferases of Arabidopsis thaliana reveals differential salicylic acid-induced expression of the plant-specific phi and tau classes. *Plant Molecular Biology* **54**(2):205-219.
- Saracco, S.A., Miller, M.J., Kurepa, J. and Richard D. Vierstra, R.D. (2007) Genetic Analysis of SUMOylation in Arabidopsis: Conjugation of SUMO1 and SUMO2 to Nuclear Proteins Is Essential. *Plant Physiology* **145**(1): 119–134.
- Scheffner, M., Nuber, U. and Huibregtse, J.M (1995) Protein ubiquitination involving an E1-E2-E3 enzyme ubiquitin thioester cascade. *Nature* **373**(6509):81-83.
- Schindelin, J., Arganda-Carreras, I., Frise, E., Kaynig,V., Longair, M., Pietzsch, T., Preibisch, S., Rueden, C., Saalfeld, S., Schmid, B., Tinevez, J., White, D.J., Hartenstein, V., Eliceiri, K., Tomancak, P. & Cardona, A. (2012) Fiji: an open-source platform for biological-image analysis. *Nature Methods* **9**: 676–682.
- Schmid, M., Davison, T.S., Henz, S.R., Pape, U.J., Demar, M., Vingron, M., Schölkopf, B., Weigel, D. and Lohmann, J.U. (2005) A gene expression map of Arabidopsis thaliana development. *Nature Genetics* **37**(5):501-506.
- Schmid, M., Davison, T.S., Henz, S.R., Pape, U.J., Demar, M., Vingron, M., Schölkopf, B., Weigel, D. and Lohmann, J.U. (2005) A gene expression map of Arabidopsis thaliana development. *Nature Genetics* **37**(5):501-506.
- Sels, J., Mathys, J., De Coninck, B.M., Cammue, B.P. and De Bolle, M.F. (2008) Plant pathogenesis-related (PR) proteins: a focus on PR peptides. *Plant Physiology and Biochemistry* **46**(11):941-950.
- Seo, P.J., Lee, A.K., Xiang, F. and Park, C.M. (2008) Molecular and functional profiling of Arabidopsis pathogenesis-related genes: insights into their roles in salt response of seed germination. *Plant Cell Physiology* **49**(3):334-344.
- Shah, J. (2003) The salicylic acid loop in plant defense. *Current Opinion in Plant Biology* **6**(4):365-371.
- Shani, E., Salehin, M., Zhang, Y., Sanchez, S.E., Doherty, C., Wang, R., Mangado, C.C., Song, L., Tal, I. and Pisanty, O. (2017) Plant stress tolerance requires auxin-sensitive Aux/IAA transcriptional repressors. *Current Biology* **27**:437–444.
- Shemorry, A., Hwang, C-S. and Varshavsky, A. (2013) Control of Protein Quality and Stoichiometries by N-Terminal Acetylation and the N-End Rule Pathway. *Molecular Cell* **50**(4): 540–551.
- Shinozaki, K., Yamaguchi-Shinozaki, K. and Seki, M. (2003) Regulatory network of gene expression in the drought and cold stress responses. *Current Opinions in Plant Biology* **6**(5):410-417.
- Shirano, Y., Kachroo, P., Shah, J., and Klessig, D. F. (2002). A gain-of-function mutation in an *Arabidopsis* Toll Interleukin1 receptor-nucleotide binding site-leucine-rich repeat type R gene triggers

defense responses and results in enhanced disease resistance. *Plant Cell* **14**: 3149–3162.
- Shirasu, K. (2009) The HSP90-SGT1 chaperone complex for NLR immune sensors. *Annual Reviews in Plant Biology* **60**:139-164.
- Shmueli, A., Tsai, Y.C., Yang, M., Braun, M.A. and Weissman, A.M. (2009) Targeting of GP78 for ubiquitin mediated proteasomal degradation by HRD1: cross-talk between E3s in the endoplasmic reticulum. *Biochemical and Biophysical Research Communications* **390**: 758–762.
- Silva, R.D. and Martinho, R.G. (2015) Developmental roles of protein N-terminal acetylation. *Proteomics* **15**(14):2402-2409.
- Simontacchi, M., Galatro, A., Ramos-Artuso, F., & Santa-María, G. E. (2015). Plant Survival in a Changing Environment: The Role of Nitric Oxide in Plant Responses to Abiotic Stress. *Frontiers in Plant Science* **6**: 977.
- Sirichandra, C., Wasilewska, A., Vlad, F., Valon, C. and Leung, J. (2009) The guard cell as a single-cell model towards understanding drought tolerance and abscisic acid action. *Journal of Experimental Botany* **60**(5):1439-1463.
- Solioz, M. and Stoyanov, J.V. (2003) Copper homeostasis in Enterococcus hirae. *FEMS Microbiology Reviews* **27:** 183-195.
- Sozzani, R., Maggio, C., Varotto, S., Canova, S., Bergounioux, C., Albani, D. and Cella, R. (2006) Interplay between Arabidopsis Activating Factors E2Fb and E2Fa in Cell Cycle Progression and Development. *Plant Physiology* **140**. 1355 - 1366.
- Smit, J.J. and Sixma, T.K. (2014) RBR E3-ligases at work. *EMBO reports* **15**(2): 142-154.
- Spallek, T., Beck, M., Ben Khaled, S., Salomon, S., Bourdais, G., Schellmann, S. and Robatzek, S. (2013) ESCRT-I mediates FLS2 endosomal sorting and plant immunity. *PLoS Genetics* **9**(12): e1004035.
- Spanu, P.D. and Kämper, J. (2010) Genomics of biotrophy in fungi and oomycetes--emerging patterns. *Current Opinions in Plant Biology* **13**(4):409-414.
- Spanu, P.D. and Panstruga, R. (2017) Biotrophic Plant-Microbe Interactions. *Frontiers in Plant Science* **8:** 192.
- Sparkes, I.A., Runions, J., Kearns, A. and Hawes, C. (2006) Rapid, transient expression of fluorescent fusion proteins in tobacco plants and generation of stably transformed plants. *Nature Protocols* **1**(4):2019-2025.
- Sponsel, V. M., Schmidt, F. W., Porter, S. G., Nakayama, M., Kohlstruk, S., & Estelle, M. (1997). Characterization of new gibberellin-responsive semidwarf mutants of Arabidopsis. *Plant Physiology* **115**(3): 1009–1020.
- Sriram, S.M., Kim, B.Y. and Kwon, Y.T. (2011) The N-end rule pathway: emerging functions and molecular principles of substrate recognition. *Nature Reviews Molecular Cell Biology* **12**(11): 735-747.
- Stangeland, B. and Salehian, Z. (2002) A improved clearing method for GUS assay in *Arabidopsis* endosperm and seeds. *Plant Molecular Biology Reporter* **20:** 107 – 114.

- Starheim, K.K., Gevaert, K. and Arnesen, T. (2012) Protein N-terminal acetyltransferases: when the start matters. *Trends in Biochemical Science* **37**(4):152-161.
- Stary, S., Yin, X.J., Potuschak, T., Schlögelhofer, P., Nizhynska, V. and Bachmair, A. (2003) PRT1 of Arabidopsis is a ubiquitin protein ligase of the plant N-end rule pathway with specificity for aromatic amino-terminal residues. *Plant Physiology* **133**(3):1360-1366.
- Stenzel, I., Otto, M., Delker, C., Kirmse, N., Schmidt, D., Miersch, O., … Wasternack, C. (2012). *ALLENE OXIDE CYCLASE* (*AOC*) gene family members of *Arabidopsis thaliana*: tissue- and organ-specific promoter activities and *in vivo* heteromerization*. *Journal of Experimental Botany* **63**(17): 6125–6138.
- Stone, S.L., Hauksdóttir, H., Troy, A., Herschleb, J., Kraft, E. and Callis, J. (2005) Functional analysis of the RING-type ubiquitin ligase family of Arabidopsis. *Plant Physiology* **137**(1):13-30.
- Stoyanov, J.V., Magnani, D. and Solioz, M. (2003) Measurement of cytoplasmic copper, silver, and gold with a lux biosensor shows copper and silver, but not gold, efflux by the CopA ATPase of Escherichia coli. *FEBS Letters* **546**(2-3):391-394.
- Strawn, M.A., Marr, S.K., Inoue, K., Inada, N., Zubieta, C. and Wildermuth, M.C. (2007) Arabidopsis isochorismate synthase functional in pathogen-induced salicylate biosynthesis exhibits properties consistent with a role in diverse stress responses. *Journal of Biological Chemistry* **282**(8):5919-5933.
- Strawn, M.A., Marr, S.K., Inoue, K., Inada, N., Zubieta, C., Wildermuth, M.C. (2007) Arabidopsis isochorismate synthase functional in pathogen-induced salicylate biosynthesis exhibits properties consistent with a role in diverse stress responses. *Journal of Biological Chemistry* **282**(8):5919-5933.
- Su, T., Xu, J., Li, Y., Lei, L., Zhao, L., Yang, H., Feng, J., Liu, G. and Ren, D. (2011) Glutathione-indole-3-acetonitrile is required for camalexin biosynthesis in *Arabidopsis thaliana*. *Plant Cell* **23**(1):364-380.
- Suh, M.C., Samuels, A.L., Jetter, R., Kunst, L., Pollard, M., Ohlrogge, J., and Beisson, F. (2005) Cuticular Lipid Composition, Surface Structure, and Gene Expression in Arabidopsis Stem Epidermis. *Plant Physiology* **139:** 1649–1665.
- Suzuki, T., Matsushima, C., Nishimura, S., Higashiyama, T., Sasabe, M., & Machida, Y. (2016). Identification of Phosphoinositide-Binding Protein PATELLIN2 as a Substrate of Arabidopsis MPK4 MAP Kinase during Septum Formation in Cytokinesis. *Plant and Cell Physiology* **57**(8): 1744–1755.
- Svistoonoff, S., Creff, A., Reymond, M., Sigoillot-Claude, C., Ricaud, L., Blanchet, A., Nussaume, L., and Desnos, T. (2007) Root tip contact with low-phosphate media reprograms plant root architecture. *Nature Genetics* **39:** 792–796.
- Swanson, R., Clark, T. and Preus, D. (2005) Expression profiling of Arabidopsis stigma tissue identifies stigma-specific genes. *Sexual Plant Reproduction* **18**: 163–171.

- Swatek, K.N. & Komander, D. (2016) Ubiquitin modifications. *Cell Research*. **26**(4):399-422.
- Taji, T., Seki, M., Satou, M., Sakurai, T., Kobayashi, M., Ishiyama, K., Narusaka, Y., Narusaka, M., Zhu, J.K., Shinozaki, K. (2004) Comparative genomics in salt tolerance between Arabidopsis and aRabidopsis-related halophyte salt cress using Arabidopsis microarray. *Plant Physiology* **135**(3):1697-1709.
- Takahashi, Y., Goldschmidt-Clermont, M., Soen, S.Y., Franzén, L.G. and Rochaix, J.D. (1991) Directed chloroplast transformation in Chlamydomonas reinhardtii: insertional inactivation of the psaC gene encoding the iron sulfur protein destabilizes photosystem I. *EMBO Journal* **10**(8):2033-2040.
- Tanaka, Y., Tanaka, N., Saeki, Y., Tanaka, K., Murakami, M., Hirano, T., Ishii, N. and Sugamura, K. (2008) c-Cbl-Dependent Monoubiquitination and Lysosomal Degradation of gp130. *Molecular and Cellular Biology* **28** (15) 4805-4818.
- Tasaki, T., Kim, S.T., Zakrzewska, A., Lee, B.E., Kang, M.J. Yoo, Y.D., Cha-Molstad, H.J., Hwang, J., Soung, N.K., Sung, K.S., Kim, S-H., Nguyen, M.D., Sun, M., Yi, E.C., Kim., B.Y. and Kwon, Y.T. (2013) UBR box N-recognin-4 (UBR4), an N-recognin of the N-end rule pathway, and its role in yolk sac vascular development and autophagy. *PNAS* **110**(10): 3800-3805.
- Tasaki, T., Mulder, L.C., Iwamatsu, A., Lee, M.J., Davydov, I.V., Varshavsky, A., Muesing, M. and Kwon, Y.T. (2005) A family of mammalian E3 ubiquitin ligases that contain the UBR box motif and recognize N-degrons. *Molecular Cell Biology* **25**(16):7120-7136.
- Tasaki, T., Sriram, S.M., Park, K.S. and Kwon, Y.T. (2012) The N-end rule pathway. *Annual Reviews of Biochemistry* **81**:261-289.
- Tasaki, T., Zakrzewska, A., Dudgeon, D.D., Jiang, Y., Lazo, J.S. and Kwon, Y.T. (2009) The substrate recognition domains of the N-end rule pathway. *Journal of Biology Chemistry* **284**(3):1884-1895.
- Thibaud, M.C., Arrighi, J.F., Bayle, V., Chiarenza, S., Creff, A., Bustos, R., Paz-Ares, J., Poirier, Y., and Nussaume, L. (2010) Dissection of local and systemic transcriptional responses to phosphate starvation in *Arabidopsis*. *Plant Journal* **64**: 775–789.
- Thines, B., Katsir, L., Melotto, M., Niu, Y., Mandaokar, A., Liu, G., Nomura, K., He, S.Y., Howe, G.A. and Browse, J. (2007) JAZ repressor proteins are targets of the SCF(COI1) complex during jasmonate signalling. *Nature* **448** (7154):661-665.
- Thomma, B. P. H. J., Nürnberger, T., & Joosten, M. H. A. J. (2011). Of PAMPs and Effectors: The Blurred PTI-ETI Dichotomy. *The Plant Cell* **23(**1), 4–15.
- Thomma, B.P.H.J., Thorsen Nürnberger, T. and Matthieu Joostena, M.A.J. (2011) Of PAMPs and Effectors: The Blurred PTI-ETI Dichotomy. *Plant Cell* **23**(1): 4–15.
- Tian, C., Zhang, X., He, J., Yu, H., Wang, Y., Shi, B., Han, Y., Wang, G., Feng, X., Zhang, C., Wang, J., Qi, J., Yu, R. & Jiao, Y. (2014) An organ boundary-enriched gene regulatory network uncovers regulatory hierarchies underlying axillary meristem initiation. *Molecular Systems Biology* **10**: 755.

- Ticconi, C.A., Delatorre, C.A., Lahner, B., Salt, D.E., and Abel, S. (2004) *Arabidopsis pdr2* reveals a phosphate-sensitive checkpoint in root development. *Plant Journal* **37**: 801–814.
- Ticconi, C.A., Lucero, R.D., Sakhonwasee, S., Adamson, A.W., Creff, A., Nussaume, L., Desnos, T. and Abel, S. (2009) ER-resident proteins PDR2 and LPR1 mediate the developmental response of root meristems to phosphate availability. *PNAS* **106**(33):14174 - 14179.
- Tsuda, K. and Katagiri, F. (2010) Comparing signaling mechanisms engaged in pattern-triggered and effector-triggered immunity. *Current Opinion in Plant Biology* **13**(4):459-465.
- Tsuda, K., Sato, M., Glazebrook, J., Cohen, J.D. and Katagiri, F. (2008) Interplay between MAMP-triggered and SA-mediated defense responses*. The Plant Journal* **53**(5):763-775.
- Turek, I., Tischer, N., Lassig, R. and Trujillo, M. (2018) Multi-tiered pairing selectivity between E2 ubiquitin-conjugating enzymes and E3 ligases. *Journal of Biological Chemistry* jbc.RA118.004226. doi:10.1074/jbc.RA118.004226.
- Turner, G.C., Du, F. and Varshavsky, A. (2000) Peptides accelerate their uptake by activating a ubiquitin-dependent proteolytic pathway. *Nature* **405**(6786): 579-583.
- Turner, N.C. & Graniti, A. (1969) *Fusicoccin*: A Fungal Toxin that opens Stomata. *Nature* **223**: 1070–1071.
- Ueki, S., Magori, S., Lacroix, B., & Citovsky, V. (2013). Transient Gene Expression in Epidermal Cells of Plant Leaves by Biolistic DNA Delivery. *Methods in Molecular Biology* (Clifton, N.J.) **940**: 17–26.
- Van Daele, I.,Gonzalez, N., Vercauteren, I., de Smet, L., Inze, D., Roldaǹ-Ruiz, I., and Vuylsteke, M.(2012) A comparative study of seed yield parameters in Arabidopsis thaliana mutants and transgenics. *Plant Biotechnology Journal* **10:** 488 – 500.
- van den Burg, H.A., Kini, R.K., Schuurink, R.C. and Takken, F.L. (2010) Arabidopsis small ubiquitin-like modifier paralogs have distinct functions in development and defense. *Plant Cell* **22**, 1998–2016.
- Van Leene, J., Eeckhout, D., Cannoot, B., De Winne, N., Persiau, G., Van De Slijke, E, Vercruysse, L., Dedecker, M., Verkest, A., Vandepoele, K., Martens, L., Witters, E., Gevaert, K. and De Jaeger, G. (2014) An improved toolbox to unravel the plant cellular machinery by tandem affinity purification of Arabidopsis protein complexes. *Nature Protocols* **10**(1):169 - 187.
- Van Leene, J., Witters, E., Inzé, D. and De Jaeger, G. (2008) Boosting tandem affinity purification of plant protein complexes. *Trends in Plant Sciences* **13**(10):517-520.
- van Loon, L.C., Rep, M. and Pieterse, C.M. (2006) Significance of inducible defense-related proteins in infected plants. *Annual Reviews in Phytopathology* **44:**135-162.
- van Tol, N., Rolloos, M., Augustijn, D., Alia, A., de Groot, H.J., Hooykaas, P.J.J. & van der Zaal, B.J. (2017) An Arabidopsis mutant with high operating efficiency of Photosystem II and low chlorophyll fluorescence. *Scientific Reports* **7:** 3314.

- van Wersch, R., Li, X. and Zhang, Y. Mighty Dwarfs: Arabidopsis Autoimmune Mutants and Their Usages in Genetic Dissection of Plant Immunity. *Frontiers in Plant Science* **7**: 1717.
- Vaneste, J.L. (2017) The Scientific, Economic, and Social Impacts of the New Zealand Outbreak of Bacterial Canker of Kiwifruit (*Pseudomonas syringae pv. actinidiae*). *Annual Review of Phytopathology* **55**:377-399.
- Varshavsky, A. (1996) The N-end rule: functions, mysteries, uses. *PNAS USA* **93**(22):12142-12149.
- Varshavsky, A. (2011) The N-end rule pathway and regulation by proteolysis. *Protein Science* **20**(8):1298-1345.
- Verma, V., Croley, F. and Sadanandom, A. (2018) Fifty shades of SUMO: its role in immunity and at the fulcrum of the growth–defence balance. *Molecular Plant Pathology* **19**(6), 1537–1544.
- Vert, G., Grotz, N., Dédaldéchamp, F., Gaymard, F., Guerinot, M.L., Briat. J.F. and Curie, C. (2002) IRT1, an Arabidopsis transporter essential for iron uptake from the soil and for plant growth. *Plant Cell* **14**(6):1223-1233.
- Vicente, J. , Mendiondo, G. M., Pauwels, J. , Pastor, V. , Izquierdo, Y. , Naumann, C. , Movahedi, M. , Rooney, D. , Gibbs, D. J., Smart, K. , Bachmair, A. , Gray, J. E., Dissmeyer, N. , Castresana, C. , Ray, R. V., Gevaert, K. and Holdsworth, M. J. (2018), Distinct branches of the N-end rule pathway modulate the plant immune response. *New Phytologist* doi:10.1111/nph.15387
- Vicente, J., Mendiondo, G.M., Movahedi, M., Peirats-Llobet, M., Juan, Y.T., Shen, Y.Y., Dambire, C., Smart, K., Rodriguez, P.L., Charng, Y.Y., Gray, J.E. and Holdsworth, M.J. (2017) The Cys-Arg/N-End Rule Pathway Is a General Sensor of Abiotic Stress in Flowering Plants. *Current Biology* **27**(20):3183-3190.
- Vierling (1991) The Roles of Heat Shock Proteins in Plants. *Annual Review of Plant Physiology and Plant Molecular Biology* **42**:579-620.
- Vierstra, R.D. (2009) The ubiquitin-26S proteasome system at the nexus of plant biology*. Nature Reviews Molecular Cell Biology* **10**(6):385-397.
- Vijn, I., das Nevas, L., van Kammen, A., Franssen, H. and Bisseling, T. (1993) Nod factors and nodulation in plants. *Science* **260**(5115):1764-1765.
- Vu, K.V., Nguyen, N.T., Jeong, C.Y., Lee, Y.H., Lee, H. and Hong, S.W. (2017) Systematic deletion of the ER lectin chaperone genes reveals their roles in vegetative growth and male gametophyte development in Arabidopsis. *The Plant Journal* **89**(5):972-983,
- Waese, J., Fan, J., Pasha, A., Yu, H., Fucile, G., Shi, R., Cumming, M., Kelley, L., Sternberg, M., Krishnakumar, V., Ferlanti, E., Miller, J., Town, C., Stuerzlinger, W. and Provart, N.J. (2017) ePlant: Visualizing and Exploring Multiple Levels of Data for Hypothesis Generation in Plant Biology. *Plant Cell* **29** (8): 1806-1821.
- Wahid, A., Gelani, S., Ashraf, M. and Foolad, M.R. (2007) Heat tolerance in plants: An overview. *Environmental and Experimental Botany* **61**(3) 199-223.

- Walsh, C.K. and Sadanandom, A. (2014) Ubiquitin chain topology in plant cell signaling: a new facet to an evergreen story. *Frontiers in Plant Science* **5**: 122.
- Wang, H., Piatkov, K. I., Brower, C. S., & Varshavsky, A. (2009). Glutamine-Specific N-Terminal Amidase, a Component of the N-End Rule Pathway. *Molecular Cell* **34**(6): 686–695.
- Wang, W., Barnaby, J.Y., Tada, Y., Li, H., Tör, M., Caldelari, D., Lee, D.U., Fu, X.D. and Dong, X. (2011) Timing of plant immune responses by a central circadian regulator. *Nature* **470**(7332):110-114.
- Wang, Y., Noguchi, K., Ono, N., Inoue, S., Terashima, I., & Kinoshita, T. (2014) Overexpression of plasma membrane H+-ATPase in guard cells promotes light-induced stomatal opening and enhances plant growth. *PNAS* **111**: 533–538.
- Wang,Y., Noguchi, K., Ono, N., Inoue, S., Terashima, I. and Kinoshita, T. (2014) Overexpression of plasma membrane H+-ATPase in guard cells promotes light-induced stomatal opening and enhances plant growth. *PNAS USA* **111**(1):533-538.
- Wasternack, C. (2007) Jasmonates: an update on biosynthesis, signal transduction and action in plant stress response, growth and development. *Annals of Botany* **100**(4):681-697.
- Wasternack, C. (2017) The Trojan horse coronatine: the COI1–JAZ2–MYC2,3,4–ANAC019,055,072 module in stomata dynamics upon bacterial infection. *New Phytologist* **213**: 972-975.
- Wasternack, C. and Hause, B. (2013) Jasmonates: biosynthesis, perception, signal transduction and action in plant stress response, growth and development. *Annals of Botan*y **111**: 1021–1068.
- Wasternack, C. and Hause, B. (2013) Jasmonates: biosynthesis, perception, signal transduction and action in plant stress response, growth and development. An update to the 2007 review in Annals of Botany. *Annals of Botany* **111**(6):1021-1058.
- Wasternack, C. and Strnad, M. (2016). Jasmonate signaling in plant stress responses and development - active and inactive compounds. *New Biotechnology* **33**: 604–613.
- Weidberg, H., Shvets, E., and Elazar, Z. (2011) Biogenesis and Cargo Selectivity of Autophagosomes. *Annual Review of Biochemistry* **80:** 125 – 156.
- Westoby, M., Falster, D.S., Moles, A.T., Vesk, P.A. and Wright, I.J. (2002) Plant ecological strategies: some leading dimensions of variation between species. *Annual Review of Ecology and Systematics* **33:** 125–159.
- Whalen, M.C., Innes, R.W., Bent, A.F., and Staskawicz, B.J. (1991) Identification of Pseudomonas syringae Pathogens of Arabidopsis and a Bacterial Locus Determining Avirulence on Both Arabidopsis and Soybean. *The Plant Cell* **3**: 49-59.
- White, M.D., Klecker, M., Hopkinson, R.J., Weits, D.A., Mueller, C., Naumann, C., O'Neill, R., Wickens, J., Yang, J., Brooks-Bartlett, J.C., Garman, E.F., Grossmann, T.N., Dissmeyer, N. and Flashman, E. (2017) Plant cysteine oxidases are dioxygenases that directly enable

arginyl transferase-catalysed arginylation of N-end rule targets. *Nature Communications* **8**:14690.
- Wiermer, M., Feys, B.J. and Parker, J.E. (2005) Plant immunity: the EDS1 regulatory node. *Current Opinion in Plant Biology* **8**(4):383-389.
- Wildermuth, M.C., Dewdney, J., Wu, G. and Ausubel, F.M. (2001) Isochorismate synthase is required to synthesize salicylic acid for plant defence. *Nature* **414**(6863):562-565.
- Wilkinson, K.A. and Henley, J.M. (2010) Mechanisms, regulation and consequences of protein SUMOylation. *Biochemical Journal* **428**: 133–145.
- Williamson, L.C., Sebastien, P.C.P. Ribrioux, Fitter, A. H. and Ottoline Leyser, O.H.M. (2001) Phosphate Availability Regulates Root System Architecture in Arabidopsis. *Plant Physiology* **126:** 75–882.
- Wilson, R., Goyal, L., Ditzel, M., Zachariou, A., Baker, D.A., Agapite, J., Steller, H. and Meier, P. (2002) The DIAP1 RING finger mediates ubiquitination of Dronc and is indispensable for regulating apoptosis. *Nature Cell Biology* **4**(6):445-450.
- Winter, D., Vinegar, B., Nahal, H., Ammar, R., Wilson, G.V. and Provart, N.J. (2007) An "Electronic Fluorescent Pictograph" Browser for Exploring and Analyzing Large-Scale Biological Data Sets. *PLOS ONE* **2**(8): e718.
- Winter, V., & Hauser, M.-T. (2006). Exploring the ESCRTing machinery in eukaryotes. *Trends in Plant Science* **11**(3): 115–123.
- Woodward. A.W and Bartel, B. (2018). Biology in Bloom: A Primer on the *Arabidopsis thaliana* Model System. *Genetics* **208:** 1337-1349.
- Wu, C.-H., Krasileva, K. V., Banfield, M. J., Terauchi, R., & Kamoun, S. (2015). The "sensor domains" of plant NLR proteins: more than decoys? *Frontiers in Plant Science* **6**: 134.
- Xin, X.F. and He, S.Y. (2013) Pseudomonas syringae pv. tomato DC3000: a model pathogen for probing disease susceptibility and hormone signaling in plants. *Annual Reviews in Phytopathology* **51**:473-498.
- Xu, F., Huang, Y., Li, L., Gannon, P., Linster, E., Huber, M., Kapos, P., Bienvenut, W., Polevoda, B., Meinnel, T., Hell, R., Giglione, C., Zhang, Y., Wirtz, M., Chen, S. and Li, X. (2015) Two N-terminal acetyltransferases antagonistically regulate the stability of a nod-like receptor in Arabidopsis. *Plant Cell* **27**(5):1547-1562.
- Xu, J., Li, Y., Wang, Y., Liu, H., Hailian, L.L., Guoqin Liu, Y. and Dongtao Ren, D. (2006) Activation of MAPK Kinase 9 Induces Ethylene and Camalexin Biosynthesis and Enhances Sensitivity to Salt Stress in Arabidopsis. *Journal of Biological Chemistry* **283**: 26996 - 27006.
- Xu, W., Ding, G., Yokawa, K., Baluška, F., Li, Q.-F., Liu, Y., Shi, W., Liang, J. and Zhang, J. (2013). An improved agar-plate method for studying root growth and response of *Arabidopsis thaliana*. *Scientific Reports* **3**: 1273.
- Yadav, R.K., Girke, T., Pasala, S., Xie, M., Reddy, G.V. (2009) Gene expression map of the Arabidopsis shoot apical meristem stem cell

niche. *Proceedings of the National Academy of Sciences* **106** (12): 4941-4946.
- Yamaguchi-Shinozaki, K. and Shinozaki, K. (2006) Transcriptional regulatory networks in cellular responses and tolerance to dehydration and cold stresses. *Annual Review of Plant Biology* **57**: 781–803.
- Yan, J., Zhang, C., Gu, M., Bai, Z., Zhang, W., Qi, T., Cheng, Z., Peng, W., Luo, H., Nan, F., Wang, Z. and Xie, D. (2009) The Arabidopsis CORONATINE INSENSITIVE1 protein is a jasmonate receptor. *Plant Cell* **21**(8):2220-2236.
- Yang, H., Li, P., Zhang, A., Wen, X., Zhang, L. and Lu, C. (2017) Tetratricopeptide repeat protein Pyg7 is essential for photosystem I assembly by interacting with PsaC in Arabidopsis. *The Plant Journal* **91**(6):950-961.
- Yang, X., Srivastava, R., Howell, S.H. and Bassham, D.C. (2015) Activation of autophagy by unfolded proteins during endoplasmic reticulum stress. *The Plant Journal* **85**(1): 83-95.
- Yang, Y., Costa, A., Leonhardt, N., Siegel, R.S. and Schroeder, J.I. (2008) Isolation of a strong Arabidopsis guard cell promoter and its potential as a research tool*. Plant Methods* **4**:6.
- Yang, Y., Kitagaki, J., Dai, R.M., Tsai, Y.C., Lorick, K.L., Ludwig, R.L., Pierre, S.A., Jensen, J.P., Davydov, I.V., Oberoi, P., Li, C.C., Kenten, J.H., Beutler, J.A., Vousden, K.H. and Weissman, A.M. (2007) Inhibitors of ubiquitin-activating enzyme (E1), a new class of potential cancer therapeutics. *Cancer Research* **67**(19):9472-81.
- Yasuda, M., Ishikawa, A., Jikumaru, Y., Seki, M., Umezawa, T., Asami, T., Maruyama-Nakashita, A., Kudo, T., Shinozaki, K., Yoshida, S. and Nakashita, H. (2008) Antagonistic interaction between systemic acquired resistance and the abscisic acid-mediated abiotic stress response in Arabidopsis. *Plant Cell* **20**(6):1678-1692.
- Yoshida, S., Ito, M., Callis, J., Nishida, I. and Watanabe, A. (2002), A delayed leaf senescence mutant is defective in arginyl-tRNA:protein arginyltransferase, a component of the N-end rule pathway in *Arabidopsis*. *The Plant Journal* **32:** 129-137
- Yuen C.Y.L., Matsumoto, K.O., and Christopher, D.A. (2013) Variation in the Subcellular Localization and Protein Folding Activity among Arabidopsis thaliana Homologs of Protein Disulfide Isomerase. *Biomolecules* **3**(4), 848-869.
- Zhang, C., Xie, Q., Anderson, R.G., Ng, G., Seitz, N.C., Peterson, T., McClung, C.R., McDowell, J.M., Kong, D., Kwak, J.M. and Lu, H. (2013) Crosstalk between the circadian clock and innate immunity in Arabidopsis. *PLoS Pathology* **9**(6): e1003370.
- Zhang, H., Gannon, L., Hassall, K.L., Deery, M.J., Gibbs, D.J., Holdsworth, M.J., van der Hoorn, R.A.L., Lilley, K.S. and Theodoulou, F.L. (2018) N-terminomics reveals control of Arabidopsis seed storage proteins and proteases by the Arg/N-end rule pathway. *New Phytologist* **218**(3):1106 - 1126.
- Zhang, H., Gannon, L., Powers, S.J., Lilley, K.S. and Theodoulou, F.L. (2015b) Quantitative proteomics analysis of the Arg/N-end rule

pathway of targeted degradation in Arabidopsis roots. *Proteomics* **15(**14): 2447 –2457.
- Zhang, J., Tripathi, D.N., Jing, J., Alexander, A., Kim, J., Powell, R.T., Dere, R., Tait-Mulder, J., Lee, J.H., Paull, T.T., Pandita, R.K., Charaka V.K., Pandita, T.K., Kastan, M.B., Walker, C.L. (2015a) ATM functions at the peroxisome to induce pexophagy in response to ROS. *Nature Cell Biology* **17**(10):1259-1269.
- Zhang, Y., Goritschnig, S., Dong, X., and Li, X. (2003). A gain-of-function mutation in a plant disease resistance gene leads to constitutive activation of downstream signal transduction pathways in suppressor of *npr1-1*, constitutive 1. *Plant Cell* **15**: 2636–2646.
- Zhang, Z., Lenk, A., Andersson, M.X., Gjetting, T., Pedersen, C., Nielsen, M.E., Newman, M-A., Hou, B-H., Somerville, S.C. and Thordal-Christensen, H. (2008) A Lesion-Mimic Syntaxin Double mutant in *Arabidopsis* reveals novel complexity of pathogen defense signaling. *Molecular Plant* **1**(3): 510- 527.
- Zhang, Z., Zheng, Y., Ham, B.K., Chen, J., Yoshida, A., Kochian, L.V., Fei, Z. and Lucas, W.J. (2016) Vascular-mediated signalling involved in early phosphate stress response in plants. *Nature Plants* **2**:16033.
- Zhao, J., Williams, C.C. and Last, R.L. (1998). Induction of Arabidopsis tryptophan pathway enzymes and camalexin by amino acid starvation, oxidative stress, and an abiotic elicitor. *Plant Cell* **10**: 359–370.
- Zheng, X., Spivey, N. W., Zeng, W., Liu, P-P., Fu, Z. Q., Klessig, D. F., He, S-Y. and Dong, X. (2012). Coronatine promotes Pseudomonas syringae virulence in plants by activating a signaling cascade that inhibits salicylic acid accumulation. *Cell Host & Microbe* **11**(6), 587–596.
- Zhou, R., Silverman, N., Hong, M., Liao, D.S., Chung, Y., Chen, Z.J. and Maniatis, T. (2005) The role of ubiquitination in Drosophila innate immunity. *The Journal of Biological Chemistry* **280**(40):34048-34055.
- Zhu, J.K. (2000) Genetic analysis of plant salt tolerance using Arabidopsis. *Plant Physiology* 124(3):941-948.
- Zhu, Z., Xu, F., Zhang, Y., Cheng, Y.T., Wiermer, M., Li, X. and Zhang, Y. (2010) Arabidopsis resistance protein SNC1 activates immune responses through association with a transcriptional corepressor. *PNAS USA* **107**(31):13960-13965.
- Zinn, K.E., Tunc-Ozdemir, M. and Harper, J.F. (2010) Temperature stress and plant sexual reproduction: uncovering the weakest links. *Journal of Experimental Botany* **61**(7): 1959–1968.
- Zipfel, C. and Robatzek, S. (2010) Pathogen-associated molecular pattern-triggered immunity: veni, vidi...? *Plant Physiology* **154**(2):551-554.
- Zipfel, C., Kunze, G., Chinchilla, D., Caniard, A., Jones, J.D., Boller, T. and Felix, G. (2006) Perception of the bacterial PAMP EF-Tu by the receptor EFR restricts Agrobacterium-mediated transformation. *Cell* **125**(4):749-760.
- Zschiesche, W., Barth, O., Daniel, K., Böhme, S., Rausche, J. and Humbeck, K. (2015), The zinc-binding nuclear protein HIPP3 acts as an upstream regulator of the salicylate-dependent plant immunity

pathway and of flowering time in Arabidopsis thaliana. *New Phytologist* **207**: 1084-1096.

Appendix: Tandem Affinity Purification of PRT1

Complex interactions of proteins in a co-ordinated and defined manner enable cellular functions to happen. PRT1 is predicted to interact with a number of different proteins in order to fulfil its function as an E3 ligase. These include regulators, substrates and E2 ubiquitin conjugating enzymes. Several different techniques are available for the identification of protein-protein interactions (Fukao, 2012). Tandem affinity purification (TAP) is a procedure performed at near physiological conditions, which allows isolation of native protein complexes whose components can be identified by mass spectrometry (Puig et al., 2001). Although early TAP studies in plants used the strong, near-constitutive CaMV35S promoter (Rubio *et al.,* 2005) where possible, it is preferable to maintain the expression of the fusion protein at a near-native level, hence the use of the endogenous PRT1 promoter in the MO14-7-1 construct (section 3.4.1).

The TAP protocol of Van Leene *et al* (2015) was modified to incorporate Bortezomib spot treatment (described in section 3.5.1) in order to investigate strong and weak interactors of PRT1. The TAP construct comprises streptavidin binding protein (SBP) and two copies of an immunoglobulin G binding domain, separated by a TEV protease cleavage site. Whole seedlings of 5 DAG MO14-7-1 was subjected to tandem affinity purification with Col-0 used as a negative control. The TAP procedure consisted of two major purification steps. During the initial purification step, native protein complexes which include the 'bait protein', in this instance PRT1, are isolated through high-affinity binding to an IgG resin. Incubation of the initial purification products with tobacco etch virus (TEV) protease, which recognises its cleavage site between the two tags, allows specific and gentle elution of weakly interacting proteins. The second purification step involves the binding of the bait protein and interactors to streptavidin beads and elution with DTT to yield the strongly interacting proteins. The TAP construct was monitored throughout the assay to ensure correct expression and stability through

anti-SBP immunoblotting (Figure 8.1). Due to technical issues, elution of the strongly interacting protein was not achieved and consequently the protein-protein interactions could not be studied through mass spectrometry.

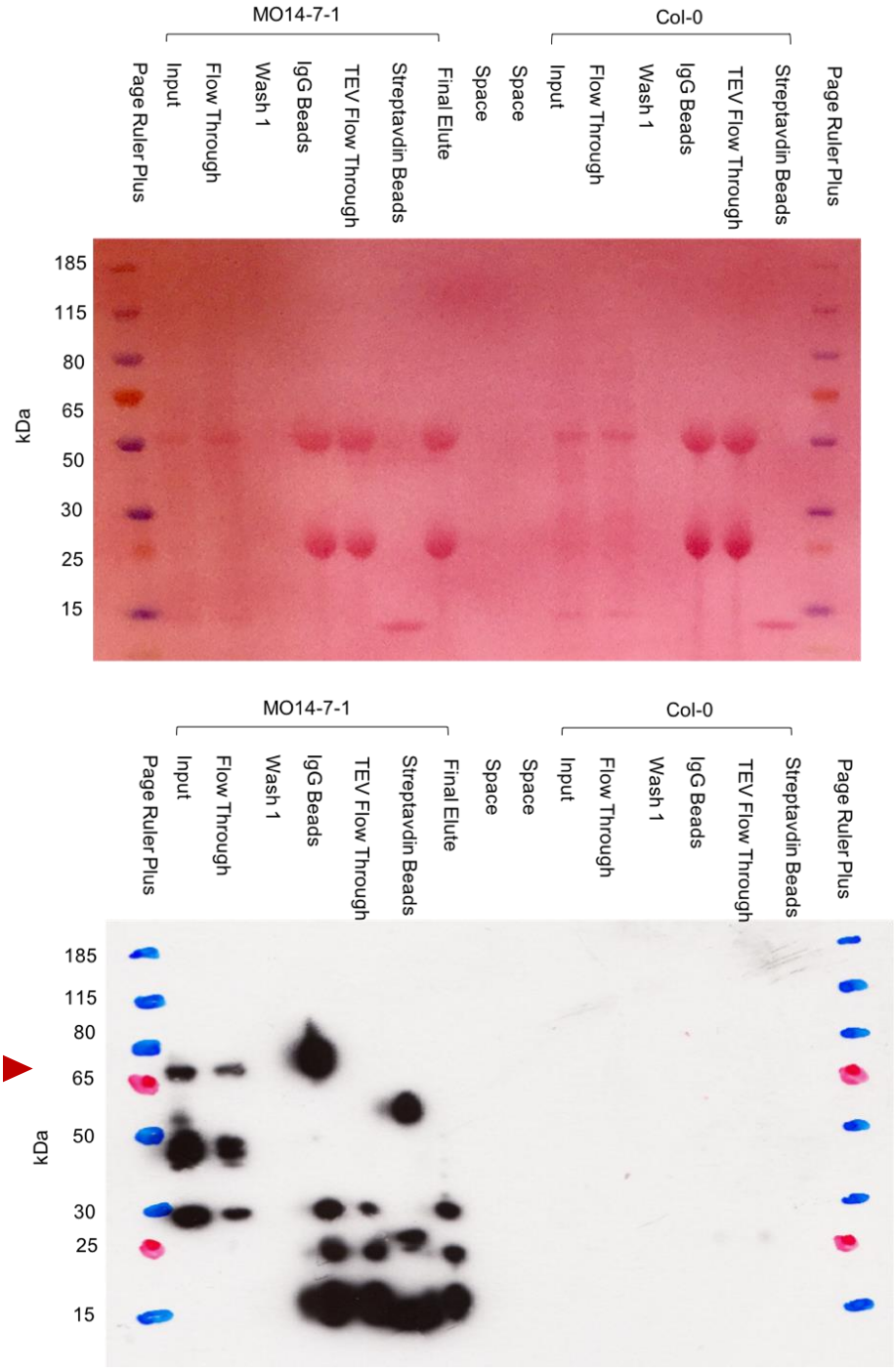

Figure 8.1: **Anti-SBP Western blot of MO14-7-1 and Col-0** (-ve) used to confirm the expression and stability of the TAP construct throughout the TAP procedure (A) Ponceau stained PVDF membrane and (B) exposed X-ray film showing the expression of the TAP in the MO14-7-1 background. PRT1-TAP protein size is ~71 KDa (SBP ~26 kDa + PRT1~45 kDa) indicated by red arrow on the blot.